# Density-Corrected Models for Soil-Gas Transport Parameters; Towards Soil Architectural fingerprints and Design of Growth Media

Chamindu, Deepagoda

*Publication date:*
2013

*Document Version*
Early version, also known as pre-print

# Density-Corrected Models for Soil-Gas Transport Parameters: Towards Soil Architectural Fingerprints and Design of Growth Media

Chamindu Deepagoda T.K.K.

PhD Dissertation

Dept. of Biotechnology, Chemistry, and Environmental Engineering

Section of Environmental Engineering

Aalborg University

April, 2012

*The Lungs of Soil*

*Soil gases move*

*In mysterious ways*

*From high C to low C*

*Around aggregate cities*

*Blocked by water locks*

*And corrected by density*

*Mostly obeying the Law of Fick*

*Searching fractured free-ways*

*And slowly revealing to us*

*The intricate architecture*

*And life-support systems*

*Of soil inner space*

*-Per Moldrup 2012*

This thesis is dedicated to all soil-gas physicists, in the past and present, for their relentless efforts and contribution to soil-gas physics.

**List of Supporting Papers**

I. **Chamindu Deepagoda, T.K.K.**, P. Moldrup, P. Schjønning, L. W. de Jonge, K. Kawamoto, and T. Komatsu. 2010. Density-corrected models for gas diffusivity and air permeability in unsaturated soil. Vadose Zone J. 10:226-238.

II. **Chamindu Deepagoda, T.K.K.**, P. Moldrup, P. Schjønning, K. Kawamoto, T. Komatsu, and L. W. de Jonge. 2011. Generalized density-corrected model for gas diffusivity in variably saturated soils. Soil Sci. Soc. Am. J. 74:1302-1317.

III. **Chamindu Deepagoda, T.K.K.**, P. Moldrup, P. Schjønning, K. Kawamoto, T. Komatsu, and L. W. de Jonge. 2012. Variable pore connectivity model linking gas diffusivity and air-phase tortuosity to soil matric potential. Vadose Zone J. doi:10.2136/vzj2011.0096.

IV. **Chamindu Deepagoda, T.K.K.**, P. Moldrup, M. P. Jensen, S. B. Jones, L. W. de Jonge, P. Schjønning, K. Scow, J. W. Hopmans, D. E. Rolston, K. Kawamoto, and T. Komatsu. 2012. Diffusion aspects of designing porous growth media for earth and space. Soil Sci. Soc. Am. J. doi:10.2136/sssaj2011.0438

V. **Chamndu Deepagoda, T.K.K**., P. Moldrup, P. Schjønning, K. Kawamoto, T. Komatsu and L. W. de Jonge. 2010. Gas-diffusivity-based connectivity analysis of aggregated soil inner and outer pore space. *In*: Proceedings from 1st International Conference and Exploratory Workshop on Soil Architecture "CESAR". Nov. 30 – Dec. 2, 2010, Faculty of Agricultural Sciences, Aarhus University, Denmark, pp. 63-68.

In this thesis, the papers will be referred to by their Roman numerals.

## Acknowledgment

This PhD thesis is based on a three-year research study (2009-2012) carried out mainly at Aalborg University (AAU), Denmark, with a short-term international stay at Saitama University (SU), Japan. This project was facilitated by the international research project Soil Infrastructure, Interfaces and Translocation processes in Inner Space (Soil-it-is), which was financed by the Danish Research Council for Technology and Production Sciences.

This thesis owes its present shape to the assistance, inspiration and guidance of many people around the world. In the first place, I express my sincere gratitude to Prof. Per Moldrup, my main supervisor, who invited me to Aalborg University and offered me a PhD position while I was in a struggle for higher studies. He introduced me to the soil-air phase, and has guided me through its intriguing tortuous pathways over the last three years. His surprising knowledge, perfect guidance, great inspiration, and wonderful ideas always impressed me and made me undiffused even after hours-long power meetings on soil gas diffusion. I am really honoured to be your PhD student.

Many thanks are also extended to Prof. Lis W. de Jonge from Research Centre Foulum for her continuous guidance and kind support throughout this study. I always had a nice time at Foulum with other colleagues, enjoyed the regular meetings at your office (but not the giant whiteboard!). I am also very thankful to Dr. Per Schjønning from Foulum whose immense experience and very useful ideas brought great value to my manuscripts. My two supervisors from SU, Prof. Toshiko Komatsu and Dr. Ken Kawamoto, are also owed my deep gratitude for their generous and continued support and also for hosting my international stay. I am thankful to Prof. Dennis Rolston, Prof. Jan Hompans, Dr. Scott Jones for excellent reviews on my manuscripts. The kind assistance of Helle Blendrup (AAU) and Dr. Hamamoto (SU) for my laboratory and research work is gratefully acknowledged.

It is always hard to get settled in a new country, many practical issues need to be fixed. To Andreas, Maria, Sam, Rune, Diana (and many others) for your helping hand to get the practical problems fixed, I am thankful. Many thanks are also due to my Danish, Japanese, Sri Lankan, and other foreign students for making my environment homely, everywhere.

I also pay sincere gratitude to my parents for patience while I am studying abroad. My beloved wife, Inoka, deserves a big hug for sharing all ups and downs during last three years with a great patience and care. Finally to my little boy, Sansithu, you never cried when I left you for office and instead greeted me with your little smile. You will be proud to see this when you are grown up.

Chamindu Deepagoda T.K.K.

Aalborg University

## Summary

Soil, the 'living skin' covering the Earth's surface, plays a fundamental role for sustaining life on the Earth. The entire terrestrial life is very much akin to soil, its properties and functions. The soil-air phase is a key component in soil functional architecture, and is responsible for controlling many essential vadose zone processes including soil aeration, subsurface migration of gaseous contaminants, and greenhouse gas emissions. Therefore, a thorough understanding of functional properties and processes linked to the soil air-phase is a prerequisite for understanding soil's life support functions and ecosystem services.

This PhD. study focused mainly on measurements and modeling of two key gas transport parameters, the soil-gas diffusivity ($D_p/D_o$, where $D_p$ and $D_o$ are the gas diffusion coefficients in soil and free air, respectively) and soil-air permeability ($k_a$), but with emphasis on gas diffusivity. The model development and validation were mainly based on literature data for soils sampled from a widely contrasting vadose zone profiles, representing a broad range of soil types and density levels. For $D_p$ and $k_a$ measurements during the present study, standard and well-documented methods were followed.

Introducing a novel, density-corrected (D-C) model approach, predictive D-C models for both $D_p/D_o$ and $k_a$ were developed from data for soils representing a wide range of soil types and density levels. Secondly, the D-C gas diffusivity model was extended to a generalized density-corrected (GDC) model to expand the predictions for an even broader range of soil types, now spanning from sand to peat. Thirdly, based on a concept of inactive pore space, an inactive-pore-space and density-corrected (IPDC) model was introduced for porous media exhibiting a distinct gas percolation threshold, especially aggregated soils. Important applications of the models, including a diffusivity-based characterization of plant growth media for Earth and Space, were also discussed.

Finally, a variable pore connectivity factor model was developed for description of the Buckingham pore connectivity-tortuosity factor, $X$, from soil matric potential ($\psi$) expressed by pF (= log $|-\psi|$). The $X$-pF model can play a duel role for predicting soil-gas diffusivity across soil types within given moisture conditions, and for soil architecture fingerprinting to better differentiate and understand effects of soil structure dynamics and compaction on soil functions..

# Table of Contents

# 1 Introduction

## 1.1 Soil: Fundamental for life

Another NASA-made Mars-bound spacecraft, the Curiosity, lifted off on 26th November 2011 and is on a 354 million-mile cruise towards Mars at the time of writing this thesis. With well-equipped devises, the Curiosity will scrutinize Martian rock and soil samples in the search for hard evidence of any form of life on Mars, now or in the history. Previous missions to Mars or the Moon have not brought any hopes of Martian or lunar life, nor have any beyond-Earth explorations so far revealed any promising signs of extraterrestrial life. It is mysterious how the terrestrial soil facilitates life on the Earth with such abundance, while the "Outer Space", including our closest neighbours, remains apparently uninhabitable (Fig. 1). While the Curiosity is in a quest for life on Martian soil, a close look into the characteristics of terrestrial soil (or simply, the "soil") may disclose very important secrets of terrestrial life.

**Fig. 1** Fundamental for life in Space: a tiny sprout emerging from a fertile terrestrial soil (left) against a barren, cold, and dry Martian soil (right) with no clues of life (image courtesy: NASA)

## 1.2 Soil architecture

Natural soil is a dynamic multi-phasic medium. The solid phase – mainly mineral particles of widely ranging sizes and shapes – makes up the skeletal structure of soil. The undecayed and partially decayed plant and animal tissues constitute the soil organic matter –another key component in the soil-solid phase. The soil-liquid phase is a solution enriched with many dissolved geochemical elements. The soil-air phase is the atmospheric counterpart in soil, but is more diverse qualitatively and quantitatively than the atmospheric air. The soil-liquid and soil-air phases are functionally complementary and transient, while they mutually share the soil total pore (or void) space. The soil pore space typically involves a wide spectrum of differently sized and shaped pores, randomly

connected and disconnected to form an intricate pore network. The soil- air (A) and -water (W), summing up to total pore space (E), and -solids (S), split into -organic matter (O) and -minerals (M), and Ever-changing system in time and space outline the soil A-W-E-S-O-M-E system (Fig. 2) and broadly define the soil functional architecture.

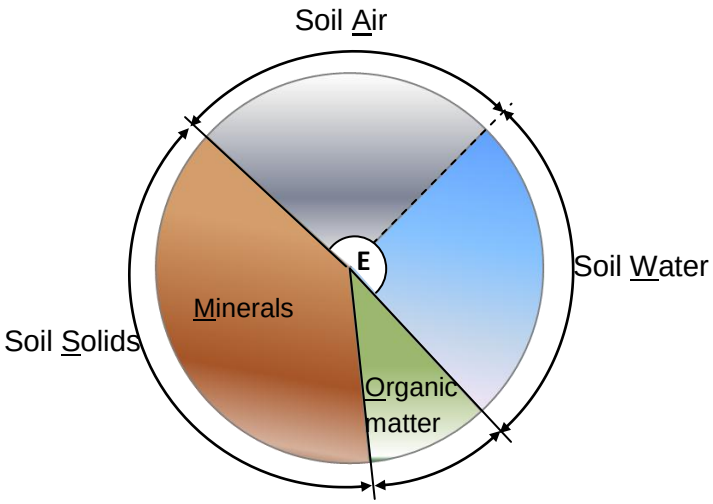


**Fig. 2** A 'snapshot' of the soil A-W-E-S-O-M-E system. The soil-water and soil-air phases share a weak boundary (denoted by a dotted line) and add up to total pore space (E) (redrawn from Moldrup et al., 2011)

The soil system is truly *awesome*, in the sense that it can potentially provide the essential infrastructure for a habitable environment, thereby making the soil an excellent abode for an extremely diverse array of soil organisms. The above-ground plant life also depends largely upon soil functional structure as extensively researched in agriculture. The entire terrestrial life, in short, is very much indebted to soil and its functions, although this has been largely ignored by the growing human population. During the last few decades, the intensified pressure on soil and its functions has given rise to a chain of environmental consequences including groundwater contamination, air pollution, climate shifts, global warming, etc. If not immediate steps are taken to control the excessive overburdening of the soil and its functions, before long the only habitable place in the universe that we know of, the Earth, will also be at risk. A thorough knowledge of soil functional architecture is a must if we are to find lasting solutions to the key environmental issues linked to soil. This thesis will mainly focus on one of the key components in soil functional architecture - the soil-air phase (except for a brief look also into the soil-liquid phase in PAPER IV), and will discuss the main processes and properties related to the functional soil-air phase.

### 1.3 Soil functional air-phase and key processes

The soil-air phase forms the 'lungs' of the soil-based living systems. A well-functioning air phase, therefore, is an essential component of a healthy soil system. While it plays a prominent role for the sustenance of plant life, it potentially also facilitates the movement of many gaseous contaminants into or out of soil, seriously affecting the environmental health. Discussed briefly below are the two key processes associated with the soil-air phase which, in perspective, have wider implications as discussed further in the supporting papers and also in this thesis.

#### (a) Soil aeration and plant life

A well-aerated root system is one of the fundamental prerequisites for successful plant growth on Earth-based (Spomer, 1974) as well as Space-based (NASA, 2002) environments. Since the plant roots (root cells) consume oxygen ($O_2$) and release carbon dioxide ($CO_2$) during respiration, the root zone -gas phase often tends to have depleted-$O_2$ and elevated-$CO_2$ concentrations compared to the atmosphere. Depleted $O_2$ levels potentially inhibit new root growth and may even lead to die off or decomposition of existing roots if $O_2$ falls below critical concentrations (Pokorny, 1979). The elevated $CO_2$ levels can also be toxic and detrimental to root growth (Whitcomb, 1979). The importance of soil aeration to sustain a stress-free rhizosphere, therefore, is twofold: the depleted soil-oxygen needs to be adequately replenished from the atmosphere, and the accumulated (toxic) soil-carbon dioxide needs to be rapidly removed from the root zone. An efficient gas exchange between the atmosphere and root cells thus becomes a crucial factor controlling the root functions.

#### (b) Greenhouse gases and gaseous phase contaminant transport

Subsurface migration and emission of greenhouse gases (i.e., methane, carbon dioxide, nitrous oxide) has raised high environmental concern during last few decades. Elevated atmospheric concentrations of greenhouse gases lead to many critical environmental problems including ozone layer depletion, regional climate shifts, and global warming (IPCC, 2007). Although the anthropogenic contribution to greenhouse gas emissions (e.g., landfills, constructed wetlands, etc) dominate following the industrial revolution, natural sources (e.g., peatlands, forests, etc.) are also responsible for a significant share of global emissions. Similarly, gaseous phase contaminants (e.g., volatile organic compounds (VOCs), agricultural fumigants, etc.) may potentially pose serious threats to local environmental health. The long-term solutions to these environmental issues will mostly depend on how accurately we can predict the subsurface movement of gases.

### 1.4 Gas Transport Parameters

Knowing the important role of the soil-gas phase functions for controlling key subsurface gas transport processes, the next step is to quantify them. A good knowledge of the main gas transport processes and the key controlling parameters is of great importance in this regard.

Transport, as opposed to equilibrium, essentially occurs when there is a *gradient* in properties. If gas transport in soil is exclusively governed by a *concentration gradient*, the gas movement occurs by diffusion and the *soil-gas diffusion coefficient*, $D_p$ ($m^3$ soil air $m^{-1}$ soil $s^{-1}$), is the most important parameter controlling the diffusive movement of gases. $D_p$ is generally scaled by $D_o$, the gas diffusion coefficient in free air, and often expressed as *gas diffusivity*, $D_p/D_o$. If, on the other hand, the gases are predominantly driven by a *pressure gradient*, the movement occurs by advection and the *air permeability*, $k_a$ ($\mu m^2$), becomes the key controlling parameter. Measurements of $D_p$ and $k_a$ are difficult due to the need for special equipment and become more complicated under *in-situ* conditions with poorly-defined initial and boundary conditions. Prediction from fast and easy-to-measure parameters (e.g., soil total or air-filled porosity; PAPERS I, II, and IV) or linking to other known soil conditions (e.g., soil moisture status or matric potential; PAPERS III and V) will be more convenient, provided the predictions can be made with adequate accuracy. Despite the existence of many predictive models for $D_p$ and $k_a$, modelling challenges still continue to exist.

*What makes the prediction of soil-gas transport parameters so challenging*?

Soils, and the conditions they are subject to, may differ markedly in many respects. Soil type/texture (from pure mineral to pure organic; PAPER I and PAPER II), structure (e.g., weakly-structured, well-structured or aggregated; PAPERS I, II, III, IV), geography and climate (e.g., from Denmark, U.S., Japan; PAPER III), geology/pedogenetics (e.g., sedimentary, glacial, alluvial, aeolian; PAPER III), land use (e.g., forest soils, urban soils, lysimeter soils; PAPER I and PAPER II), human-induced management (e.g., different tillage practices in agriculture; PAPER III, compaction in sanitary landfill caps; PAPER I and II) are just a few of them (not prioritised). These controlling factors may affect soil-gas transport parameters to varying extent. Short-term temporal variations of soil physical conditions (e.g., soil moisture status; PAPERS III and V) will also have a significant effect on gas transport parameters. For accurate predictions, a thorough understanding of how these different controlling factors affect the soil-gas transport parameters is an essential prerequisite. This is

obviously challenging, and the objectives of the present work are to discuss some of the aforementioned controlling factors and to account for them in gas transport modelling.

### 1.5 Objectives

**1.** To investigate the effects of two key controlling factors, *soil type* and *soil density*, on soil-gas transport parameters (with a greater emphasis on $D_p/D_o$) and to introduce a novel *density-corrected (D-C) modelling approach* for the predictions across soil types, spanning from sand to peat, and for widely ranging density levels.

**2.** To discuss the importance of the D-C modelling approach for two key diffusivity-based design applications:

i) Diffusivity-based characterisation of growth media as an important aspect in the design of optimal growth media for Earth- and Space-based applications.

ii) Design of the final cover layer for sanitary landfills where sufficient oxygen availability for methane oxidation is a key design criterion.

**3.** To characterise soil-gas phase tortuosity across different moisture conditions and to trace unique soil-gas phase fingerprints.

## 2 Gas diffusion modelling: Past, present, and future challenges

### Pioneers and landmarks in century-long soil-gas diffusion history

The word 'diffusion' comes from the Latin *diffundere,* meaning *pouring out*. With different meanings in different disciplines, diffusion is described in general physics as 'the intermingling of substances by the natural movement of their particles" (Oxford Dictionary). The definition is further narrowed down in soil science to describe a phenomenon in soil: "the process whereby matter is transported [in soil] under the gradient of chemical potential, activity or concentration" (Encyclopedia of Soil Science). Diffusion has been known for centuries as an important process of mass transfer in soil. An extensive experimental and modelling effort has been invested in diffusion studies with remarkable contributions from many noteworthies throughout history. This chapter is devoted to briefly revisiting an almost a century- and- a-decade long history of soil-gas diffusion modelling. The objective is to recall the pioneers and landmarks in soil-gas diffusion studies rather than a review of soil-gas diffusivity modelling. The chapter starts with a brief reflection on classical general diffusion and modelling without which the discussion becomes incomplete.

### Diffusion studies and modelling - General

Robert Brown
(1773-1858)

The first appearance of the diffusion concept, the irregular movement of small particles suspended in liquid, was made by **Robert Brown** (1773-1858), a Scottish scientist and botanist. In 1827, Brown observed the motion of granules, five to six micrometers in linear dimension, of pollens from a wildflower, and stated that "…*these motions were such as to satisfy me, after frequently repeated observation, that they arose neither from current in the fluid, nor from its gradual evaporation but belonged to the particle itself*". He first thought that there was something 'live' which drove granules, but later observed a similar motion in inclusions of quartz as well. Although he was not able to explain the phenomenon, this inherent motion of small particles is now called *Brownian motion* and the resulting movement along a concentration gradient, *Brownian diffusion*.

Thomas Graham
(1805- 1869)

Scientific studies on gas diffusion have initiated in the early eightieth century. **Thomas Graham** (1805-1869), a Glasgow-born chemist, is perhaps the pioneer of experimental studies of gas diffusion. Graham performed extensive studies on gas diffusion and published his results in 1829 and 1833, one of

them postulates what is referred to as Graham's Law: "*The diffusion or spontaneous intermixture of two gases is effected by an interchange in position of indefinitely minute volumes of the gases, which volumes are not of equal magnitude, being, in the case of each gas, inversely proportional to the square root of the density of that gas*." His extended diffusion studies to salts and liquids revealed that *diffusion in liquids is at least several thousand times slower than in gases*. Despite successful experimental work, Graham's studies fell short of mathematical explanation to diffusion phenomena.

Adolf Fick
(1829- 1901)

The most significant breakthrough in diffusion modelling came from the work of **Adolf Eugen Fick** (1829-1901), a German physiologist, who developed the mathematical framework to describe the phenomena in diffusion (he was then just 26 years old!). Inspired by the work of Graham, Fick studied diffusion of salt in water and became the first to introduce the term *diffusion coefficient, D,* the parameter this thesis has been almost entirely built upon. Fick's remarkable observations came under two fundamental laws. The Fick's first law of diffusion relates the diffusive flux to the concentration gradient as follows:

$$J = -D\frac{\partial C}{\partial x} \qquad [2.1]$$

where $J$ is the diffusive flux [$ML^{-2}\ T^{-1}$], $D$ is the diffusion coefficient [$L^2\ T^{-1}$], $C$ is the concentration [$ML^{-3}$], and $x$ is the spatial dimension [L] (the negative sign indicates the increasing diffusive flux under decreasing concentrations).

Fick's second law of diffusion couples the first law of diffusion to the continuity equation to describe the spatial-temporal relation of diffusion as follows:

$$\frac{\partial C}{\partial t} = D\frac{\partial^2 C}{\partial x^2} \qquad [2.2]$$

where $t$ is time [T].

Mathematical solutions to Fick's equations were introduced later by two prominent scientists, Jozef Stephan (1835-1893), an Austrian, and Franz Neumann (1798-1895), a German, introducing boundary conditions for solutions of the diffusion equations. A new chapter to the diffusion modelling was later added by **Albert Einstein** (1879-1955), a German, and **Marian Smoluchowski** (1872-1917), a Polish, whose independent and parallel work led to the well-known Einstein-Smoluchowski diffusion equation:

$$< x >= \sqrt{2Dt} \qquad [2.3]$$

where $< x >$ [L] represents the mean particle displacement.

**Diffusion studies and modelling - Soil physics**

**1900-1940**

E. Buckingham (1867-1940)

The gas diffusion modelling made its first breakthrough in soil science in 1904, when **Edgar Buckingham** (1867-1940), a U.S. soil physicist, performed his ground-breaking gas diffusion experiments. Employed at the United States Department of Agriculture (USDA) Bureau of Soils (BOS), Buckingham carried out aeration experiments and tested gas diffusion and convection in soils at differing moisture conditions and compaction levels. The main feature of his experiments was to treat multiple gases, carbon dioxide in particular, to collect gases from soil, and to analyse their composition. He calculated the gas diffusion coefficient, $D_p$, for four different soils and found a close relation between $D_p/D_o$ and soil air content, $\varepsilon$, as follows:

$$\frac{D_p}{D_o} = \varepsilon^2 \qquad [2.4]$$

This observation, according to Buckingham, was "*accidental, nevertheless remarkable*". Buckingham further concluded that the diffusion in soils is *not greatly dependent upon the soil texture and the structure*, but in the main on the [air-filled] porosity of soils. However, the Bulletin 25 in which he published his results was heavily criticised by F. H. King (1905) who hired Buckingham at BOS (but King left BOS a few years later). King charged Buckingham for the conclusions derived based on very limited laboratory measurements on a subject that is so complex and intricate that it cannot be solved by a "short and a direct cut". King further accused Buckingham of the "almost infinite injury done to soil science" by the premature conclusions "without a single field observation". Despite the criticism, Bulletin 25 remains the first and one of most remarkable treatises in soil-gas physics and his simple power-law model, Eq. [2.4], has proved an excellent ballpark estimate of gas diffusivity across widely different soil types. Buckingham further contributed to soil physics with the first water retention curve (Buckingham, 1907), but made no reappearance in soil-gas modelling.

No significant progress was achieved in soil-gas diffusion modelling during the next few decades, for apparently two reasons: Buckingham was far ahead of contemporary soil-gas physicists, and the conflict among the leading scientists, including Buckingham, delayed the progression. The next widely known gas diffusivity model appeared in 1940, when **H.L. Penman** (1909-1984), an English scientist, came up with a simple linear empirical equation for soil-gas diffusion as follows (Penman, 1940):

H.L. Penman
(1909-1984)

$$\frac{D_p}{D_o} = 0.66\varepsilon \qquad [2.5]$$

Penman studied gaseous diffusion through porous materials at Rothamsted Experimental Station from 1937, but he is better known for his widely used evaporation formulae. Despite wide applications, his formulae were also charged for "too empiricism". The fundamental problem with Penman's model is that it is not extendable to up to $\varepsilon = 1$, where it violates the requirement $D_p = D_o$. Worldwide recognition of his scientific work made a steady flow of local and overseas scientists to Rothamsted who contributed significantly to soil-gas diffusion modelling in the following years.

**1940-1980**

The 'hotspot' of soil-gas diffusion modelling seemed to have shifted from the West to the East during 1959-1961, when several landmark studies on predictive models appeared consecutively from Australia. Notably, a series of theoretically-based models emerged during this period. **T.J. Marshall** (1907-2008), an Australian soil physicist who also visited Penman at Rothamsted, combined the pore size distribution-based permeability equation and Darcy's law to develop a new model (Marshall, 1959):

T.J. Marshall
(1907-2008)

$$\frac{D_p}{D_o} = \varepsilon^{3/2} \qquad [2.6]$$

Eq. [2.6], as Marshall stated, replaced the constant 0.66 from the Penman model with $\varepsilon^{1/2}$. Eq. [2.6] has been successfully used as a platform model by other scientists to develop subsequent models, for example the WLR-Marshall model (Moldrup et al., 2000a), as discussed later. Marshall's contribution to soil-gas physics is only briefly highlighted, being obscured somewhat by his dedicated involvement in water transport in soils in his exceedingly long academic career (he made his last publication at the age of 98!).

**R.J. Millington** (1926-2007), another prominent Australian environmental scientist, suggested a similar theoretically-based power model, but with a slightly different power exponent. Millington followed the same derivation of diffusive flow as Marshall, but, according to Millington, Marshall had '*not recognized basic differences in wet and dry porous systems*'. The Millington (1959) model appears in the form of:

R.J. Millington
(1926-2007)

$$\frac{D_p}{D_o} = \varepsilon^{4/3} \qquad [2.7]$$

Millington went further ahead and developed a couple of more theoretically-based equations together with another Australian scientist, **J.P. Quirk** (1924-). The Millington and Quirk (1960) model was presented in the form of:

$$\frac{D_p}{D_o} = \frac{\varepsilon^2}{\Phi^{2/3}} \qquad [2.8]$$

J.P. Quirk
(1924 - )

and was followed by the Millington and Quirk (1961) model:

$$\frac{D_p}{D_o} = \frac{\varepsilon^{10/3}}{\Phi^2} \qquad [2.9]$$

Quite notably, Eq. [2.9] is almost universally accepted, highly recommended by environmental authorities (e.g., USEPA, 1996; Danish Environmental Protection Agency, 2002), and widely implemented in modern risk assessment tools (e.g., JAGG 1). Interestingly, the Millington and Quirk (MQ: 1961) study was entirely based on unsaturated water/air permeability and has not been validated for gas diffusivity against intact soils, although it has secured a firm position in soil-gas diffusion modelling. Despite the wide acceptance, the performance of the model was often found to be questionable due to significant under-prediction for wet soils. Up-scaling the model results from sample scale to, respectively, field, local, regional and global scales may lead to serious overall under-predictions and may potentially mask the true picture of critical environmental issues (e.g., methane emissions). A later study from Jin and Jury (1996) re-introduced Eq. [2.8] as a better model than Eq. [2.9], stating that Eq. [2.8] was mistakenly overlooked in the literature. Based on the results of the present study, however, we observe that Eq. [2.8] tends to markedly over-predict the measured data, but looks promising as an upper-limit model for risk assessment. We have frequently visited the MQ (1961) model throughout this study, often as a 'potential competitor' to the newly developed models.

Millington's multifaceted carrier made significant further contributions to the Australian society, including design of water supply and irrigation systems, and also the mapping of the Great Barrier Reef.

From the West, J.A. Currie, a successor to Penman at the Rothamsted Station, carried out a series of experiments on granular and aggregated soils (Currie, 1960a and b, 1961, and 1965). He is probably among the earliest to report the two-region behaviour in gas diffusivity in aggregated media, but did not make early attempts to describe this with a mathematical model. Later, Grable and Siemer (1968) from the U.S. showed that the typical gas diffusivity models, like MQ (1961), fail to describe gas diffusivity in aggregated media and they modelled the two regions independently using a power function for the inter-aggregate region and a linear (Penman-type) function for the intra-aggregate region.

D. E. Rolston
(1942- )

With increased interest in the measurement and modelling of soil-gas diffusivity, widely different laboratory methods emerged and were complicated by the use of different gas pairs (Marrero and Mason, 1972; Glinski and Stepniewski, 1985; Petersen et al., 1994), one- or multi-chamber apparatus (Currie, 1960a; Weller et al., 1974; Ball, 1981), and different calculation procedures. Field methods were even more complicated due to poorly-defined initial and boundary conditions. **Dennis E. Rolston** (1942- ), a U.S. soil physicist, made an excellent review of the different methods available, discussed the drawbacks of commonly used methods, and documented the standard method which is commonly accepted and used worldwide today. He also made a significant contribution to *in-situ* measurement methods widely used today.

**1980-2010**

Don Kirkham
(1908-1998)

Of particular interest among the models which appeared in the next few decades is the 'generalized' model presented by Troeh et al. (1982) in a study guided and co-worked by a prominent U.S. soil physicist, Don Kirkham (1908-1998). Kirkham is a pioneer in mathematical soil physics, probably the best-known soil physicist of the 20$^{th}$ century, and hence deserves a mention in any soil physics biography. Kirkham made several contributions to soil-gas

physics (e.g., Kirkham, 1946; Kirkham et al., 1958), though he is well-recognized for his work on water flow through agricultural soils.

The Troeh et al. (1982) model coupled the linear (Penman-type) and curvilinear (Buckingham-type) models to yield:

$$\frac{D_p}{D_o} = \left[\frac{\varepsilon - u}{1 - u}\right]^v \qquad [2.10]$$

The two model parameters, $u$ and $v$, have specific roles: $u$ ($0 \leq u < 1$) represents the incomplete passages of pore space (and therefore equivalent to the inactive pore space, $\varepsilon_{in}$, discussed in PAPER IV) that remain in the medium when diffusion ceases, and $v$ ($1 \leq v \leq 2$) defines the curvature of the model. However, the model seems to suffer from two drawbacks: First, with the given form, the model may become highly unrealistic within the parameter limits (e.g., $u$ = 0.99 at $\varepsilon$ = 0.99). Secondly, the usefulness of the model for predictions is questionable, as no obvious correlations have been observed between physical properties and model parameters $u$ and $v$ (Jin and Jury, 1996). The good fit observed by the authors is simply attributable to the flexibility of the model.


P. Moldrup
(1962 - )

Since the soil water was recognised as the 'number one controller' of gas diffusivity in soil (Sallam et al., 1984), many of the models in this period attempted to take the effect of water into account. **Per Moldrup** (1962- ), a Danish soil physicist, suggested several predictive models to account for water-induced effects on soil-gas diffusivity. Moldrup et al. (1996) used the Campbell soil-water characteristic (SWC) parameter, $b$, as the third parameter in the model, together with $\varepsilon$ and $\Phi$ for predictions. Moldrup et al. (1999) further combined the Campbell $b$-dependent model with the Buckingham (1904) expression to develop the so-called Buckingham-Burdine-Campbell (BBC) model.

The water-induced linear reduction (WLR)-Marshall model (Moldrup et al., 2000a) seems to be the most promising soil-gas diffusivity model among this series of models, and perhaps the best conceptually-based model of all. The WLR-Marshall model presumes that the Marshall model (Eq. [5]) holds true for dry media, and introduces a variable parameter to account for the water-induced effect as follows:

$$\frac{D_p}{D_o} = \varepsilon^{3/2}\left[\lambda(\theta)\right] \qquad [2.11]$$

where $\lambda$ ($\theta$) ($0 \le \lambda \le 1$) is the factor to account for water-induced effects. The two limiting values, $\lambda$ = 1 and $\lambda$ = 0, represent completely dry media ($\theta$ = 0) and completely wet media ($\theta = \theta_s$ or $\Phi$), respectively. Assuming a *linear reduction* with increasing water content, $\lambda$ can be expressed as:

$$\lambda(\theta) = 1 - \frac{\theta}{\Phi} \qquad [2.12]$$

Substituting in Eq. [2.11] yields:

$$\frac{D_p}{D_o} = \varepsilon^{3/2}(1 - \frac{\theta}{\Phi}) \qquad [2.13]$$

which simplifies to the widely known WLR-Marshall model as follows:

$$\frac{D_p}{D_o} = \varepsilon^{3/2}(\frac{\varepsilon}{\Phi}) \qquad [2.14]$$

Since the conceptual development of the model does not account for the properties inherent to undisturbed soils, for example soil heterogeneity, layering, soil density variations, etc., the model is preferably applicable to, and successfully tested and validated for, sieved and repacked soils. The model tends to slightly over-predict the undisturbed soils, and therefore may provide a 'safe estimate' for risk assessment. In fact, due to its simplicity (with no fitting parameters) and good performance, the WLR-Marshall model has replaced the MQ (1961) model in some risk assessment tools (e.g., the new JAGG model) while many still rely on the classical MQ (1961) model. Due to its wide acceptance, we often made a side-by-side comparison with the WLR- Marshall model when a new predictive model was evaluated.

Moldrup et al. (2000b) observed another very promising correlation (which we used in Chapter 3 for new model development) between macroporosity (defined as air-filled porosity at -100 cm suction, $\varepsilon_{100}$) and the corresponding gas diffusivity ($D_{p100}/D_o$) as follows:

$$\frac{D_{p,100}}{D_o} = 2\varepsilon_{100}^3 + 0.04\varepsilon_{100} \qquad [2.15]$$

Although not cited here, many models suggested thereafter (2000-2010) have also provided useful insights into soil-gas diffusion modelling.

**Beyond 2010 - Model challenges**

The incessant research endeavour throughout history has unquestionably brought a remarkable success to soil-gas diffusion modelling, along with the growing understanding on what controls soil-gas diffusivity. Almost a century and a decade after Buckingham, however, the key challenging

question still remains unanswered: *Is there a universal model for soil-gas diffusivity*? The question still seems to challenge soil-gas physicists, likely because there are many factors controlling gas diffusivity as yet unaccounted for or not well accounted for.

On briefly revisiting a few key models, Equations [2.7], [2.8], [2.9], and [2.14], and rewriting some in the form of interest, we get:

Millington (1959): $$\frac{D_p}{D_o} = \varepsilon^{4/3}(\frac{\varepsilon}{\Phi})^0$$

Millington-Quirk (1960): $$\frac{D_p}{D_o} = \varepsilon^{4/3}(\frac{\varepsilon}{\Phi})$$

Millington-Quirk (1961): $$\frac{D_p}{D_o} = \varepsilon^{4/3}(\frac{\varepsilon}{\Phi})^2$$

WLR-Marshall: $$\frac{D_p}{D_o} = \varepsilon^{3/2}(\frac{\varepsilon}{\Phi})$$

Note that all the equations follow the general form of:

$$\frac{D_p}{D_o} = \varepsilon^{X}(\frac{\varepsilon}{\Phi})^{Y}$$

In fact, we observed that many of the other predictive models could also be rewritten in the above form (see Table 2, PAPER II). The important term here is the ($\varepsilon/\Phi$), which was not recognised with any specific significance in most of the predictive models, except for the WLR-Marshall model, which introduced ($\varepsilon/\Phi$) as the 'water reduction factor'. Since the term $(\varepsilon/\Phi)^Y$ vanishes for dry media (i.e., $\varepsilon = \Phi$) irrespective of the magnitude of $Y$, ($\varepsilon/\Phi$) does account for water-induced effects. *Is it only water that it accounts for?*

In Chapter 3, we introduce another dimension of the ($\varepsilon/\Phi$) term to account for *density-induced effects* in gas diffusivity.

# 3 New density-corrected modelling approaches

## 3.1 Soil compaction/density

Soil compaction, by definition, is a process of *densification* whereby porosity and permeability are reduced, strength is increased and many changes are induced in the soil fabric (Soane and van Ouwerkerk, 1994). The densification of soil may result from long-term pedogenetic processes as well as from short-term anthropogenic activities. Consequently, soils with different compaction/density levels are found both in natural and engineered soil systems. Due to wide implications, we prefer to use the word 'density' in place of 'compaction' to express soil compactness. The change in density is accounted for solely by the change in soil total porosity, irrespective of the cause of the change.

The effects of soil type and soil density on soil gas diffusivity have been widely reported in many previous studies, right from the pioneering work of Buckingham (1904). Some of the concluding remarks from the selected studies are quoted below:

*We have shown that the speed of diffusion of air and carbonic acid through these soils was not greatly dependent upon texture and structure [compaction], but determined in the main by the [air filled] porosity of soils.* - Buckingham (1904)

*The relationship between soil gas diffusivity and air content did not in practice depend on soil density …* - Stepniewski (1981)

*No single curvilinear relationship can describe the change in $D/D_o$ with $\varepsilon$ especially where there are changes in both bulk density and water content, even in one soil.*

- Currie (1984)

*The gas diffusion coefficient in soils vs. air-filled porosity relationship was nearly the same irrespective of soil type, soil wetness, or soil bulk density.*

-Xu et al. (1992)

*At the same air filled porosity, the gas diffusion coefficient increased with bulk density [upon compaction] ….*

-Fujikawa and Miyasaki (2005)

*Soil compaction caused reduced water blockage effects on gas diffusion and a reduction of large-pore space, resulting in higher gas diffusivity.*

-Hamamoto et al. (2009)

The apparently inconsistent conclusions from the above studies imply a lack of understanding of the density effects on $D_p/D_o$ and modelling, which provided the main impetus for this study.

### 3.2 Soils, data and measurements

The modelling work discussed in this thesis and the supporting papers is largely based on literature data. The limited $D_p$ measurements presented in PAPER 1 and PAPER II, and all measurements presented in PAPER IV originate from the present study. The soil sampling, measurements, and calculation procedure for the selected literature data and for new data were based on standard and well-documented methods and hence will not be discussed in this thesis. We refer to Rolston and Moldrup (2002) and (2011) for details on the one-chamber gas diffusion apparatus, measurement procedure and calculations. For the two-chamber method and calculations, see Freijer (1994) and Eden (2011). Different laboratory methods for $D_p/D_o$ measurements have been discussed in Allaire et al. (2008), while the *in-situ* measurement methods of $D_p/D_o$ can be found in Tick et al. (2007).

We first selected literature $D_p$ measurements from different vadose zone profiles across Denmark for model development and validation. The sampling locations are shown in Fig. 3.1.

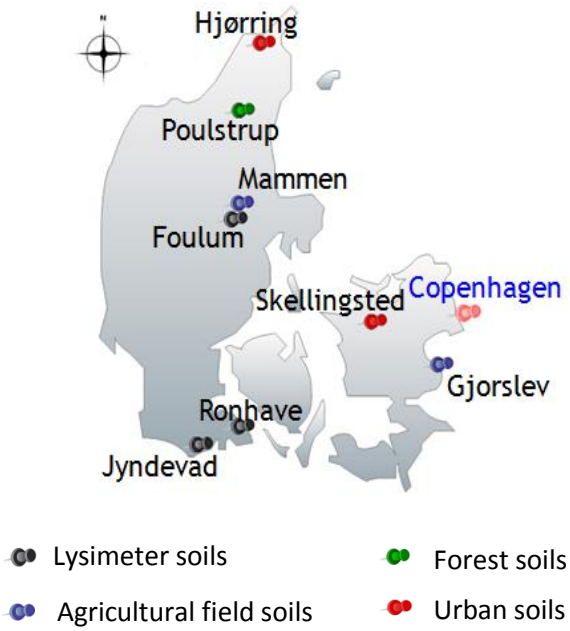


**Fig. 3.1** Sampling locations in Denmark representing different land uses. Data from Moldrup et al. (2000b), Kawamoto et al. (2006a, b), Kruse et al. (1996), Moldrup et al. (1996).

For the purpose of analysis, we first regrouped the Danish soil data according to soil type (based on total volume fraction of clay, silt and organic matter, CSO*vol*) and soil density (based on total porosity, Φ). Using CSO*vol* = 0.15 and Φ = 0.40 as the boundary values, we separated the soils into four groups, i.e. group A through D, while D* denoted a distinctive clay soil in group D as illustrated

in Fig. 3.2. The above two values were arbitrarily selected with an educated guess for the medium-dense and -textured soils, and each soil fell primarily into just one of the four groups with limited crossover. (Note that the two selected values for CSO*vol* and Φ were only used for preliminary classification and not used in subsequent modelling.)

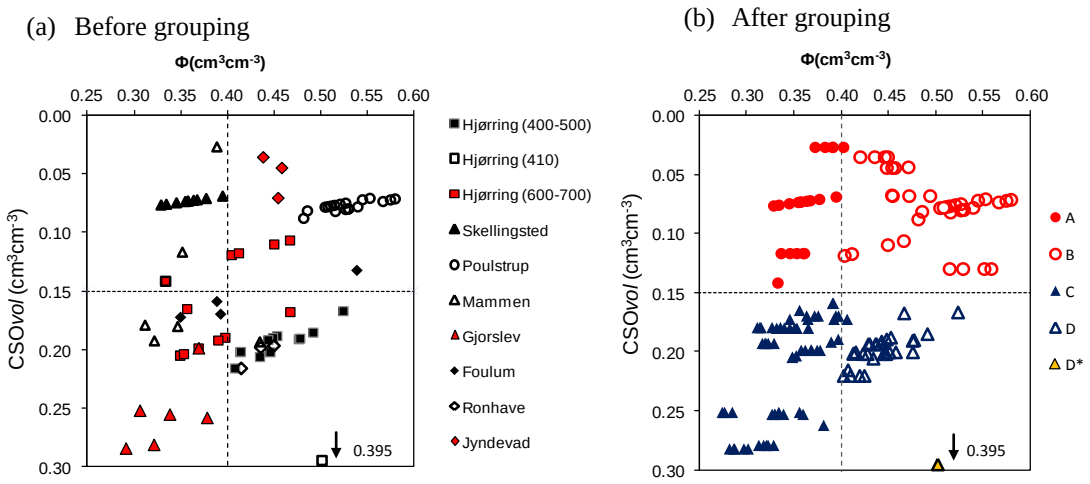


**Fig. 3.2** (a) The Danish soils, (a) before grouping and (b) after grouping, according to CSO*vol* (total volume fraction of clay, silt, and organic matter) and total porosity (Φ). Red and blue symbols represent low fine content (coarse-textured) and high fine content (fine-textured) soils, respectively, while open and closed symbols, respectively, represent less dense and highly dense soils. The yellow triangle represents a pure clay soil.

### 3.3 Soil type and density effects

*Which dominates in soil-gas diffusivity: soil type or soil density?*

Fig. 3.3 shows gas diffusivities for nine selected soils: two soils from each of A, B, C and D groups and the soil D*. Compared at a given air-filled porosity (Fig. 3.3a), soil density effects are particularly evident, and higher gas diffusivities could be observed for highly dense soils compared to the less dense ones, thus corroborating the observations of Fujikawa and Miyasaki (2005) and Hamamoto et al. (2009). Dense soils have relatively high solids contents and, therefore, at a given air-filled porosity they retain less water than the less dense soils. Recalling more pronounced effects of water-induced tortuosity than solid-induced tortuosity on soil gas phase processes, we observe enhanced gas diffusivity in high-density soils. Soil type effects, on the other hand, are not clearly evident in $D_p/D_o$ vs. $\varepsilon$ plots as also noticed by Buckingham (1904). The trends are similar for air permeability ($k_a$) but less stringent (not shown), likely being obscured by pronounced soil structure effects upon densification (note that $k_a$ occurs preferably through larger (macro) pores, whereas $D_p/D_o$ is essentially not pore size dependant) .

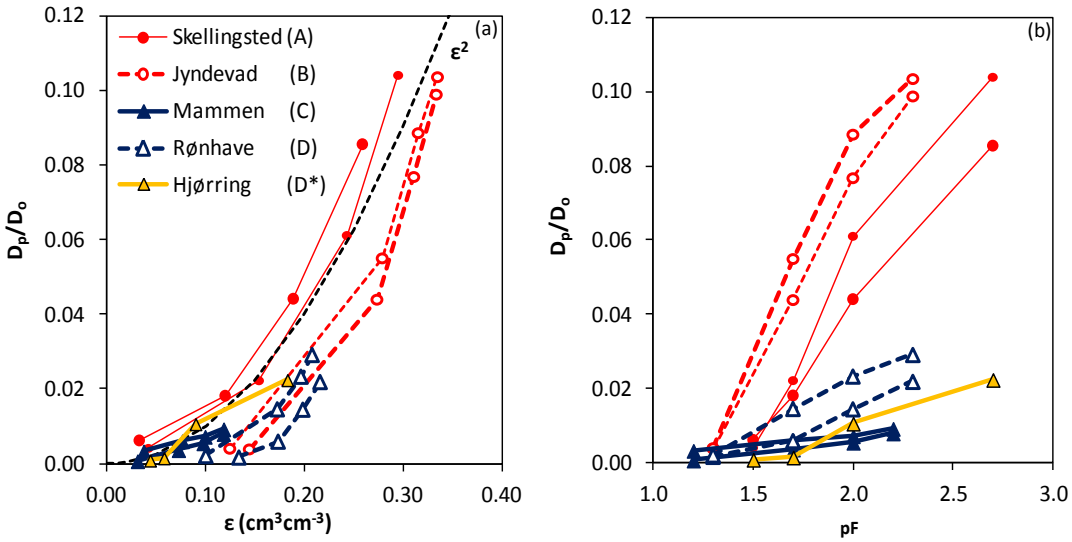


**Fig. 3.3** Soil-gas diffusivity, $D_p/D_o$, against (a) air-filled porosity, $\varepsilon$, and (b) matric potential (expressed by pF) for two soil pairs selected from each of the four selected groups, A, B, C, D, and also D*. The Buckingham model, Eq. [1], is also shown in (a) as a reference. pF = log |-$\Psi$, cm $H_2O$|.

*Do the results imply that, for example, a compacted cap layer in a sanitary landfill will cause increased methane emission?*

Certainly not, because a soil layer in natural, ambient soil conditions is more likely to stabilize at a certain *matric potential* than at a certain air-filled porosity. Taken at a given matric potential expressed by pF (= log |-$\psi$, cm$H_2O$|, after Schofield, 1935), the completely opposite trend for $D_p/D_o$ can be observed (Fig. 3.3b). Dense soils retain more water (and hence more water-induced tortuosity) and less air than the less dense soils, and exhibited lower gas diffusivity. Note the more pronounced effects of soil type in the $D_p/D_o$ vs. pF plots, since the water retention characteristics are soil type dependent.

Returning to the original question of *which one dominates in gas diffusivity*, this depends on what *basis the comparison is made*; if the comparison is based on $\varepsilon$, soil density effects are pronounced, and if the comparison is based on pF, soil type effects dominate.

### 3.4 Density-corrected models

We used the macroporosity-based relation, Eq. [2.15], as the reference model to develop the density-corrected modelling approach. The model showed very good performance at the reference pF (i.e., at pF 2), which the model was originally tested on, and yielded promising results at other pF values as well. A common feature, however, at all pF values was that the model tended to underestimate the highly dense soils and overestimate the less dense soils (see Fig. 3, PAPER 1). When the same data

are plotted against relative air-filled porosity ($\varepsilon/\Phi$), this density-induced fluctuation was diminished (Fig. 3.4).

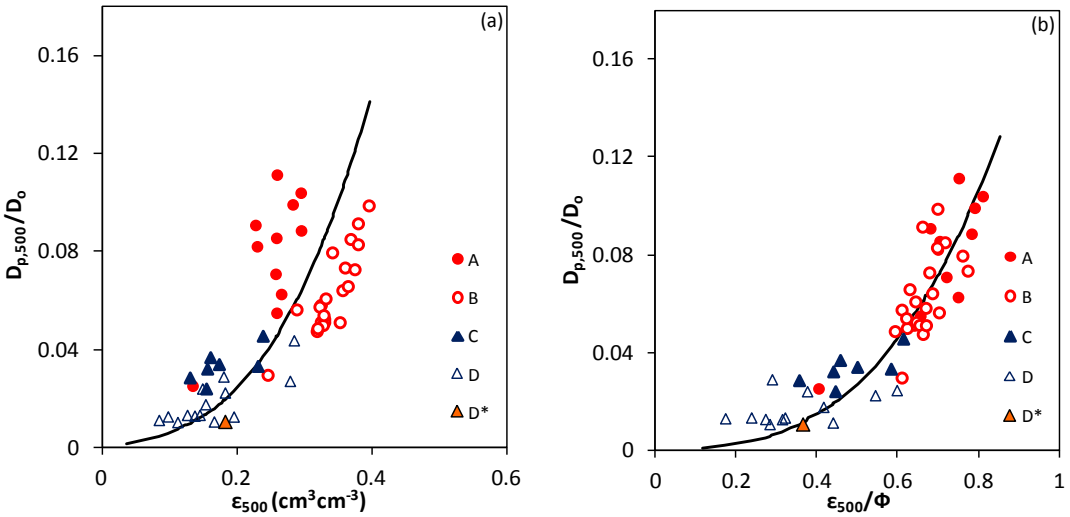


**Fig. 3.4** (a) Soil-gas diffusivity measured at -500 cm matric suction, $D_{p,500}/D_o$, against the corresponding air-filled porosity, $\varepsilon_{500}$. (b) The same $D_{p,500}/D_o$, data against relative air-filled porosity, $\varepsilon_{500}/\Phi$.

We noted that a new, analog density-corrected model could well describe the data:

$$\frac{D_p}{D_o} = 0.1\left[2\left(\frac{\varepsilon}{\Phi}\right)^3 + 0.04\left(\frac{\varepsilon}{\Phi}\right)\right] \qquad [3.1]$$

The analogous density-corrected air permeability model to predict reference-$k_a$ values takes the form of:

$$k_{a,100} = 70\left[2\left(\frac{\varepsilon_{100}}{\Phi}\right)^3 + 0.04\left(\frac{\varepsilon_{100}}{\Phi}\right)\right] \qquad [3.2]$$

The scaling factor of 0.1 in Eq. [3.1] resulted from fitting the model to all measured data. Note that combining Eq. [3.1] and [3.2] yields an important empirical relation between the two key gas transport parameters, $k_{a,\,100}$ = 700 $D_{p,100}/D_o$, (Fig. 3.5) as also observed by Kawamoto et al. (2006b) and Eden (2011).

The density-corrected $D_p/D_o$ model, in particular, performed very well when tested against the independent data and convincingly outperformed many widely used predictive models. A detailed statistical

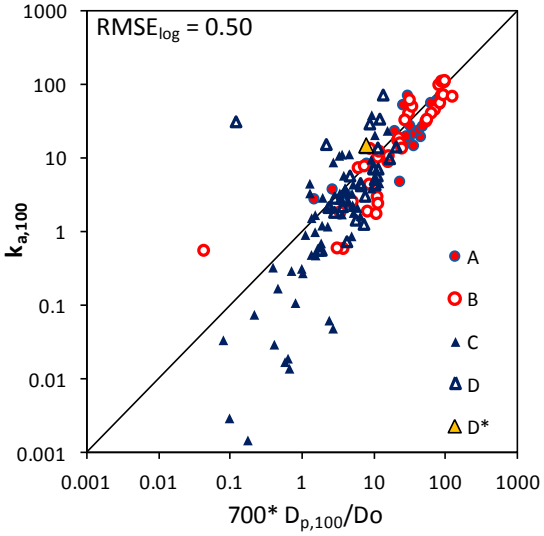


**Fig. 3.5** Scatterplot for measured $k_{a,100}$ against 700 *measured $D_p/D_o$

analysis comparing the model performances is presented in PAPER I.

### 3.5 D-C model limitations and the GDC model

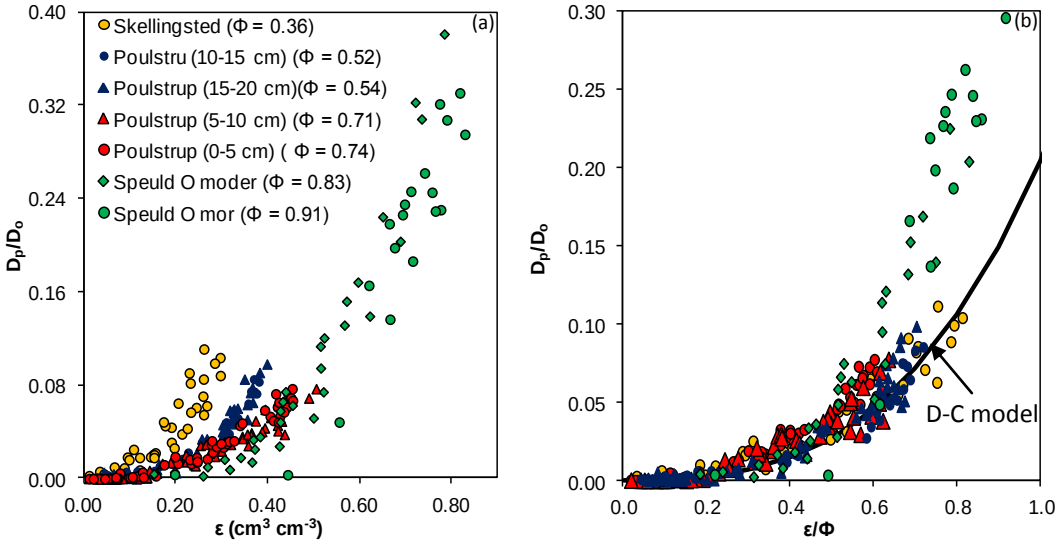


**Fig 3.6** Gas diffusivity for selected soils with varying Φ (0.52~0.91 $cm^3\,cm^{-3}$). The solid line in (b) is the D-C model, Eq. [3.1].

The D-C model is developed and validated for soils with Φ ranging from 0.27-0.54 $cm^3\,cm^{-3}$, which broadly covers the typical Φ-range for widely occurring soils. When tested against low-density soils with greater total porosities ($\Phi \approx 0.7$ $cm^3\,cm^{-3}$), we noticed the model tendency to slightly underpredict the data. Testing the model against the soils with very high total porosities, for example peat soils with $\Phi > 0.80$ $cm^3\,cm^{-3}$, resulted in serious underpredictions (Fig. 3.6). Therefore, the model required a modification to account for additional density effects resulting from high total porosities. A modified model scaling factor (presently a constant of 0.1) as a function of total porosity and/or organic matter gave no improvement, demanding a of the D-C model.

We returned to a more generalized version of the D-C model which can be written in the form of:

$$\frac{D_p}{D_o} = \left[ \alpha \left( \frac{\varepsilon}{\Phi} \right)^{\beta} + \lambda \left( \frac{\varepsilon}{\Phi} \right) \right] \qquad [3.3]$$

Setting $\lambda = 0$, as noticed for many previous gas diffusivity models, yielded a simple generalized model or the so-called Generalized Density Corrected (GDC) model as follows:

$$\frac{D_p}{D_o} = \alpha \left( \frac{\varepsilon}{\Phi} \right)^{\beta} \qquad [3.4]$$

By testing the GDC model against extensive literature measurements, we observed two important

$$\alpha = 0.5\Phi \qquad [3.5]$$

parameter links as below:

$$\beta = 3 \quad \text{or} \quad \beta = 2 + 1.38\Phi \qquad [3.6]$$

Eq. [3.5] was also suggested by Anderson et al. (2000). The model yielded comparable results for the data well described by the D-C model and, more importantly, the GDC model showed remarkable improvement over the D-C model for the very low density (i.e., high porosity) soils.

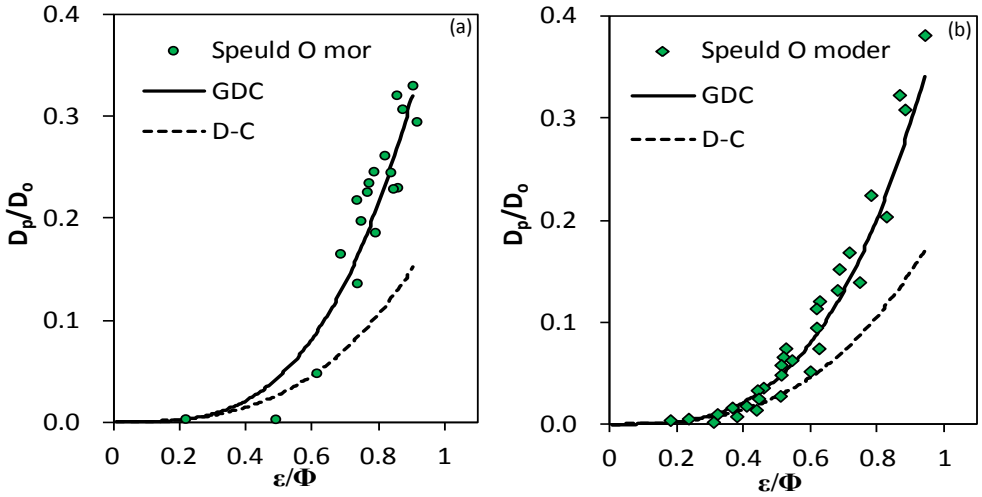


**Fig. 3.7** Results from the GDC model, predicted (from Eq. [3.4] and [3.5]) compared with the D-C model (Eq. [3.1]) for two peaty soils: (a) Speuld O mor (Φ = 0.91) and (b) Speuld O moder (Φ = 0.83). Data from Freijer (1994).

A detailed statistical analysis comparing the performance of the GDC model and the widely used predictive models is given in Table 3, PAPER II. The GDC model is simple and hence will be useful in practical engineering applications as discussed in detail in Chapter 4.

### 3.6 Gas percolation threshold, inactive pore space, and the IPDC model

The D-C and the GDC models were developed and successfully validated across a broad textural interval, and proved applicable for a wide range of density levels. A notable deviation between observed data and D-C/GDC model predictions appear for *coarse-textured* media, the gas phase functionality of which typically features a distinct *gas percolation threshold*, $\varepsilon_p$, which is the air-filled pore space below which gas diffusivity remains essentially zero, or indistinguishably small due to pronounced water blockage effects.

The soil samples for gas diffusivity measurements are commonly prepared by stepwise draining the saturated samples (from the bottom). Therefore, all the air-filled pore spaces thus created in the sample must be virtually linked to the atmosphere from the bottom, and are therefore *partially active* for gas diffusion. For the present modelling approach, however, we define the *inactive pore space*

*($\varepsilon_{in}$)* as the air-filled pore space which does not contribute to gas diffusion *across the entire sample*, although they may be partially active. Thus, below the percolation threshold ($\varepsilon < \varepsilon_p$), all the air-filled pores remain inactive since diffusion is yet to occur (Fig. 3.8), and $\varepsilon_{in}$ increases linearly (in a 1:1 line) with increasing $\varepsilon$ up to the percolation threshold ($\varepsilon_p$). With further increasing $\varepsilon$, $\varepsilon_{in}$ shows a decline which, for simplicity, is assumed here to follow a linear trend approaching $\varepsilon_{in} = 0$ at $\varepsilon = \Phi_1$ (Fig. 3.9). The behaviour can be mathematically expressed as follows (Moldrup et al., 2005):

$$\varepsilon_{in} = \varepsilon \qquad \varepsilon \le \varepsilon_p \qquad [3.7]$$

$$\varepsilon_{in} = \left[\frac{\Phi_1 - \varepsilon}{\Phi_1 - \varepsilon_p}\right]\varepsilon_p \qquad \varepsilon_p \le \varepsilon \le \Phi_1 \qquad [3.8]$$

where $\Phi_1$ ($cm^3\ cm^{-3}$) is the inter-aggregate porosity.

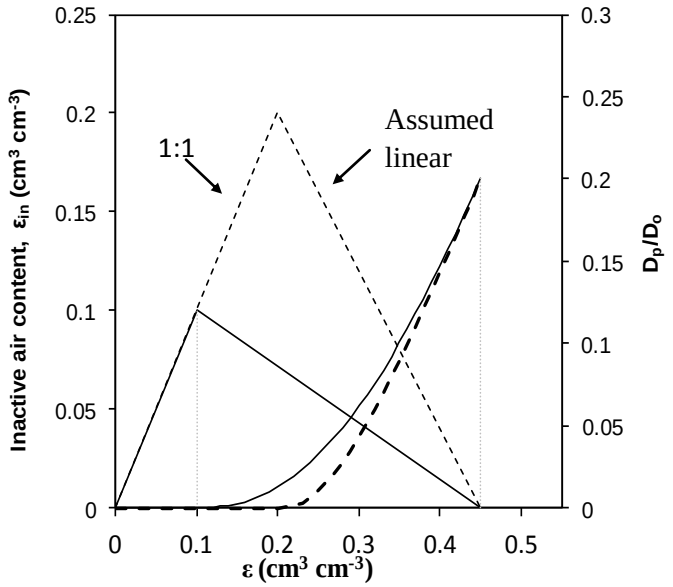


**Fig. 3.8** Illustration of the conceptual inactive pore space, Eq. [3.6] and Eq. [3.7], for two selected $\varepsilon_p$ values ($\varepsilon_p$ = 0.1 and 0.2).

By introducing the inactive pore space into the GDC model, we present the Inactive Pore and Density Corrected (IPDC) model as follows:

$$\frac{D_p}{D_o} = \alpha_1\left[\frac{\varepsilon - \varepsilon_{in}}{\Phi_1 - \varepsilon_{in}}\right]^{\beta_1} \qquad 0 < \varepsilon \le \Phi_1 \qquad [3.9]$$

$$\beta_1 = 2 + 2.75\alpha_1 \qquad [3.10]$$

$$\alpha_1 = \left.\frac{D_p}{D_o}\right|_{\varepsilon=\Phi_1} \qquad [3.11]$$

The IPDC model concept is illustrated in Fig. 3.8 for two assumed $\varepsilon_p$ values ($\varepsilon_p$ = 0.1 and 0.2). The corresponding gas diffusivity curves are also shown. To estimate $\varepsilon_{in}$ in Eq. [3.9], we used a promising linear correlation observed between $\varepsilon_{in}$ and mean particle size (See Fig. 6, PAPER IV).

### 3.7 Density-corrected models extended for bimodal media

In contrast to unimodal (structureless) soils characterised by a single pore region, bimodal (aggregated) soils typically show two distinct pore regions: Region 1 or soil outer (inter-aggregate) pore space, and Region 2 or soil inner (intra-aggregate) pore space. The D-C model (Eq. [3.1]) and GDC model (Eq. [3.3] through [3.5]) are only developed and validated for unimodal soils, but could be successfully extended to describe Region 1 in bimodal media by using inter-aggregate porosity ($\Phi_1$) in place of total porosity ($\Phi$). The IPDC model (Eq. [3.8]), on the other hand, is specifically recommended for Region 1 in bimodal media.

By assuming the implicit analogy of the two subregions (Region 1 and Region 2) and that the gas phase functions of two subregions are independent and additive, we extended the three D-C type models to the soil inner space (Region 2) as follows:

$$\left.\frac{D_p}{D_o}\right|_{\mathrm{Region2}} = \left.\frac{D_p}{D_o}\right|_{\varepsilon=\Phi_1} + \alpha_2\left(\frac{\varepsilon-\Phi_1}{\Phi-\Phi_1}\right)^{\beta_2} \qquad [3.12]$$

where the second term in Eq. [3.11] represents gas diffusivity in Region 2. The two Region 2 parameters, $\alpha_2$ and $\beta_2$, take different forms in D-C, GDC, and IPDC models (Table 3.1).

**Table 3.1** The Region 2 model parameters, $\alpha_2$ and $\beta_2$, in D-C, GDC, and IPDC models.

| Model | $\alpha_2$ | $\beta_2$ |
|---|---|---|
| D-C | $(\Phi-\Phi_1)^2$ | 2 |
| GDC | $0.5(\Phi-\Phi_1)$ | 1 |
| IPDC | fitted | 1 |

The predictions of the three models against three size fractions of Nishi-Tokyo Andisols (pasture) are presented in Fig. 3.9.

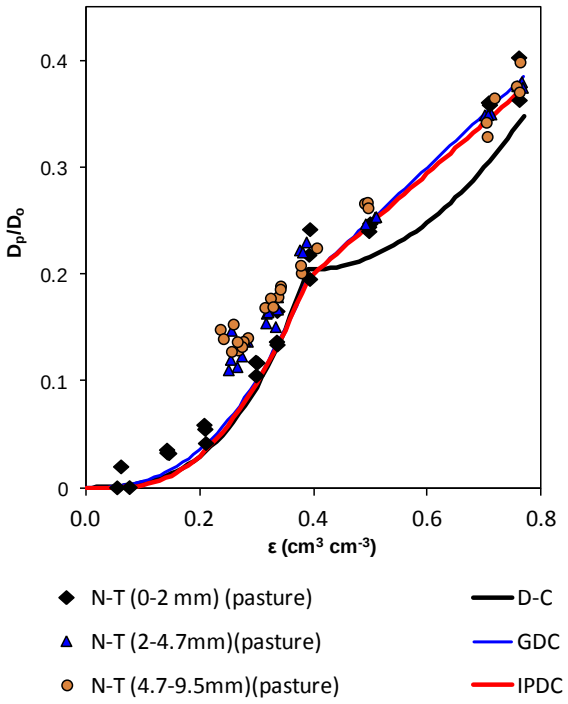


**Fig. 3.9** Predictions from the three density-corrected models, the two-region D-C and GDC models and the IPDC model, against Nishi-Tokyo (N-T) aggregated volcanic ash soils

# 4 Diffusivity-based analyses - Applications

## 4.1 Design of optimum plant growth media for space-based applications

The Earth we live on is self-sufficient; we do not bring, at least for now, anything in from outer space for our survival. A self-sufficient life support system must essentially have three basic loops closed: *food, water, and air*. Natural living systems with all the three loops simultaneously closed are rare in the universe. This is perhaps why life is so sparse in the universe, and tracing extra-terrestrial life in space has become a never-ending struggle. Our planet, the Earth, has been sustaining life for billions of years even under challenging conditions in its history, while our sister planet, Mars, presumably with more favourable conditions for life than Earth long before the Earth was inhabited (Forget et al., 2008) now "apparently" is a dead world (we await for the Curiosity to confirm this). The self-sufficiency is of equal importance also for engineered life support systems, for example International Space Stations (ISS) or an envisioned Martian/lunar human outpost which is envisioned to sustain a future human colony to facilitate interplanetary space missions.

*Why do we consider plants in space?*

In order to keep the water, air, and food loops closed in a human-based living system, a key element with exact complementary functions to those of human beings is highly beneficial, and plants can play a model role in this regard (Fig. 4.1). They have convincingly demonstrated their potential to supply clean air, drinkable water, and most food to maintain a habitable environment (Steinberg et al., 1997).

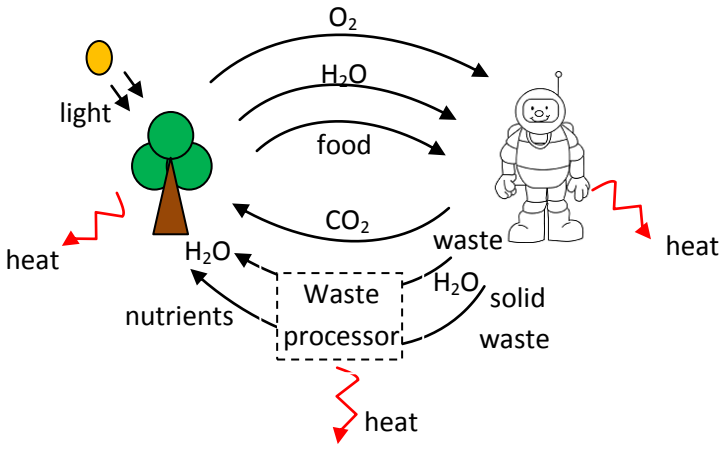


**Fig. 4.1** Human-plant complements in a closed life support system.

NASA's renewed strategic plan in year 2000 for an Advanced Life Support System (ALS) envisaged fully closed water and air loops with an optimized food loop based on the growth of crops within the ISS (NASA, 2002) (Fig. 4.2a). The same concept would also benefit an envisioned lunar or Martian base (Fig. 4.2b). Appropriate selection of growth medium is an essential prerequisite

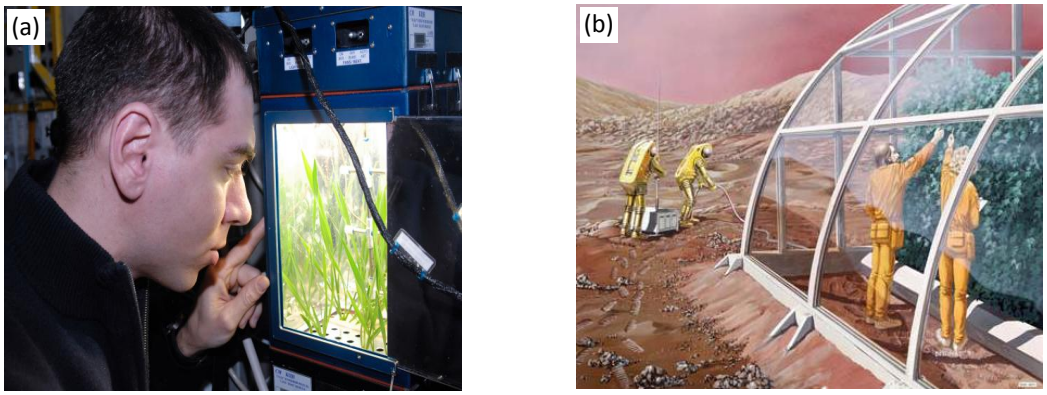


**Fig. 4.2** (a) An astronaut looking at a plant module in Russian Mir ISS. (b) An artistic view of the envisioned Mars-based greenhouse (image courtesy: NASA)

Plants, however, face many challenges in space-based environments: reduced gravity, controlled volumes, heavy vibrations at launch, to name a few. Despite the difficulties, a wide variety of plants has been tested in different growth media mainly in mixed-phase systems (e.g., hydroponics, aeroponics) and, to a lesser extent, also in separate-phase systems (i.e., solid substrates). Hydroponic culture is traditionally used in controlled environments due to high plant yields and the consistently high level of control of water, nutrients and aeration conditions that are barely achievable with solid substrates. However, microgravity-induced phase separation in mixed-phase systems is a key issue in space. In addition, the precision control of nutrients and solution chemistry (e.g., pH) is essential, which requires high-tech equipment and dedicated crew time. Although many promising techniques to control these problems have been suggested, no mixed system has yet emerged as a serious candidate for spaceflights (Steinberg et al., 2002). Separate-phase systems with porous substrates can resolve most of these problems, but need to be properly characterised to be optimised as plant growth media. Although use of native lunar or Martian regolith as growth media will be the main concern for a Lunar or Martian-based system, many terrestrial and engineered growth media have also been tested as promising candidates.

Optimal control of air (oxygen), water and nutrients at the root zone is the key for growth media design in both Earth-based and space-based environments, but is more challenging in space than on Earth. Moreover, oxygen and water/nutrient requirements are critical and complementary and are

more challenging in container-grown plants than in field-grown plants due to the physical boundaries to air and water movement.

*Critical Windows of Diffusivity (CWD)*

In order to evaluate the interplay between oxygen and nutrient diffusivities at plant critical conditions, we examined the 'critical window of diffusivity (CWD)' for oxygen and nutrients for four selected growth media.

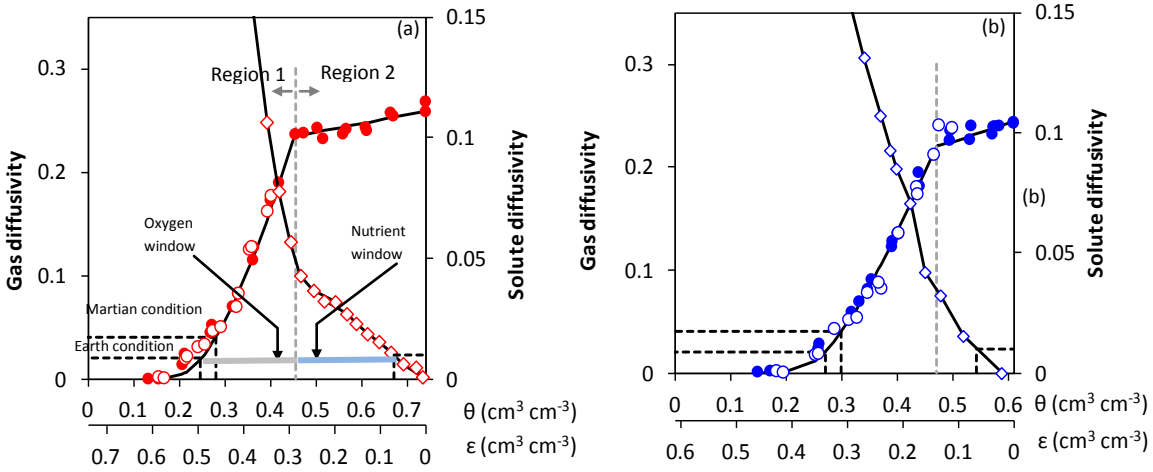


**Fig. 4.3** Gas diffusivity ($D_p(\varepsilon)/D_o$) and solute diffusivity ($D_s(\theta)/D_l$) for two prospective plant growth media for Earth and space: (a) NASA-Zeoponic, and (b) Profile. The suggested windows of diffusivity for Earth condition are also shown in (a).

Fig. 4.3 demonstrates the suggested CWD concept using two promising plant growth media: (a) Zeoponic, a NASA-made ziolite-based substrate, and (b) Profile, a stabilised baked ceramic aggregate. The measured $D_p/D_o$ and the predictions from the IPDC model are shown on the left Y-axis and solute diffusivity ($D_s/D_l$) (estimated in analog to dielectric permittivity) is shown on the right Y-axis. The critical condition with regard to aeration occurs soon after the irrigation as the water gradually occupies the outer pore space and $D_p/D_o$ falls below the threshold (minimum) value ($D_p/D_o$= 0.02). Conversely, the critical condition with regard to nutrient supply may occur just before irrigation, if the water in soil inner space falls below the critical $D_s/D_l$ (set here at $D_s/D_l$ = 0.01). We used a two-fold factor for $D_p/D_o$ (i.e., $D_p/D_o$ = 0.04) for Martian conditions (0.37-*g*) to account for the likely increase in $D_p$ at reduced gravity in a capillary-dominated water redistribution regime. We used the width of the critical window (see Fig. 4.3) as a useful index for diffusivity-based media characterisation (PAPER IV).

### 4.2 Design of final cover layer in engineered landfills

Landfills constitute one of the largest sources of global emissions of methane ($CH_4$), a powerful greenhouse gas with a high global warming potential. Nearly 10% of the global methane emissions from human-related sources originate from landfills and open dumps (IPCC, 1996). Well-maintained sanitary landfills are often equipped with gas extraction systems in which gases are burnt in flares or used as secondary energy sources. However, the emissions from most of the old landfills are still conventionally controlled by containing landfill gases using a highly compacted capping layer on top of waste layers (Fig. 4.1).

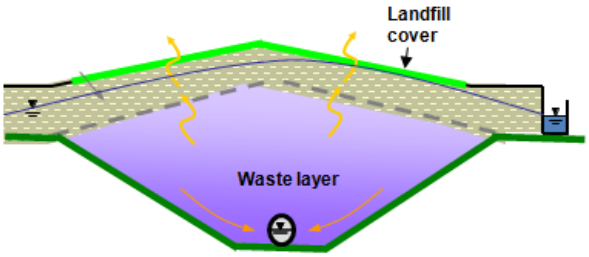


**Fig. 4.4** A typical arrangement of a landfill with a cover layer.

Although a highly-compacted cap layer can potentially restrict vertical gas movement, lateral movement of $CH_4$ and emissions off-site are uncontrollable, and have caused many fatalities in nearby households (Poulsen et al., 2001). Knowing that $CH_4$ *oxidation* (i.e., converting $CH_4$ to carbon dioxide and water in the presence of oxygen) accounts for 80% of natural global methane depletion (Kightley et al., 1995), a sufficiently aerated cover layer may facilitate $CH_4$ oxidation and thereby reduce atmospheric emissions. Only few studies have discussed oxidation in compacted soil cover layers based on gas transport parameters (e.g., Hamamoto et al., 2011; Wickramarachchi et al., 2011). The GDC model, specifically developed to account for compaction/density effects, may serve as a useful tool in the design of a sufficiently aerated compacted cover layer for a sanitary landfill.

We considered a landfill cover layer stabilised under natural, ambient conditions (suggested to occur at pF 2; PAPER II). The loss of total pore space ($\Delta\Phi$) upon compaction can be written as:

$$\Delta\Phi = \Phi^* - \Phi = -\frac{1}{\rho_s}(\rho_b^* - \rho_b) \qquad [4.1]$$

where $\Phi^*$ and $\Phi$ are total porosities at reference bulk density ($\rho_b^*$) and new bulk density ($\rho_b$), respectively, and $\rho_s$ is the particle density of soil. Assuming that the macropores (> 30 μm) are predominantly lost upon compaction, we get:

$$\frac{\varepsilon}{\Phi} = \frac{\varepsilon^* - \Delta\Phi}{\Phi^* - \Delta\Phi} \qquad [4.2]$$

where $\varepsilon^*$ and $\varepsilon$ are air-filled porosities at reference and new compaction conditions, respectively. By combining Eq. [4.1] and Eq. [4.2] with the GDC model, Eq. [3.3] through [3.5], we examined the $D_p/D_o$ variation with increasing bulk densities.

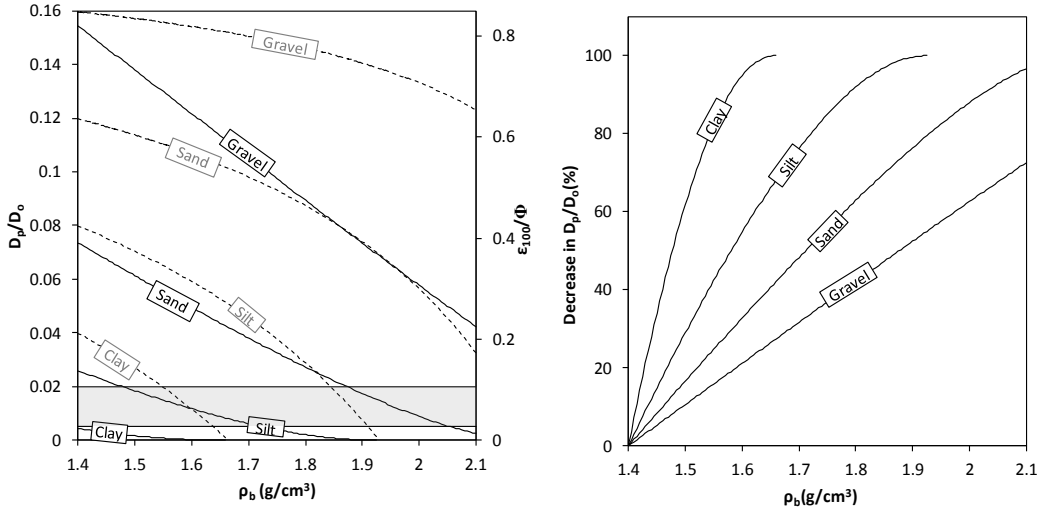


**Fig. 4.5** (a) GDC predictions for $D_p/D_o$ as a function of bulk density for different soil textures. The critical values for aeration in sandy ($D_p/D_o$ = 0.02) and clayey ($D_p/D_o$ = 0.005) soils are also shown. (b) The percent decrease in soil $D_p/D_o$ from the reference bulk density ($\rho_b$ = 1.4 gcm$^{-3}$).

Fig. 4.5 shows $D_p/D_o$ variation with dry bulk density ($\rho_b$) ranging from 1.4 g cm$^{-3}$ (loosely compacted) to 2.1 g cm$^{-3}$ (highly compacted). The shaded area demarcated by upper ($D_p/D_o$ = 0.02, the critical condition for aeration in sandy soils) and lower ($D_p/D_o$ = 0.005, the critical condition for aeration in clayey soils) lines broadly defines the critical diffusivity zone for adequate aeration. Note that gravelly soils may facilitate oxidation for the entire range of bulk densities considered, while sandy soils may fail to provide adequate aeration above 1.9 g cm$^{-3}$. Clayey soils, on the other hand, show complete loss of gas diffusivity above 1.6 g cm$^{-3}$ (Fig. 4.5b). Wickramarachchi et al. (2011) adopted the same concept to discuss the gas movement in a landfill in Saitama Prefecture in Japan. Thus, the GDC-based analysis provides a useful approach for selecting appropriate cover material for sanitary landfills.

# 5 Gas phase tortuosity analysis

## 5.1 Variable pore connectivity model

The classical approach for predicting gas diffusivity is based on air-filled porosity, as discussed in detail in Chapter 3. Acknowledging the fact that a typical soil under ambient conditions will stabilise at a certain matric potential (rather than at a certain air-filled porosity), a pF-based modelling approach will be of greater practical importance for initiating regulative measures for climate gas emissions (based on average model predictions) as well as for risk mitigation for gas phase contaminant transport (based on upper-limit model predictions).

The natural soil pore systems are inherently complicated and may differ considerably for different soil textures and structures. Since subsurface transport processes are directly linked to the functional pore network system, a thorough characterisation of the soil pore network is a key prerequisite for better understanding and prediction of the subsurface processes. A direct and most promising approach for comprehensive pore characterisation is to physically *visualise* the soil pore structure by means of modern visualisation techniques, for example X-ray CT scanning. Alternatively, indirect characterisation approaches can also provide valuable insights into the pore systems. The Buckingham pore connectivity factor, $X$ (Eq. [4.1]), and its variations with soil moisture status (e.g., matric potential or pF) is one such useful approach for diffusivity-based pore characterisation.

$$X = \frac{\log(D_p / D_o)}{\log(\varepsilon)} \qquad [5.1]$$

$X$ is derivable from any gas diffusivity model, and models suggesting constant $X$ values (e.g., $X$ = 2 (Buckingham, 1904), $X$ = 1.5 (Marshall, 1959), and $X$ = 1.33 (Millington, 1959)) and variable $X$ values (e.g., MQ, 1960 and 1961; WLR-Marshall; GDC) are available. Linking $X$ to pF, however, requires a complex combination of other models and parameters, as discussed in the *four-step approach* in PAPER III. The expressions directly linking $X$ to pF (e.g., Resurreccion et al., 2008), will be more convenient for straightforward predictions.

We hypothesised a variable pore connectivity factor, $X$, as a non-linear function of pF as follows:

$$X = X^* \left[ \frac{1 + \frac{1}{pF}}{1 + \frac{1}{pF^*}} \right]^A \qquad [5.2]$$

where $X^*$ is the reference-pore connectivity factor at the reference pF value, $pF^*$, and $A$ is the model shape factor to account for non-linearity. A preliminary analysis based on extensive soil data revealed that $X^* = 2$ at $pF^* = 3.5$ is broadly valid for wide range of soil types. The model application is specifically limited to a pF range of between 1 and 3.5, which is the likely pF range a soil will be subjected to under varying field moisture conditions.

The *X*-pF model, when tested against a wide range of soil data, exhibited a dual role of both *generalising* and *differentiating* soils as discussed in detail below.

### 5.2. Generalising soils for average and upper-limit predictions

The model played a prominent role in generalising soils across widely ranging soil types, giving promising $D_p/D_o$ predictions and comparable results to the widely-used predictive models. We observed that Eq. [4.3] with $X^* = 2$ and $A = 0.5$ is promising for general predictions of $D_p/D_o$ across a wide range of soil types, while $X^* = 1.7$ and $A = 0$ is a useful model for upper-limit predictions for risk assessment purposes. Figure 5.1 shows the scatterplot for Danish soil data with the predictions from the *X*-pF model for average (Fig. 5a) and upper-limit (Fig. 5b) model predictions (see PAPER III for further model tests).

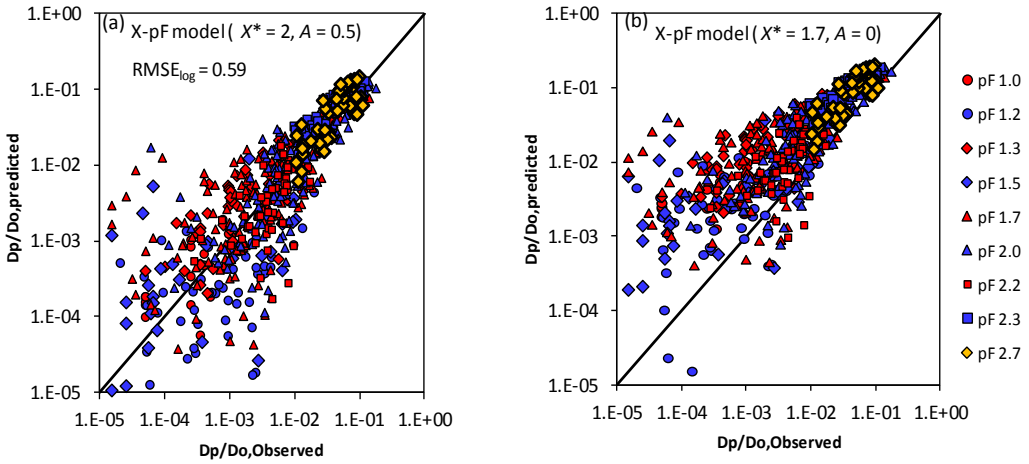


**Fig. 5.1** The performance of two *X*-pF models; (a) the Average-prediction model ($X^* = 2$, $A = 0.5$), and (b) the upper-limit model ($X^* = 1.7$, $A = 0$).

The new *X*-pF model's ability to make general (average or upper-limit) predictions distinguishes it from the previous *X*-pF models, for example the model from Resurreccion et al. (2008), which was only intended for soil architectural fingerprinting. While the present model is capable of making general predictions across soil types, it can also play an important role also for soil architectural fingerprinting as discussed below.

### 5.3 Differentiating soils for architectural fingerprinting

The *X*-pF model played a promising role in differentiating soils when the model was tested against widely contrasting soils, including differently-managed agricultural field soils (Fig. 5.2a) and soils with markedly different geographical origins (Fig. 5.2b).

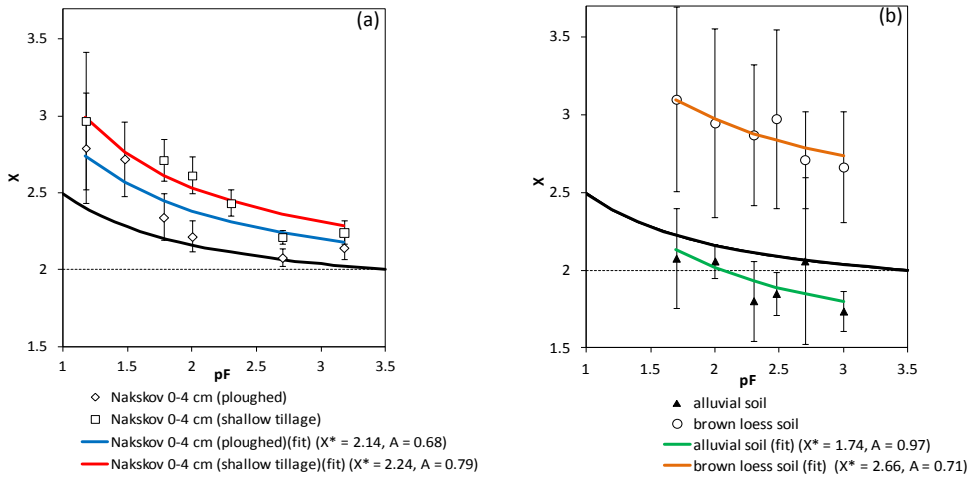


**Fig. 5.2** Buckingham-based tortuosity factor, *X*, against pF for selected soils from (a) differently-managed agricultural fields, and (b) soils from markedly different geographical origins.

Note that the observed unique structure fingerprints are broadly attributable to many time-dependent, structure-forming factors. For example, the Nakskov soil with deep ploughing (with a higher de-structuring potential) showed less tortuosity compared to the shallow-tilled soil taken at the same depth (Fig. 4.3a). The alluvial soil, with less organic matter and smaller fine fraction (hence less structure-forming potential), is expected to exhibit lower tortuosity than the brown loess soil. The contrasting observation of remarkably high tortuosity for alluvial soil is directly ascribable to its aeolian origin. Thus, the *X*-pF model approach is a useful tool to fingerprint unique soil architecture.

The extension of the pore connectivity analysis to fingerprinting aggregate soil inner space is also briefly discussed in PAPER III, based on a simple linear approach. A different non-linear approach is presented in PAPER V, based on an inner-space tortuosity factor, *X'*, to exclusively characterise the soil inner space. The complexity of soil inner-space tortuosity makes gas-diffusivity-based characterisation more challenging, and hence warrants further studies.

# 6 Conclusions

The soil-air phase is an essential component of soil architecture. The key processes and properties linked to the functional soil-air phase are crucial for sustaining life and also for controlling long-term environmental and climate health.

This study mainly focused on predicting two key transport parameters associated with the soil gaseous phase: gas diffusivity ($D_p/D_o$) and air permeability ($k_a$), with a greater emphasis on the former.

Based on a novel density-corrected approach, two Density-Corrected (*D-C*) models were presented for predicting gas diffusivity and air permeability across widely different density levels. The D-C gas diffusivity model was extended to a Generalized Density Corrected (*GDC*) model with expanded predictions for a broader textural interval. An Inactive Pore Density Corrected (*IPDC*) model was introduced for the predictions of gas diffusivity in aggregated porous media showing a distinct gas percolation threshold. An empirical linear relationship was suggested to estimate the percolation threshold from the mean particle diameter. Some important practical applications of the models on diffusivity-controlled design aspects were also discussed. A variable pore connectivity model was introduced to characterise soil-gas phase pore connectivity. The model played the dual role of generalising soils across widely contrasting soil types and differentiating soils for unique soil architecture fingerprinting.

# 7 References


Allaire,S.E., J.A. Lafond, A.R. Cabral, and S.F. Lange. 2008. Measurement of gas diffusion through soil: Comparison of laboratory methods. J. Environ. Monit. 10: 1326-1336.

Anderson A.N., J.W. Crawford, and A.B. McBratney. 2000. On diffusion in fractal soil structures. Soil Sci. Soc. Am. J. 64:19–24.

Ball, B.C. 1981. Modeling of soil pores as tubes using gas permeabilities, gas diffusivities, and water release. J. Soil Sci. 32:465–481.

Buckingham, E. 1904. Contributions to our knowledge of the aeration of soils. Bur. Soil Bull. 25. 4 U.S. Gov. Print. Office, Washington, DC.

Buckingham, E. 1907. Studies on the movement of soil moisture. USDA Bur. Soil Bull. 38. U.S. Gov. Print. Office, Washington, DC.

Currie, J.A. 1960a. Gaseous diffusion in porous media: Part 1. A non steady state method. Br. J. Appl. Phys. 11:314–317.

Currie, J.A. 1960b. Gaseous diff usion in porous media: Part 2. Dry granular materials. Br. J. Appl. Phys. 11:318–324.

Currie, J.A. 1961. Gaseous diffusion in porous media: 3. Wet granular materials. Br. J. Appl. Phys. 12:275–281.

Currie, J.A. 1965. Diffusion within soil microstructure: A structural parameter for soils. J. Soil Sci. 16:279–289

Currie, J.A. 1984. Gas diffusion through soil crumbs: The effects of compaction and wetting. J. Soil Sci. 35:1–10.

Danish Environmental Protection Agency. 2002. Guidelines on remediation of contaminated sites. Environ. Guidelines 7. Danish Ministry of the Environ., Copenhagen.

Eden, M. 2011. Gas-phase transport and structure parameters for differently managed soils. PhD. dissertation, Dept. of Agroecology Science and Technology, Aarhus University, Denmark.

Forget, F., F. Costard., and P. Lognonne. 2008. Plant Mars, Story of another world. Berlin (Alemania). Springer-Praxis.

Freijer, J.I. 1994. Calibration of jointed tube model for the gas diffusion coefficient in soils. Soil Sci. Soc. Am. J. 58:1067–1076.

Fujikawa, T., and T. Miyazaki. 2005. Effects of bulk density and soil type on the gas diffusion coefficient in repacked and undisturbed soils. Soil Sci. 170:892–901.

Glinski J., and W. Stepnewski. 1985. Soil aeration and its role for plants. CRC Press, Boca Raton, FL.

Grable, A.R., and E.G. Siemer. 1968. Eff ects of bulk density, aggregate size, and soil-water suction on oxygen diff usion, redox potentials, and elongation of corn roots. Soil Sci. Soc. Am. Proc. 32:180–187.

Hamamoto, S., P. Moldrup, K. Kawamoto, and T. Komatsu. 2009. Effect of particle size and soil compaction on gas transport parameters in variably saturated, sandy soils. Vadose Zone J. 8:1–10.

Hamamoto S., P. Moldrup, K. Kawamoto, P.N. Wickramarachchi, M. Nagamori, and T. Komatsu. 2011. Effect of extreme compaction on gas transport parameters and estimated climate gas exchange for landfill final cover soil, ASCE, J. Geotech. Geoenviron. Eng. 137, pp. 653-662.

Intergovernmental Panel on Climate Change (IPCC), 1996. Report of the Twelfth Season of the Intergovernmental Panel on Climate Change, Mexico City, 11–13 September 1996.

Intergovernmental Panel on Climate Change (IPCC). 2007. Observations: Surface and atmospheric climate change. In Climate change 2007: The physical science basis. Cambridge Univ. Press, Cambridge, UK.

Jin, Y., and W.A. Jury. 1996. Characterizing the dependence of gas diffusion coefficient on soil properties. Soil Sci. Soc. Am. J. 60:66–71.

Kawamoto, K., P. Moldrup, P. Schjønning, B.V. Iversen, D.E. Rolston, and T. Komatsu. 2006b. Gas transport parameters in the vadose zone: Gas diffusivity in field and lysimeter soil profiles. Vadose Zone J. 5:1194–1204.

Kawamoto, K., P. Moldrup, P. Schjønning, B.V. Iversen, T. Komatsu, and D.E. Rolston. 2006a. Gas transport parameters in the vadose zone: Development and tests of power-law models for air permeability. Vadose Zone J. 5:1205–1215.

Kightley D., D.B. Nedwell, and M. Cooper. 1995. Capacity for methane oxidation in landfill cover soils measured in laboratory-scale soil microcosms, Applied and Environmental Microbiology, Vol. 61, No.2, 592 – 601.

King, F.H. 1905. [Comment on] Contributions to our knowledge of the aeration of soils. Science (Washington, DC) 22:495–499.

Kirkham, D. 1946. Field method for determination of air permeability of soil in its undisturbed state. Soil Sci. Soc. Am. Proc. 11: 93-99.

Kirkham D., M. De Boodt, and L.De. Leenheer.1958. Air permeability at the field capacity as related to soil structure and yields. p. 377-391. *In* Proc. Int. Symposium on Soil Structure. Ghent, Belgium.

Kruse, C.W., P. Moldrup, and N. Iversen. 1996. Modeling diffusion and reaction in soils: II. Atmospheric methane diffusion and consumption in forest soil. Soil Sci. 161:355–365.

Marrero, T.R., and E.A. Mason. 1972. Gaseous diffusion coefficients. J.Phys. Chem.Ref. Data 1:3 118.

Marshall, T.J. 1959. The diffusion of gases through porous media. J. Soil Sci. 10:79–82.

Millington, R.J. 1959. Gas diffusion in porous media. Science 130:100–102.

Millington, R.J., and J.M. Quirk. 1960. Transport in porous media. p. 97–106. In F.A. Van Beren et al. (ed.) Trans. Int. Congr. Soil Sci., 7th, Madison, WI.14–21 Aug. 1960. Vol. 1. Elsevier, Amsterdam.

Millington, R.J., and J.M. Quirk. 1961. Permeability of porous solids. Trans. Faraday Soc. 57:1200–1207.

Moldrup, P., C.W. Kruse, D.E. Rolston, and T. Yamaguchi. 1996. Modeling diffusion and reaction in soils: III. Predicting gas diffusivity from the Campbell soil water retention model. Soil Sci. 161:366-375.

Moldrup, P., T. Olesen, J. Gamst, P. Schjønning, T. Yamaguchi, and D.E. Rolston. 2000a. Predicting the gas diffusion coefficient in repacked soil: Water induced linear reduction model. Soil Sci. Soc. Am. J. 64:1588–1594.

Moldrup, P., T. Olesen, P. Schjønning, T. Yamaguchi, and D.E. Rolston. 2000b. Predicting the gas diffusion coefficient in undisturbed soil from soil water characteristics. Soil Sci. Soc. Am. J. 64:94–100.

Moldrup, P., T. Olesen, T. Yamaguchi, P. Schjønning, and D.E. Rolston. 1999. Modeling diff usion and reaction in soils: IX. The Buckingham-Burdine-Campbell equation for gas diffusivity in undisturbed soil. Soil Sci. 164:542–551.

Moldrup, P., T.K.K Chamindu Deepagoda, L. de Jonge, S. Hamamoto, K. Kawamoto, T. Komatsu, and D.E. Rolston. 2011. Platform for regulating gas Emissions: Predicting soil-gas diffusivity across soil texture, organic matter, aggregation, compaction, and moisture. Proceedings of ASA, CSSA, SSSA annual meetings, san Antonio, TX.

Moldrup, P., T. Olesen, S. Yoshikawa, T. Komatsu, and D. E. Rolston. 2005. Predictive-descriptive models for gas and solute diffusion coefficients in variably saturated porous media coupled to poresize distribution: III. Inactive pore space interpretations of gas diffusivity. Soil Sci. 170:867–880.

National Aeronautics and Space Administration (NASA). 2002. Advanced Life Support Project Plan, 7 Document Number JSC-39168, NASA Johnson Space Center, Houston, TX, USA.

Penman, H.L. 1940. Gas and vapor movements in soil: The diffusion of vapors through porous solids. J. Agric. Sci. 30:437–462.

Petersen L.W., D.E. Rolston, P. Moldrup, and T. Yamaguchi. 1994. Volatile organic vapor diffusion and adsorption in soils. J. Environ. Qual. 23:799-805.

Pokorny, F.A. 1979. Bark potting mixtures for ornamental plants: softwood and hardwood. Georgia Nursery Notes, p.3,4,7.

Poulsen, T.G., M. Christophersen, P. Moldrup, and P. Kjeldsen. 2001. Modeling lateral gas transport in soil adjacent to old landfill. J. Environ. Eng. 127:145–153.

Resurreccion, A.C., P. Moldrup, K. Kawamoto, S. Yoshikawa, D.E. Rolston, and T. Komatsu, 2008. Variable pore connectivity factor model for gas diffusivity in unsaturated, aggregated soil. Vadose Zone J. 7, 397-405.

Rolston, D.E., and P. Moldrup. 2002. Gas diffusivity. p. 1113–1139. *In* J.H. Dane and G.C. Topp (ed.) Methods of soil analysis. Part 4. SSSA Book Ser. 5. SSSA, Madison, WI.

Rolston, D.E., and P. Moldrup. 2011. Gas transport in soils. Ch. 8. *In* P.M. Huang et al. (ed.) Handbook of soil sciences. Vol. 1. Properties and processes. 2nd ed. CRC Press, Boca Raton, FL.

Sallam, A., W.A. Jury, and J. Letey. 1984. Measurement of the gas diffusion coefficient under relatively low air-filled porosity. Soil Sci. Soc. Am. J. 48:3-6.

Schofield, R.K. 1935. The pF of the water in soil. p. 37–48. In Trans. World Congr. Soil Sci., 3rd, Oxford, UK. July–Aug. 1935. Vol. 2.

Soane, B.D., and C. van Ouwerkerk (ed.). 1994. Soil compaction in crop production. Dev. Agric. Eng. 11. Elsevier Science, Amsterdam.

Spomer, L.A. 1974. Optimizing container soil amendment: the "threshold proportion." HortScience 6:532–533.

Stepniewski, W. 1981. Oxygen diffusion and strength as related to soil compaction. Pol. J. Soil Sci. 12:3–13.

Steinberg, S.L., D.W. Ming, and D. Henninger. 2002. Plant production systems for microgravity: Critical issues in water, air and solute transport through unsaturated porous media. NASA Tech. Mem. 2002-210774. Natl. Aeronautics and Space Admin., Houston, TX

Steinberg, S.L. and D.L. Henninger. 1997. Response of tile water status of soybean to changes in soil water potentials controlled by the water pressure in microporous tubes. Plant Cell Environ. 20:1506-1516.

Tick, G.R:, C.M. McColl, I. Yolcubal, and M.L. Brusseau. 2007. Gas-phase diffusive tracer test for the in-situ measurement of tortuosity in the vadose zone. Water Air Soil Pollut. 184: 355-362.

Troeh, F.R., J.D. Jabro, and D. Kirkham. 1982. Gaseous diffusion equations for porous materials. Geoderma 27:239–253.

USEPA. 1996. Soil screening guidance: User's guide. 2nd ed. Publ. 9355.4–23. EPA/540/R-96/018. Office of Solid Waste and Emergency Response, USEPA, Washington, DC.

Weller, K.R., N.S. Stenhouse, and H. Watts. 1974. Diffusion of gases in porous solids. I. Theoretical background and experimental method. Can. J. Chem. 52: 2684: 2691.

Whitcomb, C.E. 1979. Plants, pots and drainage. Ornamentals South 1: 16-19.

Wickramarachchi P., K. Kawamoto, S. Hamamoto, M. Nagamori, P.Moldrup, and T. Komatsu. 2011. Effects of dry bulk density and particle size fraction on gas transport parameters in variably saturated landfill cover soil. Waste Manag. 12 :2464-72.

Xu, X., J.L. Nieber, and S.C. Gupta. 1992. Compaction effect on the gas diffusion coefficient in soils. Soil Sci. Soc. Am. J. 56:1743–1750.

# PAPER I

Special Section: Trace Gases

T.K.K. Chamindu Deepagoda*
Per Moldrup
Per Schjønning
Lis Wollesen de Jonge
Ken Kawamoto
Toshiko Komatsu

# Density-Corrected Models for Gas Diffusivity and Air Permeability in Unsaturated Soil

Accurate prediction of gas diffusivity ($D_p/D_o$) and air permeability ($k_a$) and their variations with air-filled porosity ($\varepsilon$) in soil is critical for simulating subsurface migration and emission of climate gases and organic vapors. Gas diffusivity and air permeability measurements from Danish soil profile data (total of 150 undisturbed soil samples) were used to investigate soil type and density effects on the gas transport parameters and for model development. The measurements were within a given range of matric potentials (−10 to −500 cm $H_2O$) typically representing natural field conditions in subsurface soil. The data were regrouped into four categories based on compaction (total porosity $\Phi$ <0.4 or >0.4 $m^3\ m^{-3}$) and soil texture (volume-based content of clay, silt, and organic matter <15 or >15%). The results suggested that soil compaction more than soil type was the major control on gas diffusivity and to some extent also on air permeability. We developed a density-corrected (D-C) $D_p(\varepsilon)/D_o$ model as a generalized form of a previous model for $D_p/D_o$ at −100 cm $H_2O$ of matric potential ($D_{p,100}/D_o$). The D-C model performed well across soil types and density levels compared with existing models. Also, a power-law $k_a$ model with exponent 1.5 (derived from analogy with a previous gas diffusivity model) used in combination with the D-C approach for $k_{a,100}$ (reference point) seemed promising for $k_a(\varepsilon)$ predictions, with good accuracy and minimum parameter requirements. Finally, the new D-C model concept for gas diffusivity was extended to bimodal (aggregated) media and performed well against data for uncompacted and compacted volcanic ash soil.

Abbreviations: D-C, density-corrected; GMP, generalized macroporosity; MQ, Millington and Quirk; OM, organic matter; WLR, water-induced linear reduction.

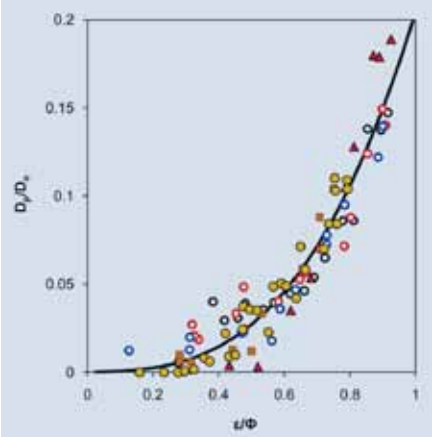


Models for predicting the soil gas diffusion coefficient and the soil air permeability from only air-filled and total porosities and which are corrected for soil dry bulk density are presented. These models were derived based on measurements on 150 intact soils representing a wide range of soil texture, compaction, and land use.

T.K.K.C. Deepagoda and P. Moldrup, Dep. of Biotechnology, Chemistry and Environmental Engineering, Aalborg Univ., Sohngaardsholmsvej 57, DK-9000 Aalborg, Denmark; P. Schjønning and L. Wollesen de Jonge, Dep. of Agroecology and Environment, Faculty of Agricultural Sciences, Aarhus Univ., Blichers Allé 20, P.O. Box 50, DK-8830 Tjele, Denmark; and K. Kawamoto and T. Komatsu, Dep. of Civil and Environmental Engineering, Graduate School of Science and Engineering, Saitama Univ., 255 Shimo-okubo, Sakura-ku, Saitama 338-8570, Japan. *Corresponding author (chamindu78@yahoo.com).

Vadose Zone J. 9
doi:10.2136/vzj2009.0137
Received 1 Oct. 2009.
Published online 7 Sept. 2010.



**The migration and emission of greenhouse gases** such as $CO_2$, $CH_4$, and $N_2O$ as well as other environmental impact gases (e.g., organic vapors at polluted sites) from terrestrial environments to the atmosphere causes increasing concern for climate, human, and ecosystem health. The enhanced atmospheric concentrations of the major greenhouse gases may potentially lead to significant regional and global climate shifts, with inherent regional and global environmental problems (Intergovernmental Panel on Climate Change, 2007). Terrestrial production of greenhouse gases occurs largely in natural systems (e.g., forest and peat lands), but rapidly expanding anthropogenic sources like agricultural fields, landfills, and constructed wetlands have also contributed significantly to increasing atmospheric concentrations (Bartlett and Harriss, 1993). For example, atmospheric $CH_4$ is a powerful greenhouse gas that contributes approximately 25% of the anticipated global warming (Mosier, 1998), and nearly one-third of global $CH_4$ emission stems from terrestrial soils (Smith et al., 2003). Landfills are a particularly large source, responsible for between 7 and 20% of global anthropogenic sources of $CH_4$ emissions (Poulsen et al., 2001), with the unsaturated final-cover soil layer being the main control of $CH_4$ migration, consumption, and emissions from landfills (Hamamoto et al., 2009b).

The uptake or emission of gases in soil systems is mainly controlled by the physical, chemical, and biological processes in the vadose zone and is strongly linked to soil physical properties such as soil texture and soil total porosity. Therefore, accurate prediction of gas movement in soils related to varying soil physical properties under natural field conditions is a prerequisite for realistic simulations of land type and management impacts on climate gas consumption or emission. Subsurface migration of gases through the soil air phase and subsequent emission across the soil–atmosphere interface occur predominantly by diffusion (Penman, 1940), and near-surface pressure fluctuations further accelerate the movement by advection (Poulsen et al., 2003).

The diffusive and advective movement of gases in soils is controlled by the soil gas diffusivity (the ratio of gas diffusion coefficients in soil and free air, $D_p/D_o$) and the soil air permeability ($k_a$), respectively. Measurements of these two gas transport parameters, however, require special equipment and are complicated to perform in situ with sufficient control of the initial and boundary conditions (Rolston et al., 1991; Rolston and Moldrup, 2002; Werner et al., 2004). Models, therefore, are frequently used to predict $D_p/D_o$ and $k_a$ as a function of easily measureable parameters such as air-filled porosity ($\varepsilon$) and total porosity ($\Phi$). Despite significant progress in developing and testing predictive models for $D_p/D_o$ and, to a lesser extent, $k_a$ during the last decade, the links between the gas transport parameters and basic soil physical properties such as texture and compaction level (as described by bulk density or total porosity) are still not well understood.

Compaction essentially decreases the pore space between soil particles, thereby decreasing the total porosity. Deleterious impacts to soil porosity may derive from long-term pedogenetic processes or from short-term anthropogenic activities (management). Dense soils are often encountered in both natural and engineered soil systems. They are also likely to occur in deep vadose zone profiles due to the weight of the overlying soil mass. In shallow urban soil profiles, compacted soils occur beneath building foundations due to the load of the superstructure and soil damage from construction activities. Traffic by heavy machinery in agricultural fields and forests creates soil compaction in the topsoil as well as in subsoil layers to ~1-m depth. This consequently affects crop productivity and soil functions related to environmental quality (Schjønning et al., 2009). Modern landfill sites are often capped with extremely compacted soil liners to reduce water permeability and trace gas emissions (Poulsen et al., 2001). Although the effects of soil density on soil aeration are recognized in general, only a few studies have examined the direct effect of soil density on the gas transport parameters (Buckingham, 1904; Stepniewski, 1981; Currie, 1984; Xu et al., 1992; Shimamura, 1992; Fujikawa and Miyazaki, 2005). Different studies have come to contradictory conclusions with regard to the effect of compaction on gas transport parameters. For example, the studies by Stepniewski (1981) and Xu et al. (1992) on gas diffusion in differently textured soils found little effect of bulk density on the relationship between $D_p/D_o$ and $\varepsilon$. On the contrary, Fujikawa and Miyazaki (2005) and Hamamoto et al. (2009a) observed increased $D_p/D_o$ with increasing bulk density at a given $\varepsilon$. Furthermore, Currie (1984) concluded that no single curvilinear relationship, even for one given soil, can describe the change in $D_p/D_o$ with $\varepsilon$ when changes occur in bulk density.

In this study, we compared soils that had reached a specific compactness through very different processes in time and space. We have chosen the term *density* for expressing the compactness. The ambition of this study expressed in general terms was to develop a simple and useful model for predicting $D_p/D_o$ and $k_a$ across soils with a range in density irrespective of the cause of that density. More specifically, the study investigated the effects of soil density and soil type on $D_p/D_o$ and $k_a$ based on data from vadose zone profiles across Denmark, including soils from urban, agricultural, and forest sites as well as a final landfill cover soil. Density-corrected model approaches were developed for both $D_p/D_o$ and $k_a$, with the models being applicable across different soil types and total porosities within the range of soil water matric potential mostly occurring under natural field conditions (between −10 and −500 cm $H_2O$).

# Materials and Methods

## Soils and Data

In this study, we used both unpublished and literature data on undisturbed soils from eight different locations with a wide geographical distribution and land uses spread across Denmark, representing a wide range of soil texture, horizons, and total porosities (we refer to each soil according to the sampling location). Measurements on a total of 150 undisturbed soil samples from the eight locations were considered. Metal rings with similar dimensions (0.034-m length, 0.061-m i.d., 100-$cm^3$ sample volume) were used for sampling at all locations. During sampling, the sharpened edge of the metal ring was carefully driven into the soil by means of a hammer and retrieved with the soil core, ensuring minimum disturbance. The end surfaces were trimmed and the edges were kneaded with a knife to prevent preferential air flow through the annular gap between the core and the sample. The samples were end-capped and stored at 2°C before measurements.

### Urban Soils

The sampling site at Skellingsted was located adjacent to an unlined municipal landfill operated as a dump of municipal solid waste and industrial waste from 1971 to 1990. The landfill was covered with 80 cm of sand and 20 cm of topsoil at the final closure (Christophersen and Kjeldsen, 2001). The lateral migration of trace landfill gases, however, caused a fatal explosion in a house near the landfill in 1991 (Poulsen et al., 2001). Samples were collected at 70-cm depth for measurements (data for both gas diffusivity and air permeability were partly presented by Poulsen et al. [2001]). Hjørring soils were sampled from a deep vadose zone profile from 4- to 5- and 6- to 7-m depths at a former municipal gas work site (gas diffusivity data were partly presented by Moldrup et al. [2000b]; air permeability data have not previously been published). The profile featured differently textured horizons including a less organic clay layer at the top (410-cm depth) and organic-matter-rich loamy soils toward the bottom of the profile.

### Agricultural and Forest Soils

Three lysimeter soils (Rønhave, Foulum, and Jyndevad) and two agricultural field soils (Mammen and Gjorslev) from Kawamoto et al. (2006a,b) were also included. The lysimeter soils with different soil textures were excavated from the three locations into large

soil bins located at Aarhus University, the Faculty of Agricultural Sciences at Research Centre Foulum in 1993. The soils were air dried, crumbled to aggregates <20 mm, and then packed in the bins incrementally in 10-cm layers to the same dry bulk density as occurred in the field. For details on management and treatment practices of the soils before sampling, and on the packing procedure into the soil bins, see Kawamoto et al. (2006b) and Lamandé et al. (2007), respectively. The two agricultural field soils (Mammen and Gjorslev) have been in agricultural use for centuries.

Two medium-organic sandy layers collected in a natural mixed hardwood forest at Poulstrup, 10- to 15-cm depth (data from Kruse et al., 1996) and 15- to 20-cm depth (data from Moldrup et al., 1996) were considered. These soils showed high $CH_4$ consumption rates probably controlled by $D_p/D_o$ and its variation with $\varepsilon$ (Kruse et al., 1996). The sampling depths, soil texture, and characteristics of each layer for the selected soils are given in Table 1.

We also used a sieved and repacked, microaggregated volcanic ash soil (Andisol) from Tsukuba, Japan (data from Osozawa, 1998) for testing a possible extension of the new gas diffusivity model to soils with bimodal pore-size distribution. We considered the soils at two compaction levels: uncompacted and uniaxially compacted at 200 kPa (Osozawa, 1998).

Table 1. The sampling locations, depths and soil physical characteristics.

| Location | Depth | Texture† | Clay | Silt | Sand | Organic matter | Total porosity‡ | Reference |
|---|---|---|---|---|---|---|---|---|
| | m | | | | % | | Φ | |
| Skellingsted | 0.70 | sand | 5.1 | 2.0 | 92.9 | 1.7 | 0.359 (0.020) | Poulsen et al. (2001) |
| Hjørring | 4.00–4.50 | sandy clay loam | 24.8 | 9.2 | 65.9 | 0.2 | 0.449 (0.040) | Moldrup et al. (2000b) ($D_p$ data), this study ($k_a$ data) |
| Hjørring | 4.10 | clay | 56.6 | 21.0 | 22.3 | 0.2 | 0.502 | |
| Hjørring | 4.50–5.00 | sandy clay loam | 26.9 | 9.2 | 63.9 | 0.2 | 0.456 (0.032) | |
| Hjørring | 6.00–6.50 | sandy loam | 15.7 | 10.8 | 73.4 | 2.1 | 0.382 (0.042) | |
| Hjørring | 6.50–7.00 | loamy sand | 11.2 | 5.0 | 83.8 | 1.6 | 0.404 (0.052 | |
| Gjorslev | 0.05–0.25 | sandy clay loam | 17.4 | 18.6 | 64.1 | 2.6 | 0.378 (0.013) | Kawamoto et al. (2006a,b) |
| Gjorslev | 0.33–0.53 | sandy clay loam | 17.2 | 14.1 | 68.7 | 0.3 | 0.369 (0.008) | |
| Gjorslev | 0.80–1.00 | sandy clay loam | 19.3 | 19.1 | 61.6 | 0.2 | 0.338 (0.013) | |
| Gjorslev | 2.05–2.25 | sandy clay loam | 24.1 | 17.3 | 58.6 | 0.2 | 0.321 (0.006) | |
| Gjorslev | 3.50–3.70 | sandy clay loam | 22.8 | 17.0 | 60.1 | 0.3 | 0.291 (0.008) | |
| Gjorslev | 4.65–4.85 | sandy clay loam | 19.7 | 15.6 | 64.7 | 0.4 | 0.306 (0.037) | |
| Mammen | 0.05–0.25 | sandy loam | 11.6 | 14.8 | 73.6 | 3.4 | 0.435 (0.005) | |
| Mammen | 0.30–0.50 | sandy clay loam | 15.2 | 12.4 | 72.4 | 0.4 | 0.347 (0.013) | |
| Mammen | 1.10–1.30 | sandy clay loam | 19.5 | 9.0 | 71.5 | 0.1 | 0.322 (0.005) | |
| Mammen | 2.05–2.15 | sandy clay loam | 17.9 | 8.6 | 73.5 | 0.1 | 0.321 (0.010) | |
| Mammen | 3.40–3.60 | sandy loam | 11.3 | 6.7 | 82.0 | 0.1 | 0.352 (0.010) | |
| Mammen | 5.40–5.60 | sand | 3.6 | 0.9 | 95.5 | 0.0 | 0.389 (0.011) | |
| Rønhave | 0.00–0.30 | sandy clay loam | 17.9 | 13.1 | 69.0 | 2.3 | 0.450 (0.025) | |
| Rønhave | 0.30–0.70 | sandy clay loam | 21.7 | 13.5 | 64.8 | 0.5 | 0.436 (0.012) | |
| Rønhave | 0.70–1.40 | sandy clay loam | 21.8 | 15.8 | 62.4 | 0.3 | 0.415 (0.010) | |
| Foulum | 0.00–0.30 | sandy loam | 11.8 | 11.3 | 77.0 | 2.3 | 0.539 (0.020) | |
| Foulum | 0.30–0.60 | sandy loam | 15.0 | 10.2 | 74.9 | 0.5 | 0.389 (0.017) | |
| Foulum | 0.60–0.90 | sandy clay loam | 16.0 | 12.0 | 71.9 | 0.2 | 0.393 (0.002) | |
| Foulum | 0.90–1.40 | sandy clay loam | 16.3 | 10.5 | 73.2 | 0.1 | 0.350 (0.005) | |
| Jyndevad | 0.00–0.30 | loamy sand | 5.9 | 2.1 | 91.9 | 1.9 | 0.469 (0.019) | |
| Jyndevad | 0.30–0.70 | loamy sand | 6.0 | 0.5 | 93.5 | 0.7 | 0.458 (0.010) | |
| Jyndevad | 0.70–1.40 | loamy sand | 5.2 | 0.7 | 94.1 | 0.2 | 0.438 (0.013) | |
| Poulstrup | 0.10–0.15 | sand | 3.7 | 3.1 | 93.2 | 3.7 | 0.519 (0.021) | Kruse et al. (1996) |
| Poulstrup | 0.15–0.20 | sand | 4.3 | 2.6 | 93.1 | 4.1 | 0.539 (0.031) | Moldrup et al. (1996) |

† Soil textures are classified based on the International Soil Science Society (ISSS) standard (Verheye and Ameryckx, 1984).
‡ Average values are given. Values in parentheses are standard deviations.

## Measurement Methods

For all samples in this study, the desired soil water matric potentials were obtained following the method proposed by Klute (1986). The 100-$cm^3$ undisturbed soil cores were first saturated inside sand boxes and subsequently drained to the intended matric potential ($\psi$) using either hanging water columns (for $\psi > -100$ cm $H_2O$) or suction and pressure plate systems (for $\psi < -100$ cm $H_2O$). The matric potentials were in the range of −10 to −500 cm $H_2O$ (at least four different potentials for each sample).

For $D_p/D_o$ measurements, the experimental setup initially suggested by Taylor (1949) and further developed by Schjønning (1985) was used. The gas diffusivity chamber was first made $O_2$–free by flushing with 100% $N_2$. Atmospheric air was then allowed to enter into the chamber through the soil sample by exposing the top surface of the soil core, and $O_2$ was measured by an electrode mounted on the chamber wall. The $O_2$ diffusion coefficient in soil ($D_p$) was calculated following Rolston and Moldrup (2002). The time taken for each measurement differed depending on the matric potential applied and was considered small enough to neglect the $O_2$ depletion due to microbial consumption (Schjønning et al., 1999).

For $k_a$ measurements, a small air pressure gradient was established across the sample by applying a constant pressure difference at the ends, and the resulting air flow (which is proportional to the air permeability) was measured by means of a flow meter. The experimental setup and procedure were outlined by Moldrup et al. (1998) and Ball and Schjønning (2002).

## Statistical Analyses

The performance of the proposed models for gas diffusivity and air permeability were evaluated and compared with existing predictive models by means of two statistical indices. To evaluate the model overall fit to the measured data, the RMSE was used:

$$\mathrm{RMSE} = \sqrt{\frac{1}{n}\sum_{i=1}^{n}(d_i)^2} \qquad [1]$$

where $d_i$ is the difference between the observed and predicted values ($D_p/D_o$ or $k_a$) and $n$ is the number of measurements in the data set.

The bias was used to assess the general overprediction (positive bias) or underprediction (negative bias) of the model compared with the observed data:

$$\mathrm{bias} = \frac{1}{n}\sum_{i=1}^{n}(d_i) \qquad [2]$$

When the statistical comparison is based on log-transformed values, Eq. [1] and [2] become $\mathrm{RMSE}_{log}$ and $\mathrm{bias}_{log}$, respectively, in which $d_i$ now corresponds to the difference between the logarithms of the observed and predicted values.

## Gas Diffusivity Models from Literature

Buckingham (1904), in one of the earliest works on soil gas physics, empirically established the following relationship between soil $D_p/D_o$ and $\varepsilon$ using four different soils in varying states of compactness and moisture content:

$$\frac{D_p}{D_o} = \varepsilon^2 \qquad [3]$$

From this, he concluded that the diffusion of gas in soils is not greatly affected by soil type. Similar single-parameter predictive models were developed later (e.g., Penman, 1940; Marshall, 1959; Millington, 1959) until the next generation of models started to incorporate some soil type and density effects through the soil total porosity ($\Phi$). Among commonly accepted soil-type-dependant models are the Millington and Quirk (MQ) (1960) model:

$$\frac{D_p}{D_o} = \frac{\varepsilon^2}{\Phi^{2/3}} \qquad [4]$$

and the Millington and Quirk (1961) model:

$$\frac{D_p}{D_o} = \frac{\varepsilon^{10/3}}{\Phi^2} \qquad [5]$$

with the latter (Eq. [5]) being almost universally accepted and recommended by the USEPA and Danish Environmental Protection Agency for risk assessment at polluted soil sites (USEPA, 1996; Danish Environmental Protection Agency, 2002). It is also frequently used for calculating climate gas emissions at different scales (from the field to a continent) and to infer gas fluxes from chamber measurements (e.g., Liu and Si, 2008; Perera et al., 2002).

The presence of water can significantly affect gas diffusion in soils. In wet soils, water held at bottlenecks (narrow pore throats between particles) can potentially create large tortuosity (prolonged pathways) for gas transport. The WLR–Marshall model (Moldrup et al., 2000a) takes this water blockage effect into account by assuming a water-induced linear reduction (WLR) of gas diffusivity:

$$\frac{D_p}{D_o} = \varepsilon^{1.5}\left(\frac{\varepsilon}{\Phi}\right) \qquad [6]$$

Rearranging Eq. [6] into the form used in this study yields

$$\frac{D_p}{D_o} = \Phi^{1.5}\left(\frac{\varepsilon}{\Phi}\right)^{2.5} \qquad [7]$$

thereby making the WLR model mathematically analogous to the widely used model for relative electrical conductivity by Mualem and Friedman (1991).

Based on gas diffusivity measurements on 126 soils representing a broad range of soil texture, horizons, and management practices,

Moldrup et al. (2000b) observed a surprisingly high correlation ($r^2$ = 0.97) between the measured gas diffusivities at −100 cm $H_2O$ of soil water potential ($D_{p,100}/D_o$) and the corresponding air-filled porosities at −100 cm $H_2O$, $\varepsilon_{100}$ (also called *macroporosity*), yielding

$$\frac{D_{p,100}}{D_o} = 2\varepsilon_{100}^3 + 0.04\varepsilon_{100} \quad [8]$$

Equation [8] (hereafter referred to as the macroporosity-dependant [MPD] relation) was successfully used in subsequent models (Moldrup et al., 2000b, 2004) as the reference-point gas diffusivity for $D_p(\varepsilon)/D_o$ models. It should be noted that the choice of −100 cm $H_2O$ as the reference state is not an arbitrary value because the natural water content at field capacity is suggested as occurring at or close to −100 cm $H_2O$ matric potential irrespective of soil texture (e.g., Schjønning and Rasmussen, 2000; Al Majou et al., 2008).

## Air Permeability Models from the Literature

The effects of soil type, texture, and compactness and especially the effect of soil structure are more pronounced for air permeability than for gas diffusivity (Buckingham, 1904). Some widely used predictive models use a reference-point value, typically $k_{a,100}$ (i.e., air permeability at −100 cm $H_2O$ of soil water potential, $\mu m^2$), together with a power-law function:

$$k_a = k_{a,100}\left(\frac{\varepsilon}{\varepsilon_{100}}\right)^{\eta} \quad [9]$$

where the exponent $\eta$ represents the combined effects of tortuosity and connectivity of the air-filled pores (Kawamoto et al., 2006a). Moldrup et al. (1998) suggested $\eta$ = 2 and Kawamoto et al. (2006a) proposed $\eta$ as

$$\eta = X - 1 \quad [10]$$

where $X$ is an exponent related to the relative air saturation term ($\varepsilon/\Phi$) in an analogous power-law gas diffusivity model. For example, $X$ equals 2.5 in the WLR—Marshall model (Eq. [7]). For reference-potential air permeability,Kawamoto et al. (2006a) used the MPD relation for gas diffusivity (Eq. [8]) together with the classical nonjointed capillary tube model (Millington and Quirk, 1964; Ball, 1981) and with given assumptions on the equivalent diameter of conducting air-filled pores, yielding

$$k_{a,100} = 700\left(2\varepsilon_{100}^3 + 0.04\varepsilon_{100}\right) \quad [11]$$

## Soil and Data Regrouping by Density and Texture Classes

As discussed above, the selected soils were widely different with respect to texture and horizons and had a wide range of total porosities reflecting different states of compactness. To categorize the soils according to texture, we express the amount of fines in terms of a volume-based fraction of clay, silt, and organic matter (OM), denoted as CSOvol, and given by

$$\text{CSOvol} = \rho_b\left(\frac{\text{clay} + \text{silt}}{2.7} + \frac{\text{OM}}{1}\right) \quad [12]$$

where CSOvol is the volume-based fraction of clay, silt, and organic matter ($cm^3\ cm^{-3}$); $\rho_b$ is the soil dry bulk density ($g\ cm^{-3}$); clay, silt, and OM are the gravimetric contents of clay, silt, and organic matter, respectively ($g\ g^{-1}$), and their denominators, 2.7 and 1, are the assumed particle densities for clay or silt and OM, respectively ($g\ cm^{-3}$) (Sumner, 2000). The value of CSOvol can range between 0 (for pure sand) and 1 (for organic soils or peat), with values in between for typical soils. A similar equation was introduced by Moldrup et al. (2007) taking into account only clay and organic matter, whereas Eq. [12] also considers silt particles as part of the finer particles potentially influencing the soil structure, pore networks, and gas transport.

Figure 1a illustrates the values of CSOvol plotted against the corresponding total porosities for the selected soils from each location.

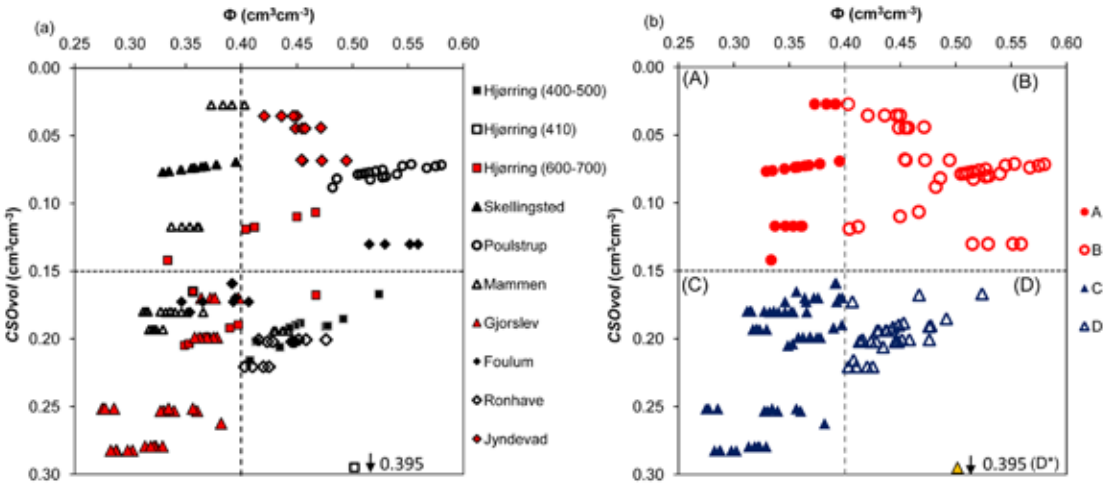


Fig. 1. (a) Volume-based fraction of clay, silt, and organic matter (CSOvol), Eq. [12], plotted against total porosity (Φ), with soils from Hjørring presented in three subhorizons; (b) soils classified into four groups, denoted as A, B, C, and D, based on compaction (Φ < 0.40 and Φ > 0.40 $cm^3\ cm^{-3}$) and texture (CSOvol < 0.15 and CSOvol > 0.15 $cm^3\ cm^{-3}$). The high-clay soil D* (sampled from Hjørring at 410-cm depth) is shown by a yellow colored triangle. The two lines of demarcation (Φ = 0.40 and CSOvol = 0.15) are shown by dashed lines in both panels.

Note that the Hjørring soils are presented in three subhorizons showing their marked differences in total porositiy and CSOvol values. For the purpose of analysis, we defined the soils with total porosity ($\Phi$) > 0.40 as less dense and $\Phi$ < 0.40 as dense. Similarly, we classified the soils having CSOvol > 0.15 as soils with high fines and those having CSOvol < 0.15 as soils with low fines. The two lines of demarcation, $\Phi$ = 0.40 and CSOvol = 0.15, were selected arbitrarily and separated the soils into four groups in such a way that each soil belonged in one of the four groups with limited crossovers. The four new groups are denoted as A, B, C, and D as shown in Fig. 1b. The soils with low fines and those with high fines are shown with red circles and blue triangles, respectively, while the open and closed symbols represent less dense and dense soils, respectively. For the ease of distinction, the high-fines (clay) soil from Hjørring (at 410-cm depth) is denoted as D* and is symbolized by a yellow triangle (Fig. 1b).

# Results, Model Development, and Tests

## Effects of Density and Soil Type

To examine the effect of soil type and density on gas transport parameters, two representative gas diffusivity curves were selected from each group A, B, C, and D and presented together in Fig. 2a. The clay soil D* is also shown for comparison. No distinct effect of soil type could be observed, supporting the observations of Buckingham (1904) and Moldrup et al. (2001). Conversely, the two soils representing Group A are markedly separated from the soils representing Group B (placed on opposite sides of the Buckingham reference model ($\varepsilon^2$) shown by a dashed line in Fig. 2a), suggesting a clear effect of density. Similar observations were made when comparing Groups C and D soils (Fig. 2a).

The observed enhanced gas diffusivity in the dense soils compared with the less dense ones at a given air-filled porosity agrees with the results of some previous studies, for example Fujikawa and Miyazaki (2005), who attributed the effect to "preferential loss" of ineffective pore space in the gas flow regime following compaction. Taken at the same air-filled porosity, dense soils with relatively higher volumetric solids content hold less water (and hence exhibit less water bridging between particles and water-induced tortuosity), resulting in increased gas diffusivity.

A further comparison of gas transport parameter behavior at a given matric potential ($\psi$) will often be of more practical interest because the soil layers throughout a vadose zone profile under natural field conditions will typically stabilize at a given matric potential (allowing a sufficiently long time after infiltration and drainage). Figure 2b shows the gas diffusivities of the same soils as in Fig. 2a but now plotted against matric potential (expressed by pF = log[$-\psi$], where $\psi$ is in cm $H_2O$, following Schofield [1935]). At a given pF, the dense soils exhibited smaller gas diffusivities than the less dense soils, thus showing an opposite trend in gas diffusivity behavior compared with Fig. 2a. At a given matric potential, the reduced gas diffusivity in the dense soils can be ascribed to the decrease in air-filled porosity as a result of the increase in water retention (Currie, 1984). Consequently, the effect of soil type or texture (giving different water retention characteristics) becomes more pronounced. The corresponding trends for air permeability (not shown) are similar but less stringent due to the pronounced effects of the soil structure on the air permeability (Moldrup et al., 2001).

In summary, the effects of soil type (texture) seemed minor and the effects of soil density seemingly dominated the effects of soil type on relative gas diffusivity and to some extent also on air permeability when the two gas transport parameters were plotted as functions of air-filled porosity. Conversely, the effects of soil type dominated when the gas transport parameters were plotted as functions of pF due to the large differences in soil water retention characteristics between finer and coarser textured soils. Thus, to discuss the effects of soil density on gas transport parameters, it should be clearly distinguished whether the comparison is made at the same air-filled porosity ($\varepsilon$) or at the same soil water matric potential (for example, given as pF) because the effects will appear different: at the same $\varepsilon$, the $D_p/D_o$ will typically be greater for a dense soil than for a less dense soil, whereas the $D_p/D_o$ at a given matric potential will typically be smaller for a dense soil than for a less dense soil.

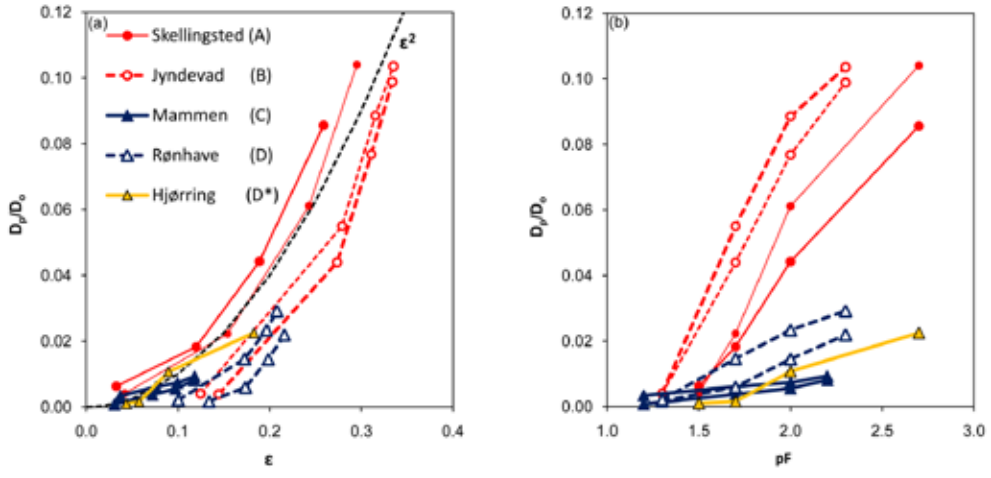


Fig. 2. Soil-gas diffusivities ($D_p/D_o$) as a function of (a) air-filled porosity ($\varepsilon$) and (b) pF (the negative logarithm of matric potential) for soil sample pairs selected to represent the four groups A, B, C and D, and additionally the soil D*. The Buckingham (1904) model, Eq. [3], is also shown (black dashed line) as a reference in (a). Data from Poulsen et al. (2001), Moldrup et al. (2000b), and Kawamoto et al. (2006a,b).

Based on the above results, with more pronounced effects of density than of soil type at the same air-filled porosity, we focused on developing density-corrected models for both $D_p/D_o$ and $k_a$ as a function of air-filled and total porosities. The models can easily be transformed into functions also of the soil water matric potential (or pF) using an appropriate soil water retention model, for example the widely used van Genuchten (1980) or Campbell (1974) models.

## Density-Corrected Gas Diffusivity Model

We first confirmed the relatively good accuracy of the MPD relation (Eq. [8]) using gas diffusivity measurements for the soils in Groups A and B at pF 2.0 (−100 cm $H_2O$ matric potential) (Fig. 3a). We further observed that the same model, when tested at pF = 2.7, still yielded promising results (Fig. 3b). Similar observations were made at pF = 1.7 as well (not shown). Based on this, we generalized the original MPD equation to yield a so-called generalized macroporosity-based (GMP) model:

$$\frac{D_p}{D_o} = 2\varepsilon^3 + 0.04\varepsilon \qquad [13]$$

The GMP model, however, shows a tendency to underestimate data for the dense soils and overestimate for the less dense soils. This tendency was observed at all the considered pF values and was highly evident at pF = 2.7 (Fig. 3b). A modification to the GMP model, therefore, was necessary to take the effect of density into account. We observed that simply plotting the measured gas diffusivities against the normalized air-filled porosity ($\varepsilon/\Phi$) largely reduced the density-induced fluctuations in the measured data (Fig. 3c and 3d) and a new, density-corrected model analogous to the GMP model could yield more accurate predictions. The density-corrected (D-C) GMP model can be written as

$$\frac{D_p}{D_o} = 0.1\left[2\left(\frac{\varepsilon}{\Phi}\right)^3 + 0.04\left(\frac{\varepsilon}{\Phi}\right)\right] \qquad [14]$$

The D-C GMP model retains the analogy to the GMP model except for the additional empirical scaling factor in front of the equation (set equal to 0.1) resulting from model fitting to the measured data for all 150 soil samples.

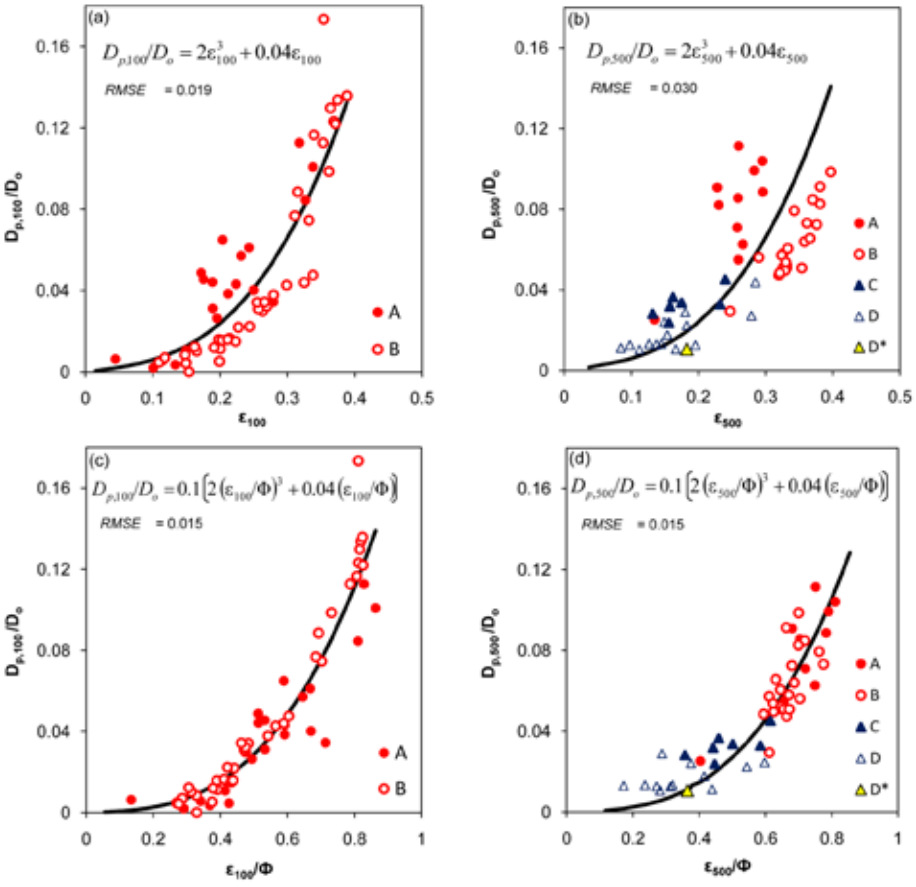


Fig. 3. The observed soil gas diffusivities ($D_p/D_o$) as a function of air-filled porosity ($\varepsilon$) (a) at pF 2.0 (−100 cm $H_2O$ suction) for the soils in Groups A and B and the predictions by the macroporosity-dependant (MPD) relation, Eq. [8], and (b) at pF 2.7 (−500 cm $H_2O$ suction) and the predictions by the MPD relation generalized also for the pF 2.7 condition; predictions by the density-corrected (D-C) gas diffusivity model, Eq. [14], at (c) pF 2.0 and (d) pF 2.7. Note the different *x* axes; RMSE values for model performance are also given.

## Test of Gas Diffusivity Models

Figure 4 shows scatterplot comparisons (in a log–log coordinate system) of predicted and measured $D_p/D_o$ for the GMP model (Eq. [13]) and the D-C GMP model (Eq. [14]) together with two existing predictive models: the Buckingham (1904) model (Eq. [3]) and the MQ (1961) model (Eq. [5]). The model performances were evaluated using the RMSE (Eq. [1]) and bias (Eq. [2]) and the analogous log-transformed indices, $RMSE_{log}$ and $bias_{log}$. Out of the four models shown, the widely accepted MQ (1961) showed a weak performance in terms of overall model fit ($RMSE_{log}$ = 0.77) and a tendency to slightly overpredict under relatively dry conditions and grossly underpredict under moist conditions, leading to a significant overall underprediction ($bias_{log}$ = −0.306). A similar behavior of the MQ (1961) model was also observed in some recent studies (Kawamoto et al., 2006b; Resurreccion et al., 2007), with some additional studies also implying a poor performance (Jin and Jury, 1996; Moldrup et al., 1996, 2003). Despite its simplicity, the Buckingham (1904) model performed remarkably well and outperformed the MQ (1961) model for most soils. A similar good performance of the classical Buckingham model was also recently observed by Resurreccion et al. (2008).

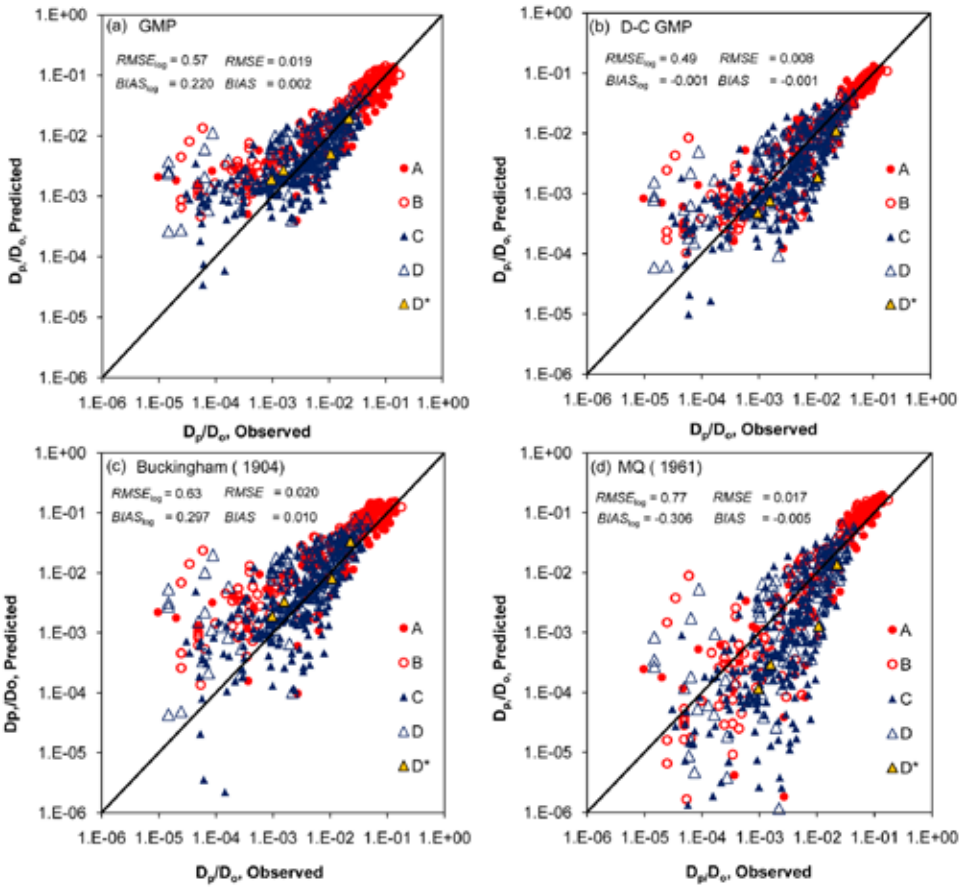


Fig. 4. Scatterplot comparison of predicted and measured gas diffusivities ($D_p/D_o$) for four predictive models: (a) the generalized macroporosity (GMP) model, Eq. [13], (b) the density-corrected (D-C) GMP model, Eq. [14], (c) the Buckingham (1904) model, Eq. [3], and (d) Millington and Quirk (MQ) (1961) model, Eq. [5]. Calculated RMSE (Eq. [1]) and bias (Eq. [2]) and $RMSE_{log}$ and $bias_{log}$ (calculated using log-transformed $D_p/D_o$ data) values are also given. Data from Poulsen et al. (2001), Moldrup et al. (1996, 2000b), Kawamoto et al. (2006a,b), Kruse et al. (1996), and this study.

The statistical indices further suggest that the D-C GMP model performed best among the four models. The results of detailed statistical analysis, for each individual group A, B, C, and D (including D*) and overall, are given in Table 2 for six predictive models including also the MQ (1960) model (Eq. [4]) and WLR–Marshall model (Eq. [6]). The new D-C GMP model, with the lowest values for both statistical indices for the individual soil groups (except for $bias_{log}$ in Groups A and B) as well as overall, seems to capture gas diffusivity behavior across soil texture and compaction levels accurately. Moreover, the new model is simple, with no additional input parameter requirements.

Applying independently measured data (i.e., data not utilized in developing the model) is an essential part of predictive model development. First, we considered measured $D_p/D_o$ data for two highly porous (and organic) topsoils sampled at 0- to 5- and 5- to 10-cm depths ($\Phi_{avg}$ = 0.72) from Poulstrup for model validation. When plotted together with the already used data for the two lower, less organic and less porous soil layers, Poulstrup (10–15- and 15–20-cm depths, $\Phi_{avg}$ = 0.53) and the very dense Skellingsted soil (70-cm depth, $\Phi_{avg}$ = 0.36), three distinctly separated curves with respect to total porosity were obtained, implying a clear effect of soil total porosity and density (Fig. 5a). Predictions by the GMP model (dashed line) corresponds to a total porosity between 0.36 (dense) and 0.53 (less dense) and therefore probably represents only gas diffusivity of medium-dense soils. The separation in the measured data dramatically narrowed when plotted against the

Table 2. Test of predictive soil gas diffusivity models against measured data. For each predictive model, the two log-transformed statistical parameters, $RMSE_{log}$ and $bias_{log}$, are also given for individual categories A, B, C, and D (including D*) and overall.

| Model† | Equation‡ | $RMSE_{log}$ | | | | | $Bias_{log}$ | | | | |
|---|---|---|---|---|---|---|---|---|---|---|---|
| | | A | B | C | D | Overall | A | B | C | D | Overall |
| Buckingham (1904) | $D_p/D_o = \varepsilon^2$ | 0.61 | 0.66 | 0.57 | 0.72 | 0.63 | 0.193 | 0.481 | 0.118 | 0.430 | 0.297 |
| MQ (1960) | $D_p/D_o = \varepsilon^2/\Phi^{2/3}$ | 0.76 | 0.81 | 0.68 | 0.88 | 0.77 | 0.488 | 0.680 | 0.435 | 0.665 | 0.560 |
| MQ (1961) | $D_p/D_o = \varepsilon^{10/3}/\Phi^2$ | 0.69 | 0.49 | 0.95 | 0.76 | 0.77 | −0.130 | 0.016 | −0.657 | −0.218 | −0.306 |
| WLR-Marshall | $D_p/D_o = \varepsilon^{1.5}(\varepsilon/\Phi)$ | 0.61 | 0.55 | 0.60 | 0.66 | 0.59 | 0.183 | 0.381 | −0.052 | 0.275 | 0.170 |
| GMP | $D_p/D_o = 2\varepsilon^3 + 0.04\varepsilon$ | 0.58 | 0.60 | 0.50 | 0.66 | 0.57 | 0.047 | 0.374 | 0.121 | 0.294 | 0.220 |
| D-C GMP | $D_p/D_o = 0.1[2(\varepsilon/\Phi)^3 + 0.04(\varepsilon/\Phi)]$ | 0.53 | 0.40 | 0.50 | 0.56 | 0.49 | 0.057 | 0.072 | −0.092 | 0.026 | −0.001 |

† MQ, Millington and Quirk; WLR, water-induced linear reduction; GMP, generalized macroporosity-dependant model; D-C GMP, density-corrected generalized macroporosity-dependant model.
‡ $D_p/D_o$, soil gas diffusivity; $\varepsilon$, air-filled porosity; $\Phi$, total porosity.

normalized air-filled porosity (Fig. 5b), and the D-C GMP model produced accurate predictions for the five soil layers across a very wide range of total porosities.

Second, we used $D_p/D_o$ data for three differently textured intact soils from Freijer (1994): a sandy soil, Kootwijk C ($\Phi = 0.389$), and two silty loam soils, BeC ($\Phi = 0.452$), and EsC ($\Phi = 0.452$), all soils with 1.4 to 1.6% OM. Although the D-C GMP model was originally developed for undisturbed soils, we further tested its applicability for repacked soils using gas diffusivity measurements for the Hjørring sandy soil (9.3% clay, 4.8% silt, 86% sand, and 0.3% OM), sieved and repacked at three different bulk densities corresponding to total porosities of 0.42, 0.36, and 0.34 $cm^3\ cm^{-3}$ (data from this study). Again, the GMP model failed to recognize the effect of density for both undisturbed and repacked soils (Fig. 6a), while the D-C GMP model yielded promising results (Fig. 6b) irrespective of the state of soil texture, structure (intact or repacked), or density.

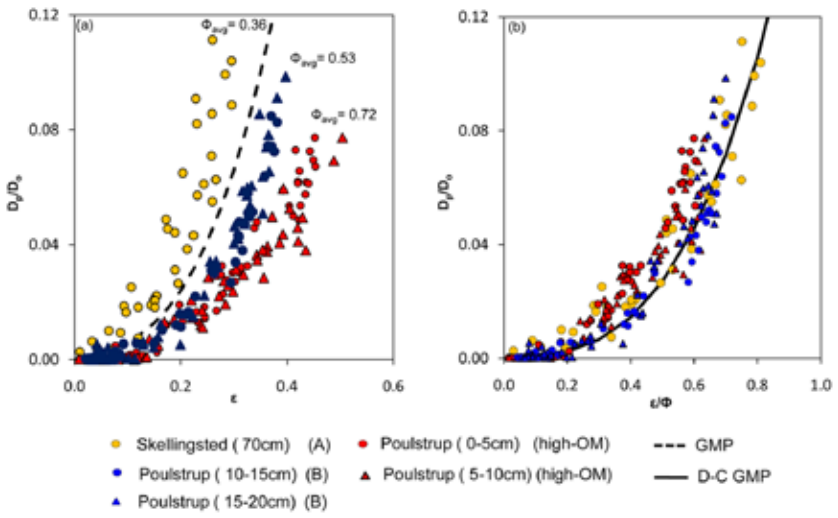


Fig. 5. Measured gas diffusivities ($D_p/D_o$) for two high-porosity and high-organic-matter (OM) soils from Poulstrup at depths of 0 to 5 and 5 to 10 cm (average total porosity $\Phi_{avg} = 0.72$) together with soils used in density-corrected model development: Poulstrup (10–15- and 15–20-cm depths, $\Phi_{avg} = 0.53$) and Skellingsted (70-cm depth, $\Phi_{avg} = 0.36$). Measured $D_p/D_o$ values are shown (a) as a function of air-filled porosity ($\varepsilon$) together with generalized macroporosity (GMP) model (Eq. [13]) predictions (dashed line), and (b) as a function of relative air-filled porosity ($\varepsilon/\Phi$) together with density-corrected (D-C) GMP model (Eq. [14]) predictions (solid line). Data from Kruse et al. (1996), Moldrup et al. (1996), and Poulsen et al. (2001).

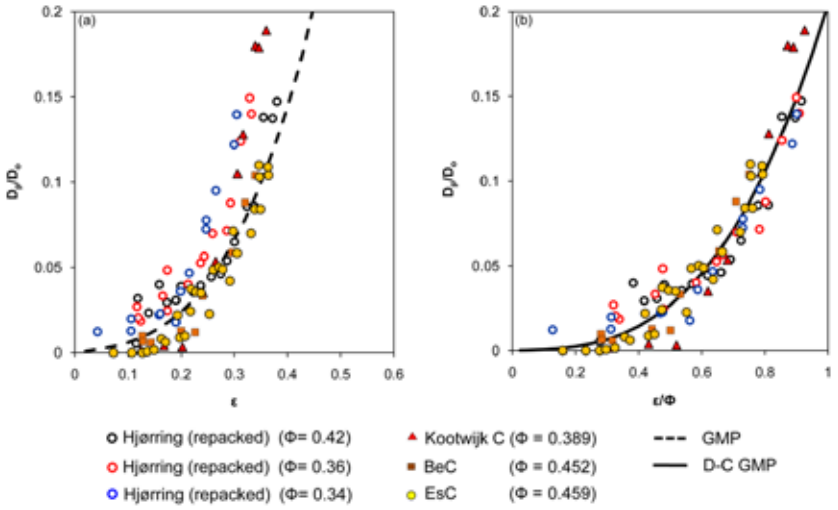


Fig. 6. Tests of new gas diffusivity ($D_p/D_o$) models against two independent data sets: (i) Hjørring soils, repacked at three bulk densities with corresponding total porosities of $\Phi$ = 0.42, 0.36, and 0.34 and (ii) three soils from Freijer (1994): Kootwijk C ($\Phi = 0.389$), BeC ($\Phi = 0.452$), and EsC ($\Phi = 0.459$). The observed $D_p/D_o$ data are shown (a) as a function of air-filled porosity ($\varepsilon$) together with generalized macroporosity (GMP) model (Eq. [13]) predictions (dashed line) and (b) as a function of relative air-filled porosity ($\varepsilon/\Phi$) together with density-corrected (D-C) GMP model (Eq. [14]) predictions (solid line).

## Density-Corrected Air Permeability Model

Following the same approach as for gas diffusivity, we first tested the performance of the macroporosity-based air permeability relation (Eq. [11]) for the soils in Groups A and B under pF 2.0 conditions. We note that at pF 2.0, the $k_a$ values for the soils in Groups C and D were mostly low and highly scattered. The model predictions are in good agreement with the measured data for Groups A and B (Fig. 7a), but the data again showed a tendency to differentiate between dense and less dense soils, as also observed for gas diffusivity (Fig. 3a). Following the same D-C approach as adopted for gas diffusivity, the density-induced differences could be reduced by plotting the observed air permeabilities against the normalized air-filled porosity (Fig. 7b). Modifying Eq. [11] as a function of relative air-filled porosity and assuming the same empirical scaling factor (0.1) as found in the case of gas diffusivity (Eq. [14]) yielded a D-C reference point air permeability model:

$$k_{a,100} = 70\left[2\left(\frac{\varepsilon_{100}}{\Phi}\right)^3 + 0.04\left(\frac{\varepsilon_{100}}{\Phi}\right)\right] \quad [15]$$

To obtain a model for $k_a$ valid not only at pF 2.0, we further assumed the validity of the general power-law model for $k_a(\varepsilon)$, Eq. [9]. Correct estimation of the power-law exponent $\eta$ (Eq. [9]) is essential for accurate predictions of air permeability as a function of air-filled porosity (Kawamoto et al., 2006a). Using the observed reference-point air permeability ($k_{a,100}$) values, we tested the performance of two power-law exponents: $\eta = 2$ as suggested by Moldrup et al. (1998), and $\eta = 1.5$, which can be derived from the analogous gas diffusivity exponent $X = 2.5$ (Eq. [7]) in

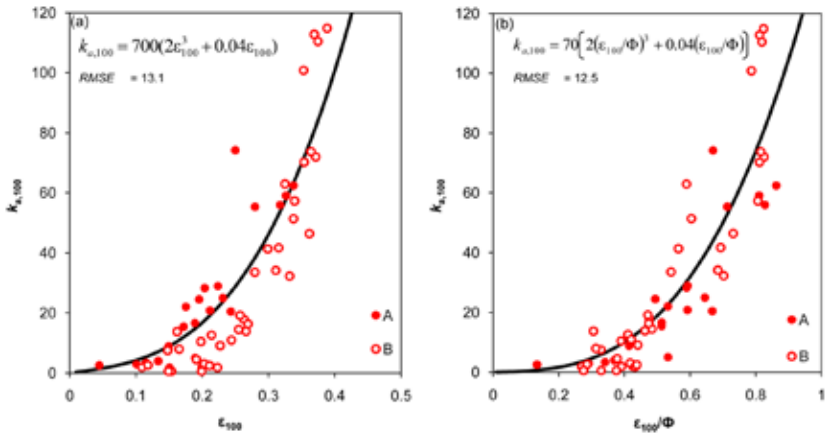


Fig. 7. Measured air permeabilities at −100 cm $H_2O$ matric potential ($k_{a,100}$) for the soils in Groups A and B: (a) as a function of air-filled porosity (ε) with predictions by the macroporosity-based (MP) model, Eq. [11], and (b) as a function of relative air-filled porosity (ε/Φ) with predictions by the density-corrected (D-C) MP model, Eq. [15]. The RMSE values for model performance are also given.

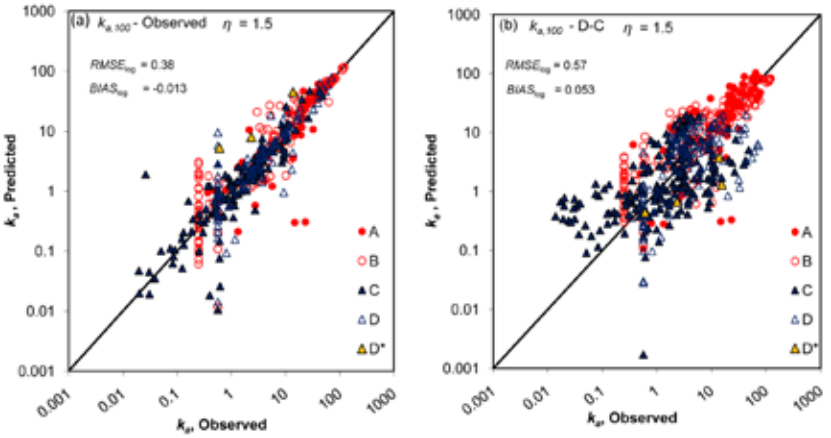


Fig. 8. Scatterplot comparison of predicted and observed air permeabilities ($k_a$). Predictions of $k_a$ are based on the power-law function, Eq. [9], with η = 1.5 and (a) using observed reference-point air permeability ($k_{a,100}$ – Observed) and (b) using predicted reference-point air permeability ($k_{a,100}$ – D-C) by the density-corrected macroporosity model (Eq. [15]). The $RMSE_{log}$ and $bias_{log}$ values calculated using log-transformed $k_a$ data are also given.

combination with Eq. [10]. The results revealed that the power-law $k_a(\varepsilon)$ model performed better with the newly derived exponent of η = 1.5 ($RMSE_{log}$ = 0.38 and $bias_{log}$ = −0.013; Fig. 8a) than with the previously proposed exponent of η = 2.0 ($RMSE_{log}$ = 0.43 and $bias_{log}$ = −0.092; not shown).

Adopting η = 1.5, we tested the performance of Eq. [9] combined with two predictive models for reference-point air permeability ($k_{a,100}$): the macroporosity (MP) model (Eq. [11]) and the density-corrected macroporosity (D-C MP) model (Eq. [15]). The D-C MP model performed better ($RMSE_{log}$ = 0.57 and $bias_{log}$ = 0.053; Fig. 8b) than the MP model ($RMSE_{log}$ = 0.61 and $bias_{log}$ = 0.203; not shown) and hence was a better approach for reference-point ($k_{a,100}$) prediction.

Overall, introducing the D-C approach to air permeability yielded only a minor improvement in $k_{a,100}$ predictions. When used in combination with the power-law model with the newly derived exponent (η = 1.5), however, $k_a$ predictions were significantly improved. Figure 8 further revealed that the power-law $k_a$ model (Eq. [9]) with η = 1.5 yielded more accurate results when used with measured $k_{a,100}$ values (Fig. 8a) than the predicted $k_{a,100}$ values using the D-C MP model (Fig. 8b). We therefore recommend using measured $k_{a,100}$, whenever possible, in Eq. [9]. In the absence of measured $k_{a,100}$ data, however, the D-C MP model can still yield reasonably accurate estimates of $k_{a,100}$.

Finally, we note that advective air flow in soils may preferentially occur through continuous macropores, for example in the presence of continuous structural cracks or wormholes, which cannot generally be explained by the above predictive models. The measurement scale is of great importance in describing such preferential air flow conditions in soils (Iversen et al., 2001) and often cannot be detected at the 100-$cm^3$ sample scale. Thus, macropore and upscaling effects on air permeability are not included in the D-C model and need to be further investigated.

## Extension of New Gas Diffusivity Model to Bimodal Soils

The new models discussed so far are developed for, and hence limited to, relatively structureless (unimodal) soils; however, the occurrence of variably compacted and highly aggregated (bimodal) soils with distinct interaggregate (Region 1) and intraaggregate (Region 2) pore spaces is not uncommon, especially for cultivated high-clay soils. We therefore extended our analysis to two-region soils by testing the new gas diffusivity models (GMP and D-C GMP) against measurements for a sieved and repacked, microaggregated Andisol at two compaction levels (uncompacted and compacted at 200 kPa) (data from Osozawa, 1998).

The observed gas diffusivities as a function of air-filled porosity (Fig. 9) clearly exhibited two-region behavior at both compaction levels, as also implied by the bimodal behavior of the soil-water retention curves (not shown). The predictions of the D-C GMP model (Eq. [14]) based on total porosity failed to capture the dual-porosity characteristics of the observed gas diffusivities and hence could not yield accurate results (shown as a dashed-dotted line in Fig. 9). Therefore, in the case of highly aggregated soils with clear bimodal behavior (e.g., judged from the soil water retention curve),

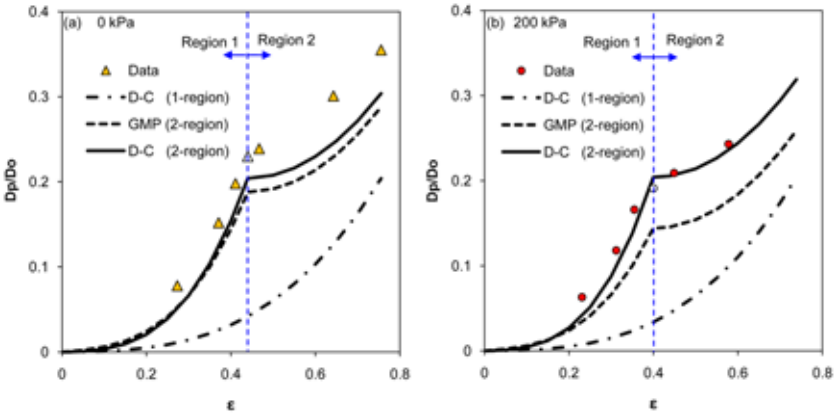


Fig. 9. Soil gas diffusivities ($D_p/D_o$) as a function of air-filled porosity ($\varepsilon$) for repacked, highly aggregated Andisols from Tsukuba, Japan, at two compaction levels: (a) uncompacted (0 kPa) and (b) compacted at 200 kPa. The open symbols represent the corresponding air-filled porosities at pF 3.0 (pF is the negative logarithm of matric potential). Also shown are the predictions of the density-corrected (D-C) model developed for relatively structureless (unimodal) soils, Eq. [14] and the predictions of the new gas diffusivity models extended for two-region soils [GMP (2-region)], Eq. [16] and Eq. [18] (dashed line), and the D-C model for two-region soils, Eq. [17] and Eq. [18] (solid line). The dotted line shown in blue color separates Regions 1 and 2; data from Osozawa (1998).

we suggest that only the D-C models to be used for the predictions in Region 1, using the interaggregate porosity in place of the total porosity. The interaggregate porosity is here considered to be the air-filled porosity at pF 3.0 near which the transition from inter- to intraaggregate pore space occurs on draining (Resurreccion et al., 2010). For the predictions in Region 2, we suggest a Buckingham (1904) type model with no additional input parameters. Thus, the GMP and D-C GMP models extended for the predictions of two-region soils can be written as follows:

For Region 1:

$$\text{GMP model: } \frac{D_p}{D_o} = 2\varepsilon^3 + 0.04\varepsilon \quad (\text{pF} \le 3.0) \qquad [16]$$

D-C GMP model:

$$\frac{D_p}{D_o} = 0.1\left[2\left(\frac{\varepsilon}{\Phi_1}\right)^3 + 0.04\left(\frac{\varepsilon}{\Phi_1}\right)\right] \quad (\text{pF} \le 3.0) \qquad [17]$$

For Region 2:

$$\frac{D_p}{D_o} = \left.\frac{D_p}{D_o}\right|_{\text{pF}=3.0} + (\varepsilon - \Phi_1)^2 \quad (\text{pF} > 3.0) \qquad [18]$$

where $\Phi_1$ is the interaggregate porosity assumed equal to the air-filled porosity measured at pF 3.0 and $D_p/D_o|_{\text{pF}=3.0}$ is the predicted gas diffusivity at pF = 3.0 using either the GMP model (Eq. [16]) or the D-C GMP model (Eq. [17]). With this bimodal approach, the performance of both models significantly improved and the D-C GMP model in particular showed promising results at both compaction levels (Fig. 9a and 9b). A similar two-region extension of the new D-C air permeability model was not examined due to the lack of appropriate data and is therefore a prospect for future research.

## Evaluation of the Density-Corrected Generalized Macroporosity Model Scaling Factor

The 150 soils used to develop the D-C models had total porosities ranging between 0.27 and 0.58 $cm^3\ cm^{-3}$ and the independent tests of the D-C GMP gas diffusivity model showed slight underprediction for the highly porous Poulstrup top layer (0–10 cm) ($\Phi$ = 0.72 $cm^3\ cm^{-3}$; Fig. 5) as well as for uncompacted aggregated soils ($\Phi$ = 0.76 $cm^3\ cm^{-3}$; Fig. 9). Furthermore, for the Poulstrup soils, the very high OM content (average OM = 17%, while the maximum OM content in the soils used to develop the DC model was 4.1%) also probably influenced the observed deviation between the model and the data. This implies that the D-C gas diffusivity model scaling factor (taken as 0.1 in Eq. [14] and [17]) may in reality be a function of the total porosity or the OM content.

Therefore, we examined whether a variable D-C GMP model scaling factor could yield improved D-C GMP model predictions. We assumed the scaling factor to be a linear function of $\Phi$ or OM content, or both, thereby including additional density and soil type effects in the overall model performance. We note that $\Phi$ and OM content are often not independent parameters because highly organic soils typically will have lesser densities and greater total porosities. Making the scaling factor a function of $\Phi$ alone, OM content alone, or both $\Phi$ and OM content did not yield overall improvements in the D-C GMP model performance for the 150 soils. We therefore conclude that using a constant scaling factor of 0.1 in Eq. [14] and [17] seems generally applicable across a wide range of soil types and densities for fairly accurate predictions of $D_p(\varepsilon)$ from only air-filled and total porosities.

For a given soil or soil profile, however, like the differently compacted aggregated Andisol or the Poulstrup soil profile representing a natural depth gradient in OM, an improved site-specific $D_p(\varepsilon)$ model can probably be obtained by making the scaling factor a function of compaction level ($\Phi$), OM content, or both. Because this could allow more accurate predictions of, e.g., climate gas emissions or uptake from vadose zone profiles containing layers of very different densities, textures, and OM contents, it should be further investigated when additional detailed $D_p(\varepsilon)$ and $k_a(\varepsilon)$ data for soil profiles and soil transects representing natural gradients in density, OM content, and clay and silt content become available.

# Conclusions

This study investigated the effect of soil type and density on gas diffusivity and air permeability under typically occurring subsurface moisture conditions (matric potentials between −10 and −500 cm $H_2O$). A significant effect of soil density on both gas transport parameters was observed, together with a less marked effect of soil type. Two D-C models were introduced for gas diffusivity and air permeability, respectively, which performed well across different soil types and density levels compared with existing predictive models.

The D-C approach for air permeability resulted in only a minor improvement in model performance at pF 2.0 (reference point); however, the new D-C-based $k_a$–ε relation at pF 2.0 used in combination with a simple power-law model (developed in analogy with a recent gas diffusivity model) produced improved and reasonably accurate $k_a(\varepsilon)$ predictions.

The new D-C gas diffusivity model was derived and successfully validated for undisturbed soils but adequately described data also for sieved and repacked soil at different compaction levels. The D-C gas diffusivity model was further extended for highly aggregated (two-region or bimodal) media with promising results for an uncompacted and compacted Andisol.

The new predictive D-C models represent a step toward a unified model concept for gas diffusivity and air permeability in undisturbed, variably saturated soils with differing densities and are useful in predicting the subsurface migration and fate of climate gases. In perspective, the new model needs to be tested against data for a wider range of soil water matric potentials and soil types, including peat, forest, and reclaimed wetland soils with typically greater OM contents and thus different soil pore structures and architecture (de Jonge et al., 2009).


## Acknowledgments

This study was made possible by the project Gas Diffusivity in Intact Unsaturated Soil (GADIUS) and the large framework project Soil Infrastructure, Interfaces, and Translocation Processes in Inner Space (Soil-it-is), both from the Danish Research Council for Technology and Production Sciences. We gratefully acknowledge the assistance of the Innovative Research Organization of Saitama University, Japan.


# References


Al Majou, H., A. Bruand, and O. Duval. 2008. The use of in situ volumetric water content at field capacity to improve prediction of soil water retention properties. Can. J. Soil Sci. 88:533–541.

Ball, B.C. 1981. Modeling of soil pores as tubes using gas permeabilities, gas diffusivities, and water release. J. Soil Sci. 32:465–481.

Ball, B.C., and P. Schjønning. 2002. Air permeability. p. 1141–1158. *In* J.H. Dane and G.C. Topp (ed.) Methods of soil analysis. Part 4. SSSA Book Ser. 5. SSSA, Madison, WI.

Bartlett, K.B., and R.C. Harriss. 1993. Review and assessment of methane emissions from wetlands. Chemosphere 26:261–320.

Buckingham, E. 1904. Contributions to our knowledge of the aeration of soils. Bur. Soil Bull. 25. U.S. Gov. Print. Office, Washington, DC.

Campbell, G.S. 1974. A simple method for determining unsaturated conductivity from moisture retention data. Soil Sci. 117:311–314.

Christophersen, M., and P. Kjeldsen. 2001. Lateral gas transport in soil adjacent to an old landfill: Factors governing gas migration. Waste Manage. Res. 19:579–594.

Currie, J.A. 1984. Gas diffusion through soil crumbs: The effects of compaction and wetting. J. Soil Sci. 35:1–10.

Danish Environmental Protection Agency. 2002. Guidelines on remediation of contaminated sites. Environ. Guidelines 7. Danish Ministry of the Environ., Copenhagen.

de Jonge, L.W., P. Moldrup, and P. Schjønning. 2009. Soil infrastructure, interfaces & translocation processes in inner space ("Soil-it-is"): Towards a road map for the constraints and crossroads of soil architecture and biophysical processes. Hydrol. Earth Syst. Sci. 13:1485–1502.

Freijer, J.I. 1994. Calibration of jointed tube model for the gas diffusion coefficient in soils. Soil Sci. Soc. Am. J. 58:1067–1076.

Fujikawa, T., and T. Miyazaki. 2005. Effects of bulk density and soil type on the gas diffusion coefficient in repacked and undisturbed soils. Soil Sci. 170:892–901.

Hamamoto, S., P. Moldrup, K. Kawamoto, and T. Komatsu. 2009a. Effect of particle size and soil compaction on gas transport parameters in variably saturated, sandy soils. Vadose Zone J. 8:1–10.

Hamamoto, S.P. P. Moldrup, K. Kawamoto, P.N. Wickramarachchi, M. Nagamori, and T. Komatsu. 2009b. Extreme compaction effects on gas transport parameters and estimated climate gas exchange for a landfill final cover soil. J. Geotech. Geoenviron. Eng.

Intergovernmental Panel on Climate Change. 2007. Observations: Surface and atmospheric climate change. *In* Climate change 2007: The physical science basis. Cambridge Univ. Press, Cambridge, UK.

Iversen, B.V., P. Moldrup, P. Schjønning, and P. Loll. 2001. Air and water permeability in differently textured soils at two measurement scales. Soil Sci. 166:643–659.

Jin, Y., and W.A. Jury. 1996. Characterizing the dependence of gas diffusion coefficient on soil properties. Soil Sci. Soc. Am. J. 60:66–71.

Kawamoto, K., P. Moldrup, P. Schjønning, B.V. Iversen, T. Komatsu, and D.E. Rolston. 2006a. Gas transport parameters in the vadose zone: Development and tests of power-law models for air permeability. Vadose Zone J. 5:1205–1215.

Kawamoto, K., P. Moldrup, P. Schjønning, B.V. Iversen, D.E. Rolston, and T. Komatsu. 2006b. Gas transport parameters in the vadose zone: Gas diffusivity in field and lysimeter soil profiles. Vadose Zone J. 5:1194–1204.

Klute, A. 1986. Water retention: Laboratory methods. p. 635–662. *In* A. Klute (ed.) Methods of soil analysis. Part 1. 2nd ed. SSSA Book Ser. 5. SSSA, Madison, WI.

Kruse, C.W., P. Moldrup, and N. Iversen. 1996. Modeling diffusion and reaction in soils: II. Atmospheric methane diffusion and consumption in forest soil. Soil Sci. 161:355–365.

Lamandé, M., P. Schjønning, and F.A. Tøgersen. 2007. Mechanical behaviour of an undisturbed soil subjected to loadings: Effects of load and contact area. Soil Tillage Res. 97:91–106.

Liu, G., and B.C. Si. 2008. Multi-layer diffusion model and error analysis applied to chamber-based gas fluxes measurements. Agric. For. Meteorol. 149:169–178.

Marshall, T.J. 1959. The diffusion of gases through porous media. J. Soil Sci. 10:79–82.

Millington, R.J. 1959. Gas diffusion in porous media. Science 130:100–102.

Millington, R.J., and J.M. Quirk. 1960. Transport in porous media. p. 97–106. *In* F.A. Van Beren et al. (ed.) Trans. Int. Congr. Soil Sci., 7th, Madison, WI. 14–21 Aug. 1960. Vol. 1. Elsevier, Amsterdam.

Millington, R.J., and J.M. Quirk. 1961. Permeability of porous solids. Trans. Faraday Soc. 57:1200–1207.

Millington, R.J., and J.M. Quirk. 1964. Formation factor and permeability equations. Nature 202:143–145.

Moldrup, P., C.W. Kruse, D.E. Rolston, and T. Yamaguchi. 1996. Modeling diffusion and reaction in soils: III. Predicting gas diffusivity from the Campbell soil water retention model. Soil Sci. 161:366–375.

Moldrup, P., T. Olesen, H. Blendstrup, T. Komatsu, L.W. de Jonge, and D.E. Rolston. 2007. Predictive-descriptive models for gas and solute diffusion coefficients in variably saturated porous media coupled to pore-size distribution: IV. Solute diffusivity and the liquid phase impedance factor. Soil Sci. 172:741–750.

Moldrup, P., T. Olesen, J. Gamst, P. Schjønning, T. Yamaguchi, and D.E. Rolston. 2000a. Predicting the gas diffusion coefficient in repacked soil: Water-induced linear reduction model. Soil Sci. Soc. Am. J. 64:1588–1594.

Moldrup, P., T. Olesen, T. Komatsu, P. Schjønning, and D.E. Rolston. 2001. Tortuosity, diffusivity, and permeability in the soil liquid and gaseous phases. Soil Sci. Soc. Am. J. 65:613–623.

Moldrup, P., T. Olesen, P. Schjønning, T. Yamaguchi, and D.E. Rolston. 2000b. Predicting the gas diffusion coefficient in undisturbed soil from soil water characteristics. Soil Sci. Soc. Am. J. 64:94–100.

Moldrup, P., T. Olesen, S. Yoshikawa, T. Komatsu, and D.E. Rolston. 2004. Three-porosity model for predicting the gas diffusion coefficient in undisturbed soil. Soil Sci. Soc. Am. J. 68:750–759.

Moldrup, P., T.G. Poulsen, P. Schjønning, T. Olesen, and T. Yamaguchi. 1998. Gas permeability in undisturbed soils: Measurements and predictive models. Soil Sci. 163:180–189.

Moldrup, P., S. Yoshikawa, T. Olesen, T. Komatsu, and D.E. Rolston. 2003. Gas diffusivity in undisturbed volcanic ash soils: Test of soil-water-characteristic-based prediction models. Soil Sci. Soc. Am. J. 67:41–51.

Mosier, A.R. 1998. Soil processes and global change. Biol. Fertil. Soils 27:221–229.

Mualem, Y., and S.P. Friedman. 1991. Theoretical prediction of electrical conductivity in saturated and unsaturated soil. Water Resour. Res. 27:2771–2777.

Osozawa, S. 1998. A simple method for determining the gas diffusion coefficient in soil and its application to soil diagnosis and analysis of gas movement in soil. (In Japanese with English summary.) Ph.D. diss. Bull. 15. Natl. Inst. Agro-Environ. Sci., Ibaraki, Japan.

Penman, H.L. 1940. Gas and vapor movements in soil: The diffusion of vapors through porous solids. J. Agric. Sci. 30:437–462.

Perera, M.D.N., J.P.A. Hettiaratchi, and G. Achari. 2002. A mathematical modeling approach to improve the point estimation of landfill gas surface emissions using the flux chamber technique. J. Environ. Eng. Sci. 1:451–463.

Poulsen, T.G., M. Christophersen, P. Moldrup, and P. Kjeldsen. 2001. Modeling lateral gas transport in soil adjacent to old landfill. J. Environ. Eng. 127:145–153.

Poulsen, T.G., P. Moldrup, M. Christophersen, and P. Kjeldsen. 2003. Relating landfill gas emissions to atmospheric pressure using numerical modelling and state-space analysis. Waste Manage. Res. 21:356–366.

Resurreccion, A.C., K. Kawamoto, T. Komatsu, P. Moldrup, N. Ozaki, and D.E. Rolston. 2007. Gas transport parameters along field transects of a volcanic ash soil. Soil Sci. 72:3–16.

Resurreccion, A.C., T. Komatsu, K. Kawamoto, M. Oda, S. Yoshikawa, and P. Moldrup. 2008. Linear model to predict soil-gas diffusivity from two soil-water retention points in unsaturated volcanic ash soils. Soils Found. 48:397–406.

Resurreccion, A.C., P. Moldrup, K. Kawamoto, S. Hamamoto, D.E. Rolston, and T. Komatsu. 2010. Hierarchical, bimodal model for gas diffusivity in aggregated, unsaturated soils. Soil Sci. Soc. Am. J. 74:481–491.

Rolston, D.E., R.D. Glauz, G.L. Grundmann, and D.T. Louie. 1991. Evaluation of an in situ method for measurement of gas diffusivity in surface soils. Soil Sci. Soc. Am. J. 55:1536–1542.

Rolston, D.E., and P. Moldrup. 2002. Gas diffusivity. p. 1113–1139. *In* J.H. Dane and G.C. Topp (ed.) Methods of soil analysis. Part 4. SSSA Book Ser. 5. SSSA, Madison, WI.

Schjønning, P. 1985. A laboratory method for determination of gas diffusion in soil. (In Danish with English summary.) Rep. S1773. Danish Inst. of Plant and Soil Sci., Tjele.

Schjønning, P., G. Heckrath, and B.T. Christensen. 2009. Threats to soil quality in Denmark: A review of existing knowledge with special emphasis on the EU Soil Thematic Strategy. DJF Rep. Plant Sci. 143. Faculty of Agric. Sci., Aarhus Univ., Tjele, Denmark.

Schjønning, P., and K.J. Rasmussen. 2000. Soil strength and soil pore characteristics for direct-drilled and ploughed soils. Soil Tillage Res. 57:69–82.

Schjønning, P., I.K. Thomsen, J.P. Møberg, H. de Jonge, K. Kristensen, and B.T. Christensen. 1999. Turnover of organic matter in differently textured soils: I. Physical characteristics of structurally disturbed and intact soils. Geoderma 89:177–198.

Schofield, R.K. 1935. The pF of the water in soil. p. 37–48. *In* Trans. World Congr. Soil Sci., 3rd, Oxford, UK. July–Aug. 1935. Vol. 2.

Shimamura, K. 1992. Gas diffusion through compacted sands. Soil Sci. 153:274–279.

Smith, K.A., T. Ball, F. Conen, K.E. Dobbie, J. Massheder, and A. Ray. 2003. Exchange of greenhouse gases between soil and atmosphere: Interactions of soil physical factors and biological processes. Eur. J. Soil Sci. 54:779–791.

Stepniewski, W. 1981. Oxygen diffusion and strength as related to soil compaction. Pol. J. Soil Sci. 12:3–13.

Sumner, M.E. 2000. Handbook of soil science. CRC Press, Boca Raton, FL.

Taylor, S.A. 1949. Oxygen diffusion in porous media as a measure of soil aeration. Soil Sci. Soc. Am. Proc. 14:55–61.

USEPA. 1996. Soil screening guidance: User's guide. 2nd ed. Publ. 9355.4–23. EPA/540/R-96/018. Office of Solid Waste and Emergency Response, USEPA, Washington, DC.

van Genuchten, M.Th. 1980. A closed-form equation for predicting the hydraulic conductivity of unsaturated soils. Soil Sci. Soc. Am. J. 44:892–898.

Verheye, W., and J. Ameryckx. 1984. Mineral fractions and classification of soil texture. Pedalogie 2:215–225.

Werner, D., P. Grathwohl, and P. Hohener. 2004. Review of field methods for the determination of the tortuosity and effective gas-phase diffusivity in the vadose zone. Vadose Zone J. 3:1240–1248.

Xu, X., J.L. Nieber, and S.C. Gupta. 1992. Compaction effect on the gas diffusion coefficient in soils. Soil Sci. Soc. Am. J. 56:1743–1750.

# PAPER II

# Generalized Density-Corrected Model for Gas Diffusivity in Variably Saturated Soils

**T.K.K. Chamindu Deepagoda***
**Per Moldrup**
Dep. of Biotechnology, Chemistry and Environmental Engineering
Aalborg Univ.
Sohngaardsholmsvej 57
DK-9000 Aalborg, Denmark

**Per Schjønning**
Dep. of Agroecology and Environment
Faculty of Agricultural Sciences
Aarhus Univ.
Blichers Allé 20
P.O. Box 50
DK-8830 Tjele, Denmark

**Ken Kawamoto**
**Toshiko Komatsu**
Dep. of Civil and Environmental Engineering
Graduate School of Science and Engineering
Saitama Univ.
255 Shimo-okubo
Sakura-ku, Saitama 338-8570, Japan

**Lis Wollesen de Jonge**
Dep. of Agroecology and Environment
Faculty of Agricultural Sciences
Aarhus Univ.
Blichers Allé 20
P.O. Box 50
DK-8830 Tjele, Denmark

Accurate predictions of the soil-gas diffusivity ($D_p/D_o$, where $D_p$ is the soil-gas diffusion coefficient and $D_o$ is the diffusion coefficient in free air) from easily measureable parameters like air-filled porosity ($\varepsilon$) and soil total porosity ($\phi$) are valuable when predicting soil aeration and the emission of greenhouse gases and gaseous-phase contaminants from soils. Soil type (texture) and soil density (compaction) are two key factors controlling gas diffusivity in soils. We extended a recently presented density-corrected $D_p(\varepsilon)/D_o$ model by letting both model parameters ($\alpha$ and $\beta$) be interdependent and also functions of $\phi$. The extension was based on literature measurements on Dutch and Danish soils ranging from sand to peat. The parameter $\alpha$ showed a promising linear relation to total porosity, while $\beta$ also varied with $\alpha$ following a weak linear relation. The thus generalized density-corrected (GDC) model gave improved predictions of diffusivity across a wide range of soil types and density levels when tested against two independent data sets (total of 280 undisturbed soils or soil layers) representing Danish soil profile data (0–8 m below the ground surface) and performed better than existing models. The GDC model was further extended to describe two-region (bimodal) soils and could describe and predict $D_p/D_o$ well for both different soil aggregate size fractions and variably compacted volcanic ash soils. A possible use of the new GDC model is engineering applications such as the design of highly compacted landfill site caps.

**Abbreviations:** D-C, density-corrected; GDC, generalized density-corrected; MQ, Millington and Quirk; WLR, water-induced linear reduction.

Natural and anthropogenic emissions of greenhouse gases ($CO_2$, $CH_4$, and $N_2O$) from terrestrial soils to the atmosphere have shown a significant increase during the last few decades. Although the contribution of natural sources (e.g., peatlands and forests) to the global greenhouse gas emission is substantial, the striking upward trends during recent decades are probably attributable to anthropogenic sources (e.g., landfills and constructed wetlands). The increased atmospheric concentrations of these gases may give rise to severe, long-term, global and regional environmental problems including global warming and regional climate shifts (Intergovernmental Panel on Climate Change, 2007; Greenhouse Gas Working Group, 2010). Localized environmental issues like indoor and outdoor air pollution may also ensue due to the migration and emission of harmful gaseous-phase contaminants (e.g., radioactive chemicals, volatile organic compounds, etc.) from contaminated soil sites (Nazaroff et al., 1985; Kliest et al., 1989; Fischer et al., 1996). Therefore, the accurate prediction of gas movement in soils will be an essential prerequisite for preventive and mitigative measures for greenhouse gas emissions and also for the implementation of risk-based corrective strategies for the cleanup of polluted soil sites.

The movement of gases in the subsurface and the emission (or uptake) across the soil–atmosphere continuum occurs mainly by diffusion (Buckingham, 1904; Penman, 1940). Soil-gas diffusion is also the key mechanism controlling the soil aeration process whereby soil $O_2$ depleted by plant roots and soil microbial consumption is continuously replenished (Currie, 1965; Russell, 1973). The soil-gas diffusion coefficient, $D_p$ ($cm^2\ s^{-1}$), is the single most important parameter controlling the diffusion of gases in

Soil Sci. Soc. Am. J. 75:1315-1329
Posted online 17 June 2011
doi:10.2136/sssaj2010.0405
Received 22 Oct. 2010.
*Corresponding author (chamindu78@yahoo.com)

soils. Hence, $D_p$ needs to be accurately determined to calculate diffusive gas fluxes in the subsurface (Jin and Jury, 1996; Moldrup et al., 2004). The need for special equipment and the complexity of the measurements, however, make $D_p$ a difficult-to-measure parameter, particularly under uncontrolled in situ conditions (Rolston et al., 1991; Rolston and Moldrup, 2002; Werner et al., 2004). Predictive models are therefore often used to estimate soil-gas diffusivity ($D_p/D_o$, where $D_o$ is the gas diffusion coefficient in free air) from easily measurable parameters such as air-filled porosity ($\varepsilon$) and soil total porosity ($\phi$). Despite the numerous gas diffusivity predictive models available today, simple models exhibiting satisfactory performance for a wide range of soil types, from less organic sandy soils to highly organic peaty soils, under varying soil physical conditions (e.g., at different compaction levels) are a rarity.

Soil compaction was defined by Soane and van Ouwerkerk (1994) as "a process of densification in which porosity and permeability are reduced, strength is increased and many changes are induced in the soil fabric and in various behavior characteristics." Soil compactness, in turn, was defined as "the state which indicates the extent to which compaction processes have influenced the packing of the constituent solid parts of the soil fabric... ." Markedly different compaction levels may result from various processes that occur spatially or temporally in soils, ranging from long-term pedogenetic processes to short-term anthropogenic activities. Consequently, dense soils are likely to occur in natural soil systems (e.g., deep vadose zone profiles) as well as in human-controlled soil systems (e.g., machinery-compacted agricultural fields, engineered landfill caps and embankments). The impact of soil density on soil functional structure may, in turn, have significant effects on gas diffusivity in soils. For example, diffuse emissions of greenhouse gases from landfills, which constitute the third largest source of anthropogenic $CH_4$ emissions worldwide (Peer et al., 1993), are significantly controlled by the commonly compacted covers and caps. Similarly, the relatively high-density soil layers often found beneath buildings may, to a greater extent, determine whether a contaminant gas plume migrating under the building will lead to indoor air pollution, if gas enters into the building, or outdoor air pollution, if the gas is emitted outside the building.

The effect of soil density (or soil compaction) on soil gas diffusivity has been studied in several previous studies (Stepniewski, 1981; Currie, 1984; Xu et al., 1992; Shimamura, 1992; Fujikawa and Miyazaki, 2005; Schjønning et al., 2007; Hamamoto et al., 2009), but progress in incorporating density effects in predictive model development has been limited. By considering soils across a wide range of density levels, Chamindu Deepagoda et al. (2010) recently developed a density-corrected (D-C) model for gas diffusivity, which gave satisfactory performance for typical Danish soils across different land types and management practices (i.e., forests, agricultural fields, landfills, etc.). The D-C model parameters were assumed to be constant values and observed to be generally applicable for the prediction of gas diffusivity for the selected soil types and density levels.

Based on literature data on Dutch and Danish soils spanning a broader interval of soil types from sand to peat, the present study extended the D-C model approach to develop a generalized density-corrected (GDC) model, which gives expanded and improved predictions of soil-gas diffusivity. For the new model development and validation, we used both undisturbed and repacked soils from widely different geographic and land use patterns. By using gas diffusivity data from the literature and this study, we further extended the GDC model to two-region (bimodal) aggregated soils with different aggregate size fractions. A possible use of the new GDC model is for engineering applications such as the design of final landfill caps, where changes in gas diffusivity due to compaction is an important design criterion.

# MATERIALS AND METHODS

## Soils and Data

### Weakly Structured (Unimodal) Soils

For model development and evaluation, we used literature data for both undisturbed and repacked soils representing a broad range of soil textures and density levels. The undisturbed soils were sampled from different horizons in Dutch and Danish soil profiles with a wide geographic contrast. The Dutch soil data were from Freijer (1994) and included eight undisturbed soils sampled from different mineral horizons (Belvedere C, Eijsden C, and Oss C), organic horizons (Speuld O moder and Speuld O mor), and from a sandy soil profile with a vertical organic matter gradient (Kootwijk AE, Kootwijk B, and Kootwijk C). Note that we only considered soils with weak to moderate structure from Freijer (1994) in this study and therefore excluded the soil Harderbos Ah due to its highly structured and aggregated, blocky nature (Freijer, 1994). The Danish data on undisturbed soils were from Andersen (1986), Schjønning and Rasmussen (2000), Kawamoto et al. (2006), and Chamindu Deepagoda et al. (2010). We classified all the undisturbed soils into groups, Groups A through D, based on the soil texture and organic matter content (Table 1). The list of soils belonging to each group is given in Table 1. We finally considered sieved, repacked soils from Denmark (data from Moldrup et al., 2000) at different compaction levels. For soil physical characteristics, see Moldrup et al. (2000).

### Structured, Aggregated (Bimodal) Soils

To investigate the extension of the GDC model to structured (bimodal) soils, we further considered five aggregated soils. First, we considered three aggregated soils from the literature with different particle size fractions: Nakskov (Thorbjørn et al., 2008), Hayden (Grable and Siemer, 1968), and Konosu (Osozawa, 1998). Except for the Konosu soils, we considered at least two aggregate size fractions from each soil. The Hayden soils include five different size fractions and also a mixture thereof, which Grable and Siemer (1968) called "soil." From the Konosu soils, we selected only the fraction <2 mm, but considered two compaction levels: uncompacted and compacted under a uniaxial stress of 200 kPa (Osozawa, 1998).

Next, we included two aggregated volcanic ash soils (Andisols) for which the data were derived from this study: Nishi-Tokyo (cultivated) soil and Nishi-Tokyo (pasture) soil. The Nishi-Tokyo (cultivated) soil was sampled at the 0- to 15-cm depth on a cultivated site and the Nishi-Tokyo (pasture) soil at the 0- to 10-cm depth on a pasture site, both sites belonging to the Field Production Science Center at the University of Tokyo, Japan. The soils (Table 1) were sieved and separated into two to three different size fractions before being repacked in sample cores to the desired bulk densities.

**Table 1. Soil physical characteristics.**

| Soil† | Texture | Clay | Silt | Sand | Organic matter | Total porosity | Interaggregate porosity‡ | Reference |
|---|---|---|---|---|---|---|---|---|
| | | | | | g kg$^{-1}$ | | | |
| | | | | Weakly structured soils | | | | |
| Group A | sand with low organic matter | 1–5 | 0–7 | > 90 | <35 | 0.35–0.50 | – | Freijer (1994), Chamindu Deepagoda et al. (2010) |
| Group B | sand with high organic matter | 1–5 | 0–6 | > 90 | >35 | 0.52–0.55 | – | Schjønning and Rasmussen (2000) |
| | organic soil | – | – | – | >850 | 0.83–0.91 | | |
| Group C | loamy sand, sandy loam, and sandy clay loam | 5–27 | 6–20 | 55–90 | <35 | 0.30–0.54 | – | Freijer (1994), Chamindu Deepagoda et al. (2010), Andersen (1986), Schjønning and Rasmussen (2000) |
| Group D | silt loam | 14–19 | 51–80 | 4–27 | 15–30 | 0.45 | – | Schjønning and Rasmussen (2000), Chamindu Deepagoda et al. (2010) |
| | clay | 56.6 | 21.0 | 22.3 | 2 | 0.50 | – | |
| | | | | Aggregated soils | | | | |
| Nakskov | silt loam | 20.3 | 15.9 | 63.8 | 24 | 0.44 | 0.19 | Thorbjørn et al. (2008) |
| Nishi-Tokyo (pasture) | silt loam | 12.0 | 42.0 | 46.0 | 110 | 0.76 | 0.39 | this study |
| Nishi-Tokyo (cultivated) | silt loam | 12.0 | 42.0 | 46.0 | NA§ | 0.74–0.76 | 0.34–0.41 | this study |
| Hayden | silty clay loam | NA | NA | NA | 68 | 0.63 | 0.42 | Grable and Siemer (1968) |
| Konosu | Andisol | NA | NA | NA | NA | 0.75 | 0.42 | Osozawa (1998) |

† Group A: Kootwijk AE, Kootwijk B, Kootwijk C, Oss C, Skellingsted, Jyndevad, Korntved, and Narita sand; Group B: Poulstrup, Speuld O moder, and Speuld O mor; Group C: Hjørring (except at 400–410-cm depth), Mammen, Gjorslev, Rønhave, Foulum, Ballum, Lerbjerg, Belvedere C, Eijsden C, Askov G4, Askov N6, Foulumgård, Rosklide, Borris 2, and Borris 3; Group D: Højer and Hjørring (400–410-cm depth). Note: each soil is named after the sampling location.

‡ Only applicable to the aggregated soils.

§ NA, not available.

## Measurement Methods

The sampling methods and measurement procedures differed for the different literature studies. For the Danish and Japanese soils, however, including the soils used in this study, similar sampling methods and measurement procedures were used as discussed below. During the sampling of undisturbed soils, 100-cm$^3$ cores were carefully retrieved from the respective soil layers, ensuring minimal soil disturbance; the ends of the cores were capped and stored at 2°C before measurements. For repacked samples, the soils were first sieved to separate the required particle size fractions and carefully packed in 100-cm$^3$ cores to the intended bulk densities. During packing of aggregated soils, particular care was taken not to crush the soil aggregates. The samples were first saturated and then drained sequentially to achieve the desired matric potentials. The different methods and apparatus used for the adjustments of matric potentials have been described in detail in many previous studies (e.g., Rolston and Moldrup, 2002; Kawamoto et al., 2006).

For gas diffusivity measurements, the one-chamber method introduced by Taylor (1950) and developed further by Schjønning (1985) was adopted. Oxygen was used as the experimental gas. The gas diffusion chamber was first flushed with 100% $N_2$ to expel all $O_2$ inside the chamber. Atmospheric air was then allowed to enter the chamber through the soil sample and the increasing concentration of $O_2$ inside the chamber was measured using an $O_2$ electrode attached to the chamber wall. Following the method proposed by Rolston and Moldrup (2002), the binary diffusion coefficient of $O_2$ and $N_2$ was calculated. By using the same gas pair in a different experimental setup, Grable and Siemer (1968) followed a similar approach to calculate the gas diffusion coefficient in repacked Hayden soil aggregates. Note that within the time frame of diffusion experiments, which varies from 2 to 3 h (on wet samples) to several minutes (on dry samples), $O_2$ depletion due to microbial consumption has been observed to be negligible (Schjønning et al., 1999) and was therefore ignored in the calculations.

For the undisturbed Dutch soils, on the other hand, Freijer (1994) used differently sized cores to collect soil samples from different horizons and profiles. The decreasing water contents for gas diffusivity measurements were achieved by stepwise evaporation from saturated samples. For gas diffusivity measurements, Freijer (1994) used $CO_2$ as the experimental gas together with $N_2$ in a two-chamber apparatus initially proposed by Reible and Shair (1982). For more details on sampling, experimental setup, and measurement and calculation procedures, see Freijer (1994). The binary diffusion coefficient of $CO_2$ and $N_2$ in free air is close to that of $O_2$ and $N_2$ (Leffelaar, 1987) and therefore the results from the two methods were assumed to be comparable.

## Statistical Analyses

Two statistical parameters, the RMSE and the bias, were used to evaluate the model performance and for comparing with existing models. The RMSE indicates the overall model fit to the observed data:

$$\mathrm{RMSE}=\sqrt{\frac{1}{n}\sum_{i=1}^{n}\left(d_i\right)^2} \qquad [1]$$

where $d_i$ is the difference between the predicted and observed gas diffusivities for the $n$ number of measurements involved.

The bias evaluates the overall model overprediction (positive bias) or underprediction (negative bias) of the observed data:

$$\mathrm{bias}=\frac{1}{n}\sum_{i=1}^{n}\left(d_i\right) \qquad [2]$$

Because both RMSE and bias have inherent tendencies to put higher weights on larger values than smaller values, we further used two corresponding log-transformed indices, $RMSE_{log}$ and $bias_{log}$, for a more balanced statistical analysis. The $RMSE_{log}$ and $bias_{log}$ can be computed from Eq. [1] and [2], respectively, by taking $d_i$ as the difference between the logarithms of the observed and predicted values.

## RESULTS AND DISCUSSION

### Model Development and Validation

Both soil type and soil density are important parameters controlling gas diffusivity in soils and hence deserve particular attention in relation to predictive model development. The effects of the two parameters on gas diffusivity are expected to differ for undisturbed and repacked soils (Moldrup et al., 2000) due to the inherent differences in their functional pore structures. By considering gas diffusivity measurements for 150 undisturbed soils representing typical soil types and density levels across Denmark, Chamindu Deepagoda et al. (2010) observed a less marked effect of soil type with a more distinct effect of soil density. They further noticed that the density-induced fluctuations observed in a typical $D_p/D_o$ vs. $\varepsilon$ plot could be greatly reduced when gas diffusivity was expressed as a function of the relative air-filled porosity ($\varepsilon/\phi$). Based on these observations, Chamindu Deepagoda et al. (2010) introduced a density-corrected (D-C) model for gas diffusivity as follows:

$$\frac{D_p}{D_o}=0.1\left[2\left(\frac{\varepsilon}{\phi}\right)^3+0.04\left(\frac{\varepsilon}{\phi}\right)\right] =0.2\left(\frac{\varepsilon}{\phi}\right)^3+0.004\left(\frac{\varepsilon}{\phi}\right) \quad [3]$$

in which the constant model parameters were generally applicable for a wide range of soil types and density levels. Notably, at complete air saturation (i.e., $\varepsilon/\phi = 1$), the D-C model essentially reduces to a constant (=0.204) irrespective of the texture and density level of the soil.

Figure 1 shows gas diffusivity data for undisturbed soils taken from different soil profiles in Denmark and also in the Netherlands. The selected soils are widely different with respect to both soil texture (Table 1) and soil density (Fig. 1). Following the D-C approach, the density-induced scatter in gas diffusivity shown in the $D_p/D_o$ vs. $\varepsilon$ plots (Fig. 1a and 1c) could be reduced to a greater extent by expressing $D_p/D_o$ as a function of $\varepsilon/\phi$ (Fig. 1b and 1d). The D-C model predictions are also shown in Fig. 1b and 1d (solid lines) with a particular emphasis on the predicted $D_p/D_o$ at $\varepsilon/\phi = 1$ (denoted by a star). At $\varepsilon/\phi = 1$, the D-C model showed satisfactory estimates of $D_p/D_o$ for less organic soils with moderate-to-high density levels ($\rho_b$ = 1.45–1.61 g cm$^{-3}$). For loose sandy soils with relatively low bulk densities ($\rho_b$ = 1.17–1.30 g cm$^{-3}$), however, and also for highly porous organic and peaty soils with very low bulk densities ($\rho_b$ = 0.15–0.30 g cm$^{-3}$), the D-C model

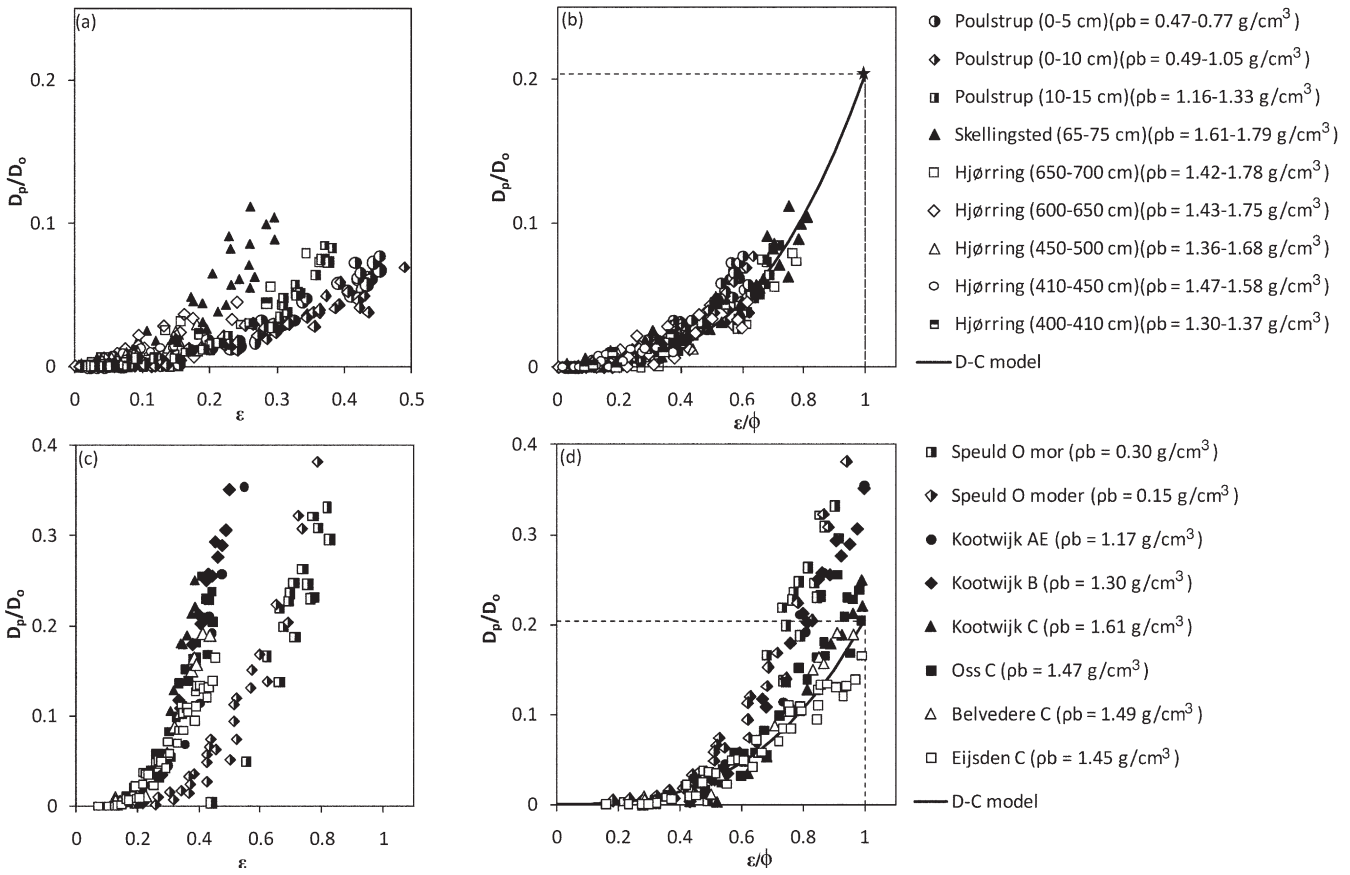


**Fig. 1. The observed gas diffusivities ($D_p/D_o$) for undisturbed soils selected from different soil profiles and horizons in Denmark and the Netherlands with different bulk densities ($\rho_b$). The $D_p/D_o$ are presented as a function of (a, c) air-filled porosity ($\varepsilon$) and (b, d) relative air-filled porosity ($\varepsilon/\phi$), where the density-corrected model (Eq. [3]) predictions are also shown (solid lines) with the predicted $D_p/D_o$ at $\varepsilon/\phi = 1$ denoted by the star. Data from Freijer (1994), Moldrup et al. (1996), and Chamindu Deepagoda et al. (2010).**

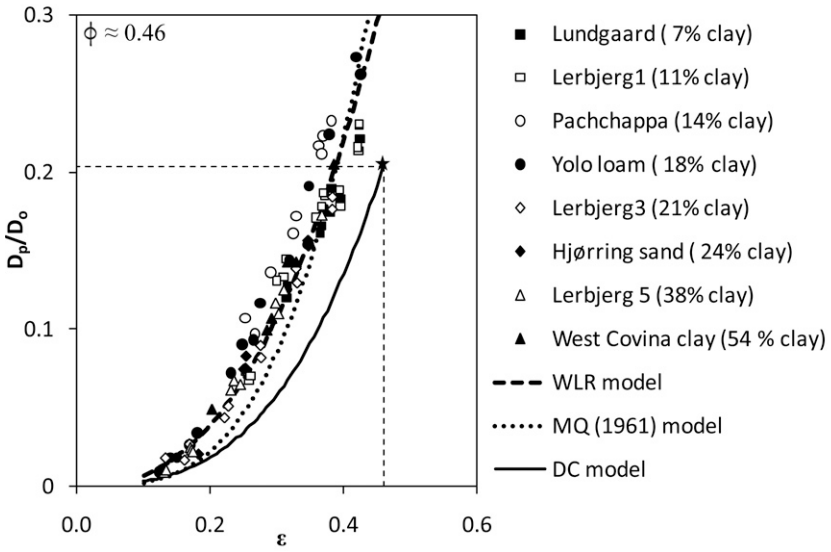


**Fig. 2. Soil-gas diffusivities ($D_p/D_o$) as a function of air-filled porosity (ε) for eight sieved, repacked soils (soil total porosity ϕ ~ 0.46) with different clay contents. Predictions from the water-induced linear reduction (WLR) Marshall model, the Millington and Quirk (MQ) (1961) model, and the density-corrected (D-C) model are also shown; The star denotes the predicted $D_p/D_o$ by the D-C model at ε/ϕ = 1. Data from Moldrup et al. (2000).**

showed a noticeable tendency to underestimate $D_p/D_o$ at ε/ϕ = 1 in combination with poor overall model predictions. This apparently poor performance of the D-C model for highly porous and low-density soils raises the need for a modification to the D-C approach to achieve improved model predictions.

To investigate the soil type effects on repacked soils, we analyzed gas diffusivity data for eight differently textured, sieved and repacked soils from Moldrup et al. (2000) (Fig. 2). The selected soils were repacked to similar bulk densities with an average total porosity of 0.46 $m^3\ m^{-3}$ and hence the density effects played only a minor role in the observed results. Despite the markedly different textures, with clay contents ranging from 0.06 to 0.54 $kg\ kg^{-1}$, no significant variation in gas diffusivity was observed, implying little effect of soil type on gas diffusivity in sieved and repacked soils. This corroborates the observations of Moldrup et al. (1997), who reported that sieved and repacked soils are much less dependent on soil type than undisturbed soils. Schjønning et al. (1999) also made similar observations for soils with widely different soil textures, and noted that disturbed soils have less continuous and more tortuous pore systems than undisturbed soils. The water-induced linear reduction (WLR)–Marshall model (Moldrup et al., 2000), a semiconceptual model particularly developed and recommended for sieved and repacked soils, described well the observed gas diffusivities, while the Millington and Quirk (1961) model, a widely used predictive model for both undisturbed and sieved and repacked soils, showed an underprediction at low air-filled porosities (Table 2, for corresponding model equations). The D-C model (Eq. [3]), which was originally developed for undisturbed soils but also tested on some sieved and repacked soils, also showed a significant underprediction of the results.

Equation [3], when expressed in a generalized form, yields

$$\frac{D_p}{D_o}=\alpha\left(\frac{\varepsilon}{\phi}\right)^{\beta}+\lambda\left(\frac{\varepsilon}{\phi}\right) \qquad [4]$$

where α, β, and λ are variable model parameters that potentially have promising links to soil type and density. In fact, when appropriate parameter values are assigned for α, β, and λ, Eq. [4] can represent most of the classical and recent predictive models for

**Table 2. Classical and recent gas diffusivity ($D_p/D_o$) models following the generalized density-corrected (GDC) model (Eq. [4]).**

| Model | Equation† | $\alpha(\varepsilon/\phi)^{\beta}+\lambda(\varepsilon/\phi)$‡ | |
|---|---|---|---|
| | | β | λ |
| Buckingham (1904) | $D_p/D_o=\varepsilon^2$ | 2 | 0 |
| Penman (1940) | $D_p/D_o=0.66\varepsilon$ | 1 | 0 |
| Millington (1959) | $D_p/D_o=\varepsilon^{4/3}$ | 1.33 | 0 |
| Marshall (1959) | $D_p/D_o=\varepsilon^{1.5}$ | 2.5 | 0 |
| Millington and Quirk (1960) | $D_p/D_o=\varepsilon^2/\phi^{2/3}$ | 2 | 0 |
| Millington and Quirk (1961) | $D_p/D_o=\varepsilon^{10/3}/\phi^2$ | 3.33 | 0 |
| Moldrup et al. (2000) (WLR§–Marshall) | $D_p/D_o=\varepsilon^{1.5}(\varepsilon/\phi)$ | 2.5 | 0 |
| Hamamoto et al. (2009) | $D_p/D_o=\varepsilon^{X}(\varepsilon/\phi)^{N}$ | $X+N$ | 0 |
| Chamindu Deepagoda et al. (2010) (density-corrected) | $D_p/D_o=0.1[2(\varepsilon/\phi)^3+0.04(\varepsilon/\phi)]$ | 3 | 0.004 |
| This study (unimodal GDC) | $D_p/D_o=0.5\phi\ (\varepsilon/\phi)^{\beta}$ | 3 or β (α) | 0 |

† ε, air-filled porosity; ϕ, total porosity.

‡ α, β, and λ are GDC model parameters (Eq. [4]).

§ WLR, water-induced linear reduction.

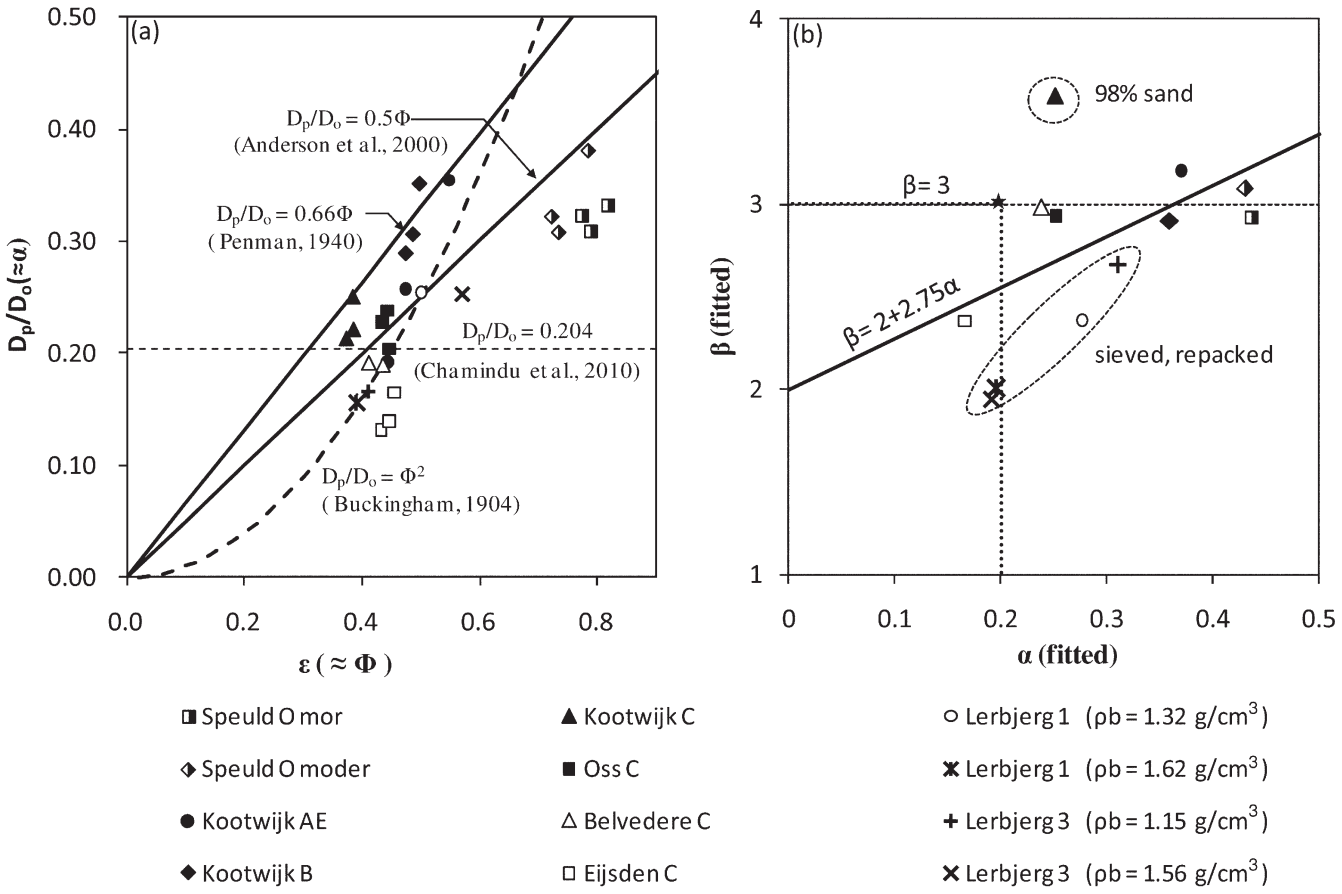


**Fig. 3. (a) Selected soil-gas diffusivity ($D_p/D_o$) measurements against air-filled porosity (ε): three measurements at or close to the driest conditions (ε ~ soil total porosity Φ) for eight undisturbed soils (data from Freijer, 1994) and one measurement under completely dry conditions (ε = Φ) for four sieved, repacked soils at different bulk densities ($\rho_b$) (data from Moldrup et al., 2000), along with predictions from the Buckingham (1904), Penman (1940), Anderson et al. (2000), and density-corrected (D-C) models; (b) for the same soils, variation of model parameters β as a function of α by fitting both the parameters in Eq. [5], with a solid line denoting a linear relation describing β as a function of α, and the star denotes (approximately) the D-C model.**

gas diffusivity (Table 2). By setting λ = 0, as is the case for most of the predictive models (except the D-C model) shown in Table 2, Eq. [4] simplifies to a two-parameter model:

$$\frac{D_p}{D_o} = \alpha\left(\frac{\varepsilon}{\phi}\right)^{\beta} \qquad [5]$$

where α represents the $D_p/D_o$ at ε/ϕ = 1 and is a function of ϕ in many previous models. The model shape factor, β, was assigned a constant in all of the above models (Table 2). Revisiting Fig. 1d reveals, however, as we justify from the results of this study discussed below, that a larger α tends to yield a larger β and vice versa, implying that β is likely to be a function of α and will thus also become a function of ϕ if α, as expected, is related to ϕ.

To further examine the possible α–ϕ and α–β relations, we considered 12 soils from the literature: eight undisturbed soils (data from Freijer, 1994) and four sieved and repacked soils (data from Moldrup et al., 2000) (Fig. 3). From each undisturbed soil, we selected three $D_p/D_o$ data points measured at the closest proximity to the completely dry condition (i.e., $D_p/D_o$ measured at and near ε = ϕ, and therefore $D_p/D_o \sim \alpha$). Except for the two peat soils (i.e., Speuld O moder and Speuld O mor), the selected measurements were made at air-filled porosities within 95 to 100% of the total porosity (i.e., at ε > 0.95ϕ). For the two peat soils, however, due to shrinkage issues under dry conditions, the last three reliable measurements were available at ε = 0.85ϕ ~ 0.95ϕ. In addition, from each repacked soil, we selected $D_p/D_o$ measurements at ε = ϕ. The variation of $D_p/D_o$ (~α) against ε (~ϕ) for the selected soils is illustrated in Fig. 3a together with predictions from four existing predictive models: Buckingham (1904), Penman (1940), Anderson et al. (2000), and Chamindu Deepagoda et al. (2010). Near ϕ = 0.4 $m^3\ m^{-3}$ representing medium density levels, the Buckingham (1904), Anderson et al. (2000), and Chamindu Deepagoda et al. (2010) models yielded, on average, promising predictions, while the Penman (1940) model appeared to give an upper-limit estimation. For the highly porous peat soils with very low densities (ϕ = 0.7–0.8 $m^3\ m^{-3}$), however, the Chamindu Deepagoda et al. (2010) model significantly underpredicted the observed data, while the Buckingham (1904) and Penman (1940) models clearly overpredicted. Of the four considered models, the Anderson et al. (2000) model yielded the best results. Note that of the six selected measurements for the two peat soils, only the measurement at ε = 0.95ϕ (the half-shaded diamond close to the $D_p/D_o$ = 0.5ϕ line in Fig. 3a) was in good agreement with the Anderson et al. (2000) model. The apparent slight overprediction of the remaining five data points measured at ε = 0.85ϕ to 0.90ϕ by the Anderson et al. (2000) model is therefore largely due to the

measurement limitations. Due to its overall good performance, we reintroduce the linear relation by Anderson et al. (2000) to establish the $\alpha$–$\phi$ relation as follows:

$$\alpha = 0.5\phi \quad [6]$$

We further examined the relationship between $\alpha$ and $\beta$ by fitting both parameters in Eq. [5] to the observed data (Fig. 3b). In Fig. 3b, we also show the D-C model with $\beta \sim 3$ (Eq. [3] with the second term omitted) for comparison (denoted by a star). Of the eight soils considered from Freijer (1994), six soils (excepting Eijsden C and Kootwijk C) also suggested $\beta = 3$ as a good approximation. A distinct outlier is Kootwijk C (encircled with a dashed line in Fig. 3b), a highly compacted sandy soil ($\rho_b$ = 1.61 g cm$^{-3}$, 98% sand) with a negligible amount of organic matter, which had a very large $\beta$ value even at an average $\alpha$.

Smaller $\beta$ values were observed for the four sieved, repacked soils (marked with a dashed line in Fig. 3b), with $\beta$ values tending to increase with increasing $\alpha$ values. Overall, an apparent linear relation was observed between $\alpha$ and $\beta$, a trend that can be adequately described by a linear function:

$$\beta = 2 + 2.75\alpha \quad [7]$$

Substituting $\alpha$ from Eq. [6] into Eq. [7] yields

$$\beta = 2 + 1.38\phi \quad [8]$$

This formulates an important parameter link in the present modeling approach. Finally, by combining Eq. [5] and [6], together with the two $\beta$ values, $\beta = 3$ and $\beta(\phi)$ (Eq. [8]), we further tested two generalized density-corrected (GDC) gas diffusivity models:

$$\frac{D_p}{D_o} = 0.5\phi\left(\frac{\varepsilon}{\phi}\right)^3 \quad [9a]$$

and

$$\frac{D_p}{D_o} = 0.5\phi\left(\frac{\varepsilon}{\phi}\right)^{2+1.38\phi} \quad [9b]$$

Figure 4 shows $D_p/D_o$ plotted against the relative air-filled porosity ($\varepsilon/\phi$) for six selected soils from Freijer (1994), together with predictions from three models: the GDC (fitted) model (Eq. [5] with fitted $\alpha$ and $\beta$; solid line), the GDC (predicted) model (Eq. [9b]; dashed line), and the D-C model (Eq. [3]; dotted line). We note that the predictions from Eq. [9a] (not shown) did not improve the results compared with Eq. [9b] and therefore we limited the analysis to Eq. [9b] for GDC model predictions. Compared with the D-C model, the GDC (predicted) model showed improved predictions for the two peat soils (Speuld O mor and Speuld O moder; Fig. 4a and 4b), and for the highly organic sandy soil (Kootwijk AE; Fig. 4c). For the less organic sandy soil (Oss C; Fig. 4d) and the two silt loams (Eijsden C and Belvedere C; Fig. 4e and 4f), both the GDC (predicted) and D-C models yielded equally good predictions.

To further test the GDC model performance, we considered two independently measured gas diffusivity data sets, 280 measurements in all, on less structured, undisturbed Danish soils. Data set I included 150 measurements (data from Chamindu Deepagoda et al., 2010), and Data Set II included 130 measurements (data from Andersen, 1986; Schjønning and Rasmussen, 2000). The data in Fig. 5 are classified into four groups (Groups A–D) according to soil texture and organic matter content (see Table 2). The two scatter plots (in a log–log coordinate system) in Fig. 5 shows the predicted and measured $D_p/D_o$ for two predictive models: the Millington and Quirk (1961) model (Fig. 5a) and the GDC model, Eq. [9b] (Fig. 5b). The Millington and Quirk (1961) model exhibited a slight overprediction under relatively dry conditions and a marked underprediction under wet conditions, a commonly noticed negative feature of the model reported in many previous studies (Kawamoto et al., 2006; Resurreccion et al., 2007). The GDC model showed a very good overall performance. Table 3 shows a detailed statistical comparison of the five predictive models against the two individual data sets, including the GDC model, the Millington and Quirk (1961) model, and three other predictive models: the Millington and Quirk (1960) model, the WLR–Marshall model, and the D-C model. We also ran the GDC model with $\beta = 3$ (Eq. [9a]) for comparison. Note that the two GDC models performed equally well for larger $D_p/D_o$ values, but the model with $\beta = 2 + 2.75\alpha$ (Eq. [9b]) performed better for smaller $D_p/D_o$ values (with smaller $RMSE_{log}$ and $bias_{log}$). Compared with other predictive models, the GDC model (Eq. [9b]) yielded lower values in both statistical parameters and in both linear and log-transformed forms, showing a good accuracy. The GDC model was outperformed only by the D-C model, particularly for Data Set I, which was used to calibrate the D-C model by Chamindu Deepagoda et al. (2010). Note that both data sets included relatively low-organic soils and moderate density levels, for which both the D-C model and the GDC model are expected to perform equally well. We await further data on highly organic soils and soils with very low density levels for a more thorough test of the GDC model.

## Extension of the Generalized Density-Corrected Model to Structured, Two-Region Soils

The foregoing discussion on model development was limited to less structured soils that exhibited typical one-region behavior in relation to gas diffusivity. Accurate prediction of gas diffusivity in structured, two-region soils is of equal importance, however, due to the wide occurrence of such soils in differently structured vadose zones.

The GDC model concept extended to encompass soils with two distinct regions (denoted as Region 1 and Region 2) presumes that gas diffusivity behaviors in the individual regions are functionally independent and mathematically additive. Thus, the one-region GDC model (Eq. [4]) can be commonly extended to describe two-region porous media as follows:

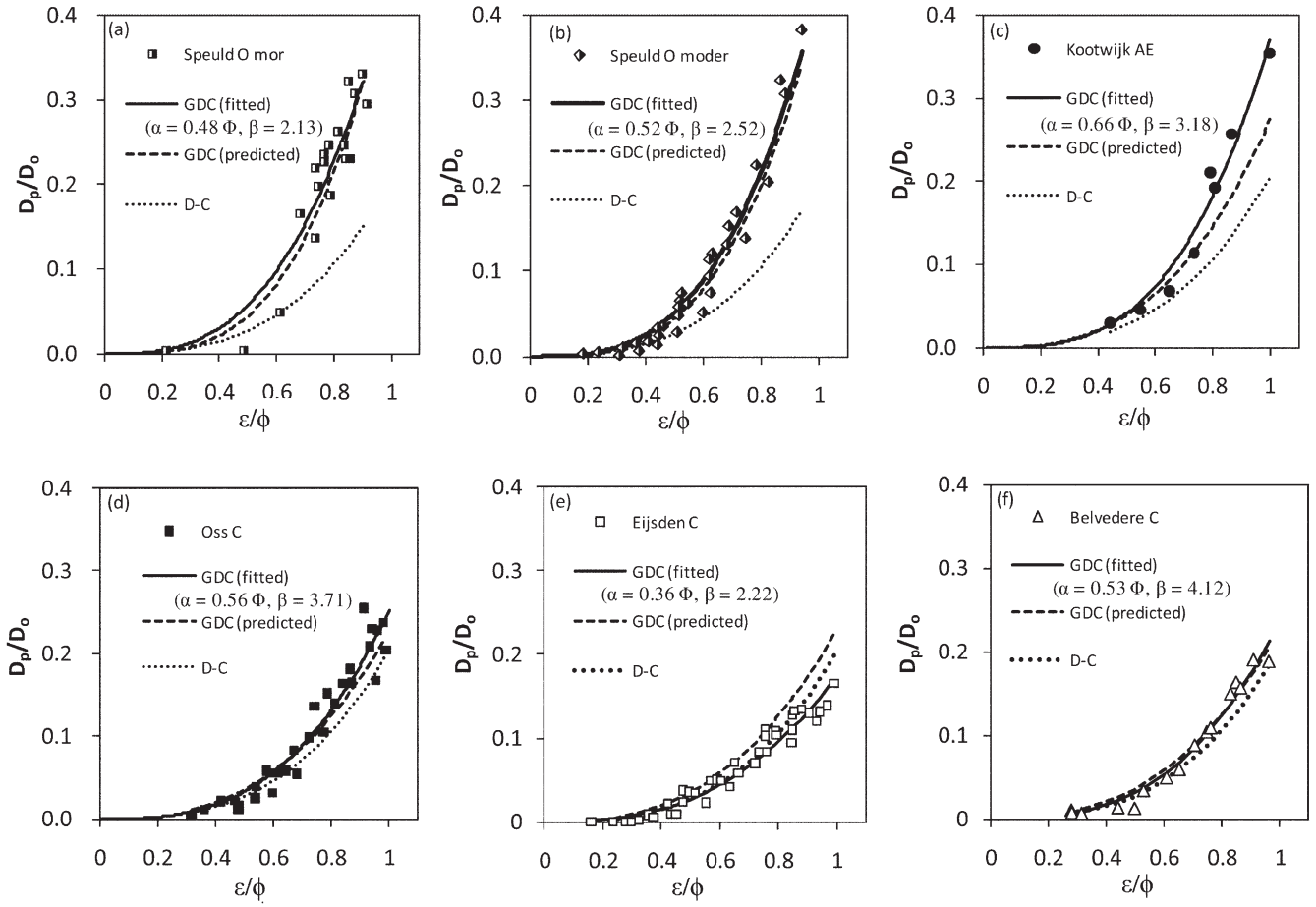


**Fig. 4. Measured soil-gas diffusivities ($D_p/D_o$) as a function of relative air-filled porosity ($\varepsilon/\phi$) for six selected soils with predictions from three models: the generalized density-corrected GDC (fitted) model (Eq. [4]; solid line), the GDC (predicted) model (Eq. [9b]; dashed line), and the density-corrected (D-C) model (Eq. [3]; dotted line). Data from Freijer (1994).**

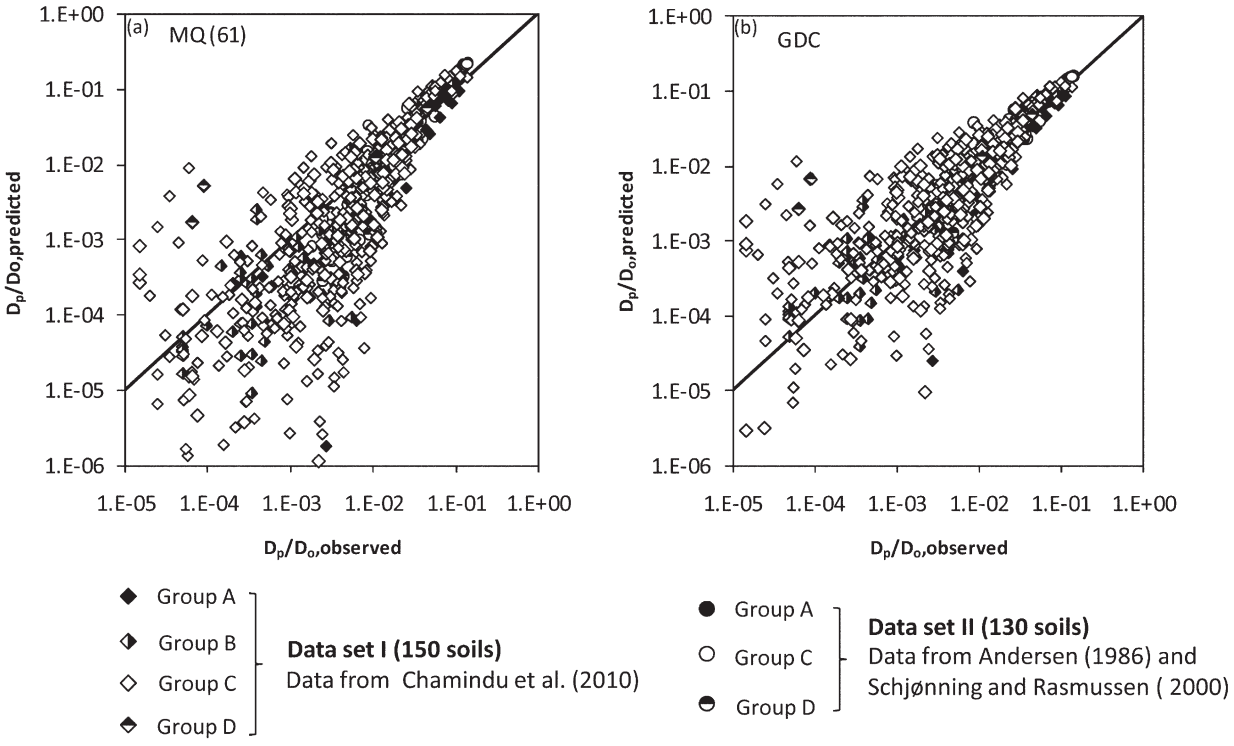


**Fig. 5. Scatter-plot comparison of predicted and measured gas diffusivities ($D_p/D_o$) for two predictive models: (a) the Millington and Quirk (1961) model and (b) the generalized density-corrected (GDC) model (Eq. [9b]). The data include 280 undisturbed soils representing the four groups (Groups A–D, Table 1) from two selected data sets.**

**Table 3. Independent test of predictive soil-gas diffusivity models against measured data for intact soils. For each predictive model, the two statistical parameters, RMSE (Eq. [1]) and bias (Eq. [2]), and their log-transformed forms are also given.**

| Model† | Equation‡ | Data set I (150 soils) | | | | Data set II (130 soils) | | | |
|---|---|---|---|---|---|---|---|---|---|
| | | RMSE | $RMSE_{log}$ | Bias | $Bias_{log}$ | RMSE | $RMSE_{log}$ | Bias | $Bias_{log}$ |
| Millington and Quirk (1960) | $D_p/D_o = \varepsilon^2/\phi^{2/3}$ | 0.047 | 0.77 | 0.029 | 0.56 | 0.049 | 0.45 | 0.036 | 0.43 |
| Millington and Quirk (1961) | $D_p/D_o = \varepsilon^{10/3}/\phi^2$ | 0.017 | 0.77 | 0.005 | −0.31 | 0.021 | 0.36 | 0.006 | −0.16 |
| WLR–Marshall | $D_p/D_o = \varepsilon^{1.5}(\varepsilon/\phi)$ | 0.026 | 0.59 | 0.013 | 0.17 | 0.025 | 0.23 | 0.015 | 0.14 |
| Density corrected | $D_p/D_o = 0.1[2(\varepsilon/\phi)^3 + 0.04(\varepsilon/\phi)]$ | 0.008§ | 0.49§ | −0.001§ | −0.001§ | 0.008 | 0.22 | −0.001 | −0.091 |
| GDC (unimodal, $\beta = 3$) | $D_p/D_o = 0.5\phi(\varepsilon/\phi)^3$ | 0.008 | 0.72 | −0.0005 | −0.26 | 0.007 | 0.32 | −0.001 | −0.18 |
| GDC (unimodal, $\beta = 2 + 2.75\alpha$) | $D_p/D_o = 0.5\phi(\varepsilon/\phi)^{2+2.75\alpha}$ | 0.009 | 0.57 | −0.003 | −0.0004 | 0.010 | 0.21 | 0.004 | −0.001 |

† WLR, water-induced linear reduction; GDC, generalized density corrected.

‡ $\varepsilon$, air-filled porosity; $\phi$, total porosity; $\alpha$ and $\beta$, GDC model parameters (Eq. [5]).

§ Data set used to calibrate the density-corrected model in Chamindu Deepagoda et al. (2010).

Region 1

$$\frac{D_p}{D_o}=\alpha_1\left(\frac{\varepsilon}{\phi_1}\right)^{\beta_1}+\lambda_1\left(\frac{\varepsilon}{\phi_1}\right);\quad \varepsilon\le\phi_1 \qquad [10a]$$

Region 2

$$\frac{D_p}{D_o}=(\alpha_1+\lambda_1)+\alpha_2\left(\frac{\varepsilon-\phi_1}{\phi_2}\right)^{\beta_2}+\lambda_2\left(\frac{\varepsilon-\phi_1}{\phi_2}\right);\quad \phi_1\le\varepsilon\le\phi \qquad [10b]$$

where $\alpha$, $\beta$, and $\lambda$ with subscripts 1 and 2 represent the corresponding model parameters in Regions 1 and 2, respectively, and $\phi_1$ and $\phi_2$ ($=\phi - \phi_1$) are the porosities associated with Regions 1 and 2, respectively.

To investigate the possible extension of the GDC model to bimodal media, we included $D_p/D_o$ data from this study and from the literature for five aggregated soils (Table 1) with different aggregate size fractions. Among the distinguishing features of aggregated soils compared with the former structureless (or weakly structured) soils is the bimodal pore size distribution, with two distinctly separate regions. Figure 6, for example, shows the pore size distribution curves for two aggregate size fractions of Nishi-Tokyo (cultivated) soils: 0 to 2 and 2 to 4.76 mm. The two distinct peaks observed for each size fraction clearly denote two separate regions: the interaggregate region (Region 1) and the intraaggregate region (Region 2). The two regions are separated in the pore size (diameter) ranges of 3 to 9 μm, which corresponds to a matric potential of pF 3.0 to 2.5 (pF = log|−ψ|, where ψ is the soil matric potential in centimeters of $H_2O$; after Schofield, 1935). This is in good agreement with the observations in previous studies, for example Schjønning (1992), who observed a bimodal pore size distribution for a number of Danish soils, typically with a boundary between two regions near 3 to 30 μm (i.e., pF 3–2). In this study, we assumed pF 3 as the boundary between the two regions for all aggregated soils for the calculations of inter- and intraaggregate porosities.

When an aggregated soil sample is saturated and sequentially drained under increasing matric suction, water held in larger pores, i.e., the pores in the interaggregate region or Region 1 (see Fig. 6), starts draining first. Gas diffusion essentially takes place only in Region 1 until all the interaggregate pores are completely drained because the intraaggregate pores (with relatively smaller pore diameters) remain water filled and hence do not contribute to gas diffusion. Gas diffusion within Region 1 of an aggregated soil is, therefore, conceptually analogous to the gas diffusion in a structureless soil (sand, for example), which has a total porosity ($\phi$) equivalent to the interaggregate porosity ($\phi_1$) of the aggregated soil. Following this conceptual analogy, which we further justify from the model results below, we use the extended two-region GDC model for Region 1 (Eq. [10a]), together with the one-region GDC model (Eq. [5–7]), to describe the gas diffusivity for Region 1 in aggregated soils:

$$\frac{D_p}{D_o}=\alpha_1\left(\frac{\varepsilon}{\phi_1}\right)^{\beta_1};\quad \varepsilon\le\phi_1 \qquad [11a]$$

where

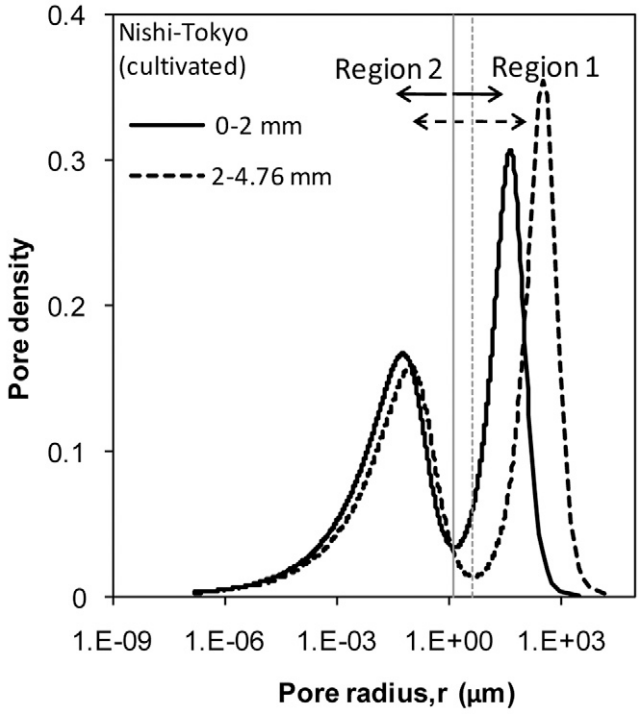


**Fig. 6. Bimodal pore size distribution (PSD) curves for two aggregate size fractions, 0 to 2 mm (solid line) and 2 to 4.76 mm (dashed line), of the sieved, repacked aggregated Nishi-Tokyo (cultivated) soil. The two vertical lines separate the interaggregate region (Region 1) from the intraaggregate region (Region 2) for each size fraction.**

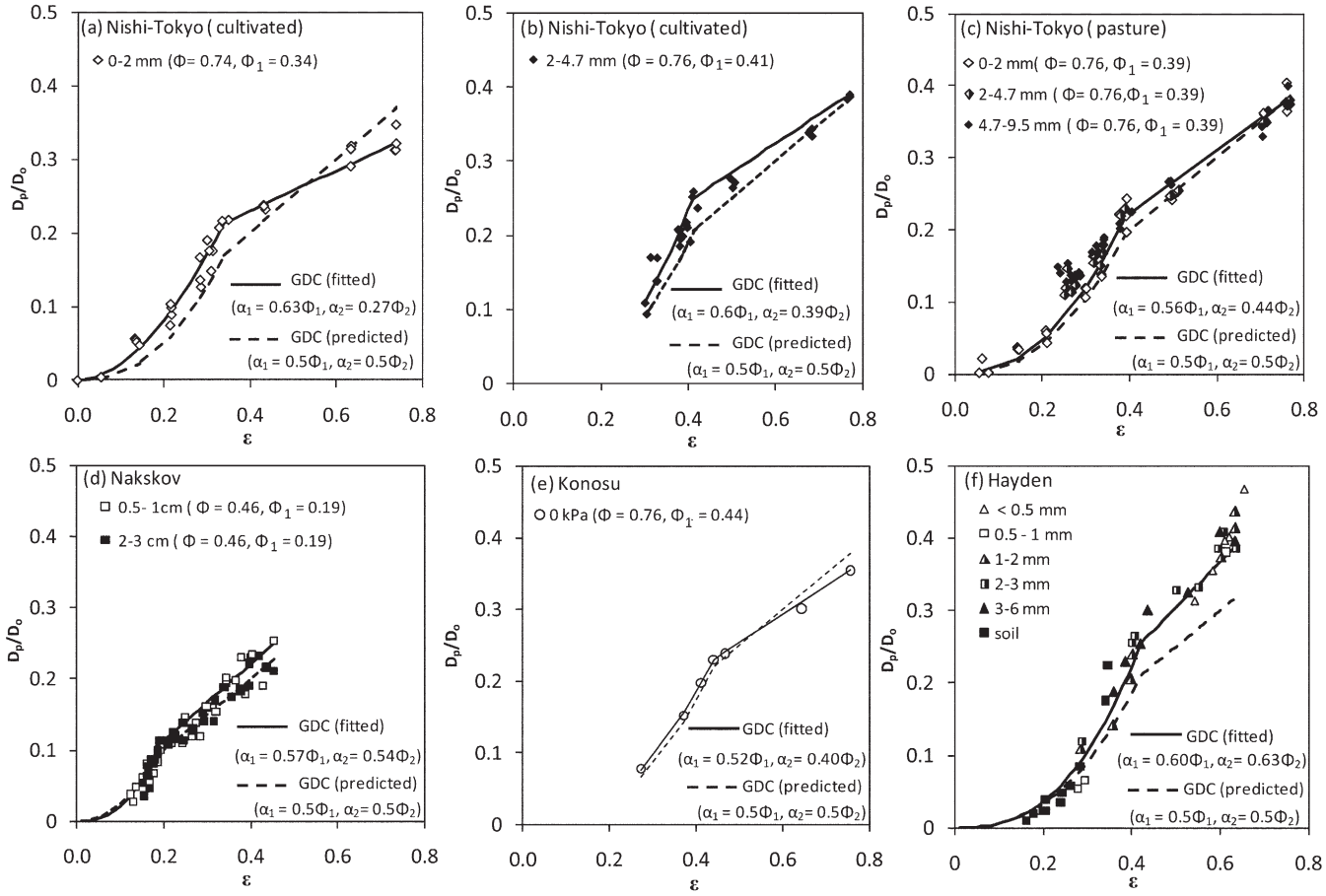


**Fig. 7. Measured gas diffusivities ($D_p/D_o$) as a function of air-filled porosity (ε) for six aggregated soils with different aggregate size fractions. Predictions from two generalized density-corrected (GDC) models are also shown: (i) GDC (fitted) model (solid line) using calculated model parameters $\alpha_1$ (= $D_p/D_o|_{\varepsilon=\phi 1}$; Eq. [11a]) and $\alpha_2$ (= $D_p/D_o|_{\varepsilon=\phi 1} - D_p/D_o|_{\varepsilon=\phi}$; Eq. [12a]) with best-fit parameter β, and (ii) GDC (predicted) model**

$$\alpha_1 = 0.5\phi_1 \qquad [11b]$$

and

$$\beta_1 = 2 + 2.75\alpha_1 \qquad [11c]$$

Further increases in matric suction in the aggregated soil sample cause the aggregates to drain, allowing gas diffusion to occur also in the intraaggregate pore region (Region 2). Within Region 2, gas diffusivity can be adequately described as a linear increase with increasing air-filled porosity (ε), as many previous studies have reported (e.g., Resurreccion et al., 2010). Therefore, by setting values for $\beta_2$ and $\lambda_2$ of 1 and 0, respectively, in Eq. [10b], the extended GDC model for Region 2 can be written as

$$\frac{D_p}{D_o} = \alpha_1 + \alpha_2\left(\frac{\varepsilon - \phi_1}{\phi_2}\right); \quad \phi_1 \le \varepsilon \le \phi \qquad [12a]$$

where $\alpha_2$, according to the GDC approach, becomes a linear function of intraaggregate porosity, $\phi_2$ (=$\phi - \phi_1$). In a generalized form, $\alpha_2$ can be expressed as

$$\alpha_2 = A\phi_2 \qquad [12b]$$

where $A$ (≤1) is a constant. If an analogous relation is assumed also for $\alpha_1$ (i.e., $\alpha_1 = A\phi_1$), Eq. [12a] reduces to a simple equation:

$$\frac{D_p}{D_o} = A\phi_1 + A\phi_2\left(\frac{\varepsilon - \phi_1}{\phi_2}\right) = A\varepsilon; \quad \phi_1 \le \varepsilon \le \phi \qquad [12c]$$

Equation [12c], despite its simplicity, has been proposed in several previous studies for gas diffusivity predictions in Region 2. For example, Grable and Siemer (1968) proposed a value for $A$ of 0.66 (analogous to the Penman [1940] model) and Resurreccion et al. (2010) a value of 0.5 (analogous to the Anderson et al. [2000] model).

Figure 7 shows the variation of gas diffusivity ($D_p/D_o$) as a function of ε for five different aggregated soils. The data for two of the aggregated soils, Nishi-Tokyo (cultivated) (Fig. 7a and 7b) and Nishi-Tokyo (pasture) (Fig. 7c), came from this study, while the data for the other three soils came from the literature: Nakskov (data from Thorbjørn et al., 2008; Fig. 7d), Konosu (data from Osozawa, 1998; Fig. 7e), and Hayden (data from Grable and Siemer, 1968; Fig. 7f). Two to five different size fractions were considered from all soils, except for the microaggregated Konosu soil from which only one size fraction (0–2 mm) at two compaction levels, uncompacted (Fig. 7e) and compacted at 200 kPa (not shown), was considered. Also shown in Fig. 7 are the predictions from the GDC (fitted) model (solid line) and the GDC (predicted) model (dashed line). For the GDC (fitted) model, we used calculated $\alpha_1$ (= $D_p/D_o|_{\varepsilon=\phi_1}$; Eq. [11a]) and $\alpha_2$ (= $D_p/D_o|_{\varepsilon=\phi_1} - D_p/D_o|_{\varepsilon=\phi}$; Eq. [12a]) values from the observed data with best-fit

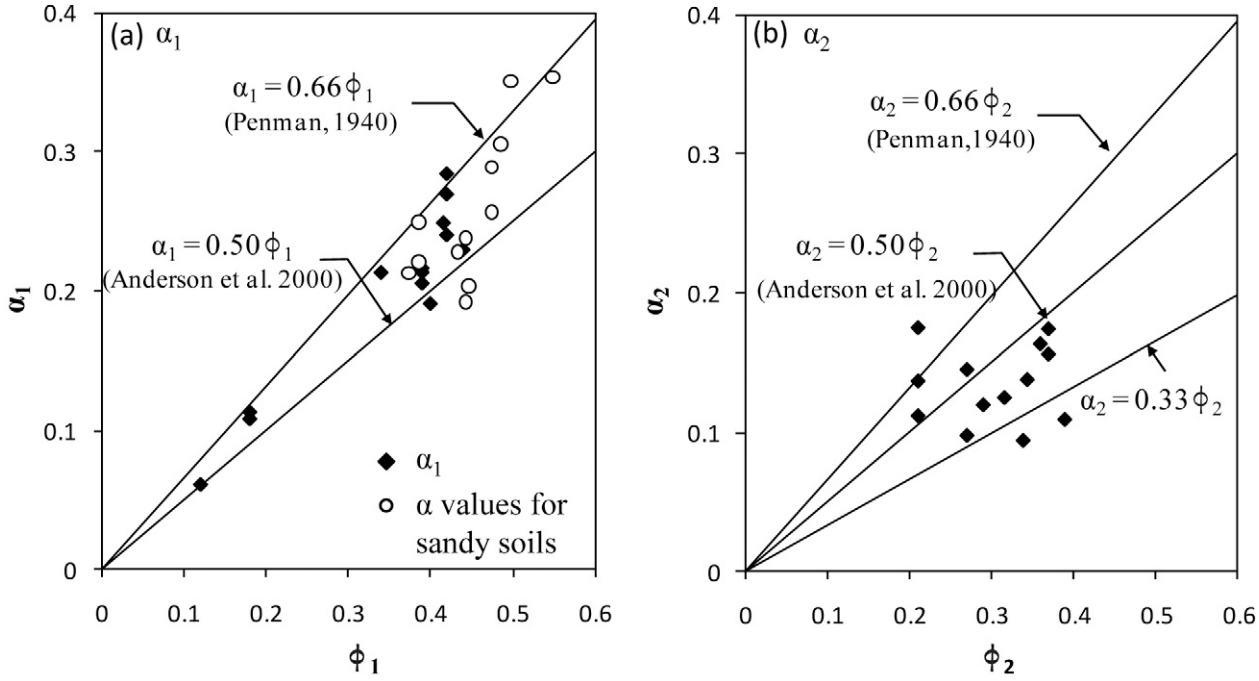


**Fig. 8. Plots for the variation of the model parameters (a) $\alpha_1$ (= $D_p/D_o|_{\varepsilon=\phi 1}$; Eq. [11a]) with interaggregate porosity ($\phi_1$) and (b) $\alpha_2$ (= $D_p/D_o|_{\varepsilon=\phi 1} - D_p/D_o|_{\varepsilon=\phi}$; Eq. [12a]) with intraaggregate porosity ($\phi_2$) for six different aggregated soils and size fractions. Variation of $\alpha$ as a function of total porosity for selected sandy soils (from Fig. 3a) is also plotted in (a) for comparison.**

$\beta_1$ (not shown). Furthermore, for both models, $\alpha_1$ and $\alpha_2$ are presented as functions of $\phi_1$ and $\phi_2$, respectively, for ease of comparison (see Fig. 7). The calculated (optimum) values for $\alpha_1$ and $\alpha_2$ lie in the ranges of (0.52–0.63) $\phi_1$ and (0.27–0.63) $\phi_2$, respectively, compared with the values from the GDC (predicted) model, where $\alpha_1 = 0.5\phi_1$ and $\alpha_2 = 0.5\phi_2$. For the predictions of gas diffusivity for Hayden soils, Grable and Siemer (1968) suggested a different power-law model for Region 1 and the Penman model for Region 2. Interestingly, with the present GDC approach, we obtained good predictions using the Penman parameters in both regions (i.e., $\alpha_1 = 0.66\phi_1$ and $\alpha_2 = 0.66\phi_2$) (not shown).

Figure 8 gives a better illustration of the variation of $\alpha_1$ and $\alpha_2$ (calculated values) against $\phi_1$ and $\phi_2$, respectively, for the aggregated soils discussed above. There was a promising linear relationship between $\alpha_1$ and $\phi_1$, and the two models, Penman (1940) and Anderson et al. (2000), were, to a large extent, able to reproduce the observed relation (Fig. 8a). Notably, the observed relation between $\alpha_1$ and $\phi_1$ was in good agreement with the previously observed relation between $\alpha$ and $\phi$ for less structured soils (Fig. 3a). To show this more clearly, we selected $\alpha$–$\phi$ relations for a few purely structureless (sandy) soils from Fig. 3a and plotted them into Fig. 8a (shown as open circles) together with the $\alpha_1$–$\phi_1$ data (shown as solid diamonds). The $\alpha$–$\phi$ relations for structureless soils are broadly similar to the $\alpha_1$–$\phi_1$ relations for aggregated soils, implying the analogy of the two subsystems that we discussed above. Similarly, $\alpha_2$ also showed a linear increase with increasing $\phi_2$ (Fig. 8b), although the trend is not as evident as for $\alpha_1$ vs. $\phi_1$. Again, the Anderson et al. (2000) model predictions looked promising, while the two models with Penman parameters ($\alpha_2 = 0.66\phi_2$) and half-Penman parameters ($\alpha_2 = 0.33\phi_2$) showed a tendency to give upper-limit and lower-limit predictions, respectively.

Finally, for aggregated soils, we examined the applicability of the new GDC model approach to describe the variation in gas diffusivity ($D_p/D_o$) as a function of matric potential expressed by pF. In Fig. 9a, we show the measured soil-water retention data and the measured $D_p/D_o$ data for the Nishi-Tokyo (cultivated) soil (0–2 mm) at differing matric potentials ranging from pF 1 (i.e., moist condition) to pF 6.9 (i.e., completely dry condition). The interaggregate pore region (Region 1) and the intraaggregate pore region (Region 2) are separated near pF 3 (shown by a vertical line; Fig. 9), which is in line with the observations of Resurreccion et al. (2007). For the predictions in soil-water characteristics, we used the bimodal van Genuchten-type retention function (Durner, 1994) (Fig. 9a, dotted line):

$$S_e = \frac{\theta-\theta_r}{\theta_s-\theta_r} = \frac{\theta_s-\theta_r-\varepsilon}{\theta_s-\theta_r} = \sum_{i=1}^{2} w_i \left[1+\left(a_i|\psi|\right)^{n_i}\right]^{-m_i} \quad [13a]$$

where $\theta_s$ is the soil-water content at saturation ($m^3\ m^{-3}$), $\theta_r$ is the residual water content ($m^3\ m^{-3}$), $w_1$ and $w_2$ are weighting factors ($0 \le w_1, w_2 \le 1$ and $w_1 + w_2 = 1$), $a_1$ and $a_2$ are model scaling factors ($cm^{-1}$), and $n_1$, $n_2$, $m_1$ (= $1 - 1/n_1$), and $m_2$ (= $1 - 1/n_2$) are model shape factors. Rearranging Eq. [13a] yields

$$\varepsilon = \left(\theta_s-\theta_r\right)\left\{1-\sum_{i=1}^{2} w_i \left[1+\left(a_i|\psi|\right)^{n_i}\right]^{-m_i}\right\} \quad [13b]$$

where

$$\psi = 10^{-pF} \quad [13c]$$

We used the $\varepsilon$–pF relation resulting from Eq. [13b] and [13c] in conjunction with the GDC [$D_p(\varepsilon)/D_o$] model (Eq. [11a] and

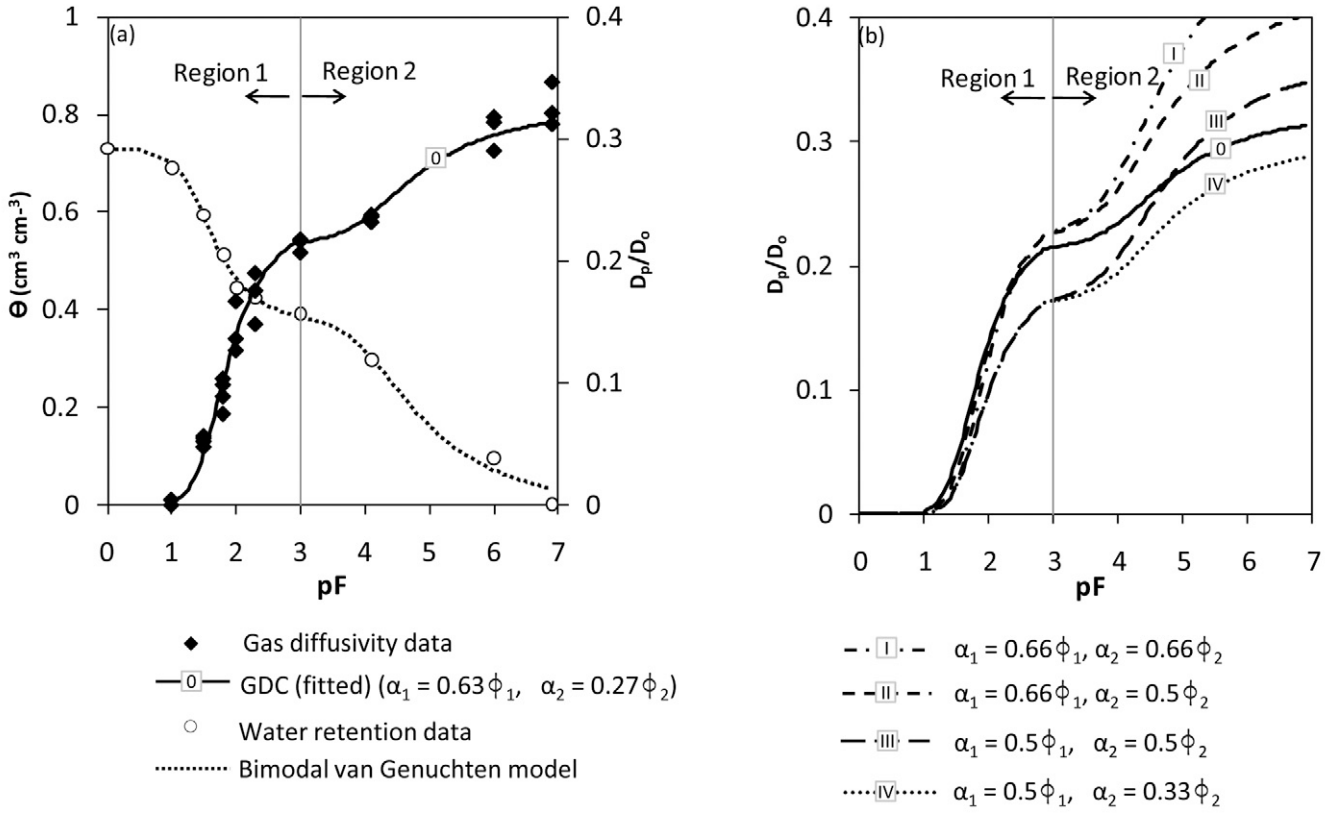


**Fig. 9. (a) Measured soil gas diffusivity ($D_p/D_o$) as a function of pF (=log|−ψ, cm $H_2O$|) together with soil-water characteristic (SWC) data (θ vs. pF) for aggregated Nishi-Tokyo (cultivated) soil (0–2 mm), with the predicted SWC curve using the dual-porosity van Genuchten model (Eq. [13a]; dotted line) and the predicted $D_p$(pF)/$D_o$ function by combining the GDC (fitted) model ($\alpha_1$=0.63$\phi_1$, $\alpha_2$=0.27$\phi_2$) with the best-fit β (Eq. [11a] and [12a] with [13b] and [13c]); and (b) the sensitivity analysis for the two-region (aggregated) generalized density-corrected model (Eq. [11a] and [12a]) parameters, $\alpha_1$ and $\alpha_2$, are shown for selected pairs of $\alpha_1$ and $\alpha_2$. The vertical lines drawn at pF 3 separate the interaggregate region (Region 1) and intraaggregate region (Region 2).**

[12a]) to make $D_p$(pF)/$D_o$ predictions. The predictions from the GDC (fitted) model are shown in Fig. 9a (solid line) with the calculated $\alpha_1$ (= 0.63$\phi_1$) and $\alpha_2$ (= 0.27$\phi_2$) values. Figure 9b shows the results of testing selected $\alpha_1$–$\phi_1$ and $\alpha_2$–$\phi_2$ pairs in the GDC model to show how sensitive the two parameters were likely to be to overall model predictions. As could be expected, changes in $\alpha_1$ seemed to affect the overall model predictions, whereas changes in $\alpha_2$ were reflected only in the predictions in Region 2.

The GDC concept may also be extended to fractured media (e.g., limestone or fractured clay) that are also commonly occurring vadose zone soils and exhibit two-region behavior (Kristensen et al., 2010) by considering a linear model ($\alpha = 0$) for the fracture region and a nonlinear model ($\lambda = 0$) for the matrix region. The extension of the GDC approach to fractured media is not discussed here but will be the focus of a future study.

Finally, for the appropriate selection of predictive models depending on different soil types and structure, we discuss below the recommended predictive models: for sieved, repacked and less-organic soils that are not highly compacted, the WLR model (Moldrup et al., 2000) seems to be precise and reliable. For intact soil systems within the pF range of 1 to 3, the D-C model (Chamindu Deepagoda et al., 2010) will be a reliable choice. For organic media, the new GDC model with $\alpha$ depending on total porosity should be used instead. For strongly aggregated or fractured soils, improvements and a test of the predictive models are still needed, especially in the dry range (pF > 3).

## Effect of Compaction on Gas Diffusivity for Different Soil Types at Natural, Ambient Soil Conditions: Generalized Density-Corrected Model Implications

Another important aspect that can be studied with the GDC modeling approach is the effects of compaction on soil gas diffusivity under natural, ambient soil conditions for different soil types. A typically occurring soil layer in the vadose zone may stabilize, if adequate time is elapsed after a rainfall event, at a particular matric potential. This potential has previously been suggested to occur at or near −100 cm $H_2O$ or pF 2 (Schjønning and Rasmussen, 2000; Al Majou et al., 2008). Let us consider a soil layer with an average bulk density of 1.4 g $cm^{-3}$ (denoted here as the reference bulk density, $\rho_b$*) at an ambient moisture condition corresponding to a matric potential of pF 2. A gradual compaction of the layer will lead to an increase in bulk density (i.e., $\rho_b > \rho_b$*) with a decrease in both total and air-filled porosities. If we assume, as evidenced in some previous studies (e.g., Osozawa, 1998; Resurreccion et al., 2007; Schjønning et al., 2007), that soil pores >30 μm (i.e., air-filled porosity at pF 2, $\varepsilon_{100}$) are predominantly lost during compaction, the relative air-filled porosity at the new bulk density ($\rho_b$) can be written as

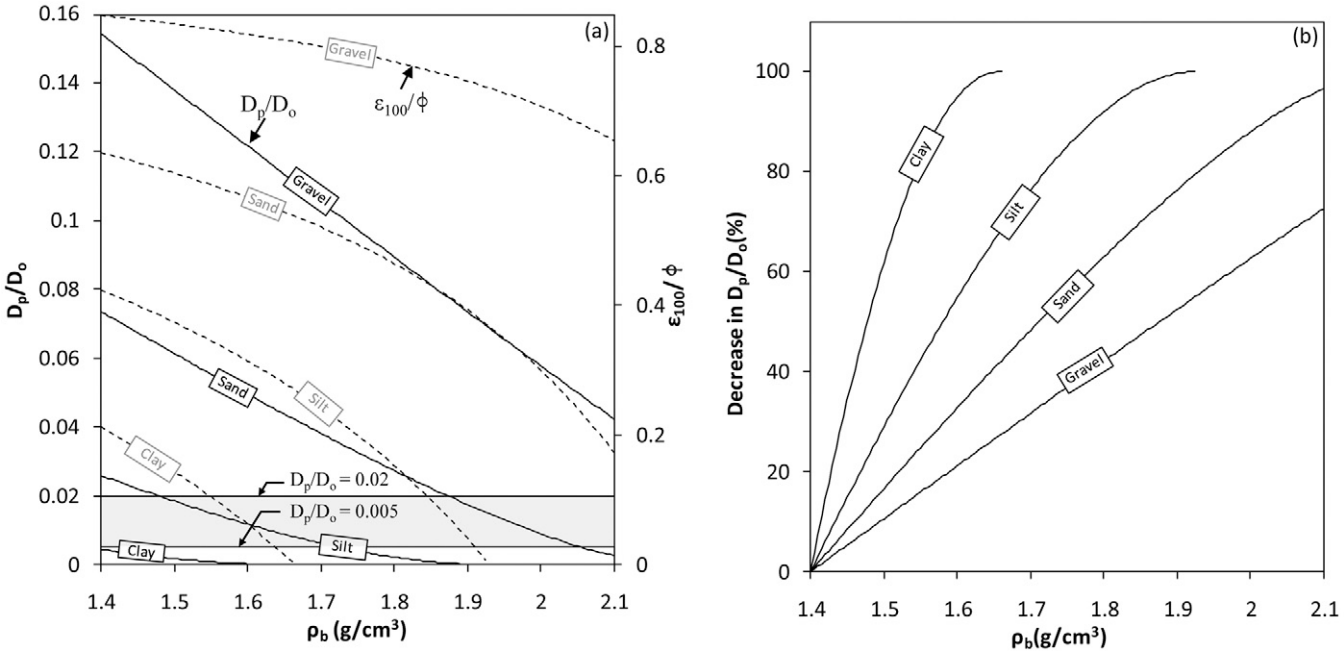


**Fig. 10. (a) Generalized density-corrected model predictions for soil gas diffusivity ($D_p/D_o$) as a function of dry bulk density ($\rho_b$) ranging from 1.4 g cm$^{-3}$ (reference dry bulk density, $\rho_b$*) to 2.1 g cm$^{-3}$ for four soil types: clay ($\varepsilon_{100}$* = 0.1), silt ($\varepsilon_{100}$* = 0.2), sand ($\varepsilon_{100}$* = 0.3), and coarse sand and gravel ($\varepsilon_{100}$* = 0.4), where $\varepsilon_{100}$* is the air-filled porosity at $\rho_b$* (solid lines), and the variations in relative air-filled porosity ($\varepsilon_{100}/\Phi$) against $\rho_b$ for these soil types (dashed lines), along with the limiting gas diffusivity for adequate soil aeration for sandy soils ($D_p/D_o$ = 0.02) and clayey soils ($D_p/D_o$ = 0.005) (shaded area); and (b) for the same soils at different $\rho_b$ values, the decrease in $D_p/D_o$ with respect to the reference gas diffusivity (i.e., $D_p/D_o$ at $\rho_b$*).**

$$\frac{\varepsilon_{100}}{\phi}=\frac{\varepsilon_{100}{}^{*}-\Delta\phi}{\phi^{*}-\Delta\phi} \qquad [14]$$

where $\Delta\phi$ is the decrease in soil total porosity with compaction, $\phi^*$ and $\varepsilon_{100}{}^*$ are the total porosity and air-filled porosity, respectively, at the reference dry bulk density ($\rho_b{}^*$), while $\phi$ and $\varepsilon_{100}$ are the two corresponding parameters at the new dry bulk density ($\rho_b$) after compaction. Note that soil total porosity ($\phi$) and the soil dry bulk density ($\rho_b$) are related, viz:

$$\phi=1-\frac{\rho_b}{\rho_s} \qquad [15]$$

where $\rho_s$ is the average soil particle density (assumed here to be 2.65 g cm$^{-3}$). Equation [14] and [15] can now be used in the GDC model, Eq. [9b], to make $D_p(\rho_b)/D_o$ predictions for different $\varepsilon_{100}{}^*$ values for the different soil types, for example for clayey ($\varepsilon_{100}{}^*$ = 0.1), silty ($\varepsilon_{100}{}^*$ = 0.2), sandy ($\varepsilon_{100}{}^*$ = 0.3), and coarse sandy and gravelly ($\varepsilon_{100}{}^*$ = 0.4) soils. Figure 10a shows the variation of $D_p/D_o$ for these four soil types (solid lines) as a function of $\rho_b$ ranging from 1.4 g cm$^{-3}$ (i.e., the reference dry bulk density representing a typical soil layer in, for example, cultivated land) to 2.1 g cm$^{-3}$ (representing, for example, an extremely compacted soil cover in a municipal solid waste depository). Note that gas diffusivity for clayey and silty soils has already ceased at a dry bulk density of less than $\rho_b$ = 2.1 g cm$^{-3}$ due to the complete loss of air-filled porosity. The two horizontal lines at $D_p/D_o$ = 0.02 and 0.005 in Fig. 10a also show the threshold (minimum) gas diffusivity values for adequate soil aeration for sandy and clayey soils, respectively (Stepniewski, 1980). At the highest compaction, only coarse sandy or gravelly soils will be able to maintain the minimum gas diffusivity requirement for adequate soil aeration. This provides useful information when selecting suitable material for a final (compacted) cover layer in a sanitary landfill where adequate $O_2$ availability is an important prerequisite for sufficient $CH_4$ oxidation. The variation in the relative air-filled porosity ($\varepsilon_{100}/\phi$) against $\rho_b$ for the four soil types is also shown in Fig. 10a (gray lines), which provides valuable information on how compaction affects the physical phase distribution for different soil types. Figure 10b, on the other hand, shows the percentage decrease in gas diffusivity ($D_p/D_o$) relative to the reference gas diffusivity (i.e., $D_p/D_o$ at $\rho_b{}^*$ = 1.4 g cm$^{-3}$) with increasing compaction. Clayey soils showed a complete (100%) loss of gas diffusivity with compaction when the bulk density just exceeded 1.6 g cm$^{-3}$, whereas gravelly soils, with the lowest percentage decrease in $D_p/D_o$ relative to the reference gas diffusivity, showed only a 70% loss even at the highest compaction considered ($\rho_b$ = 2.1 g cm$^{-3}$). Overall, the GDC model approach could be useful in some practical engineering applications, for example in designing the final capping of landfill sites, where changes in soil gas diffusivity on compaction become a controlling factor.

## CONCLUSIONS

- The D-C gas diffusivity model (Chamindu Deepagoda et al., 2010) performed well compared with previous models when tested against independently measured data representing typical less-organic soils and average density levels. For the predictions in less dense or highly porous soils (e.g., peaty soils), however, the D-C model required a modification.
- The D-C model was rewritten in a generalized form to obtain the GDC model, which could describe most previous

predictive models. The model was simplified to yield a two-parameter model (with model parameters $\alpha$ and $\beta$).

- The observed data strongly indicate that a is linearly related to $\phi$, and $\alpha = 0.5\Phi$ seems to be generally valid for soils ranging from sand to peat.
- The data further suggest that $\beta$ is also linearly related to a (and thus to $\phi$). The proposed linear relation, $\beta = 2 + 2.75\alpha$, although not strongly supported by the data, resulted in good overall model predictions.
- The GDC concept was also extended to two-region (bimodal) soils and provided satisfactory results for different size fractions of soil aggregates as well as for a Andisol at different compaction levels.
- The GDC model approach may be useful for practical engineering purposes, including the design of landfill site caps.

## ACKNOWLEDGMENTS

This study was part of the project Gas Diffusivity in Intact Unsaturated Soil (GADIUS) and the large framework project Soil Infrastructure, Interfaces, and Translocation Processes in Inner Space (Soil-it-is), both from the Danish Research Council for Technology and Production Sciences. We gratefully acknowledge the assistance of the Innovative Research Organization of Saitama University, Japan.

## REFERENCES

Al Majou, H., A. Bruand, and O. Duval. 2008. The use of in situ volumetric water content at field capacity to improve prediction of soil water retention properties. Can. J. Soil Sci. 88:533–541.

Andersen, A. 1986. Root growth in different soil types. (In Danish with English summary.) Rep. S-1827. Danish Inst. of Plant and Soil Sci., Copenhagen.

Anderson, A.N., J.W. Crawford, and A.B. McBratney. 2000. On diffusion in fractal soil structures. Soil Sci. Soc. Am. J. 64:19–24. doi:10.2136/sssaj2000.64119x

Buckingham, E. 1904. Contributions to our knowledge of the aeration of soils. Bur. Soil Bull. 25. U.S. Gov. Print. Office, Washington, DC.

Chamindu Deepagoda, T.K.K., P. Moldrup, P. Schjønning, L.W. de Jonge, K. Kawamoto, and T. Komatsu. 2010. Density-corrected models for gas diffusivity and air permeability in unsaturated soil. Vadose Zone J. 10.2136/vzj2009.0137.

Currie, J.A. 1965. Diffusion within soil microstructure: A structural parameter for soils. J. Soil Sci. 16:279–281. doi:10.1111/j.1365-2389.1965.tb01439.x

Currie, J.A. 1984. Gas diffusion through soil crumbs: The effects of compaction and wetting. J. Soil Sci. 35:1–10. doi:10.1111/j.1365-2389.1984.tb00253.x

Durner, W. 1994. Hydraulic conductivity estimation for soils with heterogeneous pore structure. Water Resour. Res. 30:211–223. doi:10.1029/93WR02676

Fischer, M.L., A.J. Bentley, K.A. Dunkin, A.T. Hodgson, W.W. Nazaroff, R.G. Sextro, and J.M. Daisey. 1996. Factors affecting indoor air concentrations of volatile organic compounds at a site of subsurface gasoline contamination. Environ. Sci. Technol. 30:2948–2957. doi:10.1021/es950912e

Freijer, J.I. 1994. Calibration of jointed tube model for the gas diffusion coefficient in soils. Soil Sci. Soc. Am. J. 58:1067–1076. doi:10.2136/sssaj1994.03615995005800040010x

Fujikawa, T., and T. Miyazaki. 2005. Effects of bulk density and soil type on the gas diffusion coefficient in repacked and undisturbed soils. Soil Sci. 170:892–901. doi:10.1097/01.ss.0000196771.53574.79

Grable, A.R., and E.G. Siemer. 1968. Effects of bulk density, aggregate size, and soil-water suction on oxygen diffusion, redox potentials, and elongation of corn roots. Soil Sci. Soc. Am. Proc. 32:180–187. doi:10.2136/sssaj1968.03615995003200020011x

Greenhouse Gas Working Group. 2010. Agriculture's role in greenhouse gas emissions & capture. Greenhouse Gas Working Group Rep. ASA, CSSA, and SSSA, Madison, WI.

Hamamoto, S., P. Moldrup, K. Kawamoto, and T. Komatsu. 2009. Effect of particle size and soil compaction on gas transport parameters in variably saturated, sandy soils. Vadose Zone J. 8:986–995. doi:10.2136/vzj2007.0144

Intergovernmental Panel on Climate Change. 2007. Observations: Surface and atmospheric climate change. p. 236–336. *In* S. Solomon et al. (ed.) Climate change 2007: The physical science basis. Cambridge Univ. Press, Cambridge, UK.

Jin, Y., and W.A. Jury. 1996. Characterizing the dependency of gas diffusion coefficient on soil properties. Soil Sci. Soc. Am. J. 60:66–71. doi:10.2136/sssaj1996.03615995006000010012x

Kawamoto, K., P. Moldrup, P. Schjønning, B.V. Iversen, D.E. Rolston, and T. Komatsu. 2006. Gas transport parameters in the vadose zone: Gas diffusivity in field and lysimeter soil profiles. Vadose Zone J. 5:1194–1204. doi:10.2136/vzj2006.0014

Kliest, J., T. Fast, J.S.M. Boley, H. van de Wiel, and H. Bloemen. 1989. The relationship between soil contaminated with volatile organic compounds and indoor air pollution. Environ. Int. 15:419–425. doi:10.1016/0160-4120(89)90057-3

Kristensen, A.H., A. Thorbjørn, M.P. Jensen, M. Pedersen, and P. Moldrup. 2010. Gas-phase diffusivity and tortuosity of structured soils. J. Contam. Hydrol. 115:26–33. doi:10.1016/j.jconhyd.2010.03.003

Leffelaar, P.A. 1987. Dynamic simulation of multinary diffusion problems related to soil. Soil Sci. 143:79–91. doi:10.1097/00010694-198702000-00001

Marshall, T.J. 1959. The diffusion of gases through porous media. J. Soil Sci. 10-79–82.

Millington, R.J. 1959. Gas diffusion in porous media. Science 130:100–102.

Millington, R.J., and J.M. Quirk. 1960. Transport in porous media. p. 97–106. *In* F.A. Van Beren et al. (ed.) Trans. Int. Congr. Soil Sci., 7th, Madison, WI. 14–21 Aug. 1960. Vol. 1. Elsevier, Amsterdam.

Millington, R.J., and J.M. Quirk. 1961. Permeability of porous solids. Trans. Faraday Soc. 57:1200–1207. doi:10.1039/tf9615701200

Moldrup, P., C.W. Kruse, D.E. Rolston, and T. Yamaguchi. 1996. Modeling diffusion and reaction in soils: III. Predicting gas diffusivity from the Campbell soil water retention model. Soil Sci. 161:366–375. doi:10.1097/00010694-199606000-00003

Moldrup, P., T. Olesen, J. Gamst, P. Schjønning, T. Yamaguchi, and D.E. Rolston. 2000. Predicting the gas diffusion coefficient in repacked soil: Water-induced linear reduction model. Soil Sci. Soc. Am. J. 64:1588–1594. doi:10.2136/sssaj2000.6451588x

Moldrup, P., T. Olesen, D.E. Rolston, and T. Yamaguchi. 1997. Modeling diffusion and reaction in soils: VII. Predicting diffusivity in undisturbed and sieved soils. Soil Sci. 162:632–640. doi:10.1097/00010694-199709000-00004

Moldrup, P., T. Olesen, S. Yoshikawa, T. Komatsu, and D.E. Rolston. 2004. Three-porosity model for predicting the gas diffusion coefficient in undisturbed soil. Soil Sci. Soc. Am. J. 68:750–759. doi:10.2136/sssaj2004.0750

Nazaroff, W.W., H. Feustel, A.V. Nero, K.L. Revzan, D.T. Grimsrud, M.A. Essling, and R.E. Toohey. 1985. Radon transport into a detached one-story house with a basement. Atmos. Environ. 19:31–46. doi:10.1016/0004-6981(85)90134-9

Osozawa, S. 1998. A simple method for determining the gas diffusion coefficient in soil and its application to soil diagnosis and analysis of gas movement in soil. (In Japanese with English summary.) Ph.D. diss. Bull. 15. Natl. Inst. Agro-Environ. Sci., Ibaraki, Japan.

Peer, R.L., A.S. Thorneloe, and L.D. Epperson. 1993. A comparison of methods for estimating global methane emissions from landfills. Chemosphere 26:387–400. doi:10.1016/0045-6535(93)90433-6

Penman, H.L. 1940. Gas and vapor movements in soil: The diffusion of vapors through porous solids. J. Agric. Sci. 30:437–462. doi:10.1017/S0021859600048164

Reible, D.D., and F.H. Shair. 1982. A technique for the measurement of gaseous diffusion in porous media. J. Soil Sci. 33:165–174. doi:10.1111/j.1365-2389.1982.tb01756.x

Resurreccion, A.C., K. Kawamoto, T. Komatsu, P. Moldrup, N. Ozaki, and D.E. Rolston. 2007. Gas transport parameters along field transects of a volcanic ash soil. Soil Sci. 172:3–16. doi:10.1097/01.ss.0000235850.55944.04

Resurreccion, A.C., P. Moldrup, K. Kawamoto, S. Hamamoto, D.E. Rolston, and T. Komatsu. 2010. Hierarchical, bimodal model for gas diffusivity in aggregated, unsaturated soils. Soil Sci. Soc. Am. J. 74:481–491. doi:10.2136/sssaj2009.0055

Rolston, D.E., R.D. Glauz, G.L. Grundmann, and D.T. Louie. 1991. Evaluation of an in situ method for measurement of gas diffusivity in surface soils. Soil Sci. Soc. Am. J. 55:1536–1542. doi:10.2136/sssaj1991.03615995005500060006x

Rolston, D.E., and P. Moldrup. 2002. Gas diffusivity. p. 1113–1139. *In* J.H. Dane and G.C. Topp (ed.) Methods of soil analysis. Part 4. SSSA Book Ser. 5. SSSA, Madison, WI.

Russell, W. 1973. Soil conditions and plant growth. 10th ed. Longman, London.

Schjønning, P. 1985. A laboratory method for determination of gas diffusion in soil. (In Danish with English summary.) Rep. S1773. Danish Inst. of Plant and Soil Sci., Tjele.

Schjønning, P. 1992. Size distribution of dispersed and aggregated particles and of soil pores in 12 Danish soils. Acta Agric. Scand. B 42:26–33.

Schjønning, P., L.J. Munkholm, S. Elmholt, and S. Olesen. 2007. Organic matter and soil tilth in arable farming: Management makes a difference within 5–6 years. Agric. Ecosyst. Environ. 122:157–172. doi:10.1016/j.agee.2006.12.029

Schjønning, P., and K.J. Rasmussen. 2000. Soil strength and soil pore characteristics for direct-drilled and ploughed soils. Soil Tillage Res. 57:69–82. doi:10.1016/S0167-1987(00)00149-5

Schjønning, P., I.K. Thomsen, J.P. Moberg, H. Jonge, K. Kristensen, and B.T. Christensen. 1999. Turnover of organic matter in differently textured soils: I. Physical characteristics of structurally disturbed and intact soils. Geoderma 89:177–198. doi:10.1016/S0016-7061(98)00083-4

Schofield, R.K. 1935. The pF of the water in soil. p. 37–48. *In* Trans. World Congr. Soil Sci., 3rd, Oxford, UK. July–Aug. 1935. Vol. 2.

Shimamura, K. 1992. Gas diffusion through compacted sands. Soil Sci. 153:274–279. doi:10.1097/00010694-199204000-00002

Soane, B.D., and C. van Ouwerkerk (ed.). 1994. Soil compaction in crop production. Dev. Agric. Eng. 11. Elsevier Science, Amsterdam.

Stepniewski, W. 1980. Oxygen diffusion and strength as related to soil compaction: I. ODR. Pol. J. Soil Sci. 13:3–13.

Stepniewski, W. 1981. Oxygen diffusion and strength as related to soil compaction: II. Oxygen diffusion coefficient. Pol. J. Soil Sci. 14:3–13.

Taylor, S.A. 1950. Oxygen diffusion in porous media as a measure of soil aeration. Soil Sci. Soc. Am. Proc. 14:55–61. doi:10.2136/sssaj1950.036159950014000C0013x

Thorbjørn, A., P. Moldrup, H. Blendstrup, T. Komatsu, and D.E. Rolston. 2008. A gas diffusivity model based on air-, solid-, and water-phase resistance in variably saturated soil. Vadose Zone J. 7:1276–1286. doi:10.2136/vzj2008.0023

Werner, D., P. Grathwohl, and P. Hohener. 2004. Review of field methods for the determination of the tortuosity and effective gas-phase diffusivity in the vadose zone. Vadose Zone J. 3:1240–1248.

Xu, X., J.L. Nieber, and S.C. Gupta. 1992. Compaction effect on the gas diffusion coefficient in soils. Soil Sci. Soc. Am. J. 56:1743–1750. doi:10.2136/sssaj1992.03615995005600060014x

# PAPER III

Special Section:
Soil Architecture and Function

T.K.K. Chamindu Deepagoda*
Per Moldrup
Per Schjønning
Ken Kawamoto
Toshiko Komatsu
Lis Wollesen de Jonge

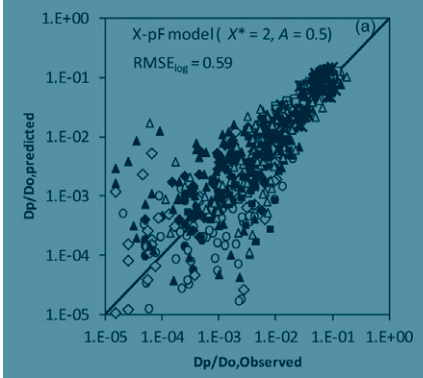


The connectivity of gas-filled pores is a major determinant in the diffusion of gases in porous media. This paper presents a model to predict the connectivity factor that appears in equations of effective diffusivity. The model relates the connectivity factor to soil matric potential and therefore to the unique pore structures of different soils.

T.K.K. Chamindu Deepagoda and P. Moldrup, Dep. of Biotechnology, Chemistry and Environmental Engineering, Aalborg Univ., Sohngaardsholmsvej 57, DK-9000 Aalborg, Denmark; P. Schjønning and L.W. de Jonge, Dep. of Agroecology, Faculty of Science and Technology, Aarhus Univ., Blichers Allé 20, P.O. Box 50, DK-8830 Tjele, Denmark; and K. Kawamoto and T. Komatsu, Dep. of Civil and Environmental Engineering, Graduate School of Science and Engineering, Saitama Univ., 255 Shimo-okubo, Sakura-ku, Saitama 338-8570, Japan. *Corresponding author (chamindu78@yahoo.com).

Vadose Zone J.
doi:10.2136/vzj2011.0096
Received 27 July 2011.



# Variable Pore Connectivity Model Linking Gas Diffusivity and Air-Phase Tortuosity to Soil Matric Potential

Soil-gas diffusivity ($D_p/D_o$) and its dependency on soil matric potential ($\psi$) is important when taking regulative measures (based on accurate predictions) for climate gas emissions and also risk-mitigating measures (based on upper-limit predictions) of gaseous-phase contaminant emissions. Useful information on soil functional pore structure, e.g., pore network tortuosity and connectivity, can also be revealed from $D_p/D_o$–$\psi$ relations. Based on $D_p/D_o$ measurements in a wide range of soil types across geographically remote vadose zone profiles, this study analyzed pore connectivity for the development of a variable pore connectivity factor, $X$, as a function of soil matric potential, expressed as pF (=log $|-\psi|$), for pF values ranging from 1.0 to 3.5. The new model takes the form of $X = X^* (F/F^*)^A$ with $F = 1 + pF^{-1}$, where $X^*$ is the pore network tortuosity at reference $F$ ($F^*$) and $A$ is a model parameter that accounts for water blockage. The $X$–pF relation can be linked to drained pore size to explain the lower probability of the larger but far fewer air-filled pores at lower pF effectively interconnecting and promoting gas diffusion. The model with $X^* = 2$ and $A = 0.5$ proved promising for generalizing $D_p/D_o$ predictions across soils of wide geographic contrast and yielded results comparable to those from widely used predictive models. The $X$–pF model additionally proved valuable for differentiating between soils (providing a unique soil structural fingerprint for each soil layer) and also between the inter- and intraaggregate pore regions of aggregated soils. We further suggest that the new model with parameter values of $X^* = 1.7$ and $A = 0$ may be used for upper limit $D_p/D_o$ predictions in risk assessments of, e.g., fluxes of toxic volatile organics from soil to indoor air at polluted soil sites.

Abbreviations: GDC, generalized density corrected; WLR, water-induced linear reduction; SWC, soil-water characteristic.

**Accurate prediction of the soil-gas diffusion coefficient,** $D_p$ ($m^3$ soil air $m^{-1}$ soil $s^{-1}$), and its variations with soil type and soil physical conditions (e.g., soil moisture status and compaction) has been a century-long research endeavor. One of the earliest and most remarkable attempts to describe $D_p$ and its dependency on soil type (texture) and soil conditions dates back to 1904, when Edgar Buckingham, from the results of his groundbreaking soil aeration experiments, suggested a simple power-law expression to estimate $D_p$ from the soil-air content ($\varepsilon$). Only a few comparable studies focused on model development during the first half of the 20th century (e.g., Penman, 1940; Taylor, 1950), but significant progress was made in the following few decades (e.g., Marshall, 1959; Millington, 1959; Millington and Quirk, 1960, 1961; Troeh et al., 1982; Moldrup et al., 2000a, 2004). A century and a decade later, accurate prediction of $D_p$ has become a major quest for today's scientists because $D_p$ has become a controlling parameter for many critical environmental issues of the day, including atmospheric emission of greenhouse gases (Intergovernmental Panel on Climate Change, 2007), migration of volatile organic compounds from contaminated sites (Petersen et al., 1994; Poulsen et al., 1999), emission of agricultural fumigants (Ashworth and Yates, 2007), and others.

Buckingham (1904) hypothesized that gas diffusivity, $D_p/D_o$ (where $D_o$ is the gas diffusion coefficient in free air), is related to $\varepsilon$ in the form of a power function:

$$\frac{D_p}{D_o} = \varepsilon^X \qquad [1]$$

where the power-law exponent, $X$, reflecting the tortuosity and connectivity of the air-filled pore space, can be calculated from measured values of $D_p/D_o$:

$$X = \frac{\log\left(D_p/D_o\right)}{\log(\varepsilon)} \quad [2]$$

A larger value of $X$ characterizes a highly tortuous and less-connected pore network that will, at a given air content, yield a smaller gas diffusivity. As the pore tortuosity decreases or the pore connectivity increases, $X$ starts decreasing and takes the minimum of $X = 1$ if the minimum tortuosity and maximum pore connectivity of the air-filled pore space is achieved (i.e., in a pore network comprising straight and parallel cylindrical pores). In natural soils, however, $X$ is typically >1 due to the solid-induced pore discontinuity. Buckingham (1904), for example, observed that $X \sim 2$ is generally valid across different soil types in near-dry conditions and concluded that the soil texture, structure, and moisture conditions may influence, but not to a great extent, the magnitude of $X$. A few subsequent studies theoretically derived constant $X$ values for dry porous media, for example $X = 1.5$ (Marshall, 1959) and $X = 1.33$ (Millington, 1959). Based on $D_p$ measurements in different dry granular materials, however, Currie (1960) revealed $X$ to be material dependent. For dry sands with different fine fractions, Shimamura (1992) observed $X$ to vary from 1.5 (for sand without fines) to $X = 2$ (for sand with >50% fines) and thus suggested that $X$ was a texture-dependent parameter.

In wetted porous media, on the other hand, water plays an important role in porous media tortuosity. The water held between particles can potentially redefine the air-filled pore boundaries, round off particle-shape-induced local irregularities (Currie, 1961; Sallam et al., 1984), and thereby make the water-induced pore discontinuity more pronounced than solid-induced tortuosity. Consequently, some studies reconsidered the solid-induced (or particle-dependent) tortuosity factors in wetted media to give greater significance to water-induced tortuosity effects (Currie, 1961). Among the subsequent studies involving water-induced pore discontinuity in gas diffusivity models, the soil-water characteristic (SWC)-dependent models (Moldrup et al., 1999) seemed promising. Moldrup et al. (1999) adopted the Campbell (1974)-based pore size distribution parameter, $b$, to describe the SWC-dependent tortuosity factor, $X = 2 + 3/b$. Notably, the SWC-based models, like most of the models we have discussed so far, assume that $X$ remains constant under different soil moisture conditions.

In a recent study, Thorbjørn et al. (2008) considered the different roles of solids (particle shape) and water on media tortuosity for differently textured undisturbed soils. They assumed that the effects of solid-induced tortuosity and water-induced pore discontinuity are independent and additive to yield:

$$X = X_{dry} + f(\theta) \quad [3]$$

where $X_{dry}$ is the solid-induced tortuosity and $f(\theta)$ is a function of the volumetric water content ($\theta$) accounting for water-induced pore discontinuity. Equation [3], when combined with a suitable water retention function, e.g., the Campbell (1974) model or the van Genuchten (1980) model, can be used to express $X$ as a function of the soil-matric potential, $\psi$.

Given sufficient time after a rainfall or irrigation event, a soil layer or profile typically stabilizes at a certain matric potential, for example at −100 cm $H_2O$, which is considered in many studies to be the natural field capacity (e.g., Schjønning and Rasmussen, 2000; Al Majou et al., 2008). A model presenting $X$ as a direct function of the soil matric potential ($\psi$) or pF (=log|−$\psi$, cm $H_2O$|; after Schofield, 1935) can provide easy prediction of the gas diffusivity and therefore may be of more practical use. Resurreccion et al. (2008) presented a symmetrical $X$–pF expression for aggregated soils:

$$X = B + A_1\left|\mathrm{pF} - \mathrm{pF}^*\right|^{A_2} \quad [4]$$

where $A_1$, $B$, $A_2$, and pF* are curve-fitting parameters. For bimodal soils, the minimum tortuosity, $X = B$, occurs at the reference matric potential, pF*, which divides the soil outer and inner pore space (Regions 1 and 2, respectively). For volcanic ash soils (Andisols), the minimum $X$ was suggested to occur near pF* = 3, at which all the water in Region 1 is assumed to have drained. Resurreccion et al. (2008) noted that Eq. [4] provides only a descriptive function for the observed nonlinearity in $X$–pF and is not intended as a prediction model for soil-gas diffusivity.

With the dual purpose of both predicting the soil-gas diffusivity and the gaseous-phase tortuosity at given soil-water matric potentials across soil types, as well as illustrating unique fingerprints of gaseous-phase tortuosity across moisture conditions (termed a *soil architectural fingerprint*) for each soil type, this study developed an extended $X$–pF model approach and application. We used widely different soils from geographically remote vadose zones, including Danish, Brazilian, Japanese, and Polish soil profiles, to present a new nonlinear $X$–pF expression valid between pF 1 and 3.5 (relatively moist conditions). Linking the new $X$–pF relation to the drained pore size, we investigated the reduced likelihood of pore connectivity (and hence lower $D_p/D_o$) in the presence of larger but fewer air-filled pores at lower pF. The new model has a dual role of generalizing (for predictions at given soil-water matric potentials) or differentiating (for unique soil architectural fingerprints). The architectural fingerprints were expanded to a wider pF range covering both outer space (interaggregate pore region) and inner space (intraaggregate pore region) of repacked soil aggregates from a volcanic ash soil (Andisol).

# Materials and Methods

## Soils and Data

We mainly used literature data on gas diffusivity in this study. For the model development, we first considered 30 undisturbed aggregated soils from Osozawa (1998): 18 Brazilian soils, five Japanese soils from Miura, Kanagawa Prefecture, and seven Japanese soils from Toyohashi, Aichi Prefecture (these soils are hereafter referred to by the sampling location). The Brazilian soils were sampled from five cultivated sites, each subjected to different plowing treatments. The soils at the sampling areas were dark red latosols. Samples from each site were taken from three to four different depths ranging between 5 and 60 cm. The sampling area for the Miura soils, characterized as light-clay Andisols, was deep-plowed, cultivated land cropped mainly with Japanese radish (*Raphanus sativus* L. var. *niger* J. Kern.). The soils were sampled at the 0- to 5-, 30- to 35-, and 50- to 55-cm depths. The Toyohashi yellow soils were sampled from two differently treated cultivated sites: one deep plowed and the normally plowed. The samples were taken at the 0- to 18-, 18- to 36-, and 36- to 70-cm depths on the deep-plowed site and at the 0- to 13-, 13- to 20-, 20- to 27-, and 27- to 60-cm depths on the normally plowed site.

Second, we considered gas diffusivity measurements for 280 undisturbed Danish soils, which were categorized into two main groups: Danish Soils I (150 soils, data from Poulsen et al., 2001; Moldrup et al., 1996, 2000b; Kawamoto et al., 2006a,b; Kruse et al., 1996), and Danish Soils II (130 soils, data from Andersen, 1986; Schjønning and Rasmussen, 2000). The soils in the two groups represent widely differing soil types and land uses across Denmark, including urban soils, agricultural field soils, lysimeter soils, forest soils, landfill cover soils, and deep vadose zone soils. A detailed description of the two soil groups can be found in Chamindu Deepagoda et al. (2011a) (Danish Soils I) and Chamindu Deepagoda et al. (2011b) (Danish Soils II).

For further testing of the *X*–pF function, we selected independently measured Danish and Polish soil data from the literature. We first considered two Danish soils from Dronninglund and Nakskov (Schjønning et al., 2011). The Dronninglund soil was primarily developed on marine sediments, whereas the Nakskov soil was derived from a glacial till; both sampling sites have been cropped for centuries and subjected to different treatment practices. Moldboard plowing and shallow tillage had been practiced at both sites 4 to 5 yr before sampling. Samples were retrieved from the 0- to 4- and 14- to 18-cm depths for the measurements. The four Polish soils include brown soil formed from loess, black earth formed from medium loam, Chernozem rendzina, and a very heavy alluvial soil, all of which were sampled from arable, humus-rich horizons (Stepniewski, 1980).

Finally, to examine soil inner structure fingerprints, we included a Nishi-Tokyo (pasture) soil, an aggregated volcanic ash soil (Andisol) from Japan (Chamindu Deepagoda et al., 2011b). The Nishi-Tokyo soil was sampled at the 0- to 10-cm depth of a pasture site. The soil included three aggregate size fractions of 0 to 2, 2 to 4.76, and 4.76 to 9.52 mm.

An overview of the soil data is given in Table 1.

Table 1. Overview of literature soil data used in the study.

| Soil | Clay | Silt | Sand | Organic matter | Total porosity | Interaggregate porosity† | Reference |
|---|---|---|---|---|---|---|---|
| | | | | g/100 g | | | |
| Model development | | | | | | | |
| Japanese and Brazilian soils | NA‡ | NA | NA | NA | 0.43–0.82 | – | Osozawa (1998) |
| Danish Soils I (150 soils) | 3.6–56.6 | 0.9–19.1 | 22.3–95.5 | 0–4.1 | 0.29–0.54 | – | Poulsen et al. (2001), Moldrup et al. (1996, 2000b), Kawamoto et al. (2006a,b), and Kruse et al. (1996) |
| Danish Soils II (130 soils) | 3.3–20.9 | 2–18.2 | 65.2–94.6 | 0.1–3.7 | 0.29–0.51 | – | Andersen (1986), Schjønning and Rasmussen (2000) |
| Independent test | | | | | | | |
| Danish soils | 7.3–11–5 | 7.7–11.5 | 66.8–78.1 | 2.2–10.2 | 0.43–0.67 | – | Schjønning et al. (2011) |
| Polish soils | 8–30 | 22–31 | 39–64 | 1.66–3.7 | 0.41–0.61 | – | Stepniewski (1980) |
| Two-region analysis | | | | | | | |
| Nishi-Tokyo (pasture) | 12.0 | 42.0 | 46.0 | 11 | 0.76 | 0.39 | Chamindu Deepagoda et al. (2011b) |

† Only applicable to the aggregated and fractured soils.
‡ Not available.

## Measurement Methods

For the Japanese, Danish, and Brazilian soils, annular metal cores of similar dimensions were used for sampling and preparation as follows: 100-cm$^3$ cores were carefully retrieved from the respective undisturbed layers with minimal soil disturbance. For the repacked Andisols, the desired size fractions were sieved out and repacked in 100-cm$^3$ cores to the desired bulk densities, taking particular care to avoid aggregate crushing. Soil-water characteristics were determined following the method of Klute (1986). The soil cores were saturated inside sand boxes and progressively drained to the intended matric potentials ($\psi$) using either a hanging water column (for $\psi \geq -30$ cm $H_2O$ or pF 1.5) or a pressure plate apparatus (for $\psi < -30$ cm $H_2O$). For Dronninglund and Nakskov soils, however, the measurements were done on independent samples (i.e., a new sample at each matric potential), with six replicate measurements. For gas diffusivity measurements, $O_2$ was used as the experimental tracer gas in a one-chamber experimental setup introduced by Taylor (1950). The $O_2$ diffusion coefficient was calculated following Rolston and Moldrup (2002).

For the Polish soils, a different procedure was followed for sample preparation and gas diffusivity measurements. The initially air-dried soils were first sifted through a 5-mm sieve to form a 10-cm-thick soil layer on a kaolin tension plate. The soil layer was moistened and drained to −100 cm $H_2O$ (pF 2) matric suction. The soil was then machine compacted inside a cylindrical vessel and the soil samples (5-cm diameter and 5-cm height) were taken from the compacted surface. The $O_2$ diffusion coefficient ($D_p$) was measured for four different compaction levels and at different matric potentials ranging between −50 cm $H_2O$ (pF 1.7) and −1000 cm $H_2O$ (pF 3). For details on the measurement and calculations of $D_p$, see Stepniewski (1981).

## Statistical Analyses

The performance of the new model against measured data was evaluated and compared with the existing models using the root mean square error (RMSE) and the log-transformed RMSE ($RMSE_{log}$), with the greatest emphasis on the latter. The RMSE indicates the closeness of model predictions—or lack of it—to the observed data:

$$RMSE = \sqrt{\frac{1}{n}\sum_{i=1}^{n}\left(d_p - d_o\right)^2} \qquad [5]$$

where $d_p$ and $d_o$ are the predicted and observed values, respectively, and $n$ is the number of measurements. The $RMSE_{log}$ can be computed by replacing both $d_p$ and $d_o$ in Eq. [5] with their corresponding log-transformed values. The $RMSE_{log}$, in particular, is a useful parameter when the smaller measured values among the measured data need to be treated with greater prominence.

# Model Relations from Basic Equations: A Four-Step Approach

As we observed in Eq. [2], the pore connectivity factor ($X$) is primarily developed using gas diffusivity ($D_p/D_o$) measured at different $\varepsilon$ values. To express $X$ as a function of matric potential (or pF), a combination of selected sets of equations is required, which can be described as a four-step procedure.

In the first step, a suitable SWC function is chosen to relate $\psi$ to the volumetric soil-water content ($\theta$). Many SWC functions are currently available and, for demonstration, we selected the Campbell (1974) model, which has also shown good predictions across the pF range of interest (pF ~ 1–3.5) in this study. The Campbell (1974) model can be written as

$$\theta = \theta_s\left(\frac{\psi}{\psi_b}\right)^{-1/b} \qquad [6]$$

where $\theta_s$ is the saturated volumetric water content, $\psi_b$ is the air-entry matric potential, and $b$ is the pore size distribution index. The representative Campbell parameters for different textural classes can be found in the literature, and Table 2 shows the corresponding values for three selected soils (extracted from Clapp and Hornberger, 1978).

In the second step, a suitable gas diffusivity predictive model is chosen—the water-induced linear reduction (WLR)–Marshall model (Moldrup et al., 2000a), for example, which can be written as

$$\frac{D_p}{D_o} = \varepsilon^{1.5}\left(\frac{\varepsilon}{\Phi}\right) \qquad [7]$$

where $\Phi$ is soil total porosity, knowing that

$$\varepsilon = \Phi - \theta \qquad [8]$$

Table 2. Campbell parameters for sand, sandy clay loam, and clay (extracted from Clapp and Hornberger, 1978).

| Soil texture | Saturated water content ($\theta_s$) | Pore size distribution index ($b$) | Air-entry matric potential ($\psi_b$) |
|---|---|---|---|
| | $cm^3\ cm^{-3}$ | | cm |
| Sand | 0.395 (0.056)† | 4.05 (1.78) | 12.1 (14.3) |
| Sandy clay loam | 0.420 (0.059) | 7.12 (2.42) | 29.9 (37.8) |
| Clay | 0.482 (0.050) | 11.4 (3.7) | 40.5 (39.7) |

† Standard deviations are given in parentheses.

In a third step, Eq. [6], [7], and [8] can be combined to yield $D_p/D_o$ as a function of pF:

$$\frac{D_p}{D_o} = f(\mathrm{pF}) \qquad [9]$$

Equations [2] and [9] can then be combined in the fourth step to obtain the $X$(pF) function:

$$X(\mathrm{pF}) = \frac{\log[f(\mathrm{pF})]}{\log(\varepsilon)} \qquad [10]$$

Because the four-step derivation of the $X$–pF relation involves complicated modeling, a simple model directly expressing $X$ as a function of pF, as discussed below, will be a useful tool.

# Results and Discussion

## Model Development

Figure 1 shows the variation of the Buckingham-based tortuosity factor $X$ (Eq. [2]) at different matric potentials given by the pF, which ranges between 1 and 3.5, for five different soil groups. The average $X$ values as well as the standard deviations (shown by the error bars) are given for each soil group. A large fluctuation in $X$ was observed under wet conditions (i.e., for smaller pF values) due to the pronounced water-induced tortuosity effects. Generally, $X$

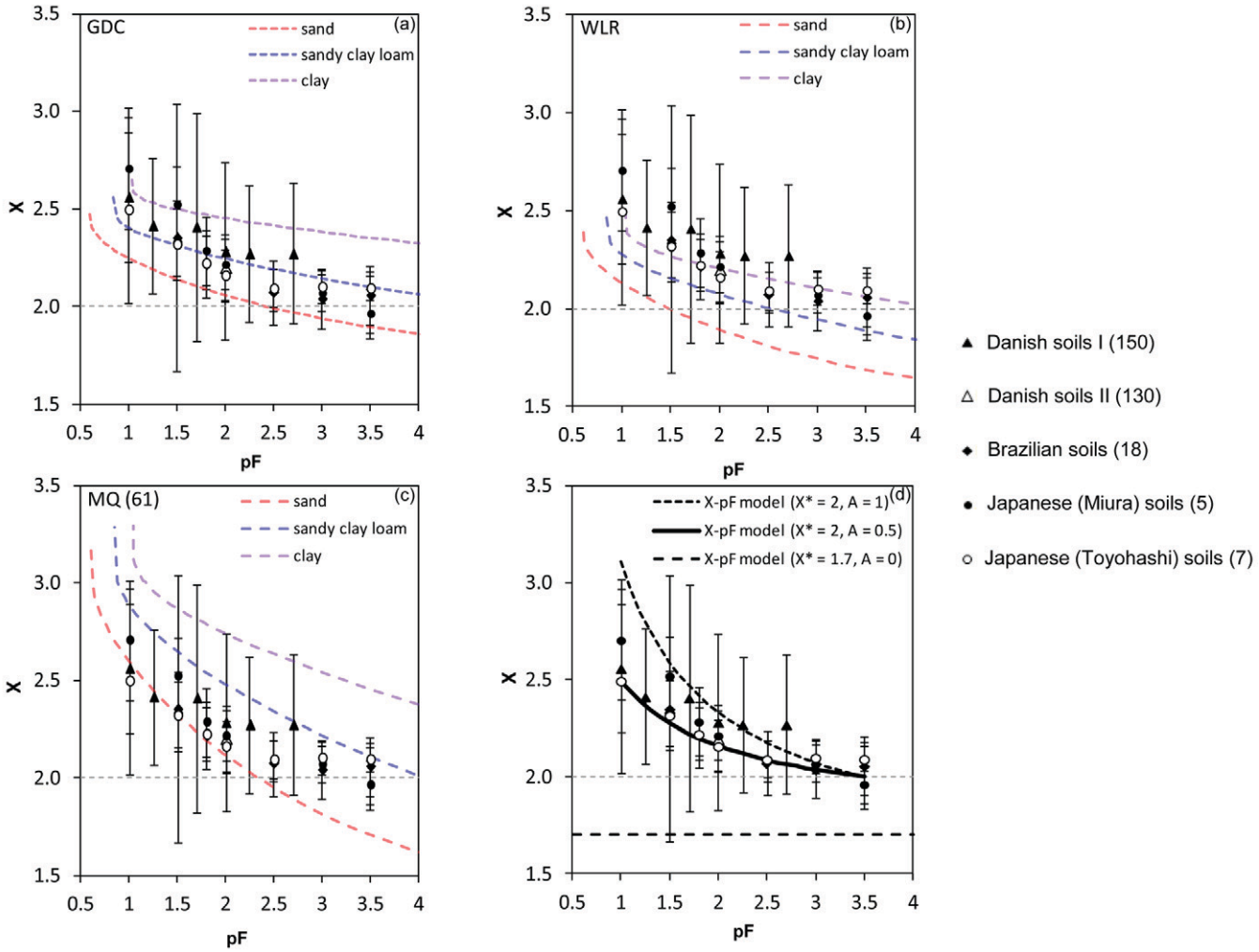


Fig. 1. Buckingham-based pore connectivity factor, $X$, as a function of pF for five selected soil groups (number of soils in each group is given in parentheses). The average $X$ values and standard deviations are shown. The dotted lines show the predictions for sand (red), sandy loam (blue), and clay (purple) from three predictive models: (a) the generalized density-corrected model, (b) the water-induced linear reduction model, and (c) the Millington and Quirk (1961) model. Predictions from the new $X$–pF model, Eq. [11], are shown in (d) with the tortuosity factor at reference pF ($X^*$) = 2 and shape factor $A$ = 1 (dotted line) and $X^*$ = 2 and $A$ = 0.5 (solid line). The $X^*$ = 1.7 and $A$ = 0 (dashed horizontal line) is also shown for upper-limit soil-gas diffusivity model predictions; pF = log |−ψ, cm $H_2O$|.

exhibited a decreasing trend with increasing pF, as opposed to a constant $X$ value for all moisture conditions, as suggested in many previous models including the Buckingham model (shown by a dotted horizontal line; Fig. 1). When the soil pore space is drained to a matric potential corresponding to pF $\sim$ 3–3.5, however, $X$ tended to approach 2.0 following the Buckingham model. Also shown in Fig. 1 are the $X$–pF predictions from three gas diffusivity predictive models: the generalized density-corrected (GDC) model (Chamindu Deepagoda et al., 2011b) (Fig. 1a), the WLR–Marshall model (Moldrup et al., 2000a) (Fig. 1b), and the Millington and Quirk (1961) model (Fig. 1c). The predictions are shown for three different soil types, including sand ($\Phi \sim 0.395$), sandy clay loam ($\Phi \sim 0.42$), and clay ($\Phi \sim 0.482$), signifying the ability of the three models to account for soil type effects. Note that the three models were combined with the Campbell (1974) model following the four-step approach discussed above to derive $X$–pF relations (see Table 2 for the Campbell parameters used for the different soil types). Of the three considered models, the GDC model, on average, yielded the best predictions, followed by the WLR model and the Millington and Quirk (1961) model in that order. Note the general underprediction of $X$ by the WLR model, which was specifically developed and validated for sieved and repacked soils with comparatively less tortuous (smaller $X$) pore networks. The significantly high $X$ values (resulting in low $D_p/D_o$) under moist conditions and slightly low $X$ values (resulting in high $D_p/D_o$) under dry conditions is a commonly noted feature of the Millington and Quirk (1961) model (Kawamoto et al., 2006b; Resurreccion et al., 2007), which often leads to marked general overpredictions of $X$.

To describe the nonlinear variation of $X$ with pF, we hypothesized that the following power-law relationship holds between $X$ and pF:

$$X = X^* \left[ \frac{1+(1/\mathrm{pF})}{1+(1/\mathrm{pF}^*)} \right]^A \qquad [11]$$

where $X^*$ is the tortuosity factor at a reference pF value denoted by pF*, and $A$ ($\geq$0) is a model shape factor to account for the observed nonlinear behavior. Adopting a reference value of $X^* = 2$ at pF* = 3.5 makes Eq. [11] a one-parameter function that, for appropriate $A$ values, may describe the $X$–pF behavior for pF $\leq$ 3.5. Note that pF* = 3.5 closely corresponds to a field condition where pores >1 μm in diameter are completely drained, which is believed to ensure a well-drained pore system. In a model sensitivity analysis with varying $A$ values for the Danish soil data, we observed that $A = 0.5$ exhibited the best overall fit (minimum $\mathrm{RMSE}_{\log}$) to the data, suggesting that $A = 0.5$ is a good estimate for general model predictions. Figure 1d shows the predictions from Eq. [11] against the selected data for three selected $A$ values: $A = 1.0$ (dotted line), $A = 0.5$ (solid line), and $A = 0$ (Buckingham model, dotted horizontal line). Further shown in Fig. 1d is $X^* = 1.7$, $A = 0$ (dashed horizontal line) which, as discussed below, will be useful for upper-limit $D_p/D_o$ predictions.

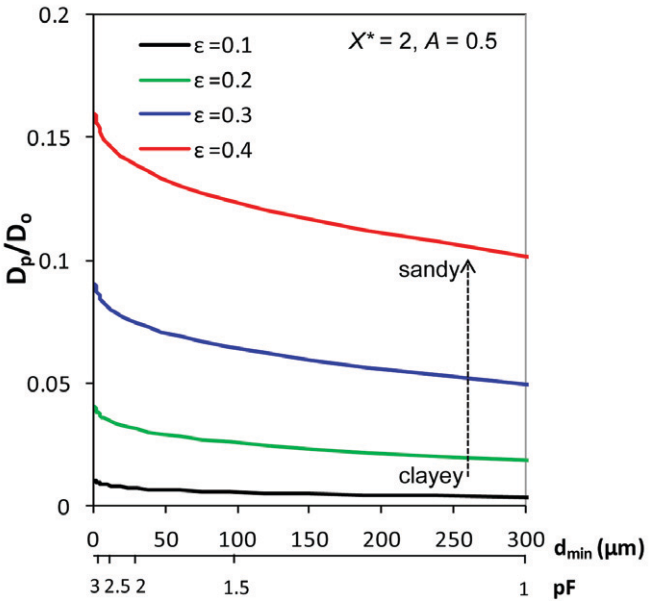


Fig. 2. The pore connectivity factor ($X$)–pF model (Eq. [11] with tortuosity factor at reference pF $X^* = 2$, and shape factor $A = 0.5$) illustration for soil-gas diffusivity, $D_p/D_o$, as a function of minimum drained pore diameter, $d_{min}$, and pF at four selected air-filled porosities (ε); $d_{min}$ (μm) = $3000/10^{pF}$ and pF = log |−ψ, cm $H_2O$|.

## Linking Model Relation to Pore Diameter

Because pF can be directly linked to the minimum drained pore diameter, $d_{min}$ (μm) (=$3000/10^{pF}$), the new $X$–pF model offers the added advantage of easily relating $D_p/D_o$ (and thereby $D_p/D_o$-derived parameters) to $d_{min}$. Figure 2 shows the variation of $D_p(\mathrm{pF})/D_o$ as a function of $d_{min}$ for four selected ε values: 0.1, 0.2, 0.3, and 0.4 $\mathrm{cm^3\ cm^{-3}}$. Moving from large drained (or air-filled) pore sizes to smaller pore sizes (from right to left) along each line (i.e., constant ε), a gradual increase in $D_p/D_o$ can be observed, with a greater increase for larger ε values (e.g., ε = 0.4 $\mathrm{cm^3\ cm^{-3}}$, representing more sandy soils) compared with the smaller ε values (e.g., ε = 0.1 $\mathrm{cm^3\ cm^{-3}}$, representing clayey soils). Note that larger ε values associated with smaller, but more abundant, air-filled pores imply the presence of a large number of small pores, which results in increased pore connectivity and gas diffusivity. Conversely, larger ε values with fewer, but larger, air-filled pores result in a less connected pore system, yielding low gas diffusivity. It is important to note here that $D_p/D_o$ is not essentially pore size dependent and is dependent only on the *interconnected* air-filled pore space. Because the presence (or the absence) of smaller pores can significantly control the probability of pore connectivity, the pore size can also play an important role in the $D_p/D_o$ behavior.

## Model Tests

To examine the new $X$–pF model performance, we tested the model across a wide range of soils. We used $\mathrm{RMSE}_{\log}$ to statistically evaluate the model performance and compare it with the existing

models. The reason for using the $RMSE_{log}$ (instead of RMSE) for the model evaluation was twofold: first, the $X$–pF model (Eq. [11]) is anchored at the selected dry end (i.e., at $pF^* = 3.5$) and hence is forced to perform adequately for the measured large $D_p/D_o$ values for which an RMSE-based evaluation is generally preferred; second, to describe the smaller values of the measured data (under moist conditions), which was our main concern, the $RMSE_{log}$ is a more appropriate parameter than the RMSE.

## Using the Model for Generalizing Soil-Gas Diffusivity Predictions

Figure 3 shows scatterplot comparisons for Danish Soils I using two $X$–pF models: $X^* = 2$, $A = 0.5$ (Fig. 3a) and $X^* = 1.7$, $A = 0$ (Fig. 3b), together with the predictions from four other predictive models: the Buckingham model (Fig. 3c), the GDC model (Fig. 3d), the WLR model (Fig. 3e), and the Millington and Quirk (1961) model (Fig. 3f). Note that the $X$–pF model with $X^* = 2$, $A = 0.5$ (Fig. 3a) is suggested as an average-prediction model, while the model with $X^* = 1.7$, $A = 0$ (Fig. 3b) is suggested for upper-limit predictions. Overall, the $X$–pF model ($X^* = 2$, $A = 0.5$) yielded promising predictions, showing its ability to generalize the predictions across widely contrasting soils. In fact, the $X$–pF model ($RMSE_{log} = 0.59$, RMSE = 0.016) clearly outperformed the widely used Millington and Quirk (1961) model ($RMSE_{log} = 0.77$, RMSE = 0.016) and the Buckingham model ($RMSE_{log} = 0.63$, RMSE = 0.012), with slightly better predictions than the WLR model ($RMSE_{log} = 0.59$, RMSE = 0.026) as well. The $X$–pF model was only outperformed by the GDC model ($RMSE_{log} = 0.57$, RMSE = 0.010), which, as discussed above, seems to be a very promising predictive model for undisturbed soils.

To further examine the model robustness in generalizing $D_p/D_o$ predictions, we extended the model test to independently measured Danish and Polish soil data. We carefully selected literature soils derived from markedly contrasting geographic origins (e.g., marine sediments, glacial, loess, alluvial, etc.). The soils included two Danish soils, Dronninglund and Nakskov, sampled from two differently treated sites (moldboard plowed and shallow tilled) and at two different depths (0-4 and 14-18 cm) (data from Schjønning et al., 2011). We further used four Polish soils

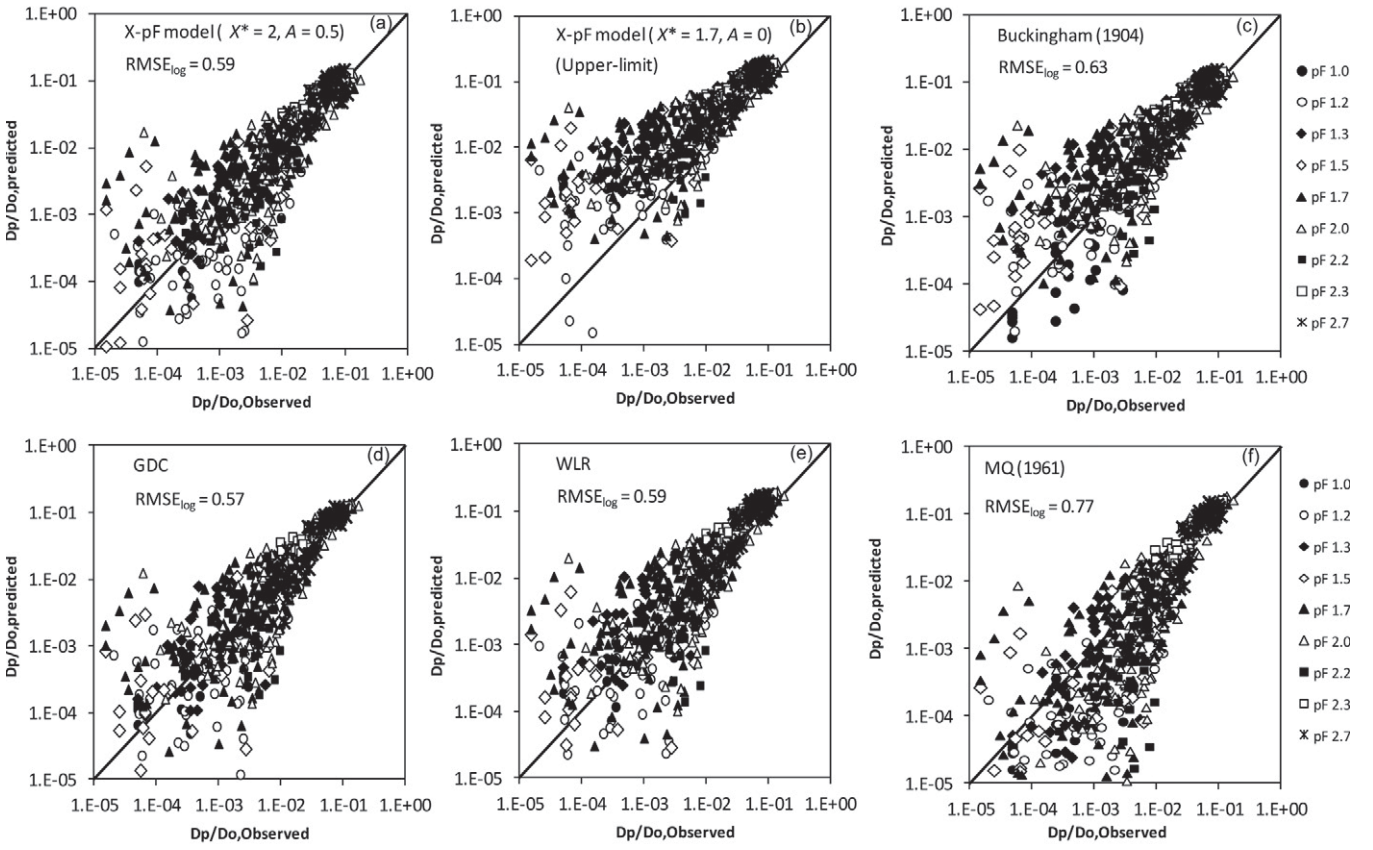


Fig. 3. Scatterplot comparisons of predicted and measured soil-gas diffusivities ($D_p/D_o$) using six predicted models: two pore connectivity factor ($X$)–pF models (Eq. [11]) using (a) tortuosity factor at reference pF ($X^*$) = 2 and shape factor $A = 0.5$ (for average $D_p/D_o$ predictions) and (b) $X^* = 1.7$ and $A = 0$ (for upper-limit $D_p/D_o$ predictions), (c) the Buckingham model (Eq. [1]), (d) the generalized density-corrected (GDC) model, (e) the water-induced linear reduction (WLR)–Marshall model (Eq. [7]), and (f) the Millington and Quirk (1961) model. Measured values are given for nine pF values. Calculated log-based RMSE values are also given. Data from Poulsen et al. (2001), Moldrup et al. (1996, 2000a), Kawamoto et al. (2006a,b), and Kruse et al. (1996); pF = log |−ψ, cm $H_2O$|.

(a Chernozem rendzina, a very heavy alluvial soil, a black earth, and a brown loess soil) from Stepniewski (1980) for the model test. Figure 4 shows scatterplot comparisons for the data using six different models: the two $X$–pF models and the four existing models compared in Fig. 3. Due to the highly tortuous structure observed for brown loess soils, all the models showed a tendency to markedly overpredict the data (open circles). The model comparisons are based on three $RMSE_{log}$ values: (i) $RMSE_{log}$ for all Polish soils, (ii) $RMSE_{log}$ for the Polish soils excluding the brown loess soil, and (iii) $RMSE_{log}$ for the two Danish soils. Clearly, the $X$–pF model ($X^* = 2, A = 0.5$) yielded promising results compared with most of the other predictive models, suggesting the ability of the new $X$–pF model to generalize $D_p/D_o$ predictions across soils with distinct geographic origins. The $X$–pF model with $X^* = 1.7$ and $A = 0$ (Fig. 4b), as noted above, continued to give promising upper-limit model predictions.

## Using the Model for Differentiating Structure Fingerprints

We observed the usefulness of the new model for generalizing $D_p/D_o$ predictions across different soils and soil structures. Can we use the model also to differentiate wide contrasts in soil structures? By revisiting the Danish and Polish soils discussed above, we examined the ability of the new model to differentiate unique soil structures with the view of soil architecture fingerprinting of soil structure.

Figure 5 shows the variation in $X$ as a function of pF for the Danish and Polish soils discussed above. With regard to soil functional structure, the soils exhibited unique $X$–pF fingerprints that may likely be linked to many time-dependent, structure-forming factors including soil type (influenced by different pedogenic origins and processes), management (including

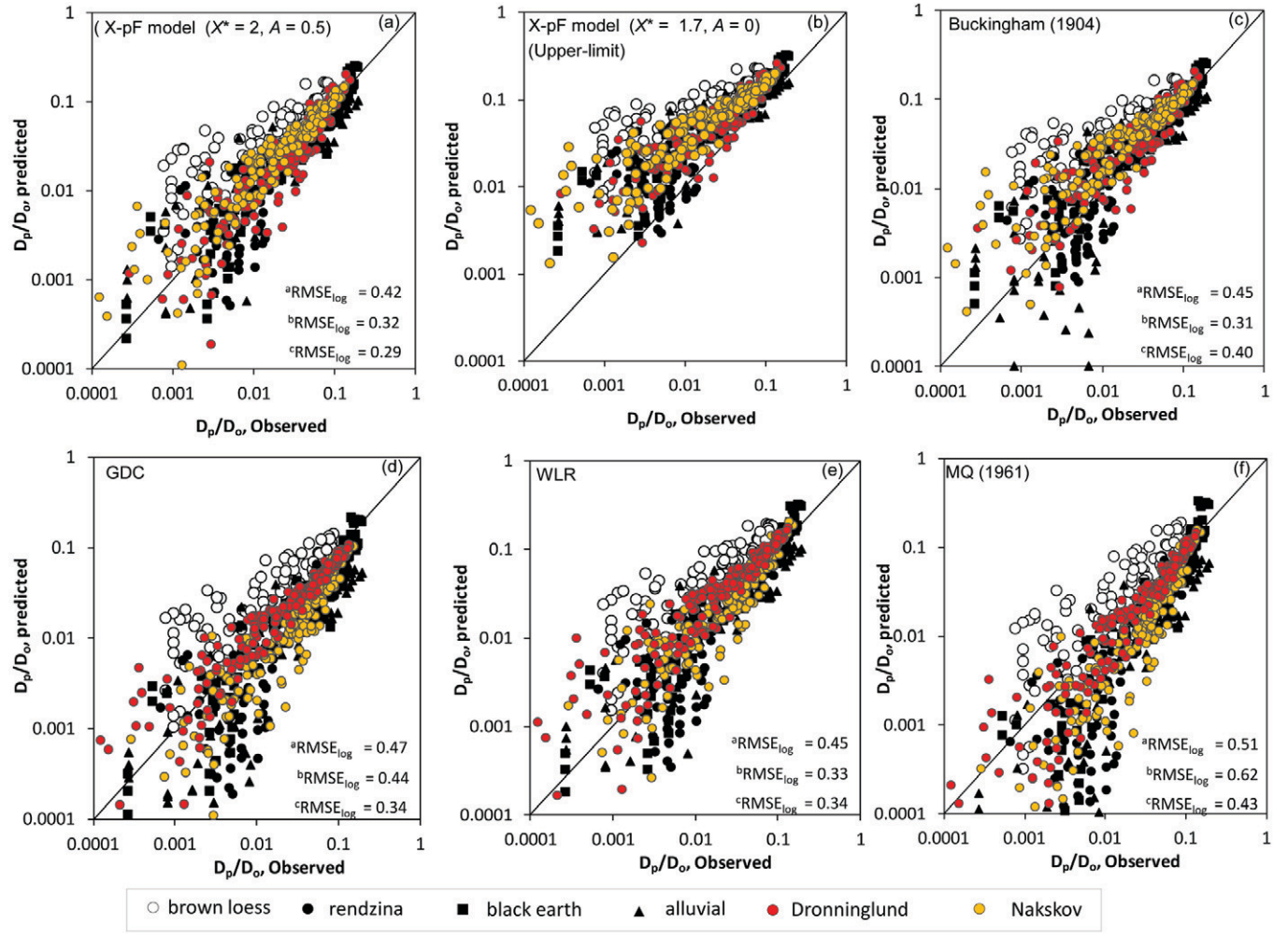


Fig. 4. Scatterplot comparisons of predicted and measured soil-gas diffusivities ($D_p/D_o$) for two Danish soils and four Polish soils: two pore connectivity factor ($X$)–pF models (Eq. [11]) using (a) tortuosity factor at reference pF ($X^*$) = 2 and shape factor $A = 0.5$ (for average $D_p/D_o$ predictions) and (b) $X^* = 1.7$ and $A = 0$ (for upper-limit $D_p/D_o$ predictions), (c) the Buckingham model (Eq. [1]), (d) the generalized density-corrected (GDC) model, (e) the water-induced linear reduction (WLR)–Marshall model (Eq. [7]), and (f) the Millington and Quirk (1961) model. Calculated log-based RMSE values are given for all four Polish soils ($^aRMSE_{log}$), three Polish soils excepting the brown loess soil ($^bRMSE_{log}$), and two Danish soils ($^cRMSE_{log}$). Data from Schjønning et al. (2011) and Stepniewski (1980); pF = log |−ψ, cm $H_2O$|.

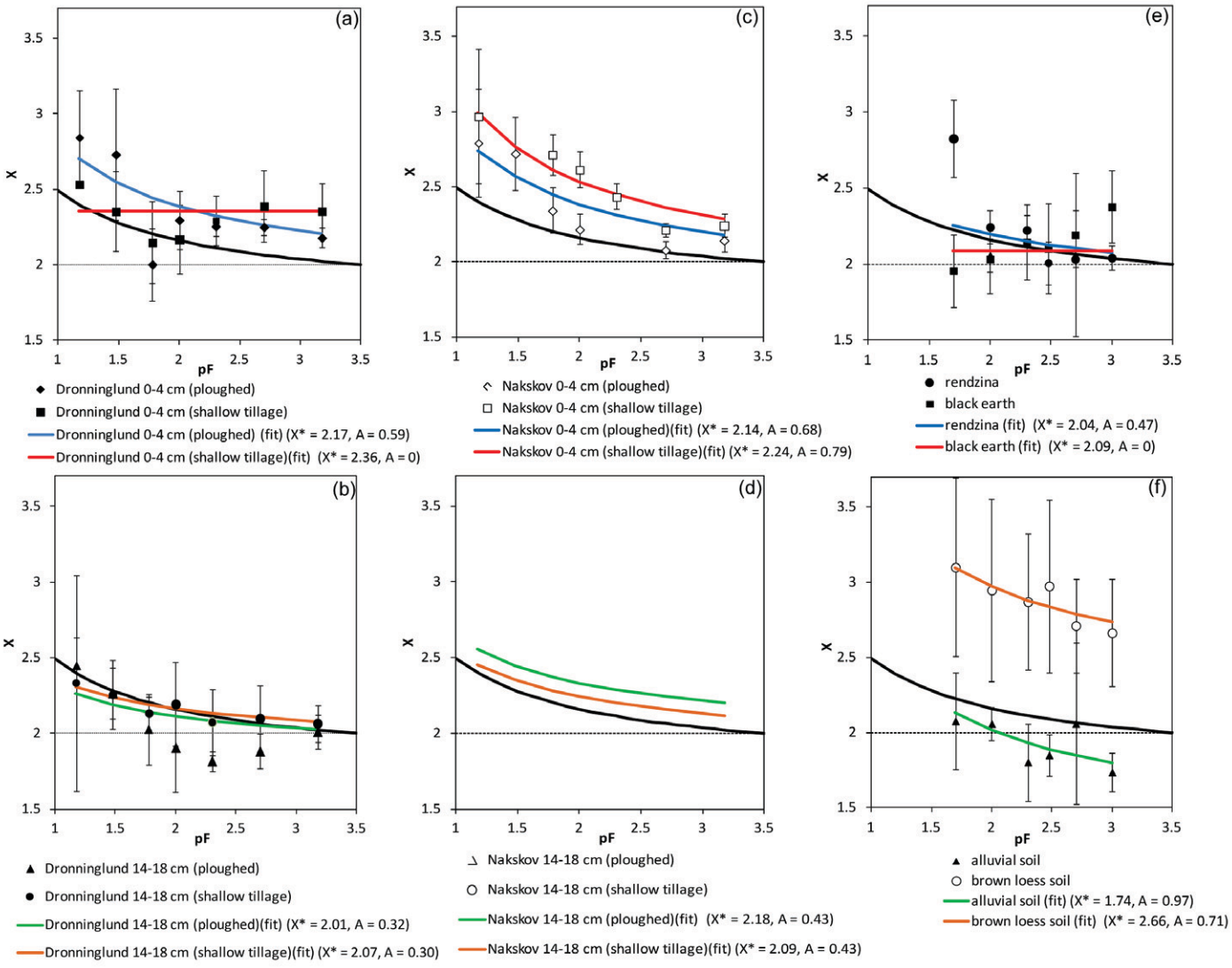


Fig. 5. Buckingham-based tortuosity factor, $X$, as a function of pF for two Danish soils, (a,b) Dronninglund and (c,d) Nakskov, and also for (e,f) four Polish soils. The Danish soil data are given for two sampling depths (0-4 and 14-18 cm) and for two treatment practices (shallow tillage and moldboard plow). The predictions from the $X$–pF model (Eq. [11]) are shown for each soil with given tortuosity at reference pF ($X^*$) and shape factor $A$ (best-fit) pairs. The $X$–pF model with $X^* = 2$ and $A = 0.5$ (black solid line) and $X^* = 2$, $A = 0$ (Buckingham model, dotted horizontal line) are also shown. Data from Schjønning et al. (2011) and Stepniewski (1980); pF = log |−ψ, cm $H_2O$|.

different treatment practices), organic matter, climate, and so on. For example, Dronninglund is a sorted soil dominated by fine sand and silt with very modest clay content, which may potentially yield a weak soil structure. The high organic matter content resulting from many years of arable farming seems to have created some structure-forming potential, however, as reflected by the $X$–pF plot. In contrast, Nakskov is a texturally graded soil with a higher clay content and hence shows a higher structure-forming potential despite the comparatively low organic matter content. At Nakskov, the shallow-tilled topsoil (hence less tendency for soil destructuring) showed a more pronounced pore tortuosity (i.e., higher $X$) as opposed to the moldboard-plowed soil from the same depth. At Dronninglund there were no evident effects of different treatments, effects perhaps being obscured by considerable mixing of organic matter during treatment. Of the Polish soils, the brown loess soil exhibited strikingly higher $X$ values at all pF values, which is probably attributable to its aeolian origin (note that brown loess has the lowest organic matter content and smallest clay fraction of the Polish soils and hence the texture- or organic-matter-induced soil structure formation is less likely to be the cause of the markedly high $X$ values). Thus, to account for the unique $X$–pF behavior exhibited by the selected soils, we produced descriptive $X$–pF relations for each soil (see Fig. 5) using different $X^*$ and $A$ pairs (we used the $X$ at the maximum measured pF value as $X^*$ and best-fit $A$ to describe each soil). The $X$–pF model thus proved to be promising for differentiating soil structures and therefore can be a useful tool for soil structure fingerprinting.

## Using the Model for Fingerprinting Aggregate Soil Inner Space

Our study essentially limited the pore connectivity analysis to the wet range in less-structured soils, closely restricted to the range of $1 \leq \text{pF} \leq 3.5$. An insight into the internal pore network structure in two-region media can be gained by extending the analysis to also include the soil inner pore space ($3.5 \leq \text{pF} \leq 6.9$). Although a detailed discussion of $X$–pF modeling for soil inner space awaits further measurements, we describe below a simple approach toward this using the available data.

Figure 6a presents basic soil-water characteristic curves for the sieved and repacked Nishi-Tokyo (pasture) soil (0-2-mm fraction)—a volcanic ash soil (Andisol) that typically exhibits a microaggregated pore structure (Chamindu Deepagoda et al., 2011b). The SWC data (θ vs. pF) are shown (left $y$ axis) together with predictions from the two-region van Genuchten model (Durner, 1994). Also shown are the $D_p/D_o$ vs. pF variation and the SWC-based pore size distribution (right $y$ axis). The $D_p/D_o$ data and the SWC data show the two-region behavior of the aggregated soil, which is more clearly evidenced from the SWC-derived pore size distribution. The boundary between the outer space (Region 1) and the inner space (Region 2) occurs close to pF ~ 3.0 to 3.5, thus corroborating the observations of Resurreccion et al. (2008), who suggested pF 3 as the region boundary for Andisols.

The variations in $X$ (Eq. [2]) against pF are shown in Fig. 6b for three different size fractions of the same soil: 0 to 2, 2 to 4.76, and 4.76 to 9.52 mm. Note the typical variation of $X$ in bimodal media characterizing a gradual decrease in $X$ with pF in Region 1, followed by an increase in $X$ in Region 2 (Resurreccion et al., 2008). The variation of $X$ with pF showed apparent linear and symmetric behavior in the two regions:

$$X = X^* + B|3.5 - \text{pF}| \quad [12]$$

where $B$ is a constant describing the slope of the linear $X$–pF relation.

The sieved and repacked soils generally showed a less tortuous pore network than the undisturbed soils due to reduced effects of heterogeneity, layering, soil density, etc., on remolding. To account for this decreased pore tortuosity, Moldrup et al. (2000a) reintroduced $X^* \sim 1.5$ (Marshall, 1959) as a good estimate for the predictions of sieved and repacked soils. We, therefore, used the two-region symmetric $X$–pF model (Eq. [12]) with $X^* \sim 1.5$

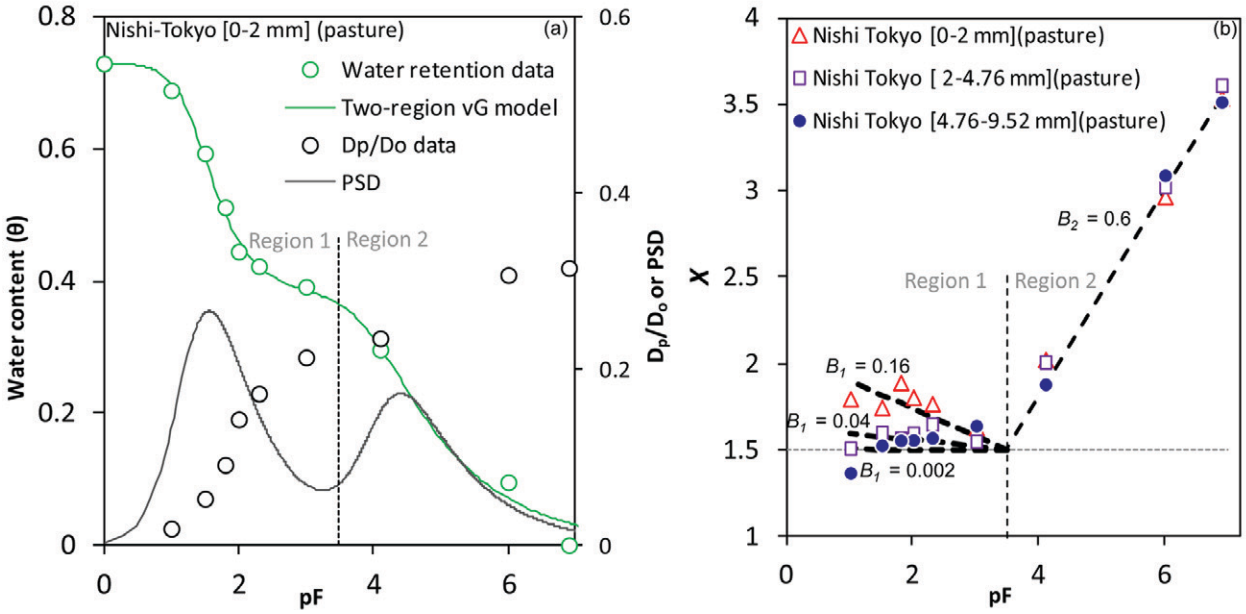


Fig. 6. Soil inner space tortuosity analysis for aggregated Nishi-Tokyo (pasture) soil (0-2 mm fraction): (a) measured soil water characteristic (SWC) (θ vs. pF) data and predictions from the two-region van Genuchten (vG) model (left $y$ axis) and the measured soil-gas diffusivity ($D_p/D_o$) and the SWC-derived pore size distribution (PSD; right $y$ axis); (b) variation in connectivity factor $X$ (Eq. [2]) vs. pF (range 1–6.9) for three different size fractions. The vertical dotted line at pF = 3.5 shows the boundary separating Regions 1 and 2. Predictions from a two-region linear $X$–pF relation (Eq. [12]) are also shown, with tortuosity at reference pF ($X^*$) = 1.5 and different $B$ values (slopes) for Region 1 ($B_1$) and Region 2 ($B_2$). The Marshall (1959) model, $X^* = 1.5$ and $B = 0$, is also shown (dotted horizontal line). Data from Chamindu Deepagoda et al. (2011b); pF = log|−ψ, cm $H_2O$|.

to characterize the observed behavior in the sieved and repacked Andisol. Figure 6b further shows linear $X$–pF relations for the three size fractions in Regions 1 and 2, with slopes denoted by $B_1$ and $B_2$, respectively. For Region 1, individual linear relations are presented for the three size fractions, with $B_1$ decreasing with increasing aggregate size. Interestingly, for Region 2, a single linear relation could describe the $X$–pF variation for all three size fractions, suggesting the broad similarity in pore network structure in the soil inner space, irrespective of the significant differences in physical aggregate size. Thus, the new $X$–pF model seems to be promising for fingerprinting aggregate soil inner space. Further analysis using additional measurements is required, however, to confirm the observations. With the help of additional data, a future study will be devoted to examining the $X$–pF relations in bimodal soils to further explore soil inner space architecture.

## Conclusions

A nonlinear empirical model was presented to predict the classical Buckingham model based tortuosity factor, $X$, as a function of matric potential expressed as pF, for pF values ranging from 1 to 3.5. The novelty and the usefulness of the new $X$–pF concept and model can be described as follows:

1. The model facilitates easy prediction of soil-gas diffusivity in a soil layer or soil profile at a given soil-water matric potential condition (e.g., drained to −100 cm $H_2O$ or pF 2, typically considered to be natural field capacity).
2. With a modified set of model parameters ($X^*$ = 1.7 and $A$ = 0), the new model enables a realistic upper-limit $D_p/D_o$ prediction, useful with regard to, e.g., indoor or outdoor air risk assessment at soil sites contaminated with volatile organics or soil emissions of climate gases.
3. In the case where $D_p/D_o$ is measured from wet to dry conditions, a unique soil structure (architecture) fingerprint of the functional pore space is derived from the soil-gas diffusivity. This can be compared with the average soil behavior as predicted by the new $X$–pF model, allowing us to see where a given soil is distinctly different and unique in functional pore-space behavior.
4. The $X$–pF expression linked to the drained pore size can explain the lower probability of the larger but fewer air-filled pores at lower pF effectively interconnecting and promoting gas diffusion.


### Acknowledgments

This study was made possible by the project Gas Diffusivity in Intact Unsaturated Soil ("GADIUS") and the large framework project Soil Infrastructure, Interfaces, and Translocation Processes in Inner Space ("Soil-it-is"), both from the Danish Research Council for Technology and Production Sciences. We gratefully acknowledge the assistance of the Innovative Research Organization of Saitama University, Japan.


## References


Al Majou, H., A. Bruand, and O. Duval. 2008. The use of in situ volumetric water content at field capacity to improve prediction of soil water retention properties. Can. J. Soil Sci. 88:533–541. doi:10.4141/CJSS07065

Andersen, A. 1986. Root growth in different soil types (Rodvækst i forskellige jordtyper). Rep. S-1827 (In Danish with English summary). Danish Inst. of Plant and Soil Science, Copenhagen.

Ashworth, D.J., and S.R. Yates. 2007. Surface irrigation reduces the emission of volatile 1,3-dichloropropene from agricultural soils. Environ. Sci. Technol. 41:2231–2236. doi:10.1021/es062642d

Buckingham, E. 1904. Contributions to our knowledge of the aeration of soils. Bur. Soil Bull. 25. U.S. Gov. Print. Office, Washington, DC.

Campbell, G.S. 1974. A simple method for determining unsaturated conductivity from moisture retention data. Soil Sci. 117:311–314. doi:10.1097/00010694-197406000-00001

Chamindu Deepagoda, T.K.K., P. Moldrup, P. Schjønning, L.W. de Jonge, K. Kawamoto, and T. Komatsu. 2011a. Density-corrected models for gas diffusivity and air permeability in unsaturated soil. Vadose Zone J. 10:226–238. doi:10.2136/vzj2009.0137

Chamindu Deepagoda, T.K.K., P. Moldrup, P. Schjønning, K. Kawamoto, T. Komatsu, and L.W. de Jonge. 2011b. Generalized density-corrected model for gas diffusivity in variably saturated soils. Soil Sci. Soc. Am. J. 75:1315–1329..

Clapp, R.B., and G.M. Hornberger. 1978. Empirical equation for some soil hydraulic properties. Water Resour. Res. 14:601–604. doi:10.1029/WR014i004p00601

Currie, J.A. 1960. Gaseous diffusion in porous media: 1. A non-steady state method. Br. J. Appl. Phys. 11:314–317. doi:10.1088/0508-3443/11/8/302

Currie, J.A. 1961. Gaseous diffusion in porous media: 3. Wet granular materials. Br. J. Appl. Phys. 12:275–281. doi:10.1088/0508-3443/12/6/303

Durner, W. 1994. Hydraulic conductivity estimation for soils with heterogeneous pore structure. Water Resour. Res. 30:211–223. doi:10.1029/93WR02676

Intergovernmental Panel on Climate Change. 2007. Observations: Surface and atmospheric climate change. In S. Solomon et al. (ed.) Climate change 2007: The physical science basis. Contribution of Working Group I to the Fourth Assessment Report of the Intergovernmental Panel on Climate Change. Cambridge Univ. Press, Cambridge, UK.

Kawamoto, K., P. Moldrup, P. Schjønning, B.V. Iversen, T. Komatsu, and D.E. Rolston. 2006a. Gas transport parameters in the vadose zone: Development and tests of power-law models for air permeability. Vadose Zone J. 5:1205–1215. doi:10.2136/vzj2006.0030

Kawamoto, K., P. Moldrup, P. Schjønning, B.V. Iversen, D.E. Rolston, and T. Komatsu. 2006b. Gas transport parameters in the vadose zone: Gas diffusivity in field and lysimeter soil profiles. Vadose Zone J. 5:1194–1204. doi:10.2136/vzj2006.0014

Klute, A. 1986. Water retention: Laboratory methods. p. 635–662. In A. Klute (ed.) Methods of soil analysis. Part 1. 2nd ed. SSSA Book Ser. 5. SSSA, Madison, WI.

Kruse, C.W., P. Moldrup, and N. Iversen. 1996. Modeling diffusion and reaction in soils: II. Atmospheric methane diffusion and consumption in forest soil. Soil Sci. 161:355–365. doi:10.1097/00010694-199606000-00002

Marshall, T.J. 1959. The diffusion of gases through porous media. J. Soil Sci. 10:79–82. doi:10.1111/j.1365-2389.1959.tb00667.x

Millington, R.J. 1959. Gas diffusion in porous media. Science 130:100–102. doi:10.1126/science.130.3367.100-a

Millington, R.J., and J.P. Quirk. 1960. Transport in porous media. p. 97–106. *In* F.A. Van Beren et al. (ed.) Trans. Int. Congr. Soil Sci., 7th, Madison, WI. 14–21 Aug. 1960. Vol. 1. Elsevier, Amsterdam.

Millington, R.J., and J.P. Quirk. 1961. Permeability of porous solids. Trans. Faraday Soc. 57:1200–1207. doi:10.1039/tf9615701200

Moldrup, P., C.W. Kruse, D.E. Rolston, and T. Yamaguchi. 1996. Modeling diffusion and reaction in soils: III. Predicting gas diffusivity from the Campbell soil water retention model. Soil Sci. 161:366–375. doi:10.1097/00010694-199606000-00003

Moldrup, P., T. Olesen, J. Gamst, P. Schjønning, T. Yamaguchi, and D.E. Rolston. 2000a. Predicting the gas diffusion coefficient in repacked soil: Water-induced linear reduction model. Soil Sci. Soc. Am. J. 64:1588–1594. doi:10.2136/sssaj2000.6451588x

Moldrup, P., T. Olesen, P. Schjønning, T. Yamaguchi, and D.E. Rolston. 2000b. Predicting the gas diffusion coefficient in undisturbed soil from soil water characteristics. Soil Sci. Soc. Am. J. 64:94–100. doi:10.2136/sssaj2000.64194x

Moldrup, P., T. Olesen, T. Yamaguchi, P. Schjønning, and D.E. Rolston. 1999. Modeling diffusion and reaction in soils: IX. The Buckingham–Burdine–Campbell equation for gas diffusivity in undisturbed soil. Soil Sci. 164:542–551. doi:10.1097/00010694-199908000-00002

Moldrup, P., T. Olesen, S. Yoshikawa, T. Komatsu, and D.E. Rolston. 2004. Three-porosity model for predicting the gas diffusion coefficient in undisturbed soil. Soil Sci. Soc. Am. J. 68:750–759. doi:10.2136/sssaj2004.0750

Osozawa, S. 1998. A simple method for determining the gas diffusion coefficient in soil and its application to soil diagnosis and analysis of gas movement in soil. (In Japanese with English summary.) Ph.D. diss. Bull. 15. Natl. Inst. Agro-Environ. Sci., Ibaraki, Japan.

Penman, H.L. 1940. Gas and vapor movements in soil: The diffusion of vapors through porous solids. J. Agric. Sci. 30:437–462. doi:10.1017/S0021859600048164

Petersen, L.W., D.E. Rolston, P. Moldrup, and T. Yamaguchi. 1994. Volatile organic vapor diffusion and adsorption in soils. J. Environ. Qual. 23:799–805. doi:10.2134/jeq1994.00472425002300040026x

Poulsen, T.G., M. Christophersen, P. Moldrup, and P. Kjeldsen. 2001. Modeling lateral gas transport in soil adjacent to old landfill. J. Environ. Eng. 127:145–153. doi:10.1061/(ASCE)0733-9372(2001)127:2(145)

Poulsen, T.G., P. Moldrup, T. Yamaguchi, P. Schjønning, and J.A. Hansen. 1999. Predicting soil-water and soil-air transport properties and their effects on soil-vapor extraction efficiency. Ground Water Monit. Rem. 19:61–70. doi:10.1111/j.1745-6592.1999.tb00225.x

Resurreccion, A.C., K. Kawamoto, T. Komatsu, P. Moldrup, N. Ozaki, and D.E. Rolston. 2007. Gas transport parameters along field transects of a volcanic ash soil. Soil Sci. 172:3–16. doi:10.1097/01.ss.0000235850.55944.04

Resurreccion, A.C., P. Moldrup, K. Kawamoto, S. Yoshikawa, D.E. Rolston, and T. Komatsu. 2008. Variable pore connectivity factor model for gas diffusivity in unsaturated, aggregated soil. Vadose Zone J. 7:397–405. doi:10.2136/vzj2007.0058

Rolston, D.E., and P. Moldrup. 2002. Gas diffusivity. p. 1113–1139. In J.H. Dane and G.C. Topp (ed.) Methods of soil analysis. Part 4. SSSA Book Ser. 5. SSSA, Madison, WI.

Sallam, A., W.A. Jury, and J. Letey. 1984. Measurement of the gas diffusion coefficient under relatively low air-filled porosity. Soil Sci. Soc. Am. J. 48:3–6. doi:10.2136/sssaj1984.03615995004800010001x

Schjønning, P., and K.J. Rasmussen. 2000. Soil strength and soil pore characteristics for direct-drilled and ploughed soils. Soil Tillage Res. 57:69–82. doi:10.1016/S0167-1987(00)00149-5

Schjønning, P., I.K. Thomsen, S.O. Petersen, K. Kristensen, and B.T. Christensen. 2011. Relating soil microbial activity to water content and tillage-induced differences in soil structure. Geoderma 163:256–264. doi:10.1016/j.geoderma.2011.04.022

Schofield, R.K. 1935. The pF of the water in soil. p. 37–48. In Trans. World Congr. Soil Sci., 3rd, Oxford, UK. July–Aug. 1935. Vol. 2.

Shimamura, K. 1992. Gas diffusion through compacted sands. Soil Sci. 153:274–279. doi:10.1097/00010694-199204000-00002

Stepniewski, W. 1980. Oxygen diffusion and strength as related to soil compaction: I. ODR. Pol. J. Soil Sci. 13:3–13.

Stepniewski, W. 1981. Oxygen diffusion and strength as related to soil compaction. Pol. J. Soil Sci. 14:3–13.

Taylor, S.A. 1950. Oxygen diffusion in porous media as a measure of soil aeration. Soil Sci. Soc. Am. Proc. 14:55–61. doi:10.2136/sssaj1950.036159950014000C0013x

Thorbjørn, A., P. Moldrup, H. Blendstrup, T. Komatsu, and D.E. Rolston. 2008. A gas diffusivity model based on air-, solid-, and water-phase resistance in variably saturated soil. Vadose Zone J. 7:1276–1286. doi:10.2136/vzj2008.0023

Troeh, F.R., J.D. Jabro, and D. Kirkham. 1982. Gaseous diffusion equations for porous materials. Geoderma 27:239–253. doi:10.1016/0016-7061(82)90033-7

van Genuchten, M.Th. 1980. A closed-form equation for predicting the hydraulic conductivity of unsaturated soils. Soil Sci. Soc. Am. J. 44:892–898. doi:10.2136/sssaj1980.03615995004400050002x

# PAPER IV

# Diffusion Aspects of Designing Porous Growth Media for Earth and Space

**Chamindu Deepagoda T.K.K***
**Per Moldrup**
Dep. of Biotechnology, Chemistry and Environmental Engineering
Aalborg University
Sohngaardsholmsvej 57
DK-9000 Aalborg, Denmark

**Maria P. Jensen**
NIRAS A/S
Vestre Havnepromenade 9
DK-9100 Aalborg, Denmark

**Scott B. Jones**
Dep. of Plants, Soils and Climate
Utah State University
Logan, UT 84322-4820

**Lis Wollesen de Jonge**
**Per Schjønning**
Dep. of Agroecology and Environment
Faculty of Science and Technology
Aarhus University
B. Allé 20
P.O. Box 50
DK-8830 Tjele, Denmark

**Kate Scow**
**Jan W. Hopmans**
**Dennis E. Rolston**
Dep. of Land, Air, and Water Resources
University of California
Davis, CA 95616

**Ken Kawamoto**
**Toshiko Komatsu**
Dep. of Civil and Environmental Engineering
Graduate School of Science and Engineering
Institute for Environmental Science and Technology (IEST)
Saitama University
255 Shimo-okubo, Sakura-ku
Saitama, 338-8570, Japan

**Growing plants in extraterrestrial environments, for example on a space station or in a future lunar or Martian outpost, is a challenge that has attracted increasing interest over the last few decades. Most of the essential plant needs for optimal growth (air, water, and nutrient supply, and mechanical support) are closely linked with the basic physical properties of the growth media. Diffusion is the main process whereby oxygen and nutrients are supplied to plant roots, and gas and solute diffusivity are the key parameters controlling the diffusive movement of oxygen and nutrients in the root zone. As one among several essential aspects of optimal porous media design for plant growth, this study presents a diffusion-based characterization of four commercial, aggregated growth media. To account for the observed large percolation threshold for gas diffusivity in the selected media, an inactive pore and density corrected (IPDC) model was developed and excellently described measured gas diffusivity in both inter- and intraaggregate pore regions. A strong relation ($r^2$ = 0.98) between percolation threshold for gas diffusivity and mean particle (aggregate) diameter was found and suggested to be used in future design models. Also, critical windows of diffusivity (CWD) was defined identifying the air content range where gas diffusivity (hence, oxygen supply) and solute diffusivity or the analogous electrical conductivity (hence, nutrient supply) are above pre-defined, critical minimum values. Assuming different critical values for gas diffusivity under terrestrial and Martian conditions, the four growth media were compared and it was found that one medium did not fulfill the pre-set criteria. Overall, the analyses suggested that particle (aggregate) sizes below 0.25 and above 5 mm should likely be avoided when designing safe plant growth media for space. The CWD concept was also applied to a natural volcanic ash soil (Nishi-Tokyo, Japan), and the natural soil was found competitive or better than the tested commercial growth media. This could bear large perspectives for Martian outpost missions, since NASA has found that Martian dust/soil mostly resembles volcanic ash soil among terrestrial materials.**

**Abbreviations:** ALS, advanced life support system; CWD, critical windows of diffusivity; EGME, ethylene glycol monoethyl ether; GDC, generalized density corrected; IPDC, inactive pore density corrected; ISS, international space stations; NASA, National Aeronautics and Space Administration; PSD, pore size distribution; SSA, specific surface area; SWC, soil-water characteristics; TDR, time domain reflectometry.

Sufficient aeration and adequate water and nutrient availability at the root zone are among the most essential physiological demands of plants. The soil-gaseous phase is the main source of plant oxygen, while the soil-liquid phase (or soil solution) provides plant water and nutrients. However, since the two phases are complementary and transient in nature, the oxygen, water, and nutrient requirements of plants are not adequately met all the time. If any of these requirements reaches limiting conditions, it can have significant impact on plant

Soil Sci. Soc. Am. J.
doi:10.2136/sssaj2011.0438
Received 19 Dec. 2011.
*Corresponding author (chamindu78@yahoo.com).

life and crop productivity. In the absence of induced movement of gases and liquids, the exchange of gases and nutrients between plant roots and the surrounding environment can become diffusion-limited (Porterfield, 2002). The soil-oxygen diffusion coefficient, $D_p$ ($m^3$ soil air $m^{-1}$ soil $s^{-1}$), and the solute diffusion coefficient in soils, $D_s$ ($m^3$ soil water $m^{-1}$ soil $s^{-1}$), are the two key parameters controlling the diffusion of oxygen and solutes (nutrients), respectively. They are often expressed by gas diffusivity ($D_p/D_o$) and solute diffusivity ($D_s/D_l$), respectively, where $D_o$, and $D_l$ are the diffusion coefficients of, respectively, oxygen in free air and solutes in free water.

Growing plants in containerized porous media has long been a common horticultural practice. In container-grown plants the volume constraints can potentially create intensive conditions, demanding better controls over liquid and gaseous behavior in root zone environments. The porous media characteristics are among the important physical factors governing liquid and gaseous behavior in solid substrates (Jones and Or, 1998b). For example, a fine-textured medium (with predominantly small pores) remains largely saturated after irrigation, resulting in a poorly aerated root zone (Spomer, 1974). On the other hand, in a coarse-textured medium consisting of large particles, water tends to create bridges between the particles, thereby significantly restricting the movement of gases. This suggests the presence of a particular range of particle size favoring optimum plant growth—an important factor to be considered in the design of an optimal plant growth medium. Similar to soil texture, changes in soil functional structure (i.e., particle and pore network) may also markedly affect the physical suitability of a plant growth medium. For example, differently compacted soils will differ in water retention and aeration properties (Chamindu Deepagoda et al., 2011a) and hence will behave differently as plant growth media. Notably, both soil texture and structure significantly influence soil total porosity and pore size distribution—two other important properties to be considered in the design of optimum plant growth media.

Compared to unrestricted environments where depleted water and nutrients can be adequately replenished across the natural soil continuum by mass transport, the plants grown in finite volumes have very limited access to such resources. The ability to reserve plant essential water and nutrients, therefore, becomes another important media property for container-grown plants. Among the widely different natural and manufactured terrestrial materials tested, coarse-textured/aggregated media have been found to be well suited for plants grown in controlled volumes (Jones et al., 2003) due to the presence of large total pore spaces, wide (multimodal) pore size distributions and a sufficiently large specific surface area (serving as potential nutrient and chemical reserves).

The concept of growing plants in extra-terrestrial environments, for example in international space stations (ISS) or in the envisioned lunar or Mars base, has recently sparked renewed interest among researchers in various scientific disciplines. The early plants grown on-board the ISS were meant to offer psychological comfort to the crew on long-duration space missions (Nechitailo and Mashinsky, 1993). The National Aeronautics and Space Administration (NASA), with its expanded vision of advanced life support system (ALS), envisions regenerating air, water, and food within the ISS to ensure self-sufficiency on long-term space missions (NASA, 2002). A future lunar or Mars base is also believed to sustain a self-sufficient human colony, and would further serve as a remote outpost to facilitate inter-planetary space missions. Plants, if successfully grown in these controlled (reduced gravity) environments, provide food, oxygen supply and carbon dioxide removal and therefore will function as part of a bioregenerative life support system. A substantial research endeavor has been devoted to examining a wide range of plants grown in soilless environments (e.g., in hydroponic systems) (Dreschel et al., 1989; Steinberg et al., 2002; Wheeler et al., 2003) and, to a lesser degree, also in solid-support substrates (Steinberg et al., 2000; Heinse et al., 2007). Due to growing concern within NASA's ALS program, "define requirements for the ideal substrate for microgravity" was laid under the critical areas of research in microgravity soil physics (Steinberg et al., 2002).

Due to limited opportunities and financial constraints, however, reduced gravity experiments have not been widely conducted. In a few past studies, the liquid behavior in porous substrates under microgravity conditions has been well described (Bingham et al., 2000; Heinse et al., 2007; Or et al., 2009), and some valuable insight into the substrate gaseous diffusion as well (Porterfield, 2002; Monje et al., 2005). Knowing that diffusion is exclusively a concentration-dependent (not gravity-dependent) phenomenon, the gravity effects on the liquid-gaseous interface will likely be the controlling factor affecting reduced gravity gas diffusion processes in a porous matrix. In a recent gravity-controlled study, Or et al. (2009) showed that the gravity effects on the pore scale liquid-gaseous interfacial configuration are insignificant in coarse-grained media with particle sizes in the range of a few millimeters. They further revealed that $D_p$ measurements at zero gravity (0-*g*) and terrestrial gravity (1-*g*) conditions yielded comparable results, suggesting the broad applicability of results from ground-performed diffusion experiments for reduced gravity conditions as well. Since the key plant metabolic processes were also proved to be gravity independent (Monje et al., 2005), the proper selection of growth media will be of great value for successful plant growth on Earth and also in space. Despite a few promising attempts mainly on conceptually-based media characterization for optimal growth design (e.g., Jones and Or, 1998a; Jones et al., 2009), physically-based studies involving direct measurements of transport properties for more descriptive media characterizations remain limited.

In this study, we present a diffusion-based comparison of four prospective aggregated growth media: Profile, Zeoponic, Turface and pumice, each having unique transport properties and physical characteristics. To account for large percolation thresholds on gas diffusivity in the selected media, we invoke the concept of inactive pore space and use in a recent density-

corrected gas diffusivity model. Based on the measurements of oxygen diffusivity and dielectric properties (analog to solute diffusivity via water content) at varying soil moisture conditions, we examine CWD for oxygen and nutrients at predefined critical conditions on Earth and also on Mars. We further look at a "critical water storage window" to evaluate water availability before the plants wilt due to water deficiency. For all the three critical windows, we consider a situation *in between irrigations*, where the system is drained to a certain matric potential. For the oxygen diffusivity window, we consider the oxygen diffusion through interaggregate pore space (or Region 1) to the root zone. For the nutrient diffusivity window and the water window, we look at the nutrient diffusion and water availability in the intra-aggregate pore space (or Region 2) for local supply of nutrients and water at plant roots. We note here that we have not considered transient water flow and nutrient transport during and just after irrigation where the resupply of water and nutrients to the depleted root zone occurs.

We further introduce a "design diagram" to help select the optimal range of particle sizes for plant growth and discuss its applications on Earth and also on a Martian base. Finally, we discuss the implications of the CWD concept to examine Japanese volcanic ash soil (Andisol) as a candidate for future space-based applications. We emphasize that the diffusion-based characterization we discuss herein is only one of many essential aspects in optimal plant growth media design considerations, particularly under microgravity conditions where many other factors may also play critical roles in overall design process (Steinberg et al., 2002).

## MATERIALS AND METHODS

### Porous Media and Properties

In this study, we mainly considered four aggregated growth media with different particle size fractions (given in square brackets throughout the text) as follows: Pumice [3.2–9.5 mm] (Charley's Greenhouse and Garden, Mount Vernon, WA), Turface [2.0–5.0 mm] (Aimcor, Deerfield, IL), Profile [0.25–0.85 mm] (Aimcor, Deerfield, IL), and Zeoponic [0.25–1.0 mm] (Rocky Mountain Zeolites LLC, Golden, CO). The pumice originates from volcanic parent materials from the Washington State area (Blonquist et al., 2006). Turface and Profile are stabilized baked ceramic aggregates which have been widely tested as prospective substrates in many previous microgravity plant experiments (Steinberg and Poritz, 2005; Heinse et al., 2007). Zeoponic, a NASA-developed zeolite-based synthetic substrate, is also a promising growth medium that has been tested in many gravity-controlled environments (Steinberg et al., 2000). A detailed characterization of the four growth media based on soil-water retention and dielectric properties has been presented by Blonquist et al. (2006). Some useful physical properties relevant to the present study are also given in Table 1 (data from Blonquist et al. (2006) and present study).

For the validation of the IPDC model, we considered two aggregated soils from the literature: a crumb soil [1–2 mm] (data from Currie, 1984) and a pumice [~1 mm] (referred hereafter as Currie-pumice, data from Currie, 1961). The crumb soil, a silty clay loam, was sampled from a 100-yr-old Highfield permanent pasture at Rothamsted and showed high water stability against swelling and shrinking (Currie, 1984). No information is available with regard to the origin, texture, and packing of Currie-pumice, but the measured water-retention characteristics (not shown) revealed clear evidence of two-region behavior (Currie, 1961).

We finally considered a Japanese volcanic ash soil (Andisol), the Nishi-Tokyo aggregated soil [2–4.76 mm], in this study (data from Chamindu Deepagoda et al., 2011b). The soil was sampled at 5 to 10-cm depth on a pasture site at Field Production Science Center, the University of Tokyo. The soil was first sieved to separate the desired particle size fraction and then repacked ($\rho_b$ = 0.76 g cm$^{-3}$) for measurements.

### Measurement of Soil-Water Characteristics

For the four aggregated growth media, we used literature measurements on soil-water characteristics SWC) (data from Blonquist et al., 2006). Two additional measurements were performed for each medium at two different matric potentials, −100 cm $H_2O$ (at pF 2) and −800 cm $H_2O$ (at pF 2.9) and confirmed the compatibility of results (pF = log |−ψ, m $H_2O$|, where ψ is the soil matric potential; following Schofield, 1935). For the additional measurements, 100-cm$^3$ samples were packed (in triplicates) to the same dry bulk density as given in Blonquist et al. (2006) (see Table 1) and saturated samples drained to the above matric potentials inside a sandbox. By using similar sized samples, Chamindu Deepagoda et al. (2011b) made water content adjustments for Nishi-Tokyo soils by first draining inside a sandbox (below pF 2) and then inside a pressure plate apparatus (from pF 2–4.2), followed by two evaporation steps at air-dry (pF ~ 6.0) and oven-dry (pF ~ 6.9) conditions.

### Soil-Gas Diffusivity Measurements

For gas diffusivity ($D_p/D_o$) measurements in the four aggregated growth media, 100-cm$^3$ samples were packed to

**Table 1. Physical properties of the growth media**

| Media | Physical properties | | | | | |
|---|---|---|---|---|---|---|
| | Aggregate size range | Bulk density | Total porosity | Interaggregate porosity | Surface area | |
| | | | | | Blonquist et al. (2006)† | This study‡ |
| | mm | g cm$^{-3}$ | cm$^3$ cm$^{-3}$ | | m$^2$ g$^{-1}$ | |
| Pumice | 3.2–9.5 | 0.36 | 0.83 | 0.45 | 18 | 13.9 |
| Turface | 2.0–5.0 | 0.62 | 0.75 | 0.42 | 55 | 101.4 |
| Zeoponic | 0.25–1.0 | 0.97 | 0.61 | 0.44 | 140 | 94.2 |
| Profile | 0.25–0.85 | 0.65 | 0.74 | 0.42 | 56 | 95.8 |

† Estimated by water adsorption method.

‡ Measured by ethylene glycol monoethyl ether (EGME) method.

the desired bulk densities as given in Table 1. Different water contents for $D_p/D_o$ measurements were achieved by stepwise evaporation from saturated samples. The one-chamber method suggested by Taylor (1950) and developed further by Schjønning (1985) was adopted for oxygen diffusivity measurements. The diffusion chamber was first flushed with 100% $N_2$ to get rid of all the oxygen inside the chamber. The sample was mounted on the chamber and the top surface of the sample was exposed to the air, allowing atmospheric oxygen to diffuse into the chamber through the sample. An oxygen sensor mounted on the chamber wall continuously measured the oxygen concentration inside the chamber. The gas diffusion coefficient in soil ($D_p$) was calculated based on the steady-state method following Rolston and Moldrup (2002). The length of time taken for each measurement (varied from 2–3 h to a few minutes, depending on the soil moisture condition) was assumed to be short enough to ignore the oxygen depletion caused by microbial consumption (Schjønning et al., 1999).

The $D_p/D_o$ measurements for the four growth media were first performed at the University of California, Davis (UCDavis) with a traditional, commonly-used gas diffusion apparatus and then independently tested using a newly-developed experimental-set up at Aalborg University (AAU), Denmark. The two apparatus, in principle, consist of the same components, except for the pneumatically-controlled tightening mechanism implemented in the new setup to ensure a perfectly airtight system. Further, the hard-to-push opening/closing slide available in the old setup is replaced with an easily-movable rotary slide in the new apparatus.

Currie (1984) used differently-sized sample rings to pack initially air-dried soil crumbs for the measurements of gas diffusivity. The uncompacted samples were first equilibrated at −50 cm $H_2O$ (pF 1.7) matric suction and then compacted to different bulk densities. The samples were subsequently rewetted and re-equilibrated at pF 1.7 before achieving different moisture conditions by progressive wetting or drying. Using hydrogen as the experimental gas in an experimental setup described in Currie (1960a), gas diffusion measurements were done for both crumb soils and Currie-pumice.

### Dielectric Permittivity Measurements

Blonquist et al. (2006) used time domain reflectometry (TDR) measurements to determine the dielectric permittivities for the four aggregated growth media. The TDR measurements were undertaken by means of a custom-designed measurement cell with a parallel-plate probe arrangement. The aggregated growth media samples were first vacuum saturated with NaCl solution, and then packed in the cell for the TDR measurements. The measurements were made using a standard Tektronix 1502b cable tester.

### Specific Surface Area Measurements

The specific surface area (SSA) for the four aggregated growth media (Table 1) were determined independently by two different methods: (i) estimated from the bound water fraction on a mass basis (data from Blonquist et al., 2006), and (ii) measured in the present study using the ethylene glycol monoethyl ether (EGME) method (Petersen et al., 1996; Pennell, 2002; Cerato and Lutenegger, 2002). The SSA estimated from the water adsorption method assumed monolayer coverage of water and an area of 9 square angstroms per water molecule.

The SSA measured by EGME was found to be similar to those measured by $CO_2$ (de Jonge et al., 2000). The observed discrepancy of the results from the two different methods (Table 1) has also been reported in the literature (Petersen et al., 1996; Yukselen and Kaya, 2006) and was mostly attributed to the differences in extent to which water or EGME tend to access the internal surface areas of the minerals. The EGME method, in particular, was observed to yield more reliable predictions over several other widely-used methods. We therefore rely on the measured SSA from the EGME method in the media comparisons.

## MODELING APPROACHES

### Soil-Water Characteristics and Pore Size Distribution

In contrast to typical structureless (or unimodal) soils, the aggregated media are often characterized by two distinct (bimodal) pore regions: interaggregate or external pore region (Region 1) where pores occupy the region between the aggregates, and intra-aggregate or internal pore region (Region 2) where pores occupy the region inside the aggregates. Consequently, the classical unimodal functions frequently used to describe SWC for structureless soils, for example the van Genuchten model (van Genuchten, 1980), are not directly applicable to the bimodal aggregated media. The widely accepted approach to represent the two-region behavior in bimodal media involves algebraic superposition of two individual unimodal functions, assuming the two subporous systems (Region 1 and Region 2) are functionally independent. In this study, we used the bimodal van Genuchten-type water retention function (Durner, 1994) as follows:

$$S_e = \frac{\theta - \theta_r}{\theta_s - \theta_r} = \sum_{i=1}^{2} w_i \left[1 + a_i |\psi|^{n_i}\right]^{-m_i} \qquad [1]$$

where $\theta_s$ is the soil-water content at saturation ($cm^3\ cm^{-3}$); $\theta_r$ is the residual water content ($cm^3\ cm^{-3}$); $w_1$ and $w_2$ are weighting factors ($0 \le w_1, w_2 \le 1$ and $w_1 + w_2 = 1$); $a_1$ and $a_2$ are model scaling factors ($cm^{-1}$); $n_1, n_2$, $m_1 (= 1-1/n_1)$, $m_2$ $(= 1-1/n_2)$ are model shape factors. The weighting factors, scaling factors, shape factors and residual water content were estimated as curve-fitting parameters by using the nonlinear, curve-fitting routine SOLVER in MS Excel (Wraith and Or, 1998).

The first derivative of the SWC function yields the soil specific moisture capacity, $C^*$ $(= d\theta/d\psi)$ which can be used to determine the equivalent PSD as follows (Durner, 1994):

$$\frac{d\theta(r)}{d\log_{10} r} = \frac{d\theta(pF)}{d(pF)} = \frac{d\theta(\psi)}{d\log_{10}|\psi|}$$

$$\frac{d\psi}{d\log_{10}|\psi|}=\frac{d\theta(\psi)}{d\psi}=[\log_e 10]|\psi|C^* \qquad [2]$$

where $r$ is the pore radius which is related to the soil matric potential by,

$$r(\mu m)=\frac{146}{g|-\psi(m)|} \qquad [3]$$

where $g$ is the acceleration of gravity, used as a constant ($g$ = 9.81 ms$^{-2}$) throughout this study. (Note: 1m of water head ≈10 kPa.)

## Soil-Gas Diffusivity and Pore Connectivity

Similar to the bimodal soil-water retention models, the two-region gas diffusivity models developed for aggregated media also assume that the two regions (Region 1 and Region 2) are functionally independent and additive (e.g., Resurreccion et al. [2008, 2010]; Chamindu Deepagoda et al. [2011a, 2011b]). A notable feature of aggregated media with relatively large particles (like the media considered in the present study) is the presence of large *percolation thresholds* ($\varepsilon_p$) for gas diffusivity. At air-filled porosities below the percolation threshold ($\varepsilon \le \varepsilon_p$), gas diffusivity remains essentially zero (i.e., $D_p/D_o = 0$), since all the air-filled pores are made virtually "inactive" for gas diffusion by the interconnected water films around the particles. The *inactive air-filled pore space for gas diffusion* ($\varepsilon_{in}$) increases linearly with increasing air content (i.e., with draining) and will reach a maximum value at the percolation threshold ($\varepsilon_{in} = \varepsilon_p$). As the draining progresses ($\varepsilon > \varepsilon_p$), the water films start disconnecting, allowing the hitherto disconnected air-filled pores to gradually become interconnected, resulting in a decrease in inactive pore space (Troeh et al., 1982). The inactive pore space can be assumed to reach zero at complete air saturation of interaggregate pore space (i.e., at $\varepsilon = \Phi_1$, where $\Phi_1$ is the interaggregate porosity), provided that other factors that cause inactive pores (for example, heavy compaction; Shimamura, 1992) are not playing a significant role. Depending on the texture and the pore network structure of the soil, the decreasing trend may be nonlinear (e.g., Sahimi, 1994), but a linear decrease will be a simple and reasonable approximation (Moldrup et al., 2005). Figure 1 illustrates the variation of $\varepsilon_{in}$ (the left $y$ axis) with increasing air-filled pore space ($\varepsilon$) for two selected $\varepsilon_p$ values: $\varepsilon_p$ = 0.1 (solid line), and $\varepsilon_p$ = 0.2 (dashed line). The $\varepsilon_p$- $\varepsilon$ relation can be mathematically described by the following equations (Moldrup et al., 2005):

$$\varepsilon_{in} = \varepsilon \qquad \varepsilon \le \varepsilon_p \qquad [4a]$$

$$\varepsilon_{in} = \left[\frac{\Phi_1 - \varepsilon}{\Phi_1 - \varepsilon_p}\right]\varepsilon_p \qquad \varepsilon_p < \varepsilon \le \Phi_1 \qquad [4b]$$

By incorporating the concept of inactive pore space into a recently developed two-region generalized density corrected (GDC) model for gas diffusivity (Chamindu Deepagoda et al., 2011b), we introduce an IPDC model for gas diffusivity predictions (in Region 1) in aggregated growth media as follows:

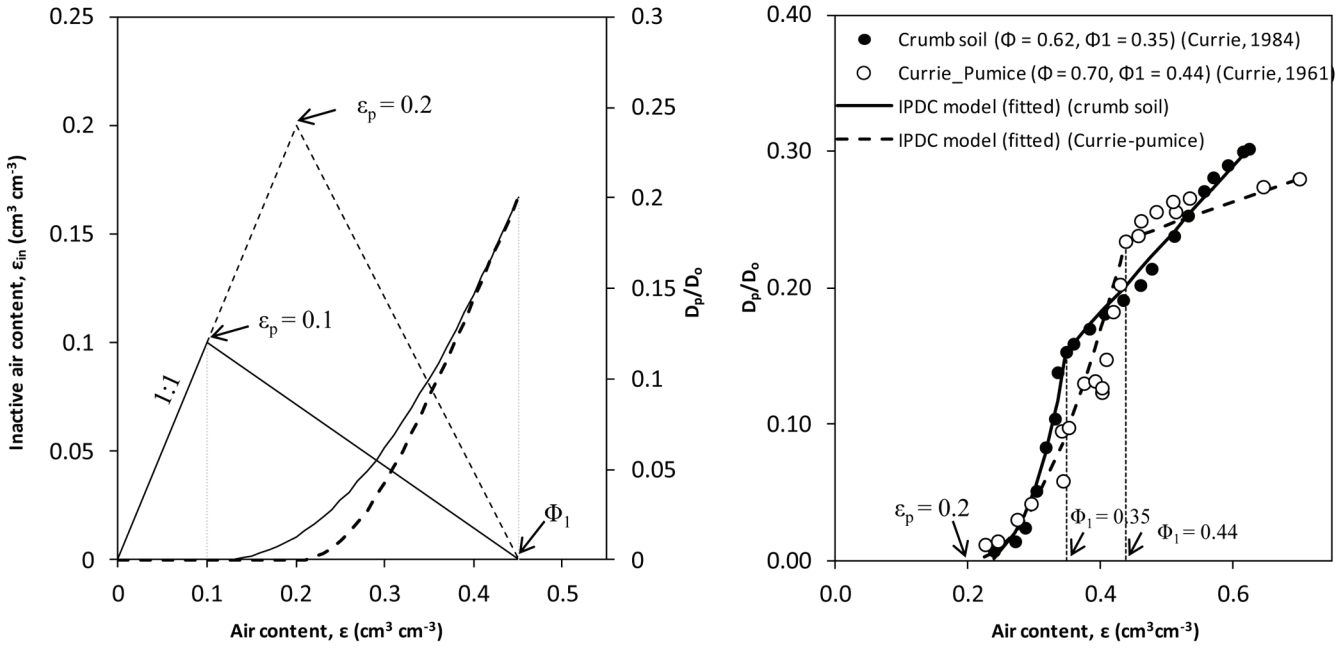


**Fig. 1. Illustration of inactive pore space and inactive pore and density corrected (IPDC) model. (a) Variation of inactive air content ($\varepsilon_{in}$) (left $y$ axis) as a function of air content ($\varepsilon$) are represented by two lines: a 1:1 line (Eq. [4a]) below the percolation threshold ($\varepsilon_p$), and an assumed linear variation (Eq. [4b]) between the percolation threshold ($\varepsilon_p$) and the interaggregate porosity ($\Phi_1$). Also shown are the IPDC model predictions (Eq. [4a] through Eq. [4g]) demonstrated using two assumed $\alpha_1$ values (right $y$ axis), $\alpha_1$ = 0.1 and $\alpha_1$ = 0.2, each for two selected $\varepsilon_p$ values: $\varepsilon_p$ = 0.1 (thin solid line), and $\varepsilon_p$ = 0.2 (dotted line). (b) IPDC model performance on two selected soils: a crumb soil (Currie, 1984) and the Currie-Pumice (Currie, 1961).**

### Region 1:

$$\frac{D_p}{D_o} = \alpha_1 \left[ \frac{\varepsilon - \varepsilon_{in}}{\Phi_1 - \varepsilon_{in}} \right]^{\beta_1} \quad 0 < \varepsilon \le \Phi_1 \qquad [4c]$$

where

$$\alpha_1 = \left. \frac{D_p}{D_o} \right|_{\varepsilon=\Phi_1} \qquad [4d]$$

The parameter $\beta_1$ is the model shape factor which can be calculated from $\alpha_1$ following the suggested linear relation (Chamindu Deepagoda et al., 2011b):

$$\beta_1 = 2 + 2.75\alpha_1 \qquad [4e]$$

Thus, Eq. [4a] through [4e] can then be used to make gas diffusivity predictions in Region 1 for the aggregated growth media. Note that $\varepsilon_p$ and $\alpha_1$ are the two controlling parameters of the IPDC model behavior, as the other two model parameters, $\varepsilon_{in}$ and $\beta_1$, are linked to $\varepsilon_p$ and $\alpha_1$, respectively. The model sensitivity to $\varepsilon_p$ and $\alpha_1$ are demonstrated in Fig. 1 using two selected $\alpha_1$ values, $\alpha_1$ = 0.2 and $\alpha_1$ = 0.3, and for each $\alpha_1$ value, model predictions are shown (right $y$ axis) for two assumed $\varepsilon_p$ values of 0.1 and 0.2.

For the predictions in Region 2, we assume the linear relation proposed by Chamindu Deepagoda et al. (2011b) as follows:

### Region 2:

$$\frac{D_p}{D_o} = \alpha_1 + \alpha_2 \left[ \frac{\varepsilon - \Phi_1}{\Phi - \Phi_1} \right] \qquad [4f]$$

where

$$\alpha_2 = \left. \frac{D_p}{D_o} \right|_{\varepsilon=\Phi} - \left. \frac{D_p}{D_o} \right|_{\varepsilon=\Phi_1} \qquad [4g]$$

The applicability of the IPDC model concept for bimodal media is demonstrated in Fig. 1b using gas diffusivity measurements from two well-aggregated soils from the literature; a crumb soil (data from Currie, 1984), and Currie-pumice (data from Currie, 1960b). The IPDC model could describe well the two differently-structured soils with significantly large percolation thresholds.

Since gas diffusion essentially occurs in the interconnected pore network, the variation of $D_p/D_o$ with $\varepsilon$ can reveal useful information on pore network connectivity in differently-structured porous media. The Buckingham (1904)-based pore connectivity factor, $X$, is a widely used parameter to describe pore network connectivity (e.g., Resurreccion et al., 2008; Chamindu Deepagoda et al., 2011c). The parameter $X$ can be computed from measured $D_p/D_o$ at different values of $\varepsilon$ by:

$$X = \frac{\log\left(\frac{D_p}{D_o}\right)}{\log(\varepsilon)} \qquad [5]$$

### Solute Diffusivity

Similar to $D_p/D_o$ models, expressions predicting solute diffusivity ($D_s/D_l$) as a function of soil-water content ($\theta$) are mainly available for structureless soils (e.g., Millington and Quirk, 1961; Olesen et al., 2001; Moldrup et al., 1997) and reliable predictive models for structured/aggregated media are lacking (Hamamoto et al., 2009a). Due to laborious and time-consuming experimental work for the measurements of $D_s$, it was often found convenient to estimate $D_s/D_l$ from relatively fast and easily measureable media properties. Electrical conductivity (EC) is a widely accepted analog parameter to solute diffusivity (Ullman and Aller, 1982; Tuli and Hopmans, 2004; Hamamoto et al., 2009a) and functional relationships have been proposed to estimate $D_s/D_l$ from relative electrical conductivity (Tuli and Hopmans, 2004). Solute transport modeling under microgravity conditions using EC sensor-based data have also been discussed (NASA, 2002). Since the dielectric permittivity ($E$) is a strictly analogous parameter to EC (Robinson and Friedman, 2005), we assume that the following implicit analogy holds between relative dielectric permittivity and solute diffusivity:

$$\frac{D_s(\theta)}{D_l} = \frac{E(\theta) - E_s}{E_b - E_s} \qquad [6]$$

where $E_s$ and $E_b$ are corresponding dielectric permittivity values for solid phase and bulk water, respectively.

## RESULTS AND DISCUSSION

### Physical Properties and Soil-Water Characteristics

The observed basic physical properties for the four growth media are given in Table 1. In striking contrast to typical structureless soils, all the media showed remarkably high total porosity (>0.60 $cm^3\ cm^{-3}$) and low bulk density (<0.90 $g\ cm^{-3}$), both are highly favorable for root growth and permeation and also to facilitate quick drainage after a rainfall or irrigation. Soil-water characteristic curves for the four growth media clearly exhibited strong dual porosity characteristics (Fig. 2a and 2c). The PSD derived from the SWC for the four growth media are also shown in Fig. 2b and 2d. The two main steps in calculating PSD involve (i) estimation of pore radius ($r$, μm) from the soil-matric potential ($\psi$, m), Eq. [3], and (ii) the derivation of pore density from the $\psi$ ($\theta$) function, Eq. [2] (shown by arrows from Fig. 2a and 2b). The PSD curves also clearly exhibited bimodal behavior with two separate peaks for all the aggregated media. A distinguishing feature of the four PSD curves for the selected media compared to those for typical aggregated soils is the distinct separation of the two pore regions (i.e., internal and external pore regions) without an overlapping region, suggesting very strong two-region characteristics. The two photos (inset

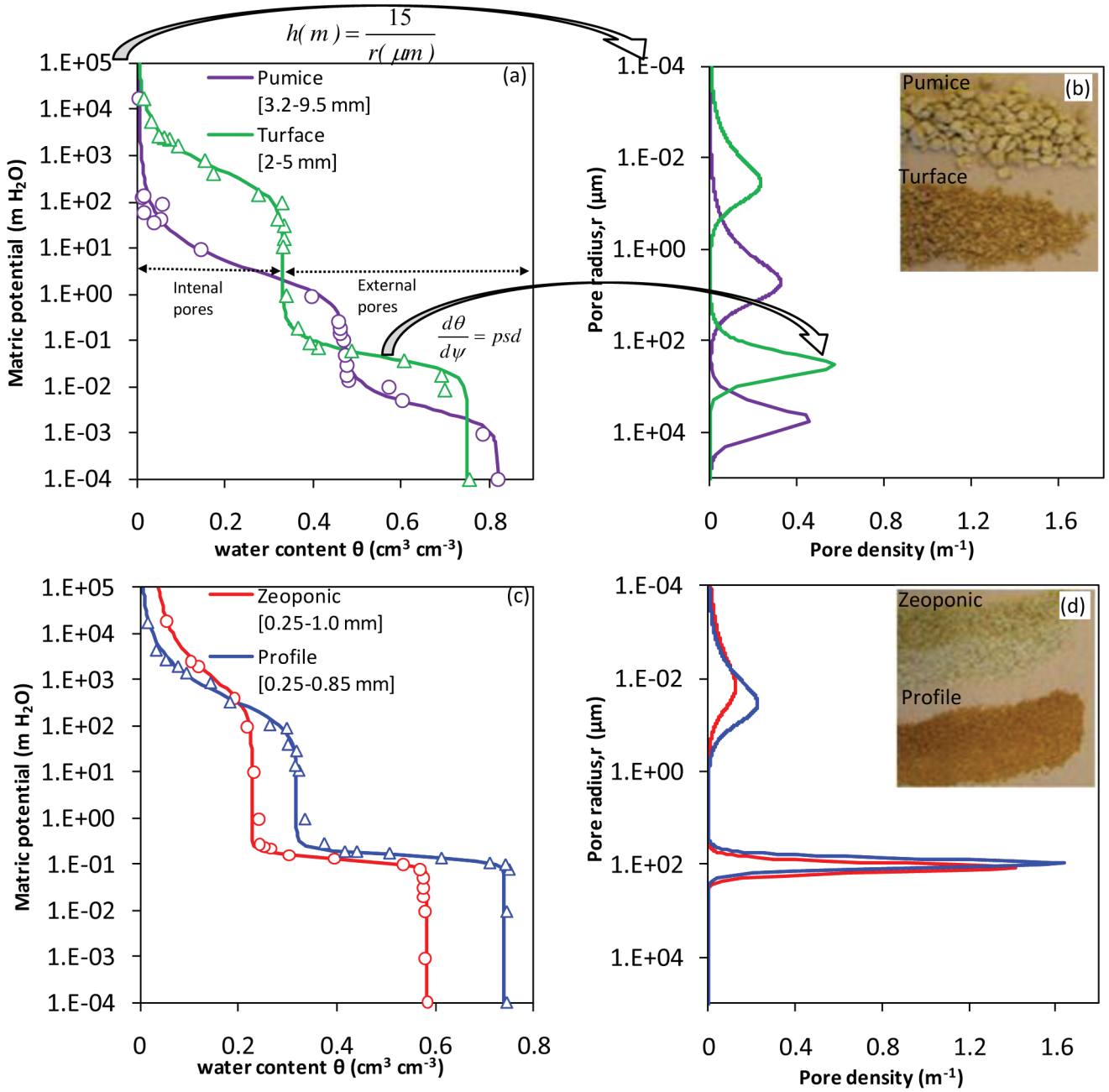


**Fig. 2. (a and c) Observed and predicted soil water characteristic (SWC) data and (b and d) corresponding pore size distribution (PSD) curves for the four aggregated growth media. The two main steps involved in derivation of PSD from SWC are also shown by arrows. Insets: (in b) photos of pumice, Turface, (in d) Zeoponic, and Profile.**

in Fig. 2b and 2d) depicting the four growth media used in this study clearly indicate their relative grain sizes.

## Growth Media Fingerprints with Pore Connectivity Factor

The variation of Buckingham (1904)-based pore connectivity factor, *X*, with air content (ε) followed generally a similar trend for the selected growth media, as demonstrated for Zeoponic and Profile in Fig. 3, and were in good agreement with previous observations (e.g., Resurreccion et al., 2008). The relatively larger *X* values at wet conditions (i.e., at small ε) are due to the high water-induced pore discontinuity and are expected to be larger for media with larger particles (with more pronounced water blockage effects) than with smaller particles. With increasing ε (draining), *X* showed a monotonic decrease due to enhanced pore connectivity, and reached a minimum when all the external pores were completely drained. Note that in fine-textured media (e.g., Zeoponic and Profile), the remaining water after each drainage step tends to get distributed over the particle surfaces, leaving less water to create water bridges between particles, which results in a more steady decrease in *X*. Conversely, in coarse-grained media, water is mostly held between particles as water bridges, and irregular discontinuity of them with drainage causes a scatter in *X* with a decreasing trend. Further drainage causes aggregates to drain themselves, allowing gases to diffuse also into the internal pores (Region 2). The

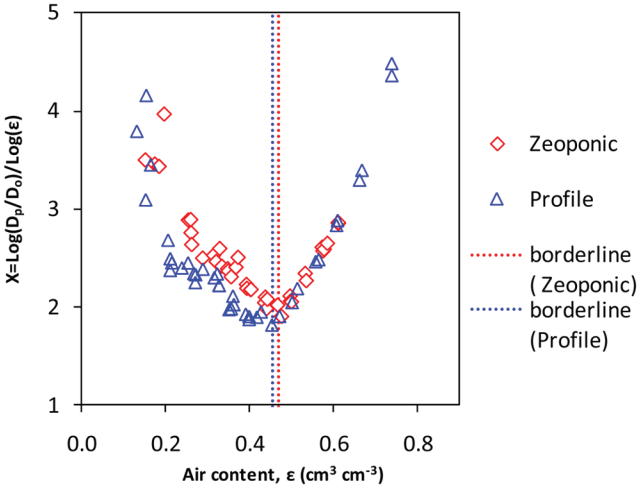


**Fig. 3. Variation of Buckingham pore connectivity factor, *X* (Eq. [5]), for Zeoponic and Profile, as a function of air content (ε). The two vertical lines demarcate the boundary between the interaggregate pore region (Region 1) and intra-aggregate pore region (Region 2) for the selected media.**

diffusion of gases through remote and highly tortuous internal pores leads to an increase in *X*. Unlike the considerable scatter observed for Region 1, the *X*-ε behavior within Region 2 for the four media showed a striking agreement in all media, suggesting a strong similarity in their internal pore structure despite wide contrasts in size, physical properties, and origin. The air content at which minimum *X* occurs demarcates the boundary between the external (Region 1) and internal (Region 2) pore regions for each medium (shown by dotted lines; Fig. 3), and therefore gives useful information on the porosities associated with each region. In this study, we defined the air content at minimum *X* as the external porosity to give the soil *functional* pore space (determined from $D_p$ measurements) a greater significance.

## Oxygen and Nutrient Diffusivities and Plant Limiting Criteria

Figure 4 shows data for gas diffusivity ($D_p/D_o$) measured at both UCDavis (open circles) and AAU, Denmark (closed circles), as a function of soil-air content (ε). The two independent measurements generally showed a good agreement and thus verified the consistency of the measurements from the two different apparatus. The two-region IPDC model, Eq. [4a] through Eq. [4g], described well the observed data and hence proved to be a useful tool for well-aggregated media with distinct percolation thresholds. Also shown in Fig. 4 are the results for solute diffusivity (estimated in analogy with relative dielectric permittivity, $E/E_o$) as a function of soil water content (θ) for the four growth media. The solute diffusivity variation also exhibited a noticeable two-region behavior as observed in many previous studies related to bimodal media (e.g., Hamamoto et al., 2009a) and was generally consistent with the two-region behavior shown by gas diffusivity data.

With a combined illustration of gas and solute diffusivities in the entire range of air and water contents, Fig. 4 further provides a useful platform for evaluating the ability of the growth media to meet simultaneously the air and nutrient requirements for plant growth. We here discuss the limiting criteria with respect to gas and nutrient diffusion for optimal plant growth under Martian conditions (referred to as Mars criteria), while showing the corresponding values also for terrestrial (reference) conditions (referred to as Earth criteria). For the limiting Earth criterion for gas diffusivity we used the value $D_p/D_o = 0.02$ reported in many studies as the threshold (minimum) value for adequate soil aeration in uncontrolled (field) conditions (Stepniewski, 1980; Schjønning et al., 2003). Jones et al. (2011) used the same threshold value to discuss gas diffusivity in containerized media while Nkongolo and Caron (2006) and Allaire et al. (1996) also observed a threshold near $D_p/D_o \approx 0.015$ in containerized peat substrates. There is no analogous well-documented criterion for solute diffusivity/relative permittivity ($E/E_o$), we therefore evaluated and compared the media for critical nutrient supply based on a value of $E/E_o = 0.01$, at which there is assumed to be sufficient media connectivity to facilitate movement of solutes in root zone environments.

As we previously discussed, the gravity effects on pore scale phase distribution were less pronounced for gas diffusivity, particularly at less saturated conditions. In typical root modules of relatively large scale (e.g., 10 cm in height), however, the macroscopic gas transport properties will be controlled by wetting front morphology and phase entrapment, where gravity effects may also play a role (Or et al., 2009). For example, at reduced gravity conditions water tends to get more uniformly distributed over the sample volume. Consequently, the increased water-induced pore tortuosity at reduced gravity may result in a decrease in $D_p$. For a sample of nearly 10 cm thickness, Jones et al. (2003) showed a decrease in $D_p$ by 1.5 to 2.0 times at zero gravity (0 *g*) relative to terrestrial gravity (1 *g*). Therefore, to account for the likely underprediction in gas diffusion coefficient under reduced gravity, we applied a safety factor of 2.0 to define the Mars criterion for gas diffusivity (i.e., $D_p/D_o = 0.04$). The effect of reduced gravity on solute diffusivity is not well examined but Or et al. (2009) theoretically argued for negligible reduced-gravity effects on pore-scale (microscopic) water distribution and configuration. In the present study the critical (limiting) conditions for solute diffusivity is assumed to occur in between irrigation events where the water is mainly present as interaggregate water held tightly by capillary forces and this together with the theoretical results by Or et al. (2009) leads to our assumption of negligible effects of gravity change from 1 *g*.

## Critical Diffusivity Windows for Oxygen and Nutrients

Plants grown in volume-constrained modules, under terrestrial gravity or reduced gravity, are typically subjected to a predefined periodic irrigation to ensure that plant water and nutrient requirements are adequately met at all times. When substantial time has elapsed after an irrigation event, the water held in the external pores will be nearly drained, and most of the plant water and nutrient requirements will be supplied by the water available in the internal pores. As mentioned above, the

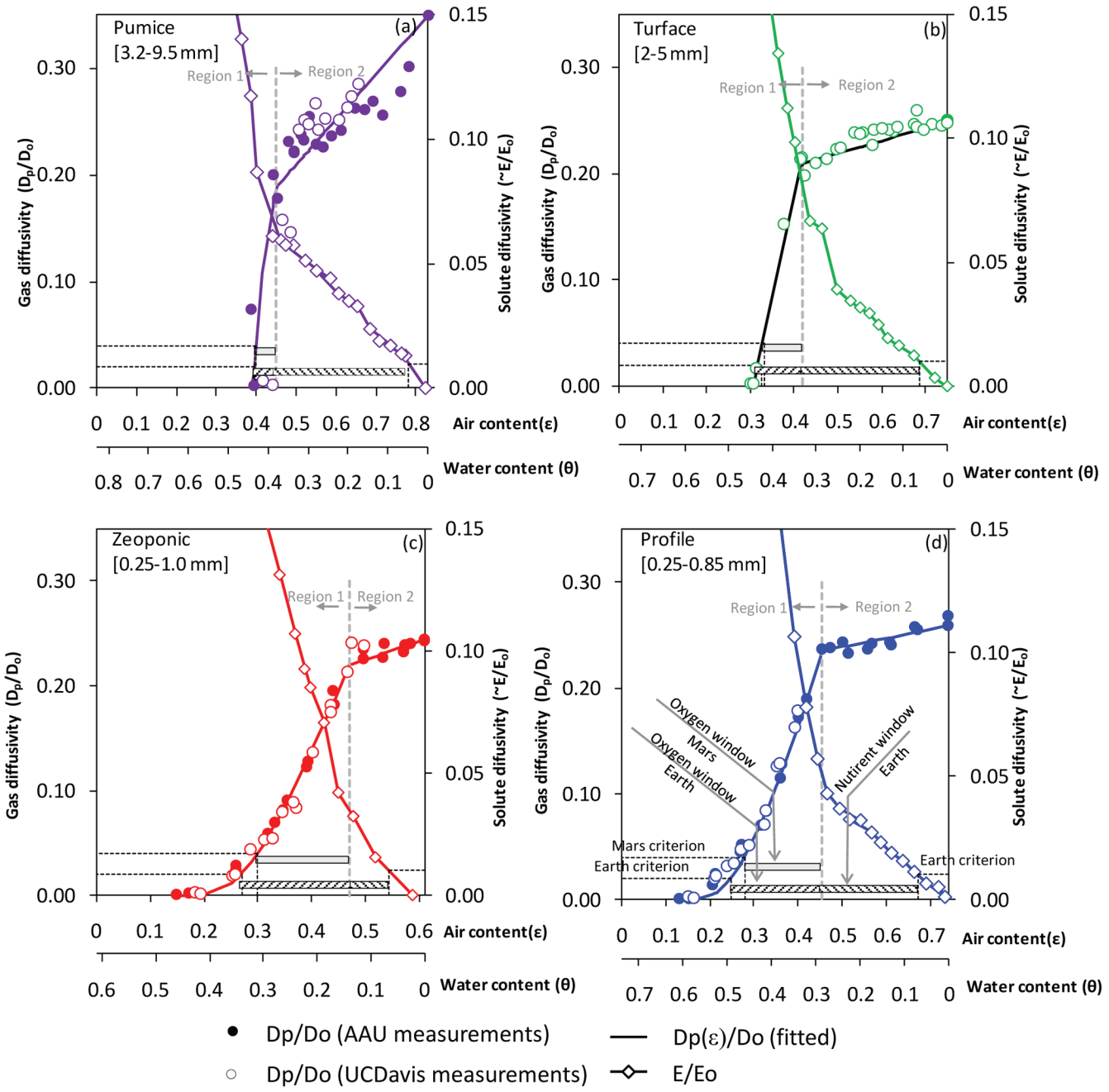


**Fig. 4. Oxygen diffusivity ($D_p/D_o$) and solute diffusivity (estimated from relative dielectric permittivity, $E/E_o$) as a function of air content (ε) and water content (θ), respectively, for the four aggregated growth media. The independent $D_p/D_o$ measurements done at the University of California, Davis (UCDavis) (open circles) and at the Aalborg University (AAU), Denmark (closed circles) are shown, together with the inactive pore density corrected (IPDC) model predictions (Eq. [4a] through Eq. [4g]). The "windows" for oxygen diffusivity and solute (nutrient) diffusivity are also shown by differently shaded horizontal bars at both Martian and terrestrial conditions (see Fig. 4d for details). Note: Earth and Mars criteria for limiting oxygen diffusivity are $D_p/D_o$ = 0.02 and $D_p/D_o$ = 0.04, respectively. $E/E_o$ = 0.01 was used to evaluate nutrient diffusivity window for Earth.**

critical condition with regard to nutrient diffusion occurs some time after cease of irrigation when the internal pores also start draining (i.e., moving from the vertical dashed line toward the right in Fig. 4) and the water content falls below the limiting values for solute diffusivity. The critical condition for oxygen diffusion, on the other hand, occurs soon after irrigation, when the external pore space is being gradually occupied by water (i.e., moving from the vertical dotted line toward the left in Fig. 4), causing the soil-air content to fall below the value corresponding to limiting oxygen diffusivity. Thus, in order for plants to survive at both the critical conditions, the growth media should have sufficiently large CWD; the media with the larger CWD (for oxygen and nutrients) will likely provide a more favorable environment for plants at limiting conditions. The oxygen and nutrient CWD for the four growth media at Earth condition and the oxygen CWD for and Martian condition are shown in Fig. 4 (in differently shaded horizontal bars) and the corresponding details are given for convenience in Fig. 4d. Table 2 shows the measured widths (intervals of air content) of the CWD for each growth medium. The media having smallest CWD, highlighted

**Table 2. Critical windows for oxygen and solute diffusivity and water availability at Earth and Mars conditions. (The window width is measured in air contents)**

| Media | For Earth condition Diffusivity windows | | For Martian condition | | |
|---|---|---|---|---|---|
| | Oxygen | Solute† | | Oxygen diffusivity at pF 1.3 | Water window θ at pF 1.3–pF 4.2 |
| Pumice | **0.054‡** | 0.331 | **0.051** | **0** | 0.442 |
| Turface | 0.096 | 0.266 | 0.087 | 0.124 | 0.067 |
| Zeoponic | 0.200 | **0.073** | 0.170 | 0.087 | **0.034** |
| Profile | 0.207 | 0.216 | 0.175 | 0.108 | 0.138 |

† Critical window for solute diffusivity was evaluated based on $E/E_o = 0.01$.

‡ Bold numbers refer to the lowest value among the four growth media.

in bold (Table 2), were pumice (for oxygen at Earth and Mars conditions) and Zeoponic (for nutrients at Earth condition). We emphasize that the present CWD concept is based on static pore-water conditions where the critical (limiting) situations for gas and solute diffusivity will occur in between irrigation events. The CWD approach is at present not linked to dynamic water flow conditions and the results from the previous studies (e.g., Scovazzo et al., 2001) on dynamic nutrient supply to plant roots by moving water (convective transport) therefore have not been taken into account.

## Field Capacity and Critical Water Storage Windows

Another key approach to evaluate the growth media for adequate soil aeration is to observe oxygen diffusivity at *field capacity* conditions (note that the term "field capacity" here refers to the potentials imposed in controlled volumes that are comparable to those in the field at field capacity). At field capacity, the excess water will be drained, and the media will stabilize at a certain matric potential or pF. This potential has been suggested to occur at or near −100 cm $H_2O$ or pF 2 for a wide range of texture intervals at terrestrial gravity conditions (Schjønning and Rasmussen, 2000; Al Majou et al., 2008). However, Madsen (1976) observed that −50 cm $H_2O$ (or pF 1.7) would be a better approximate to mimic field capacity in coarse-textured media. This is also in agreement with the study by Allaire et al. (1996) who used −50 cm $H_2O$ as the limiting potential of "easily available water (EAW)" for containerized media. In reduced gravity conditions, for example at Martian gravity (0.37 $g$), the corresponding matric potential may occur at −19 cm $H_2O$ or pF 1.3 (i.e., in equilibrium with free water held 19 cm below the gravity vector), assuming the equilibrium matric potential scales linearly with the gravitational force (Jones et al., 2011). Figure 5 shows the measured $D_p/D_o$ data for the four growth media as presented in Fig. 4, but now as a function of pF. The predictions from the combined two-region IPDC model (Eq. [4a] through [4 g]) and the bimodal water retention function (Eq. [1] with $|\psi| = 10^{pF}$) are also shown (solid line). The star symbol denotes the limiting gas diffusivity for soil aeration ($D_p/D_o = 0.04$) near field capacity (pF = 1.3) in Mars conditions. Profile, Turface, and Zeoponic exhibited oxygen diffusivity at pF 1.3 significantly above the limiting value (marked by a dotted arrow), and therefore *passed* the oxygen diffusivity-based evaluation. Pumice, on the other hand, *failed* to satisfy the minimum requirement for soil aeration due to its significantly large percolation threshold for oxygen diffusivity.

At field capacity, the media should also ensure adequate water and nutrient storage, or a sufficiently large "critical water window", for optimum plant growth. A great variety of plants reportedly have a permanent wilting point at pF 4.2 irrespective of soil types (Schofield, 1935), which essentially limits the water availability for plant growth/survival. We calculated the width of the critical water windows for Mars conditions at water contents between pF 1.3 (field capacity) and pF 4.2 (plant wilting point, with a reasonable assumption that it will remain unaffected by reduced gravity). Note that the adopted water window is also one of the limiting criteria in the widely used least limiting water range (LLWR) concept to assess overall soil physical quality for plant growth (da Silva et al., 1994; Lapen et al., 2004).

Revisiting Fig. 5, water retention results are also shown, together with the model predictions (dotted line) using the bimodal water retention function. The shaded area illustrates the critical water window for each medium, showing the smallest window for Zeoponic (see also Table 2). Note that pumice shows good water storage properties with the largest critical water window, but it already showed very poor aeration near field capacity. Overall, Profile showed the best results with fairly balanced oxygen and nutrient windows at limiting conditions and with satisfactory performances also at field capacity. In addition, the results suggest that Turface is a promising plant growth medium for future space-based applications. Further, out of the four growth media, Profile and Turface have the largest specific surface areas (measured with the EGME method, Table 1), which may potentially serve as additional storage for plant essential nutrients.

## Mean Particle–Pore Size Relations and Design Diagram for Optimal Growth Media

As the above diffusivity-based analysis implied, the proper selection of particle size will be an essential prerequisite for the optimal design of a plant growth medium. The particle size likely controls the mean pore size and also the percolation threshold for oxygen diffusivity in the medium, and can therefore significantly alter soil aeration properties. Previous studies have also reported promising correlations between particle size distribution and soil aeration characteristics. Verhagen (1997) and Caron et al. (2005), for example, observed strong relationship between the soil-air content at a specific matric potential and the finer particle fraction (<1mm) in different peat mixes. Figure 6 shows the percolation threshold ($\varepsilon_p$) values for the six considered porous media plotted against the corresponding mean particle sizes ($D_{mean,}$ μm). Percolation threshold ($\varepsilon_p$) showed an increase with increasing $D_{mean}$ following a very promising linear relationship ($r^2 = 0.98$). The observed $\varepsilon_p$–$D_{mean}$ linear relation will be of great utility in future studies when estimating $\varepsilon_p$ for different media, particularly in the absence of measured $D_p/D_o$ data.

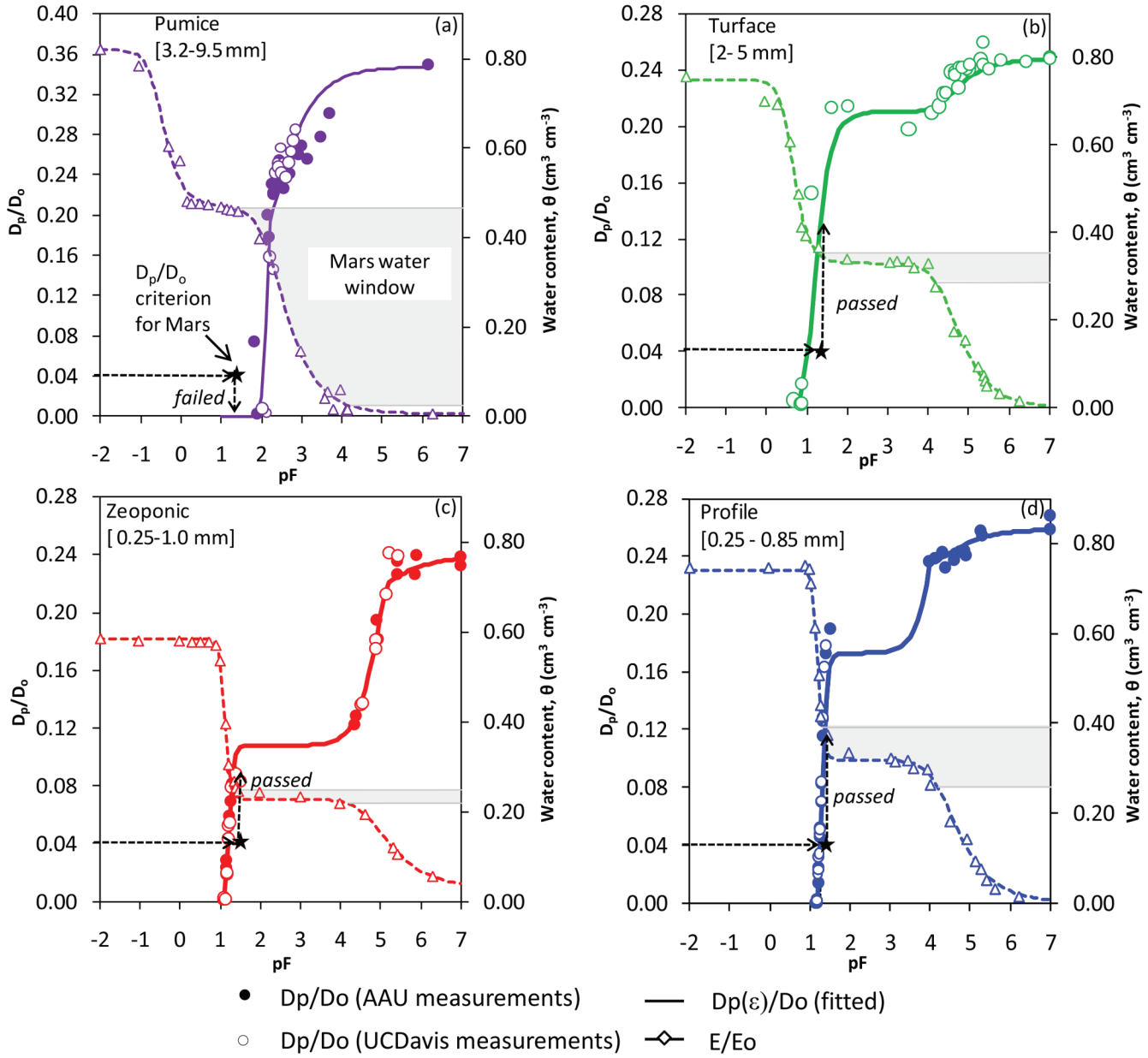


**Fig. 5. Measured oxygen diffusivity ($D_p/D_o$) for the four aggregated growth media as given in Fig. 4, but as a function of pF ( = log |−ψ, cm $H_2O$|). The $D_p/D_o$ predictions (solid line) are made by combining inactive pore density corrected (IPDC) model (Eq. [4a] through Eq. [4g]) with the van Genuchten type bimodal soil-water characteristics (SWC) function (Eq. [1] and $|\psi| = 10^{pF}$). The star (★) denotes the limiting oxygen diffusivity criterion at Martian field capacity (i.e., $D_p/D_o$ = 0.04 at pF 1.3) and the dotted arrows indicate whether the media satisfies the limiting criterion (marked as *passed*) or not (marked as failed). Also shown are the observed and predicted (dashed line) soil water characteristics. The suggested "Mars water window" (i.e., water content between pF 1.3 and pF 4.2) is also shown for each medium (the shaded area).**

Among the factors controlling gas percolation threshold ($\varepsilon_p$), the local distribution and geometries of water films and water bridges between particles dominate. Since such pore scale water distribution configurations are not significantly affected by gravity (Or et al., 2009), the percolation threshold may likely remain unchanged under reduced gravity conditions. Further, a preliminary water drainage simulations for different column lengths suggested less pronounced effects of column length on bulk soil water content profile. However, correct design of water application and drainage system under microgravity is important to ensure that local areas with encapsulated soil-air is minimized, and this needs to be optimized in further modeling and experimental studies (e.g., Chau et al., 2005).

Figure 7 shows mean particle diameter ($D_{mean}$) plotted against pF and drained pore diameter ($d$), together with the linear relation, $d$ = 0.27 $D_{mean}$ suggested by Hamamoto et al. (2009b) for coarse-textured media. The two vertical dotted lines, drawn at pF 1.7 (or $d$ = 60 μm) and 1.3 (or $d$ = 150 μm), correspond to the above assumed terrestrial condition (i.e., field capacity of −50 cm $H_2O$) and Martian condition (i.e., field capacity of −19 cm $H_2O$), respectively. This implies that, for example, at a field capacity of pF = 1.7, all the pores >60 μm will be drained, and therefore a medium with pores predominantly larger than 60 μm will provide optimum aeration for plant growth. Assuming the relation $d = 0.27D_{mean}$ holds, this corresponds to a mean particle diameter ($D_{mean}$) of 220 μm, suggesting a medium

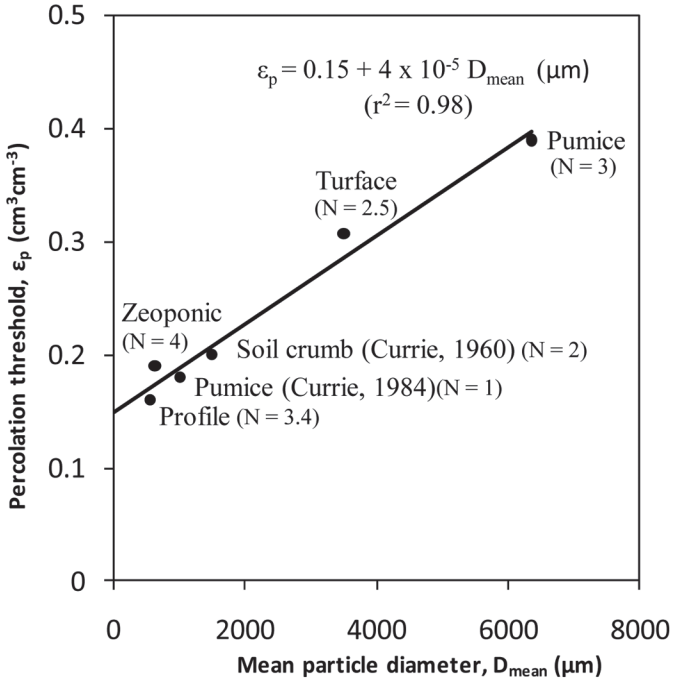


**Fig. 6. Observed percolation threshold ($\varepsilon_p$) as a function of mean particle diameter ($D_{mean}$, μm) for the six considered growth media, together with the best-fit linear regression model (solid line). The ratio of maxium to minimum particle size, denoted as *N*, is also shown for each growth media.**

with $D_{mean}$ >220 μm (shown by the area shaded in orange) will ensure good soil aeration at terrestrial field capacity. The similar criterion at Martian field capacity (at pF 1.3) is $D_{mean}$ >550 μm (shown by the area shaded in brown; Fig. 7). Note that both Zeoponic and Profile, the two smallest particle size fractions, satisfied the minimum particle size criterion at both terrestrial and Martian conditions (shown by two dotted horizontal lines; Fig. 7). Therefore, the two coarser media, Turface and pumice also obviously satisfied the minimum criterion for both Earth and Mars conditions, suggesting the suitability of all five media in Earth-based and Mars-based applications. Note that media with very large particles (e.g., pumice) will also suffer from poor soil aeration due to a larger percolation threshold, suggesting the existence of a limiting value also for maximum $D_{mean}$. Our results show that $D_{mean}$ <5000 μm will be an appropriate upper-limit criterion for adequate oxygen diffusivity. Note that the suggested aggregate size range for adequate soil aeration (0.2–5 mm) on Earth is broadly in good agreement with the observed optimal aggregate size interval for seed-to-aggregate contact based on best plant emergence and minimum evaporation (Braunack, 1995; Håkansson et al., 2011). The suggested minimum aggregate size for Martian condition ($D_{mean}$ >0.5 mm) also agrees well with the observations from Jones et al. (2011), who noted that the particle diameter above 1 mm and narrow particle (and pore) size distribution may potentially minimize the capillary force dominance on water distribution under reduced gravity conditions. This can be best examined by numerical simulations of fluid phase behavior in different growth media with different aggregate size distributions (and thus different soil-water (θ-ψ) and soil-air (ε-ψ) characteristic curves) under full and reduced gravity as illustrated in Jones et al. (2011), combined with growth experiments under different gravity conditions.

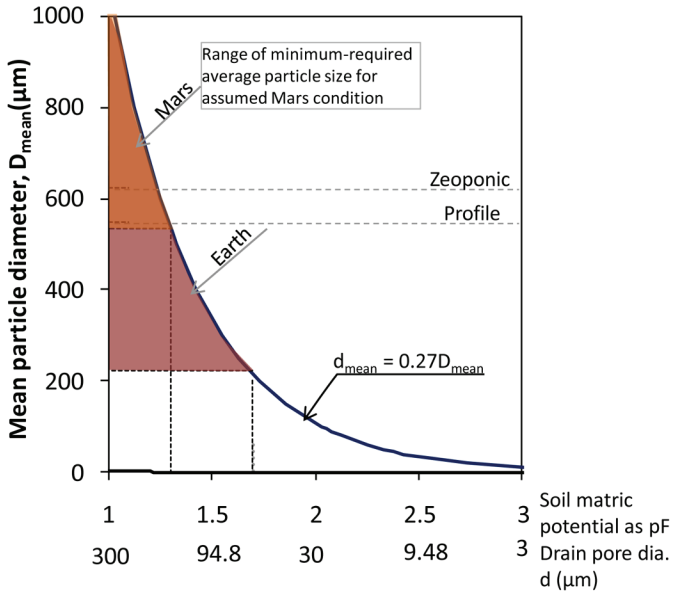


**Fig. 7. The proposed design diagram for selection of optimum particle size based on different drainage conditions (pF values) for terrestrial and Martian conditions. The range of minimum average particle sizes for assumed Earth condition (field capacity –50 cm $H_2O$ or pF 1.7; brown colored area) and Mars (field capacity –19 cm $H_2O$ or pF 1.3; orange colored area) condition are shown for the linear relation $d_{mean}$ = 0.27 $D_{mean}$ (Hamamoto et al., 2009b). pF = log |–ψ, cm $H_2O$|.**

We emphasize that the lower and upper limits for $D_{mean}$ suggested herein for the selection of an optimum particle size range are based only on adequate aeration. The media properties ensuring sufficient water and nutrient supply should also be embraced when selecting an optimal plant growth medium.

## Volcanic Ash Soil in Space: Implications from the Diffusivity-based Analysis

Among the basic properties we discussed in relation to a promising plant growth medium are high total porosity and low bulk density, accompanied by strong dual porosity characteristics. Of the naturally occurring soils endowed with such useful properties, volcanic ash soils (Andisols) are well known and widely regarded as highly suitable growth media (Shoji and Takahashi, 2002). A deep rooting zone, large water holding capacity, and good drainage properties are common in typical Andisols (Shoji et al., 1993). These distinctive Andic properties are generally attributed to the presence of allophane-dominated hollow spherical morphology, which allows free movement of water/air molecules into and out of the structure (Nanzyo, 2002). Besides, some soils derived from volcanic origins (e.g., JSC Mars-1 Martian regolith simulant) are reported to have a close spectral similarity to the bright regions of Mars, and are widely recognized as promising terrestrial analogs to the Martian soils (Robinson et al., 2009). A diffusivity-based analysis, in addition, will also provide further insight into the characteristics of the volcanic ash soils.

Figure 8 shows observed gas diffusivity as a function of air content for a Nishi-Tokyo volcanic ash soil [2–4.76 mm] (data from Chamindu Deepagoda et al., 2011b). The measured data were limited at the wet region, particularly near the percolation threshold, and therefore we used the $D_{mean}$ - $\varepsilon_p$ relation (Fig. 6) to estimate the percolation threshold for the selected size fraction. Together with the IPDC model, Eq. [4a] through Eq. [4g], we reasonably predicted the observed gas diffusivity (solid line). The observed CWD for oxygen corresponding to Mars conditions (shown by the shaded bar; Fig. 8) is comparable to that of Turface. The soil also *passed* the evaluation test for sufficient aeration at Martian field capacity, since the observed value of $D_p/D_o$ at pF 1.3 was well above the limiting value ($D_p/D_o$ = 0.04). The width of the critical water window at Mars conditions (not shown) was also observed to be comparable to those for Turface and Profile. Solute diffusivity/electrical permittivity measurements for the selected particle size fraction of the soil are needed to examine the corresponding CWD for nutrients. Further shown in Fig. 8 are the observed soil-water retention data together with model-fit (Eq. [1]; dashed line), which suggest distinct dual porosity characteristics. The observed very large SSA (227.2 $m^2$ $g^{-1}$, comparable to the JSC Mars-1 simulant's SSA of 200 $m^2$ $g^{-1}$) by the EGME method provides further evidence of its physical suitability as an excellent growth medium. In summary, the observed oxygen diffusivity and media properties for the Nishi-Tokyo Andisol are comparable to well-performing growth media and therefore it can, in a future perspective, be a promising growth medium candidate for space-based applications.

An important aspect we did not consider as part of the CWD concept is the volume displacement by roots. The root intrusion to substrate macropore space, up to nearly 20% of pore space in the given media, will be within the region of gas percolation threshold (see Fig. 4 and Fig. 8) and hence will not adversely affect gas diffusivity. In addition, some other important issues, including container geometry (Fonteno, 1989), have not been addressed here.

Due to its widespread potential use and importance, we re-emphasize that the diffusion-based media characterization we mainly focused in the present study is only one important aspect of broad considerations in growth media design. The final plant growth media characterization must essentially include many physical, chemical, and biological considerations for both terrestrial and reduced gravity conditions while the reduced gravity systems may involve additional issues, for example, shuttle launch vibrations (Steinberg et al., 2002).

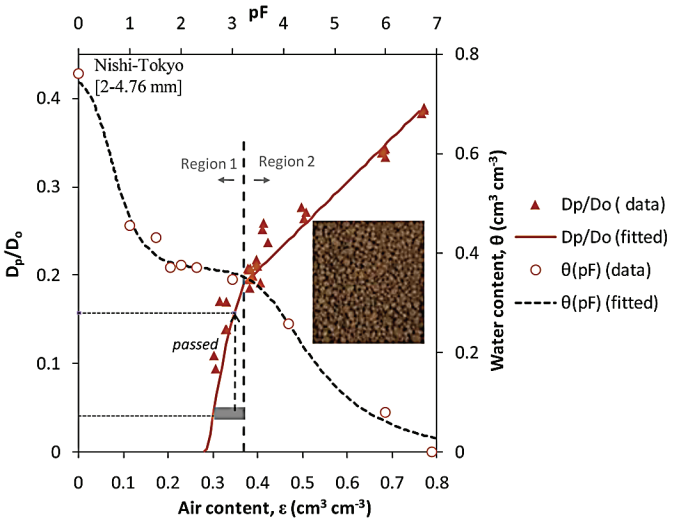


**Fig. 8. Measured oxygen diffusivity ($D_p/D_o$) as a function of air content (ε) for Nishi-Tokyo volcanic ash soil (Andisol) [2–4.76 mm], together with the inactive pore density corrected (IPDC) model predictions, Eq. [4a] through Eq. [4 g] (solid line). The "window" for oxygen diffusivity is shown (shaded horizontal bar) for Martian condition. The oxygen diffusivity at Martian field capacity (i.e., at pF 1.3) (shown by dotted vertical and horizontal lines) exceeds the limiting $D_p/D_o$ value for Mars (i.e., $D_p/D_o$ = 004; horizontal dashed line) and hence *passed* the evaluation criterion. Also shown in (a) are the observed soil water retention data, together with the best-fit to bimodal van Genuchten type model (Eq. [1]). The vertical dashed line separates the external pore (Region 1) and internal pore (Region 2) regions. Inset: a photo of Nishi-Tokyo [2–4.76 mm] soil aggregates. Data from Chamindu Deepagoda et al. (2011b). pF = log |–ψ, cm $H_2O$|.**

## CONCLUSIONS

· The appropriate selection of particle size for optimal plant growth was discussed based on a mean particle size and pore size-based design diagram. As an important part of this, a. strong relation ($r^2$ = 0.98) between percolation threshold for gas diffusivity and mean particle (aggregate) diameter was found. The overall results implied to avoid mean particle sizes below 0.2 mm (due to insufficient aeration) and above 5 mm (due to large percolation threshold) when selecting optimal plant growth media for Earth and, especially, Martian conditions.

· A new IPDC model could describe well the observed gas diffusivity data for the selected media, all with a distinct percolation threshold.

· Japanese volcanic ash soil (Andisol) with 2- to 4.76-mm sized aggregates showed good aeration characteristics comparable to well-performing growth media. All potential growth media, however, need to be investigated for other critical aspects in plant growth media design before making final selections.

· Based mainly on the concept of CWD for oxygen and nutrients, this study presented a comparison of four prospective growth media (pumice, Turface, Zeoponic, and Profile) to select best-performing media under the terrestrial and Martian conditions. Among the tested media, Profile showed best overall performance, followed by Turface and Zeoponic in that order. Pumice showed a poor performance due to inadequate aeration for plant growth.


## ACKNOWLEDGMENTS

This study was part of the project Gas Diffusivity in Intact Unsaturated Soil ("GADIUS") and the large framework project Soil Infrastructure, Interfaces, and Translocation Processes in Inner Space ("Soil-it-is"), both from the Danish Research Council for Technology and Production Sciences. We gratefully acknowledge the assistance of Innovative Research Organization of Saitama University, Japan.

## REFERENCES


Allaire, S.E., J. Caron, L.E. Parent, I. Duchesne, and J.A. Rioux. 1996. Air-filled porosity, relative gas diffusivity, and tortuosity: Indices of Prunus x cistena sp. growth in peat substrates. J. Am. Soc. Hortic. Sci. 121:236–242.

Al Majou, H., A. Bruand, and O. Duval. 2008. The use of in situ volumetric water content at field capacity to improve prediction of soil water retention properties. Can. J. Soil Sci. 88:533–541. doi:10.4141/CJSS07065

Bingham, G.E., S.B. Jones, D. Or, I.G. Podolski, M.A. Levinskikh, V.N. Sytchov, T. Ivanova et al. 2000. Microgravity effects on water supply and substrate properties in porous matrix root support systems. Acta Astronaut. 47:839–848. doi:10.1016/S0094-5765(00)00116-8

Blonquist, J.M., Jr., S.B. Jones, I. Lebron, and D.A. Robinson. 2006. Microstructural and phase configurational effects determining water content: Dielectric relationships of aggregated porous media. Water Resour. Res. 42:W05424 10.1029/2005WR004418. doi:10.1029/2005WR004418

Braunack, M.V. 1995. Effect of aggregate size and soil water content on emergence of soybean (*Glycine max* L. Merr.) and maize (*Zea mays* L.). Soil Tillage Res. 33:149–161. doi:10.1016/0167-1987(94)00444-J

Buckingham, E. 1904. Contributions to our knowledge of the aeration of soils. Bur. Soil Bull. 25. U.S. Gov. Print. Office, Washington, DC.

Caron, J., L.M. Reviere, and G. Guillemain. 2005. Gas diffusion and air filled porosity: Effect of some oversize fragments in growing media. Can. J. Soil Sci. 85:57–65. doi:10.4141/S03-086

Cerato, A.B., and A.J. Lutenegger. 2002. Determination of surface area of fine-grained soils by the Ethylene Glycol Monoethyl Ether (EGME) method. Geotech. Testing J., ASTM. 25:314–320.

Chamindu Deepagoda, T.K.K., P. Moldrup, P. Schjønning, L.W. de Jonge, K. Kawamoto, and T. Komatsu. 2011a. Density-corrected models for gas diffusivity and air permeability in unsaturated soil. Vadose Zone J. 10:226–238. doi:10.2136/vzj2009.0137

Chamindu Deepagoda, T.K.K., P. Moldrup, P. Schjønning, K. Kawamoto, T. Komatsu, and L.W. de Jonge. 2011b. Generalized density corrected model for gas diffusivity in variably saturated soils. Soil Sci. Soc. Am. J. 74:1302–1317.

Chamindu Deepagoda, T.K.K., P. Moldrup, P. Schjønning, K. Kawamoto, T. Komatsu, and L.W. de Jonge. 2011c. Variable pore connectivity model linking gas diffusivity and air-phase tortuosity to soil matric potential. Vadose Zone J. 11: 10.2136/vzj2011.0096.

Chau, J.F., D. Or, and M.C., Sukop. 2005. Simulation of gaseous diffusion in partially saturated porous media under variable gravity with lattice Boltzmann methods. Water Resour. Res. 10.1029/2004WR003821.

Currie, J.A. 1960a. Gaseous diffusion in porous media: Part 1. A nonsteady state method. Br. J. Appl. Phys. 11:314–317. doi:10.1088/0508-3443/11/8/302

Currie, J.A. 1960b. Gaseous diffusion in porous media: Part 2. Dry granular materials. Br. J. Appl. Phys. 11:318–324. doi:10.1088/0508-3443/11/8/303

Currie, J.A. 1961. Gaseous diffusion in porous media: Part 3. Wet granular materials. Br. J. Appl. Phys. 12:275–281. doi:10.1088/0508-3443/12/6/303

Currie, J.A. 1984. Gas diffusion through soil crumbs: The effects of compaction and wetting. J. Soil Sci. 35:1–10. doi:10.1111/j.1365-2389.1984.tb00253.x

da Silva, A.P., B.D. Kay, and E. Perfect. 1994. Characterization of the least limiting water range of soils. Soil Sci. Soc. Am. J. 58:1775–1781. doi:10.2136/sssaj1994.03615995005800060028x

de Jonge, H., L.W. de Jonge, and C. Mittelneijer-Hazeleger. 2000. The microporous structure of organic and mineral soil materials. Soil Sci. 165:99–108. doi:10.1097/00010694-200002000-00001

Dreschel, T.W., R.M. Wheeler, J.C. Sager, and W.M. Knott. 1989. Factors affecting plant growth in membrane nutrient delivery. In: R.D. MacElroy, editor, Controlled ecological life support systems: CELSS '89 Workshop. NASA Tech. Mem. 1989-102277. Ames Res. Ctr., Moffett Field, CA.

Durner, W. 1994. Hydraulic conductivity estimation for soils with heterogeneous pore structure. Water Resour. Res. 30:211–223. doi:10.1029/93WR02676

Fonteno, W.C. 1989. An approach to modeling air and water status of horticultural substrates. Acta Hort. 238:67–74.

Håkansson, I., T. Rydberg, and J. Arvidsson. 2011. Effects of seedbed properties on crop emergence: 2. Effects of aggregate size, sowing depth and initial water content under dry weather conditions. Acta Agric. Scand. B-S. 61:469–479.

Hamamoto, S., P. Moldrup, K. Kawamoto, and T. Komatsu. 2009b. Effect of particle size and soil compaction on gas transport parameters in variably saturated, sandy soils. Vadose Zone J. 8:986–995. doi:10.2136/vzj2007.0144

Hamamoto, S., M.S.A. Perera, A.C. Resurreccion, K. Kawamoto, S. Hasegawa, T. Komatsu, and P. Moldrup. 2009a. The solute diffusion coefficient in variably compacted, unsaturated volcanic ash soils. Vadose Zone J. 8:942–952. doi:10.2136/vzj2008.0184

Heinse, R., S.B. Jones, S.L. Steinberg, M. Tuller, and D. Or. 2007. Measurements and modeling of variable gravity effects on water distribution and flow in unsaturated porous media. Vadose Zone J. 6:713–724. doi:10.2136/vzj2006.0105

Jones, S.B., B. Bugbee, R. Heinse, D. Or, and G.E. Bingham. 2009. Porous plant growth media design considerations for lunar and martian habitats. Soc. Automot. Eng. Techn. Paper no. 2009-01-2361.

Jones, S.B., and D. Or. 1998a. Design of porous media for optimal gas and liquid fluxes to plant roots. Soil Sci. Soc. Am. J. 62:563–573. doi:10.2136/sssaj1998.03615995006200030002x

Jones, S.B., and D. Or. 1998b. Particulated growth media for optimal liquid and gaseous fluxes to plant roots in microgravity. Adv. Space Res. 22:1413–1418. doi:10.1016/S0273-1177(98)00221-X

Jones, S.B., D. Or, and G.E. Bingham. 2003. Gas diffusion measurement and modeling in coarse-textured porous media. Vadose Zone J. 2:602–610.

Jones, S.B., D. Or, R. Heinse, and M. Tuller. 2011. Beyond earth: Designing root zone environments for reduced gravity conditions. Vadose Zone J. 11. 10.2136/vzj2011.0081.

Lapen, D.R., G.C. Topp, E.G. Gregorich, and W.E. Curnoe. 2004. Least limiting water range indicators of soil quality and corn production, eastern Ontario, Canada. Soil Tillage Res. 78:151–170. doi:10.1016/j.still.2004.02.004

Madsen, H. 1976. Soil water content of some soils in Jutland. (In Danish.) Folio Geographica Danica X (4).

Millington, R.J., and J.M. Quirk. 1961. Permeability of porous solids. Trans. Faraday Soc. 57:1200–1207. doi:10.1039/tf9615701200

Moldrup, P., T. Olesen, D.E. Rolston, and T. Yamaguchi. 1997. Modeling diffusion and reaction in soils: VII. Predicting gas and ion diffusivity in undisturbed and sieved soils. Soil Sci. 162:632–640. doi:10.1097/00010694-199709000-00004

Moldrup, P., T. Olesen, S. Yoshikawa, T. Komatsu, and D.E. Rolston. 2005. Predictive-descriptive models for gas and solute diffusion coefficients in variably saturated porous media coupled to pore size distribution: III. Inactive pore space interpretations of gas diffusivity. Soil Sci. 170:867–880. doi:10.1097/01.ss.0000196770.45951.06

Monje, O., G. Stutte, and D. Chapman. 2005. Microgravity does not alter plant stand gas exchange of wheat at moderate light levels and saturating $CO_2$ concentration. Planta 222:336–345. doi:10.1007/s00425-005-1529-1

Nanzyo, M. 2002. Unique properties of volcanic ash soils. Glob. Environ. Res. 6:99–112.

National Aeronautics and Space Administration. 2002. Advanced life support project plan. Document no. JSC-39168. NASA Johnson Space Center, Houston, TX.

Nechitailo, G.S., and A.L. Mashinsky. 1993. Space biology: Studies at orbital stations. Mir Publ., Moscow.

Nkongolo, N.V., and J. Caron. 2006. Pore space organization and plant response in peat substrates. II. Dendradethum Ramat. Scientific Res. and Essays 1:93–102.

Olesen, T., P. Moldrup, T. Yamaguchi, and D.E. Rolston. 2001. Constant slope impedance factor model for predicting the solute diffusion coefficient in unsaturated soil. Soil Sci. 166:89–96. doi:10.1097/00010694-200102000-00002

Or, D., M. Tuller, and S.B. Jones. 2009. Liquid behavior in partially-saturated porous media under variable gravity. Soil Sci. Soc. Am. J. 73:341–350. doi:10.2136/sssaj2008.0046

Pennell, K.D. 2002. Specific surface area. In: J. H. Dane and G. C. Topp, editors, Methods of soil analysis. Part 4: Physical methods. SSSA Book Ser. 5. SSSA, Madison, WI. p. 295–315.

Petersen, L.W., P. Moldrup, O.H. Jacobson, and D.E. Rolston. 1996. Relations between specific surface area and soil physical and chemical properties. Soil Sci. 161:9–22. doi:10.1097/00010694-199601000-00003

Porterfield, D.M. 2002. The biophysical limitations in physiological transport and exchange in plants grown in microgravity. J. Plant Growth Regul. 21:177–190. doi:10.1007/s003440010054

Resurreccion, A.C., P. Moldrup, K. Kawamoto, S. Hamamoto, D.E. Rolston, and T. Komatsu. 2010. Hierarchical, bimodal model for gas diffusivity in aggregated, unsaturated soils. Soil Sci. Soc. Am. J. 74:481–491. doi:10.2136/sssaj2009.0055

Resurreccion, A.C., P. Moldrup, K. Kawamoto, S. Yoshikawa, D.E. Rolston, and T. Komatsu. 2008. Variable pore connectivity factor model for gas diffusivity in unsaturated, aggregated soil. Vadose Zone J. 7:397–405. doi:10.2136/vzj2007.0058

Robinson, D.A., and S.P. Friedman. 2005. Electrical conductivity and dielectric permittivity of sphere packings: Measurements and modeling of cubic lattices, randomly packed monosize spheres and multi-size mixtures. Physica A 358:447–465. doi:10.1016/j.physa.2005.03.054

Robinson, D.A., S.B. Jones, J.M. Blonquist, Jr., R. Heinse, I. Lebron, and T.E. Doyle. 2009. The dielectric response of the tropical Hawaiian mars soil simulant JSC Mars-1. Soil Sci. Soc. Am. J. 73:1113–1118. doi:10.2136/sssaj2008.0297

Rolston, D.E., and P. Moldrup. 2002. Gas diffusivity. In J.H. Dane and G.C. Topp, editors, Methods of soil analysis. Part 4. SSSA Book Ser. 5. SSSA, Madison, WI. p. 1113–1139.

Sahimi, M. 1994. Applications of percolation theory. Taylor and Francis, London.

Schjønning, P. 1985. A laboratory method for determination of gas diffusion in soil. Rep. S1773. Danish Inst. of Plant and Soil Sci., Tjele. (In Danish with English summary.)

Schjønning, P., and K.J. Rasmussen. 2000. Soil strength and soil pore characteristics for direct-drilled and ploughed soils. Soil Tillage Res. 57:69–82. doi:10.1016/S0167-1987(00)00149-5

Schjønning, P., I.K. Thomsen, J.P. Møberg, H. de Jonge, K. Kristensen, and B.T. Christensen. 1999. Turnover of organic matter in differently textured soils: I. Physical characteristics of structurally disturbed and intact soils. Geoderma 89:177–198. doi:10.1016/S0016-7061(98)00083-4

Schjønning, P., I.K. Thomsen, P. Moldrup, and B.T. Christensen. 2003. Linking soil microbial activity to water- and air-phase contents and diffusivities. Soil Sci. Soc. Am. J. 67:156–165. doi:10.2136/sssaj2003.0156

Schofield, R.K. 1935. The pF of the water in soil. In: Trans. World Congr. Soil Soc., 3rd, Oxford, UK. July–Aug. 1935. Vol. 2. p. 37–48.

Scovazzo, P., T.H. Illangasekare, A. Hoehn, and P. Todd. 2001. Modeling of two-phase flow in membranes and porous media in low gravity as applied to plant irrigation in micro-gravity. Water Resour. Res. 37:1231–1243. doi:10.1029/2000WR900311

Shimamura, K. 1992. Gas diffusion through compacted sands. Soil Sci. 153:274–279. doi:10.1097/00010694-199204000-00002

Shoji, S., and T. Takahashi. 2002. Environmental and agricultural significance of volcanic ash soils. Glob. Environ. Res. 6:113–135.

Shoji, S., M. Nanzyo, and R.A. Dahlgren. 1993. Volcanic ash soils: Genesis, properties, and utilization. Elsevier Amsterdam, the Netherlands. p. 1–288.

Spomer, L.A. 1974. Optimizing container soil amendment: The "threshold proportion.". HortScience 6:532–533.

Steinberg, S.L., D.W. Ming, K.E. Henderson, C. Carrier, J.E. Gruener, D.J. Barta, and D.L. Henninger. 2000. Wheat response to differences in water and nutritional status between Zeoponic and hydroponic growth systems. Agron. J. 92:353–360.

Steinberg, S.L., D.W. Ming, and D. Henninger. 2002. Plant production systems for microgravity: Critical issues in water, air and solute transport through unsaturated porous media. NASA Tech. Mem. 2002-210774. Natl. Aeronautics and Space Admin., Houston, TX.

Steinberg, S.L., and D. Poritz. 2005. Measurement of hydraulic characteristics of porous media used to grow plants in microgravity. Soil Sci. Soc. Am. J. 69:301–310. doi:10.2136/sssaj2005.0301

Stepniewski, W. 1980. Oxygen diffusion and strength as related to soil compaction. Pol. J. Soil Sci. 12:3–13.

Taylor, S.A. 1950. Oxygen diffusion in porous media as a measure of soil aeration. Soil Sci. Soc. Am. Proc. 14:55–61. doi:10.2136/sssaj1950.036159950014000C0013x

Troeh, F.R., J.D. Jabro, and D. Kirkham. 1982. Gaseous diffusion equations for porous materials. Geoderma 27:239–253. doi:10.1016/0016-7061(82)90033-7

Tuli, A., and J.W. Hopmans. 2004. Effect of degree of fluid saturation on transport coefficients in disturbed soils. Eur. J. Soil Sci. 55:147–164. doi:10.1046/j.1365-2389.2003.00551.x

Ullman, W., and R.C. Aller. 1982. Diffusion coefficients in near shore marine sediments. Limnol. Oceanogr. 27:552–555. doi:10.4319/lo.1982.27.3.0552

van Genuchten, M.Th. 1980. A closed-form equation for predicting the hydraulic conductivity of unsaturated soils. Soil Sci. Soc. Am. J. 44:892–898. doi:10.2136/sssaj1980.03615995004400050002x

Verhagen, J.B.G.M. 1997. Particle size distribution to qualify milled peat: A prediction of air content of ultimate mixtures. In: G. Schmileski, editor, Peat in horticulture. Proceedings of the International Peat Conference, Amsterdam, the Netherlands. 2–7 Nov. 1997. p. 53–57.

Wheeler, R.M., J.C. Sager, R.P. Prince, W.M. Knott, C.L. Mackowiak, G.W.Stutte et al. 2003. Crop production for advanced life support systems: Observations from the Kennedy space center breadboard project. NASA Tech. Mem. 2003-211184. NASA, Cape Canaveral, FL.

Wraith, J.M., and D. Or. 1998. Nonlinear parameter estimation using spreadsheet software. J. Nat. Resour. Life Sci. Educ. 27:13–19.

Yukselen, Y., and A. Kaya. 2006. Prediction of cation exchange capacity from soil index properties. Clay Miner. 41:827–837. doi:10.1180/0009855064140222

# PAPER V

# Gas-Diffusivity-Based Connectivity Analysis of Aggregated Soil Inner and Outer Pore Space

**Chamindu Deepagoda T.K.K. (1), Per Moldrup (1), Per Schjønning (2), Lis Wollesen de Jonge (2), Ken Kawamoto (3) and Toshiko Komatsu (3)**

(1)Dept.of Biotechnology, Chemistry and Environmental Engineering, Aalborg University, Sohngaardsholmsvej 57, DK-9000 Aalborg, Denmark. (2) Dept. of Agroecology and Environment, Faculty of Agricultural Sciences, Aarhus University, Blichers Allé 20, P.O.BOX 50, DK-8830 Tjele, Denmark. (3) Dept. of Civil and Environmental Engineering, Graduate School of Science and Engineering, Saitama University, 255 Shimo-okubo, Sakura-ku, Saitama, 338-8570, Japan.

dc@bio.aau.dk

## Summary

A pore connectivity analysis based on gas diffusivity measurements is presented to fingerprint the outer (inter-aggregate) and inner (intra-aggregate) pore spaces in aggregated soils. We developed an empirical model to express the Buckingham-based pore connectivity factor, $X$, as a function of soil matric potential ($\psi$) given by pF (= $\log|\psi|$), for the predictions in the outer pore space (pF 1.0 to 3.5). The new $X$ (pF) model was validated with independently measured data and performed better than a widely used predictive model. We further derived an inner space pore connectivity factor, $X'$, to gain exclusive fingerprints for the soil inner space functional structure. A two-region gas diffusivity model developed by combining three classical model approaches predicted well the observed bimodal gas diffusivity data. The predicted $X'$-pF and $X'$-$\varepsilon$ relations showed unique characteristics in soil inner space architecture.

## Introduction

Subsurface migration of greenhouse gases and gaseous phase contaminants occur predominantly by diffusion (Penman, 1940) and soil-gas diffusion coefficient, $D_p$ ($cm^2/s$), is the key parameter controlling diffusion of gases in soils. Accurate description of $D_p$ and its variation with differing soil moisture conditions has been a century-long research endeavour, and still continues to progress with our expanding knowledge on soil functional architecture.

Buckingham (1904) suggested a simple power-law model to predict gas diffusivity $D_p/D_o$ (where $D_o$ is the gas diffusion coefficient in free air) from air-filled porosity ($\varepsilon$) as follows:

$$D_p/D_o = \varepsilon^X \quad (1)$$

where the power-law exponent $X$ , a factor representing soil-pore network tortuosity and connectivity, can be calculated from the measured $D_p/D_o$ values by,

$$X = \frac{log\left(D_p/D_o\right)}{log\left(\varepsilon\right)} \quad (2)$$

Buckingham suggested empirically a constant value for $X$ (i.e., $X$ = 2) based on the measurements for differently-textured soils at near-dry conditions. On the contrary, some later studies suggested non-constant $X$ values for dry media and noted $X$ to be particle shape-dependant or texture-dependant. The presence of water has more pronounced effects on media tortuosity than the solid particles (Moldrup et al., 2000), and hence water-induced tortuosity factors are common in studies related to wetted media (Moldrup et al., 2000). However, only few studies have focused on the variation of $X$ with pF (= $\log|\psi, \text{cm } H_2O|$, where $\psi$ is soil matric potential). For example, for well-aggregated Andisols, Resurreccion et al. (2008) proposed the following $X$-pF relationship:

$$X = B + A_1 \left| pF - pF^* \right|^{A_2} \quad (3)$$

where $A_1$, $A_2$, B, and pF* are curve fitting parameters.

Based on gas diffusivity measurements, this study presents a pore connectivity analysis to characterize the outer and inner pore spaces in aggregated soils. A non-linear $X$-pF expression was developed to predict outer space pore tortuosity and connectivity factor as a function of pF. Considering an exclusive intra-aggregate pore connectivity factor, $X'$, we examined distinct fingerprints also in the soil inner space.

## Methods

We used soil gas diffusivity data from Ozosawa (1998) for undisturbed aggregated soils including 18 Brazilian soils, 5 Japanese (Mura) soils, 7 Japanese (Toyohashi) soils, 2 Japanese (Tsumagoi) soils (cultivated and non-cultivated) and also a non-aggregated Kashima dune sand. We further used undisturbed Danish soil data (Danish soil I and Danish soil II) and repacked Nishi-Tokyo (0-2mm) soil data from Chamindu et al. (2010). For sampling, preparation, soil properties, and gas diffusivity measurements, see Ozosawa (1998) and Chamindu et al. (2010).

## Results

Figure 1(a) illustrates variation of $X$, Eq. (2), for selected soils at differing matric potentials ranging from pF 1.0 to 3.5. Aggregated soils typically have their outer pore space (inter-aggregate region) fully drained at pF 2.0-3.5. All the considered soils showed an average $X$ value of 2.0 (Fig. 1a) near pF 3.5, and therefore showed a good agreement with Buckingham (1904).

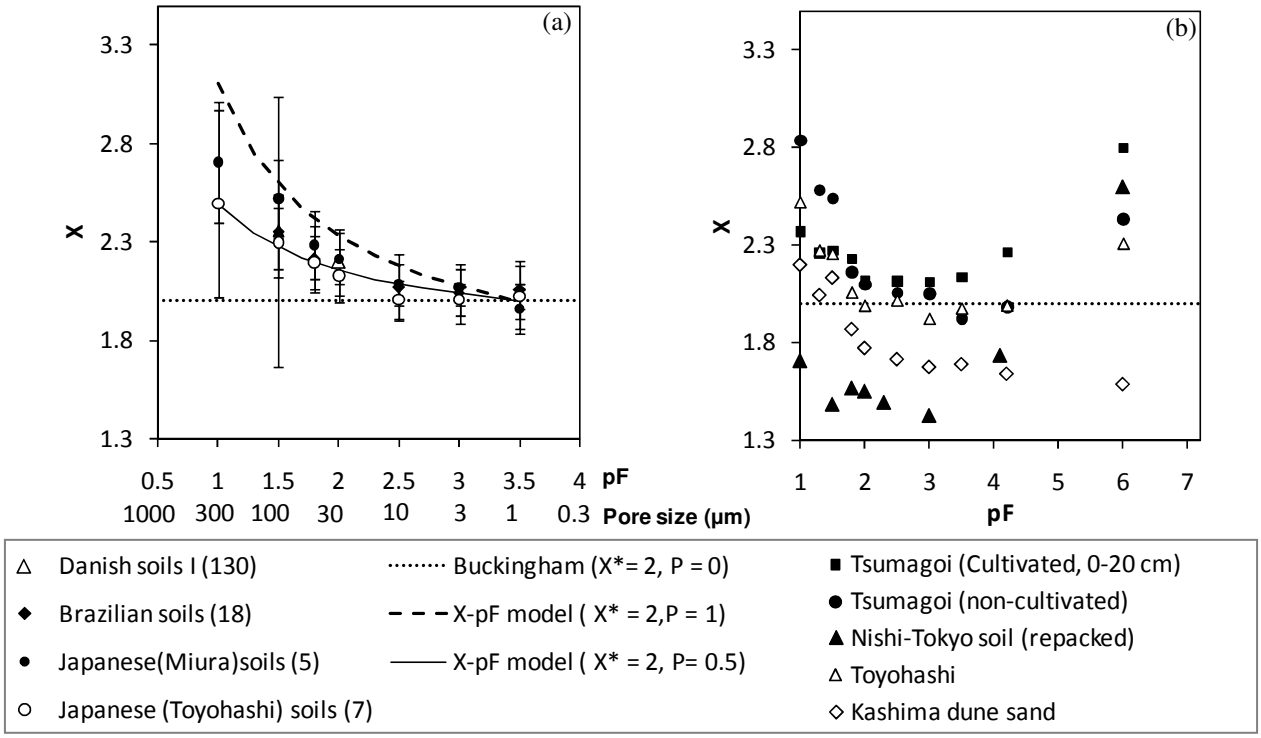


However, contrary to Buckingham (1904), $X$ showed a monotonic increase with decreasing pF, due to the enhanced water blockage effects at wet conditions. To describe this non-linear variation of $X$ with pF, we suggest a simple $X$ -pF model as follows:

$$X = X^* \left[ \frac{1 + \frac{1}{pF}}{1 + \frac{1}{pF^*}} \right]^P \tag{4}$$

where $X^*$ is the tortuosity factor at a reference-pF value denoted by pF*, and $P(\geq 0)$ is the model shape factor to account for the non-linear behavior. Considering a reference value of $X^*$= 2.0 at pF = 3.5, we tested the $X$-pF model for three different $P$ values (Fig. 1a): $P$ = 0 (Buckingham model), $P$ = 1.0, and P = 0.5. Of the three tested $X$-pF models, the model with $X^*$ = 2 and $P$ = 0.5 yielded best predictions, suggesting the following $X$-pF model for the outer pore space:

$$X = 2 \left[ \frac{1 + \frac{1}{pF}}{1 + \frac{1}{3.5}} \right]^{0.5} \tag{5}$$

Figure1 (b) shows variation of $X$ over a wider range of pF values, ranging from pF 1.0 to 6.0, for five different Japanese soils. Except for the Kashima dune sand, all other soils are aggregated soils with a well developed inner pore space (intra-aggregate region). $X$ showed a decrease with increasing pF up to pF = 3.0(~3.5) as observed in Fig 1(a), followed by a gradual increase again at higher pF values. This increase can be attributed to the draining of intra-aggregate pores, allowing gas diffusion to occur also in remote

and more tortuous pores within the aggregates in addition to main diffusion pathways. Compared to the two undisturbed Tsumagoi Andisols, the sieved and repacked Nishi-Tokyo Andisols showed a smaller $X$ in the inter-aggregate region due to less particle cementation as a result of breakdown of soil structure. However, this difference in $X$ is less pronounced at larger pF values (e.g., at pF 6), implying the structure changes are less affected to the intra-aggregate tortuosity. Kashima dune sand, on the other hand, consists mainly of non-aggregated uniform coarse sand particles and hence its $X$-pF behavior is self-explanatory.

To develop the $X$-pF model, Eq. (5), we mainly considered data for aggregated soils measured in a wide range of pF values, together with limited measurements also on

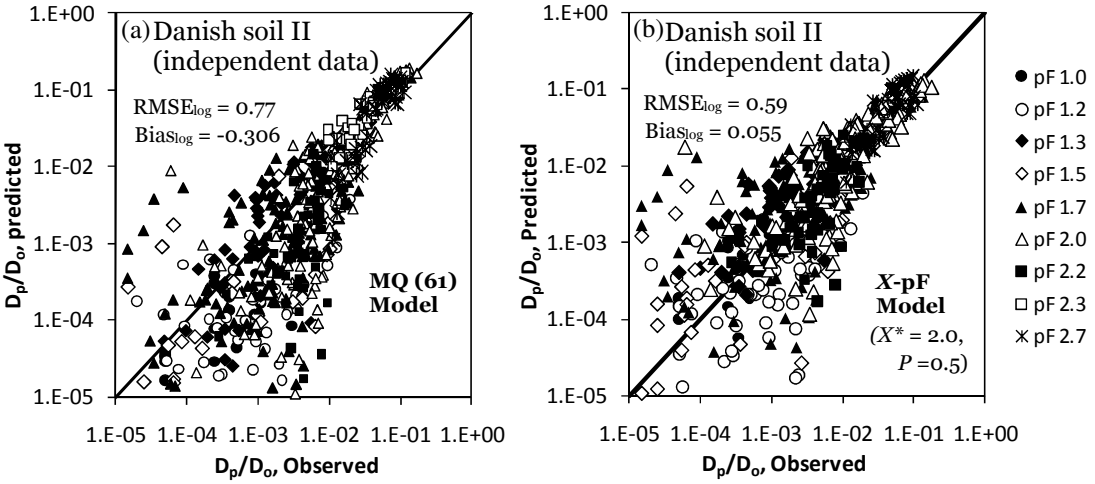


**Fig. 2** Scatterplot comparison for Danish soil II data with (a)MQ (1961) model, and (b) $X$-pF model, Eq. (5)

non-aggregated soils (Danish soil I). For model validation, we used independent $D_p/D_o$ data (Danish soil II) for 150 soils measured at 9 different pF values ranging from 1.0 to 2.7. Fig. 2 shows the scatterplot comparison of observed and predicted $D_p/D_o$ using two predictive models: the widely used Millington and Quirk (MQ: 1961) model (Fig.2a), and the $X$-pF model, Eq. (5) (Fig.2b). According to statistical analyses, MQ (61) model exhibited a poor fit (RMSE$_{log}$=0.77) with a marked overall under-prediction (Bias$_{log}$ = -0.306) and the $X$-pF model, in comparison, showed a better overall performance (RMSE$_{log}$=0.59, Bias$_{log}$ = 0.055).

In order to gain further insight into the inner pore space tortuosity and connectivity in aggregated porous media, we revisited the measured data for Nishi-Tokyo (0-2 mm) aggregated soil (data from Chamindu et al., 2010). The pore size distribution curve for the soil (Fig.3a) clearly demonstrated the presence of the two distinct regions, inter-aggregate region (Region 1) and intra-aggregate region (Region 2), which are separated near pore dia. of 3 μm (corresponding to pF 3). A similar two-region behavior was also observed for $D_p/D_o$ (Fig. 3b), and the Buckingham model (dotted line) failed to describe the observed data. In this study, we use the two-region Buckingham (1904)-Penman (1940)-Call (1957) model (BPC model) for the $D_p/D_o$ predictions:

Region 1:

$$D_p/D_o = (\varepsilon - \varepsilon_p)^{\beta} \qquad (\varepsilon_p \le \varepsilon < \Phi_1) \tag{6}$$

Region 2:

$$D_p/D_o = (\Phi_1 - \varepsilon_p)^{\beta} + H(\varepsilon - \Phi_1) \qquad (\Phi_1 \le \varepsilon \le \Phi) \tag{7}$$

where $\beta$ and $H$ are model fitting parameters and $\varepsilon_p$ and $\Phi_1$ are, respectively, the percolation threshold and the inter-aggregate porosity. To gain a quantitative insight into the inner space pore tortuosity, we separately considered the intra-aggregate tortuosity, denoted by $X'$, which can be written as,

$$X' = \frac{log\left(D_p/D_o - D_p/D_o\big|_{\varepsilon=\Phi_1}\right)}{log\,(\varepsilon - \Phi_1)} \qquad (\Phi_1 < \varepsilon \le \Phi) \tag{8}$$

By using Eq. (7) and Eq. (8) in combination with the bimodal van Genuchten(vG) water retention function (Durner, 1994), we obtained variation of $X'$ as functions of ε (Fig. 3c) and pF (Fig.3d), both showing useful fingerprints in the inner pore space.

Finally, we examined the sensitivity of two model parameters, the BPC model parameter $H$ (Eq.(7)) and the two-region vG model fitting parameter $\alpha_2$, on the overall $X'$ (pF) predictions (Fig. 4). The vG $\alpha_2$ did not show a significant effect on $X'$-pF behavior whereas $H$ showed a marked effect on overall model predictions.

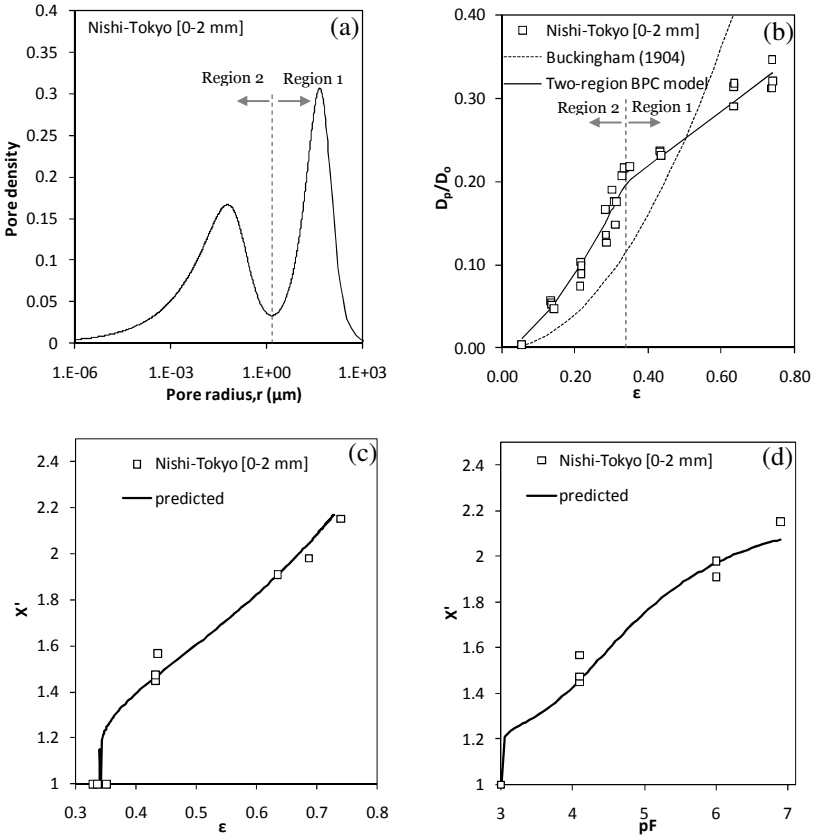


**Fig. 3** Measured and predicted data for Nishi-Tokyo (0-2 mm) soil: (a) pore size distribution, (b) gas diffusivity (c) $X'$ with ε, and (d) $X'$ with pF.

## Conclusions

- An empirical model was presented to predict the classical Buckingham model-based tortuosity factor, $X$, as a function of pF ranging from pF 1 to 3.5. The model showed promising results when tested against independently measured gas diffusivity data, and performed better than a widely used predictive model.

• A two-region gas diffusivity model developed by combining three classical model approaches predicted well the observed bimodal behavior in gas diffusivity for aggregated soils.

• A valuable insight into the soil inner space could be gained by considering exclusively an intra-aggregate pore tortuosity-connectivity factor, *X′*. The predicted *X′*-ε and *X′*-pF relations offered unique functional structure fingerprints.

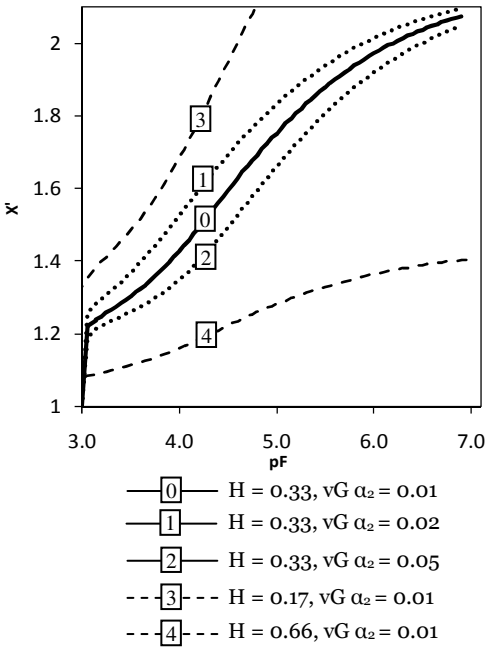


0 — H = 0.33, vG $\alpha_2$ = 0.01
1 — H = 0.33, vG $\alpha_2$ = 0.02
2 — H = 0.33, vG $\alpha_2$ = 0.05
3 - - - H = 0.17, vG $\alpha_2$ = 0.01
4 - - - H = 0.66, vG $\alpha_2$ = 0.01

**Fig. 4** Sensitivity analysis for two model parameters: *H* (Eq. (7)), and vG $\alpha_2$.


## Acknowledgements

This study was supported by the projects Gas Diffusivity in Intact Unsaturated Soil ("GADIUS") and Soil Infrastructure, Interfaces, and Translocation Processes in Inner Space ("Soil-it-is") from the Danish Research Council for Technology and Production Sciences.


## References


Buckingham, E., 1904. Contributions to our knowledge of the aeration of soils. Bur. Soil Bull. 25. U.S. Gov. Print. Office, Washington, DC.

Call, F., 1957. Soil fumigation: V. Diffusion of ethylene dibromide through soils. *J Sci. Food Agric* 8, 143-150.

Chamindu Deepagoda, T.K.K., Moldrup, P., Schjønning, P., Kawamoto, K., Komatsu, T. and de Jonge, L. W., 2010. Generalized density corrected model for gas diffusivity in variably saturated soils. *Soil Sci. Soc. Am. J.* (submitted).

Durner, W., 1994. Hydraulic conductivity estimation for soils with heterogeneous pore structure. Water Resour. Res. 30, 211–223.

Millington, R.J., and Quirk, J.M., 1961. Permeability of porous solids. *Trans. Faraday Soc.* 57, 1200–1207.

Moldrup, P., Olesen, T., Gamst, J., Schjønning, P., Yamaguchi, T., and Rolston, D.E., 2000. Predicting the gas diffusion coefficient in repacked soil: Water-induced linear reduction model. *Soil Sci. Soc. Am. J.* 64, 1588–1594.

Osozawa, S., 1998. A simple method for determining the gas diffusion coefficient in soil and its application to soil diagnosis and analysis of gas movement in soil. (In Japanese with English summary.) *Ph.D. diss. Bull.* 15. Natl. Inst. Agro-Environ. Sci., Ibaraki, Japan.

Penman, H.L., 1940. Gas and vapor movements in soil: The diffusion of vapors through porous solids. *J. Agric. Sci.* 30, 437–462.

Resurreccion, A.C., Moldrup, P., Kawamoto, K., Yoshikawa, S., Rolston, D.E., and Komatsu, T., 2008. Variable pore connectivity factor model for gas diffusivity in unsaturated, aggregated soil. *Vadose Zone J.* 7, 397–405.